

# UC Davis

## UC Davis Electronic Theses and Dissertations

### Title

Modeling riparian geomorphology and vegetation on a regulated river to assess change, prioritize ecological restoration areas, and inform restoration design

### Permalink

<https://escholarship.org/uc/item/29g03887>

### Author

McConnell, Clancy

### Publication Date

2023

Peer reviewed|Thesis/dissertation

Modeling riparian geomorphology and vegetation on a regulated river to assess change, prioritize ecological restoration areas, and inform restoration design

By

CLANCY ROBERT MCCONNELL  
DISSERTATION

Submitted in partial satisfaction of the requirements for the degree of

DOCTOR OF PHILOSOPHY

in

Geography

in the

OFFICE OF GRADUATE STUDIES

of the

UNIVERSITY OF CALIFORNIA

DAVIS

Approved:

---

Steven E. Greco, Chair

---

James H. Thorne

---

Eric W. Larsen

Committee in Charge

2023

Copyright © 2023 by Clancy R. McConnell

## **Abstract**

This dissertation is a three-part geographic study of the historical ecology and applied ecological restoration of Lower Putah Creek, California. It uses state-of-the-art tools in geographic information systems (GIS) to analyze historical and modern datasets. Findings are intended to inform riparian management, restoration planning, and restoration design.

In Chapter 1, a century of geomorphic change is analyzed using flow frequency analysis and a suite of topographic metrics to characterize channel shape over time. Most notably, it uses height above river (HAR), which is the height ( $z$ ) of an  $x$ - $y$  location above the nearest channel's thalweg or edge of low-flow (baseflow) river surface. Results show that the dams on Putah Creek reduced channel-forming peak flows by at least 82% in volume, and now maintain a perennial baseflow. Between 1905 and 2005, there was significant channel incision along the entire creek, a change from a U-shaped channel to a V-shaped channel, and a narrowing of the baseflow channel by half, although with significant reach-scale variation. These findings can inform channel-appropriate restoration designs or dam diversion strategies to manage geomorphic processes.

In Chapter 2, land cover change is analyzed between 1937 (pre-dam) and 2009 (post-dam) using machine learning image classification tools and forest-based classification methods. Those techniques were used to identify the importance of three topographic variables in predicting land cover: HAR, bank slope, and distance-to-baseflow surface. Results support previous studies, which show that a regulated flow regime enables longer-term plant succession and establishment of woody vegetation. Analysis by topographic variables show that woody vegetation tracked downward channel incision, and that the riparian zone became compressed in a narrower channel with steeper banks. Bank slope, HAR, and distance-to-baseflow surface had

equal importance in predicting land cover types in both 1937 and 2009 image classifications. Findings demonstrate that these methods can be used in other systems to characterize vegetation change.

In Chapter 3, first, inundation modeling and machine learning image classification are used to establish that HAR is well-correlated to discharge and vegetation. Then, HAR is used in a random forest classification to predict land cover types, and the output classification is used to create HAR zones relevant for restoration planning. Next, 25 reaches of Lower Putah Creek are delineated based on relatively homogeneous geomorphic characteristics and each is then ranked according to the sum of two independent rankings: (1) the in-channel relative area of their combined core riparian and marginal riparian zones; and (2) the in-channel relative area of their combined aquatic and transition zones. While 18 of the 21.22 miles of creek analyzed qualify as “degraded,” lowering of just half of the transition zone to floodplain HAR level could double the riparian zone, indicating a significant opportunity to recover endangered riparian forest in the Sacramento Valley. Finally, the relative area of aquatic and transition zones were used to prescribe geomorphological restoration actions. Of the degraded sections, 13.64 miles qualify for floodplain lowering, 7.05 miles qualify for baseflow narrowing, and 3.21 miles qualify for both, indicating that radical geomorphological change is needed to maximize the riparian habitat potential of Lower Putah Creek. The HAR zones created in this study can be directly incorporated into existing terrain design tools for restoration on Lower Putah Creek, and these methods can be implemented in many other river systems using publicly-available GIS datasets.

## Table of Contents

Abstract .....	ii
Table of Contents .....	iv
List of Figures .....	vii
List of Tables .....	ix
Acknowledgments.....	x
Introduction.....	1
Historical background on Lower Putah Creek.....	5
Chapter 1 Using height above river to characterize a century of geomorphic change on a dredged and regulated river .....	9
Highlights.....	9
Abstract .....	9
1. Introduction.....	10
2. Study Area .....	13
3. Methods.....	17
3.1 Flow frequency .....	17
3.2 Geomorphology .....	20
4. Results.....	26
4.1 Flow frequency .....	26
4.2 Geomorphology .....	30
5. Discussion.....	36
5.1 Flow frequency .....	36
5.1 Geomorphology .....	37
6. Conclusion .....	41
Chapter 2 Modeling pre- and post-dam geomorphological drivers of riparian vegetation distribution using machine learning imagery classification on a California coast range river .....	43
Highlights.....	43
Abstract .....	43
1. Introduction.....	45
2. Study Area .....	48
3. Methods.....	50
3.1 Creating imagery mosaics.....	50

3.2 Support vector machine (SVM) image classification .....	54
3.3 Random forest classification.....	56
3.5 Reach-scale analysis .....	57
4. Results.....	57
4.1 Creating imagery mosaics.....	57
4.2 Support vector machine (SVM) image classification .....	58
4.3 Random forest classification.....	62
4.4 Geomorphic analysis.....	63
4.5 Reach-scale analysis .....	75
5. Discussion.....	79
6. Conclusion .....	84
Chapter 3 Assessing reach-scale geomorphology using height above river zones to prioritize riparian restoration sites and inform restoration design on an incised and regulated California coast range river .....	85
Highlights.....	85
Abstract.....	85
1. Introduction.....	87
2. Study Area .....	90
3. Methods.....	92
3.1. 1-D flow modeling.....	95
3.2 Support vector machine imagery classification and geomorphic distribution.....	96
3.3 Random forest imagery classification using height above river .....	98
3.4 Identifying potential restoration sites.....	99
3.5 Prescribing restoration actions .....	100
4. Results.....	101
4.1 1-D flow modeling.....	101
4.2 Support vector machine imagery classification and geomorphic distribution.....	104
4.3 Random forest imagery classification using height above river .....	112
4.4 Identifying potential restoration sites.....	120
4.5 Prescribing restoration actions .....	129
5. Discussion.....	131
6. Conclusion .....	136
Intellectual Merit.....	138

Bibliography .....	139
Appendix.....	152



## List of Figures

Figure 1.1. Location of the Putah Creek Watershed.....	15
Figure 1.2. Pre- and post-dam average annual hydrographs for Lower Putah Creek.....	16
Figure 1.3. Study boundary.....	20
Figure 1.4. A 1905 USGS topographic quadrangle, Merritt, used in the study.....	22
Figure 1.5. An example of the HAR maps.....	25
Figure 1.6. Flow frequency values for selected recurrence intervals in pre-dam and post-dam. .	28
Figure 1.7. Flow frequency curves for pre-dam and post-dam.....	29
Figure 1.8. DEM subtraction map and accompanying 1905 and 2005 cross-sections. ....	30
Figure 1.9. The distribution of area by HAR for 1905 and 2005.....	31
Figure 1.10. Cross-sections sampled from the 41 representative cross-sections in Appendix Figure A.1. ....	33
Figure 1.11. Longitudinal plots by river-mile.....	35
Figure 1.12. Thalweg elevation profiles for 1905 and 2005.....	36
Figure 1.13. Cross-sections that could serve as reference sites for geomorphic restoration. ....	41
Figure 2.1. Black and white 1937 aerial photograph for a section of Lower Putah Creek.....	51
Figure 2.2. Mosaicked aerial imagery for 1937 and 2009.....	53
Figure 2.3. Classified imagery for 1937 and 2009 and the land cover transition map. ....	59
Figure 2.4. The distribution of land cover type by HAR for 1937 and 2009.....	66
Figure 2.5. Proportional cover of each class by HAR in 1937 and 2009. ....	67
Figure 2.6. Distribution of woody vegetation by HAR in 1937 and 2009.....	68
Figure 2.7. The distribution of land cover type by bank slope for 1937 and 2009.....	70
Figure 2.8. Proportional cover of each class by bank slope in 1937 and 2009.....	71
Figure 2.9. Distribution of cover type by distance to baseflow surface for 1937 and 2009.....	73
Figure 2.10. Proportional cover by distance to baseflow surface in 1937 and 2009.....	74
Figure 2.11. Land cover transition map for the reach-scale analysis.....	78
Figure 3.1. Locations and extents of major restoration projects on Lower Putah Creek in relation to the study boundary and river-miles. ....	92
Figure 3.2. Flowchart of study methods, including input and output datasets for each step.....	94
Figure 3.3. Inundation areas for modeled recurrence intervals, overlaid on the HAR raster. .	102
Figure 3.4. Total inundated area by discharge.....	103
Figure 3.5. Mean HAR of inundation surface edge by discharge.....	104
Figure 3.6. Aerial imagery and SVM land cover classification.....	106
Figure 3.7. Distribution of each SVM-classified cover type by HAR.....	109
Figure 3.8. Relative cover of each vegetation cover type by HAR. ....	110
Figure 3.9. Inundated area of each cover type by discharge.....	112
Figure 3.10. Maps showing (a) HAR, (b) the random forest classification, and (c) the reclassified HAR zones. ....	114
Figure 3.11. Distribution of each cover type by HAR in the random forest classification. ....	119

Figure 3.12. Relative cover by HAR in the random forest classification. ....	119
Figure 3.13. Boundaries of the 25 planning reaches, numbered from downstream (east) to upstream (west).....	122
Figure 3.14. Reaches in relation to river-miles and place names. ....	123
Figure 3.15. Examples of the four reach types, ranked by relative area of riparian zone and relative area of transition and aquatic zones. ....	126
Figure 3.16. Reach-scale rankings by larger-scale reach, or section. ....	128
Figure A.1. Representative cross-sections from Chapter 1 geomorphic analyses.....	154
Figure A.2. HAR zone maps by reach. ....	171

## List of Tables

Table 1.1. Flow frequency values for selected recurrence intervals.....	28
Table 2.1. Total area in acres of each cover class in 1937 and 2009.....	58
Table 2.2. Transition matrix for land cover change between 1937 and 2009.....	60
Table 2.3. Confusion matrices for the SVM imagery classification for 1937 and 2009. ....	62
Table 2.4. Mean and standard deviation of each geomorphic variable for each cover type in 1937 and 2009.....	64
Table 2.5. Transition cover for the Winters upstream reach.....	76
Table 2.6. Transition cover for the middle reach.....	76
Table 2.7. Transition cover for the South Fork reach. ....	77
Table 2.8. Reach-scale geomorphology in 1905 and 2005, including channel slope and bank slope, and incision between 1905 and 2005.....	77
Table 3.1. Recurrence interval flows used for creating flood inundation polygons. ....	96
Table 3.2. SVM-classified land cover area and proportional cover, including absolute cover and relative cover.....	105
Table 3.3. Confusion matrix for the SVM imagery classification accuracy assessment. ....	107
Table 3.4. Mean and standard deviation of the HAR values of each land cover type in the SVM classification. ....	109
Table 3.5. Random forest-classified land cover area and proportional cover across the entire 1,551-acre study area. ....	113
Table 3.6. Random forest classification of land cover area masked to the same coverage as the SVM classified output.....	115
Table 3.7. Random forest classification of land cover area.....	116
Table 3.8. Confusion matrix for the random forest classification validation. ....	117
Table 3.9. Total area of each HAR zone across the study area. ....	121
Table 3.10. Sum ranking of reaches by HAR zones. ....	125
Table A.1. Pre-dam Weibull-plotted flow frequency tables, sorted by flow rank.....	152
Table A.2. Post-dam Weibull-plotted flow frequency tables, sorted by flow rank. ....	153
Table A.3. Reach-scale geomorphological statistics. ....	165
Table A.4. Reach-scale area of each land cover type in the SVM classification of 2020 NAIP imagery. ....	166
Table A.5. Reach-scale relative area of each land cover type in the SVM classification of 2020 NAIP imagery. ....	167
Table A.6. Reach-scale area of each HAR zone from the random forest classification and zone analysis.....	168
Table A.7. Reach-scale relative area of each HAR zone within the channel. ....	169
Table A.8. Place names associated with each reach. ....	170

## **Acknowledgments**

This is not just the end of my degree, but the end of 25 years of schooling in the public education system, over 11 years of which I spent at UC Davis. I have only been able to reach this point because of the enormous support of the people in my "village." I would like to take a moment to thank them.

First and foremost, my major professor, Dr. Steven Greco, saw something in me eight years ago and took a chance. With his propensity for patience borne of decades of teaching, which inspired me to get into GIS in the first place, he saw me through to the end. My dissertation committee member, Dr. Jim Thorne, a brilliant and humorous scientist who contributed greatly to my project, also saw something in me and was generous enough to hire me as a postdoc right out the gate. I will do my best to rise to the occasion. My other dissertation committee member, Dr. Eric Larsen, asked me poignant questions from the beginning of the formulation of my project, questions that helped me contextualize everything I was planning to do, and helped me write a "good story." He also made me feel welcome, a hard thing to do in academia. My qualifying exam committee members, Drs. Truman Young and Mark Grismer, helped me build the valuable foundational knowledge I needed to become a scientist, and graciously gave their time to reviewing my dissertation proposal.

I owe a bottomless pit of thanks to the Program Coordinator of the Geography Graduate Group, Carrie Armstrong-Ruport, for enabling me to succeed at every critical juncture, from paperwork and funding to jolly ranchers and impromptu "shut-the-door" conversations. I also owe the chair of Geography, Dr. Diana Davis, much gratitude for giving me graduate teaching opportunities and consulting with me about my dissertation and career. Diana was another person who made me feel welcome and needed in academia. To my PI on the zoning atlas project, Dr.

Catherine Brinkley, I owe many thanks for being the most level-headed, straightforward, and supportive boss I've ever had. She also gave me priceless opportunities to lead projects that advanced my career. I owe my GIS course supervisor, Dr. Isaya Kisekka, many thanks for encouraging me to keep my heart in teaching, even when the going gets rough. I'd also like to thank Dr. Susan Ustin for consulting with me about my image classification methods; her advice proved essential.

My Mom and Dad believed in me when I didn't believe in myself, never hesitated to ask the hard questions when it was in my best interests, and—perhaps most importantly—always sent me back to school loaded with care packages, trays of lasagna, and boxes of cookies. My brother, Patrick, took countless late-night phone calls from me about hard situations, good news when it came—however few and far between—and what was the latest in the railroading world. These calls got me through grad school. My wonderful girlfriend, Annie, encouraged me on many bad days, celebrated with me on the infrequent good days, and for nearly six years has been the light of my life. My mentor, Dr. Paul Salitsky, has been a steadfast supporter of mine for eight years in both career and life, and has taught me how to be a better athlete, teacher, and person; I consider him family.

I shared many comical writing and teaching days with my lab colleagues, Drs. Monica Parisi and Kim Chacon, who overcame much more than me to get their degrees; they inspired me to see this through. I also shared fascinating conversations over coffee with Putah Creek Streamkeeper Rich Marovich, who warmly supported me and made me feel that my research was valued. For the hardest GIS questions, I always went to Dr. Sean Hogan, who had a simple solution to every problem and taught me how to fly drones with a little flair. For awarding me the funds that enabled this project, I thank Robin Kulakow and Bill Julian of the Yolo Basin

Foundation, the UC Davis Geography Graduate Group, the UC Davis Jastro endowment, and the Central Sierra Audubon Chapter. To all of my running, college, marching band, and grad school friends, I am grateful for the memories, camaraderie, and laughs over these many years.... Here's to the end of an era.

Finally, I would like to acknowledge that the Putah Creek region has been the home of the Patwin people for many centuries. They managed and stewarded the land sustainably, and elders continue to instruct youth in the ways their culture is tied to this landscape. Today, they live on in at least three tribes: Cachil DeHe Band of Wintun Indians of the Colusa Indian Community, Kletsel Dehe Wintun Nation, and Yocha Dehe Wintun Nation. I am honored to have worked and studied on their traditional lands.

## **Dedication**

This work is dedicated to my grandparents:

Sandra Wells, who took me hiking in the mountains, initiated my obsessions with Harry Potter and Star Trek, and inspired me to enjoy every day.

Barbara McConnell, who taught me the power of reading and writing and edited my early drafts, from grade school into college.

George McConnell, who helped me get into playing music at an early age and instilled in me that any job worth doing is worth doing right.

Bill Dailey, who showed me that friends are the family you choose for yourself.

## Introduction

*“Putah Creek...is a treasure.... It’s an entire ecosystem in the middle of a heavily farmed, agricultural environment. And in my view, it’s not just a question of whether Putah Creek is just as good...or worse off...but simply that Putah Creek is different.”*

Judge Richard K. Park

Issued in his ruling for year-round flows for Lower Putah Creek

April 8, 1996

Dams change rivers, hydrologically, ecologically, and geomorphologically.

Anthropogenic changes like dams and gravel mining can make it more challenging to study bio-physical relationships in degraded rivers, especially when attempting to establish baseline conditions, but these changes are often the reason we study these systems: to better rehabilitate them as functional habitat. Reconstructions of historical ecological and physical conditions are an integral part of informing the management of river ecosystems, and the use of comparative methods in historical ecology can help piece together a mix of data into reasonably realistic pictures of the past. Indeed, if we are to "restore" rivers, even if only in function and not in form, it is essential to understand the drivers of change, whether past, present, or potential future.

Like any science, historical ecology studies must be framed within the context of the ways their data were collected: usually by people from generations in the past with no connection to present research objectives and no idea of how the data they were collecting would be used with future technology. In this sense, these studies can contribute to science by making novel and creative use of existing data as well as create knowledge about past ecosystems. Since much of the data used in historical ecology was collected in the last two centuries, it is also a reminder that the historical reconstructions created from these data are really only snapshots from a time when the ecosystems they document, in many cases, had already been developed, and in many more cases, had been managed for centuries or millennia by indigenous people. Indeed, to understand pre-settlement conditions, it is essential to review prehistoric data



(Whipple et al., 2011); after all, two centuries only provides a relatively narrow view of long-term ecological processes, such as evolution, and often cannot account for the way indigenous people managed their landscapes for thousands of years (Anderson, 1993; Beller et al., 2017). Additionally, these snapshots were often taken at irregular intervals without controlling for external variables or the benefit of modern research design to reduce bias; the picture may be fuzzy at best (O'Brien, 2001).

Why study rivers in particular? Wetlands and rivers are among the most changed and degraded ecosystems on the planet, and are considered endangered in heavily-developed areas (Best, 2019; Petsch et al., 2023). They critically need to be restored or rehabilitated to avoid the loss of riparian species and critical ecosystem functions. One of these areas is California's Sacramento Valley, where just 8.7% of riparian, or river-adjacent, habitat remains from pre-colonial times (Geographical Information Center, 2003; Roberts et al., 1980). Fortunately, new tools and methods in geography are enabling scientists to study rivers in more descriptive and efficient ways. Of perhaps most importance in developing new tools for river science are geographic information systems (GIS), which combine a database management system with a graphical user interface to manipulate a wide range of data easily and quickly. In this dissertation, I made extensive use of a wide variety of tools in GIS, from topographic workflows to machine learning.

A relatively new GIS tool (developed for widespread GIS use starting in 2008) that forms a cornerstone of this project is height above river (HAR), or relative elevation, which describes the height of every spot in a study area relative to the nearest baseflow river surface (Dilts et al., 2010; Greco et al., 2008). Its usefulness in applied hydrology and river restoration has already been demonstrated in a number of ways (Bair et al., 2021; Bureau of Reclamation, 2013; Greco

et al., 2008; Griggs, 2009; Schwindt et al., 2020), but only in static conditions; HAR has not yet been used to analyze change over time, and thus, this is a particularly novel aspect of this research. Also, while HAR has been used to identify areas suitable for riparian restoration (Benda et al., 2011; California Department of Water Resources, 2017; cbec, 2023) and to design planting zones in geomorphologically-restored rivers (Bair et al., 2021), no studies have used a HAR-classified land cover model to assess geomorphology, quantify restoration potential, and plan restoration design. The following three chapters make extensive and novel use of GIS to characterize change, identify degraded and reference areas, prioritize rehabilitation, and prescribe restoration actions at the river and reach scales.

As is the case in many branches of science, contextualized findings from one river system can be useful in managing other similar river systems. In the following chapters, a case study approach was used to analyze change and evaluate restoration potential along nearly the entire below-dam section of Putah Creek (referred to as Lower Putah Creek) from river-miles 1.54-22.76, a medium-sized dammed river in the southwestern Sacramento Valley (downstream of river-mile 1.54, near the convergence of Putah Creek with the Yolo Bypass, was too affected by the hydrology and management of the Yolo Bypass to be included in this project). This study area was chosen because it was: (a) accessible and most proximate to the researchers' campus, (b) large enough that findings can be relatable to dozens of other dammed river systems in the region but small enough that nearly the entire lower creek could be studied, (c) possessed enough historical and current data for productive analyses and these data had not yet been analyzed for the purposes of characterizing historical conditions, and (d) presented interesting and novel riparian phenomena that would be a valuable contribution to science. Additionally, major modifications to Lower Putah Creek have transformed it into a novel ecosystem (Hobbs et al.,

2009; Moyle, 2014), one that only partially resembles its former pre-settlement state and to which it can never return. Because of this, coordinated and scientifically-informed rehabilitation efforts in its channel have been challenging to develop and implement. Methods from this project can be applied in other river systems, and findings from this project can be used immediately to enhance Lower Putah Creek.

The objectives of this dissertation are to:

Chapter 1:

- Demonstrate the effectiveness of a geomorphological metric, height above river, in characterizing historical geomorphic change from 1905 to 2005 using a case study approach on Lower Putah Creek, California;
- Identify the potential causes of change, whether from damming, channelization, dredging, or industrial agriculture; and
- Characterize the hydrologic changes caused by flow regulation in Lower Putah Creek using peak flow frequency analyses.

Chapter 2:

- Characterize the type, magnitude, and distribution of vegetation change between the pre-dam and post-dam states of Lower Putah Creek;
- Use machine learning to identify the possible topographic drivers of vegetation change; and
- Demonstrate the effectiveness of topographic variables, including HAR, bank slope, and distance to baseflow surface, in characterizing vegetation change.

Chapter 3:

- Use height above river to predict riparian vegetation zones;

- Characterize reaches based on their area and distribution of HAR zones to identify which reaches have functional riparian morphology;
- Identify the nature of geomorphological restoration required in each reach to produce a functional riparian floodplain morphology, as well as the potential riparian area that could be gained through geomorphological restoration; and
- Use HAR zones to prescribe reach-scale geomorphological restoration actions.

While Judge Park was right when he said that Putah Creek is different now than it used to be, it does not change the fact that Putah Creek could be better. In this dissertation, I attempt to fill a few gaps in the story of this unique river, how it has changed, and how it could be enhanced to gain back at least a little of what has been lost. I will end with a quote by Stanford et al. (1996: 391), whose approach to restoring regulated rivers helps frame this project:

*“Although restoration to aboriginal state is not expected, nor necessarily desired, recovering some large portion of the lost capacity to sustain native biodiversity and bioproduction is possible by management for processes that maintain normative habitat conditions.”*

### **Historical background on Lower Putah Creek**

It cannot be determined the full extent to which damming affected the geomorphology of Lower Putah Creek, because settlers first began altering the creek in the mid-1800s before any physical data were recorded, and no topographic data exists from the time immediately preceding or following dam construction. Before the area began to be farmed or grazed by Mexican and U.S. settlers, a riparian forest up to two miles wide straddled the banks of Putah Creek, and valley oak woodlands extended up to several miles beyond that (Geographical Information Center, 2003; Holmes and Nelson, 1915; Tuil, 2019). This forest had been sustainably used and

maintained for 1,500 years by Native Americans, but starting in the 1840s, settlers rapidly cut it down for cattle fencing, housing, and other uses on the area's Ranchos (Vaught, 2007).

Thereafter, they fought catastrophic flooding from Putah Creek for decades, often by building ineffective makeshift levees.

By 1873, organized channel construction had begun: ranchers east of Davisville (now called Davis) sought to redirect flood waters from their farms by scraping material from the floodplain eastward of the creek's 90-degree northward bend to create a new channel, south of their cattle farms (now known as the South Fork of Putah Creek). Early on, this shallow channel was ineffective and filled at least halfway with sediment after moderate flows, but persistent efforts to maintain its depth and width, combined with scouring from major flows uninhibited by vegetation (which had been denuded by this point for cattle fencing), slowly increased the channel's size until it had reached the same depth as the old channel at the intersection, or fork, with the old channel, and then surpassed its depth (Vaught, 2007). By the time the USGS topographically surveyed the Central Valley in 1905, the new channel had been scoured about five feet deeper than the old channel by some combination of earth-moving and human-induced flood scouring; the creek filled the old channel only during large flows, though major floods still occasionally wetted the northern floodplain, including the UC Davis campus and downtown Davis. By 1905, it was, and had been for at least 60 years, in a state of major change. This would continue through most of the 1900s, and gravel mining further contributed to localized channel deepening as late as the 1970s, when UC Davis dredged aggregate from their reach of the creek to build campus roads and buildings (P. Moyle, personal communication, 2018). In 1948, the U.S. Army Corps of Engineers placed an earthen dam on the old channel at the intersection of the old and new channels, permanently redirecting all flow into the new channel and creating the

“pond” or “slough” in the old channel that would officially become the UC Davis Arboretum in the former North Fork channel (Parker, 2006). Even after this final modification to the creek's hydrology, a major storm in 1973 flooded the city of Davis. The campus Arboretum, now serving as a stormwater detention basin, overtopped its banks and flooded as far north as 7<sup>th</sup> Street, about a half-mile away from the old channel (Larkey, 1969). While this region of California has been channelized, drained, and developed beyond recognition, these occasional severe storms continue to remind residents of the "inland sea" they inhabit (Kelley, 1989).

By the 1940s, industrial agriculture in Yolo and Solano counties had depleted regional groundwater, and enough political clout was raised to implement the Solano Project and dam Putah Creek (Rubin, 1988). In 1957, Monticello Dam created Lake Berryessa and Putah Diversion Dam created Lake Solano, redirecting an average of 70% of the volume of water received in the upper watershed to farmers in Solano County.

During a severe drought in the 1980s, the reservoir operator, Solano County Water Agency, reduced flows into Lower Putah Creek to zero during the driest months of the year, resulting in a dry creekbed, nearly total loss of the fish population, and stressed riparian vegetation (Hammond, 1989; Jacinto et al., 2023). While the creek did occasionally run dry in some sections in September and October before the dam was constructed, the sudden change from a perennial creek to a desiccated set of puddles led to public outcry. After a decade of litigation from the non-profit Putah Creek Council, which was formed as a response to the drying up of the creek in 1988, a judge ruled that Lower Putah Creek required a year-round minimum baseflow. In 2000, the Putah Creek Accord stipulated that Solano County Water Agency needs to: (1) maintain a minimum flow in Lower Putah Creek year-round, (2) appoint a streamkeeper to look out and manage restoration on the creek and relations with its many riparian landowners,

and (3) allocate funding each year for education and stewardship, the vast majority of which has since been contracted to Putah Creek Council.

While Lower Putah Creek has been studied in some ways, no one has yet characterized the pre-dam/post-dam geomorphological or vegetation change, and river-scale assessments have not analyzed the drivers of riparian vegetation distribution. UC Davis Professor Peter Moyle and his associated aquatic biologists have studied in great detail the fish populations of Lower Putah Creek, documenting the benefit that the Accord's flow regime has had to native fish populations (Jacinto et al., 2023; Kiernan et al., 2012; Moyle, 2014; Moyle et al., 1998). Dr. Melanie Truan (UC Davis) and her associated wildlife biologists have studied the riparian habitat diversity and wildlife and bird populations on Putah Creek for many years, including habitat enhancements (Dybala et al., 2018; Lin et al., 2022; Truan et al., 2010). Solano County Water Agency has studied a number of facets relevant to riparian management (Jones and Stokes, 1992), including the bathymetry (Yates, 2003) and invasive vegetation (Lower Putah Creek Coordinating Committee, 2005). Dr. Mark Grismer (UC Davis) has demonstrated the importance of groundwater to riparian vegetation in at least some reaches of Lower Putah Creek (2018), and Dr. JayLee Tuil (UC Davis) modeled the possible prehistoric distribution of riparian forest and oak woodland in the lower Putah-Cache landscapes (2019).

## **Chapter 1 Using height above river to characterize a century of geomorphic change on a dredged and regulated river**

### **Highlights**

- Height above river provides valuable insight into geomorphic changes
- A suite of geographic tools provides most comprehensive picture of change
- Flow regulation reduced peak streamflows on Putah Creek by at least 80%
- Reduction in peak streamflows led to significant incision and channel narrowing

### **Abstract**

Quantifying geomorphic change is critical to watershed management and stream restoration. The development of efficient methods in geographic information systems (GIS) has made quantifying riverine change more approachable. A particularly useful GIS-based metric for describing riparian systems is height above river (HAR), or relative elevation, which is the height (z) of an x-y location above the nearest channel's thalweg or edge of low-flow river surface. HAR has been used to identify vegetation zones, depth to groundwater, flood risk, and channel and planting design in ecological restoration. However, no studies have used HAR to characterize change in channel shape over time. In this study, a flow frequency analysis and HAR-based geomorphic analysis were used to characterize change between the pre- and post-dam states of a regulated river, Lower Putah Creek, a tributary to the Sacramento River in California, USA. Flow frequency analyses indicate that the dam has reduced channel-forming peak flows by at least 82% in volume. The historical HAR analysis examined two time periods, 1905 and 2005, and found significant channel deepening (incision) as well as a change from a U-shaped to a V-shaped channel. Longitudinal analyses show channel incision along the entire creek, with an average incision of 8.5 ft and a maximum incision depth of 17 ft, as well as a



mean 49% narrowing of the baseflow channel width and narrowing along almost the entire creek. These landscape-scale methods for studying historical riverine geomorphology can inform channel-appropriate restoration designs or dam diversion strategies to manage geomorphic processes.

**Keywords:** height above river, GIS, flow regulation, dams, historical reconstructions, flow frequency, riparian geomorphology

## 1. Introduction

Rivers are critical components in landscape ecosystems and support human society. Riverine and riparian ecosystems alone are home to over a third of the world's human population and many of its biodiversity hotspots (Best, 2019). Directly and indirectly, rivers provide many ecosystem services, but most large river ecosystems are severely degraded due to watershed modification and flow regulation by human infrastructure (Best, 2019; Petsch et al., 2023). Dams are by far the largest source of anthropogenic change to river systems; 63% of the world's longest rivers are dammed, only 23% of all the world's rivers remain undammed, while 2.8 million dams worldwide impound and divert flow to support developed regions (Grill et al., 2019). In California alone, 1,530 dams impound up to 45 million acre-feet of water, yet this volume may not be enough to support the state's population and industry under projected climate change (Escriva-Bou et al., 2019; "National Inventory of Dams," 2023).

Dams have been shown to affect downstream flow timing and volume (Magilligan and Nislow, 2005; Petts and Gurnell, 2005; Richter and Richter, 2000), sediment aggradation and degradation (Ronco et al., 2010), floodplain geomorphology (Bair et al., 2021; Marren et al., 2014), and ecological life cycles and ecological disturbance (Poff and Hart, 2002). Annual peak streamflow, the maximum instantaneous flow recorded during a water year, is an important

hydrologic metric because large flows transport sediment and gravel, scour material and vegetation, and serve as the main source of secondary succession in floodplain river ecosystems. Additionally, peak streamflow is used to calculate flow frequency, or recurrence interval, which is an important criterion for designing infrastructure, such as bridges and levees, and for assessing flood risk in developed areas.

While many studies have characterized the effects of dams on downstream rivers, each river system is unique and managed, to a large degree, based on its environmental conditions, surrounding land uses, and demands from water users. Also, though some hydrogeomorphic responses to damming are relatively consistent across all dammed systems, some responses, such as changes to daily minimum flows, can vary significantly across sites (Magilligan and Nislow, 2005). For this reason, geomorphic studies are still conducted for individual river systems to inform watershed management, and it remains important to continue to develop more efficient and effective methods for studying rivers.

The advancement of geographic information systems (GIS) technology has enabled efficient, low-cost examination of entire watersheds or rivers with straightforward tools, useable not only by trained field hydrologists but also by physical geographers and other GIS users. One of those tools is height above river, or HAR. HAR is a GIS method for characterizing lateral channel topography, where any x-y value in a river reach study area can be assigned a height (z-elevation) value relative to the nearest channel thalweg or low-flow (baseflow) river surface edge (Dilts et al., 2010; Greco et al., 2008; Nobre et al., 2011; Poole et al., 2002). HAR was first used in geology studies in the 1940s to describe the sequence of soil horizons, and by the 1970s, it was being used as a field method to identify elevation zones for riparian vegetation (Teversham, 1973). Serving as a proxy for vegetation zonation is the most common use of HAR today, and

studies have used it to approximate groundwater depth (height above groundwater; Greco et al., 2008) and flood inundation (Bair et al., 2021; California Department of Water Resources, 2017; Greco et al., 2008; Sagers et al., 1996; Vondrasek, 2015), create flood risk maps (Ureta et al., 2020), and design channel shape and planting zones in river restoration (Bair et al., 2021). Dilts et al. (2010) found HAR to be superior in accuracy and ease of implementation over digital or field-collected cross-sections; others have found remote sensing methods of inland waters, like HAR, to be superior for their scalability to large areas and, in the case of satellite data, their temporal frequency (Palmer et al., 2015). Additionally, many GIS methods can easily be executed over an entire study area, negating the need for representative statistical sampling (Daniel, 2012).

However, for as long as HAR has been a useful metric, it has not yet been applied to characterize geomorphic change over time. While standard hydrologic transects between time periods can show site-scale changes in a river channel, a high density of them is required to provide a generalized picture of longitudinal change in channel shape across an entire river or reach. As a raster elevation model, HAR is capable of describing these changes across an entire study area with a level of precision equal to the input datasets.

The objectives of this study are to:

- Demonstrate the effectiveness of HAR in characterizing historical geomorphic change from 1905 to 2005 using a case study approach on Lower Putah Creek, California;
- Identify the possible causes of change, whether from damming, channelization, dredging, or industrial agriculture; and

- Characterize the hydrologic changes caused by flow regulation in Lower Putah Creek using peak flow frequency analyses.

## 2. Study Area

Historically, Putah Creek was an ephemeral, semi-arid river that drained a 654-square-mile watershed in the Inner Northern Coast Range of California eastward to the Yolo Bypass, a component of the Sacramento River flood control system. Ultimately, Putah Creek is a tributary to the Sacramento River, the largest river system in California. A large dam on Putah Creek creates a large reservoir, Lake Berryessa, that results in constant outflow now making it a perennial river. Putah Creek was the main component of the Solano Project, a water storage system developed to support agricultural and urban development in Solano County, California. East of the city of Winters, the 304-ft-tall Monticello Dam impounds Lake Berryessa, the state's longest reservoir at 17 miles. Berryessa captures an average of 93% of the volume of precipitation received in the Putah Creek watershed (UC Berkeley GeoData Repository, 2023), and can store over four times the average annual precipitation in its captured watershed (Yolo Bypass Working Group et al., 2001). The lowest 30 miles of creek, below the outfall from Lake Berryessa, have been heavily modified by large infrastructure projects, damming, dredging, agriculture, invasive species, and recreation, creating a novel riparian ecosystem (Hobbs et al., 2009; Moyle, 2014) that only partially resembles the historical ecosystem.

Seven miles downstream of the Lake Berryessa outfall, the Putah Diversion Dam shunts an average of 70% of its outflow each year into the Putah South Canal for farm irrigation and municipal use in Solano County. Due to the location of the dams and the unique shape of the Putah Creek watershed (**Figure 1.1**), 97% of the total watershed area and an average of 98% of the total volume of water are regulated and diverted by major dams. One minor tributary, Dry

Creek, and a small portion of watershed area located downstream of Putah Diversion Dam contribute little to the creek's overall hydrograph dynamics (Petts and Gurnell, 2005). The remaining 30% of water that runs down Lower Putah Creek does so according to reservoir operations, which are determined by supply and demand and—to a certain extent—flood management, as well as by the Putah Creek Accord (a legal agreement signed in 2000). Since the Accord, a minimum baseflow has been required year-round to protect native fish species and other ecosystem functions (Somach, 2000), including critically important restoration efforts in the Putah Sinks region of the Yolo Bypass Wildlife Area (Yolo Bypass Working Group et al., 2001). The flow regime based on the Accord has had a positive effect on native fish communities in Lower Putah Creek (Jacinto et al., 2023), although geomorphic effects have not yet been studied. Legacy water rights and illegal pumping drain an unknown and variable amount of water out of Lower Putah Creek (California Department of Fish and Game, 2008), and complex groundwater connections through gravel deposits (i.e., gaining and losing reaches) may influence flow by relatively small amounts according to season and reach/location (Grismer, 2018; Harvey et al., 1993), although these connections were much more important before dam regulation created a perennial baseflow (Huberty and Johnston, 1941; Rubin, 1988).

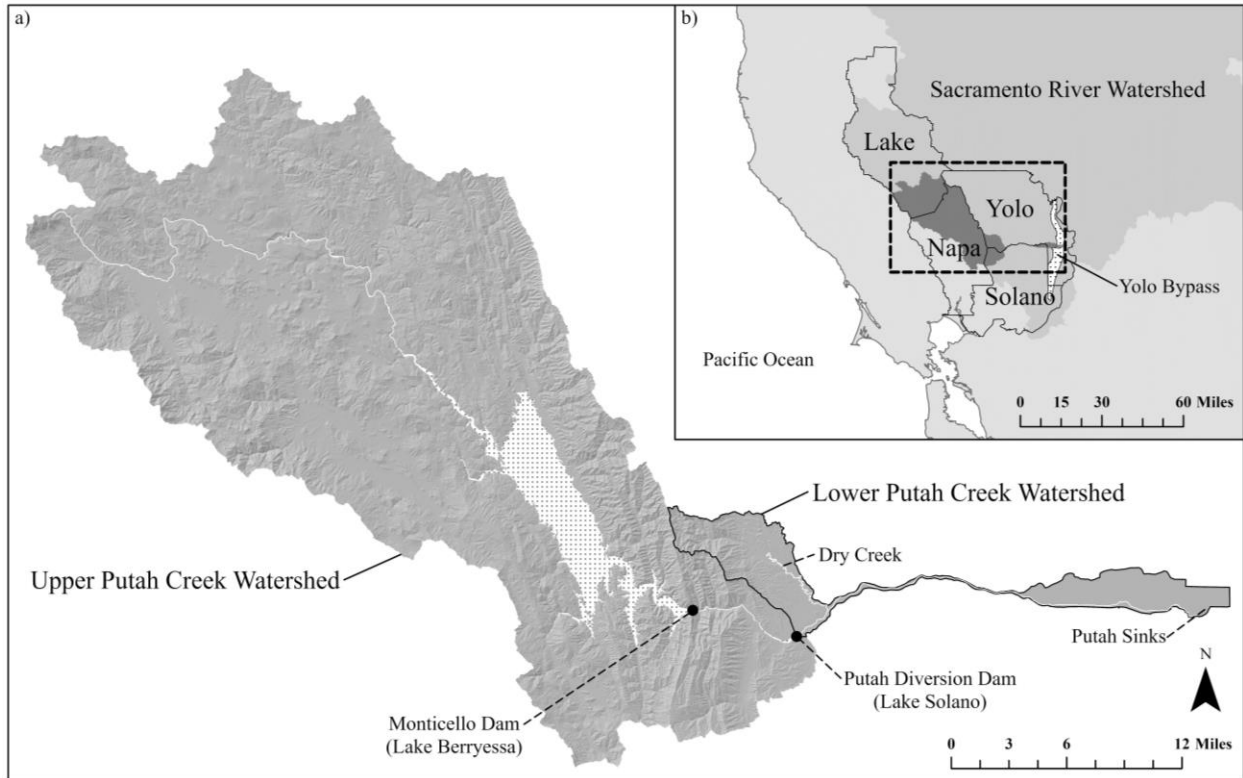


**Figure 1.1.** Location of the Putah Creek Watershed. a) Upper and lower watersheds of Putah Creek, hydrologically divided by the Putah Diversion Dam, and b) inset map of the location of the entire Putah Creek watershed (dark gray) in relation to the Sacramento River watershed (medium gray), its four host counties, the Yolo Bypass (white dotfill), and the Northern California coastline (Solano County Water Agency, 2009; US Census Bureau, 2023; USGS, 2022).

While the 2000 Accord modified the annual hydrograph of Lower Putah Creek to benefit aquatic ecology, it had little impact on geomorphology because the newly-required perennial baseflow has limited power to transport or scour sediment (Larsen et al., 2006), and any other supplemental environmental flows were within the established range of annual peak streamflows for the post-dam system. The dams on Putah Creek have a typical and predictable impact on the annual hydrograph of the lower river: increased summer baseflows and reduced winter runoff flows (**Figure 1.2**) (Magilligan and Nislow, 2005). Peak streamflow, the largest flow recorded in each water year (a water year is defined from October 1<sup>st</sup> to the following September 30<sup>th</sup>, due to the Mediterranean climate), was most dramatically affected after 1957, when the dams were

completed (**Figure 1.2**). The largest flow recorded pre-dam, in 1940, was 81,000 cubic feet per second (cfs), and was the last flood from Putah Creek to submerge the city of Davis (Larkey, 1969). The largest flow since 1957 has been just 18,700 cfs, and occurred in 1983.

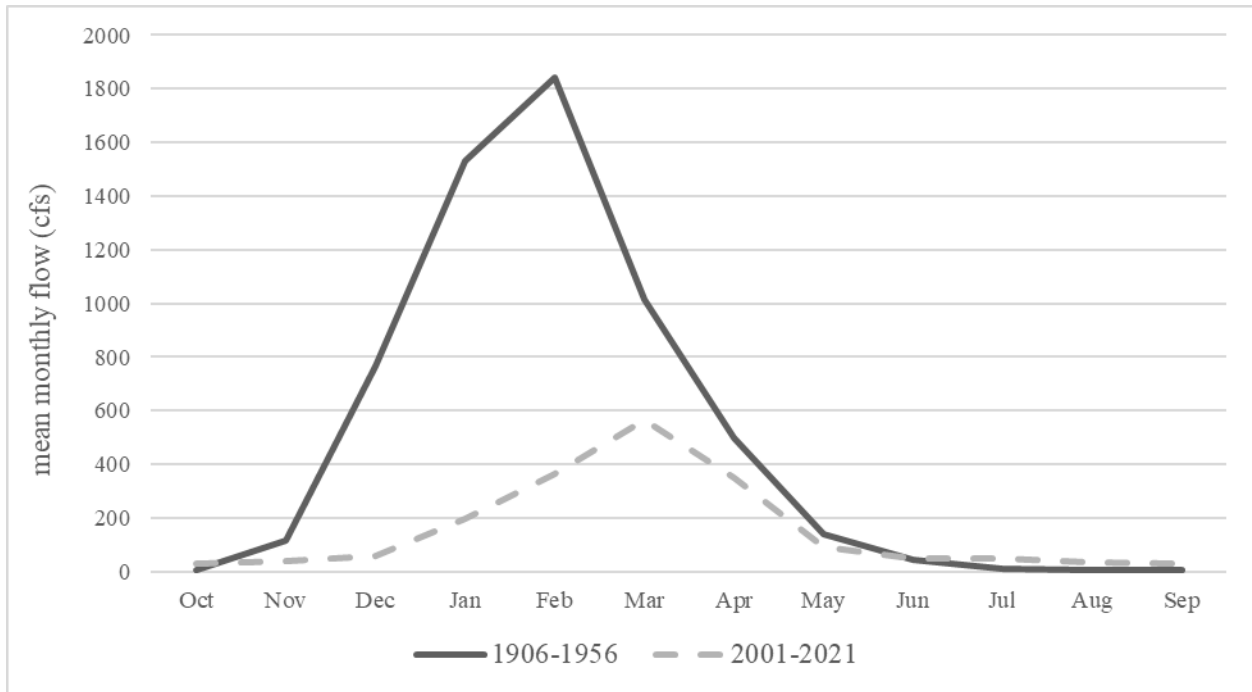


**Figure 1.2.** Pre- and post-dam average annual hydrographs for Lower Putah Creek. There was a major reduction in winter flows, minor increase in summer flows, and total average reduction in flow of 69%. Monthly average post-dam flow data was only available after 2000 (Bureau of Reclamation, 2023).

Nearly all of the land uses adjacent to the current channel are agricultural, including row crops, orchards, and flooded alfalfa, as well as rural residential, except for a 1.5-mi urban section along the north bank in the city of Winters. The watershed of Lower Putah Creek is primarily agricultural, with small portions of undeveloped grassland and oak woodland in the Dry Creek watershed, as well as a small area of developed land near and on the campus of the University of California (UC), Davis.

### **3. Methods**

#### **3.1 Flow frequency**

Annual peak streamflow tables for Lower Putah Creek were downloaded from the US Geological Survey (USGS) National Water Information System for gages 11454500 (water years 1906-1930) and 11454000 (water years 1931-2021) (USGS, 2023). These data were broken into two time periods: 1906-1956 (pre-dam, unregulated flow) and 1957-2021 (post-dam, regulated flow) and were analyzed using different flow frequency methods.

Unregulated flow can be analyzed using traditional, statistical methods since it is comprised entirely of stochasticity; regulated flow cannot be analyzed using traditional methods because the downstream flow is determined primarily by reservoir release schedules, not environmental stochasticity (Buchberger, 1980). Flow frequencies for the pre-dam, unregulated flow data (water years 1906-1956) were analyzed using the NRCS Frequency Curve Determination spreadsheet, which uses the Log-Pearson Type III regression, the standard unregulated (natural) flow regression formula recommended by the USGS (England et al., 2019; Yochum, 2017). This formula has been found to have the most appropriate mathematical fit for peak flow data (Interagency Committee on Water Data (IACWD), 1981), which do not fit a single statistical distribution. It has been used by federal agencies for unregulated flow modeling since 1967 (NRCS, 2015; U.S. Water Resources Council, Subcommittee on Hydrology, 1967). The mean in this model is approximately the 2-year peak discharge. Standard deviation is the slope of the line, and the regional skew is the curvature of the line (England et al., 2019; NRCS, 2015). The output from the spreadsheet is a logarithmic plot of the predictive curve and a readable table that can output a flow size for any recurrence interval, or vice versa.



There is currently no standardized guidance for modeling flow frequency for regulated rivers, even from U.S. resource agencies (England et al., 2019). Traditional statistical techniques cannot be used to calculate flow frequency for regulated systems, though some basic graphical techniques can be used to estimate a frequency curve (England et al., 2019; NRCS, 2015, 2007). The Log-Pearson type III curve can still be used as a rough estimator in some systems, but caution must be taken in interpreting the results due to the lack of an error estimate. In most regulated systems, a frequency curve is not necessarily useful because the discharges are determined by demand and reservoir operations, rather than by the stochastic natural processes that can be modeled in a frequency curve. Some researchers (e.g. Buchberger, 1980; Ergish, 2010; Lee et al., 2017; Tomic, 1998) have developed complex novel methods, some involving reservoir routing, to separate stochastic from deterministic components in flow frequency analyses for the purposes of reservoir management, and the US Army Corps of Engineers prescribes a complex method requiring watershed simulation in HEC-HMS (or a similar program) to create synthetic floods in order to develop an “unregulated” frequency curve from which to “subtract” the reservoir (regulated) output (Ayalew et al., 2013; “Hydrologic Frequency Analysis: EM 110-2-1415,” 1993). These methods were not used for the following reasons: (1) they are all time-intensive hydrologic routing methods and are beyond the scope of this project, (2) the required reservoir data were unavailable to the researchers, (3) results from this study are not likely to be used to manage reservoir outflows since they are fixed through the Putah Creek Accord, and (4) even the large post-dam recurrence interval flows in this system (e.g. 65-year flow) are not nearly large enough to cause flooding outside the levees or to damage infrastructure (Hosking and Wallis, 1997; Somach, 2000).

To estimate post-dam flow frequency, we used recurrence intervals of actual annual peak flow events using the Weibull plotting position formula (Interagency Committee on Water Data (IACWD), 1981), which is a simple, non-parametric method that can be used in regulated systems. We modeled peak flows for the 64 years of peak streamflow data that were available for the post-dam system. While this method does not calculate error, it has been used to roughly estimate the effects of damming on flow in large river systems by management agencies, such as the Bureau of Reclamation and California Department of Water Resources (Interagency Committee on Water Data (IACWD), 1981), and is appropriate for graphical comparisons. This formula may provide unreliable estimates at extremely high and low flood events, but is intuitive and simple. Since it is a non-predictive formula, it cannot return flow sizes for requested recurrence intervals; rather, it assigns each data point to a recurrence interval based on its rank and size relative to the other point values. The Weibull formula for flow frequency determination is:

$$\text{Probability exceedance} = m/(n+1)$$

Where:

n = sample size (number of years of peak streamflow records)

m = rank (peak streamflow record ranking from largest (e.g. 50) to smallest (1))

The peak streamflow data were ranked, then recurrence intervals and exceedance probabilities were calculated from these using the Weibull formula, and plotted. The complete tables are included as **Appendix Tables A.1** and **A.2**.

### 3.2 Geomorphology

Physical change in the channel was analyzed using a combination of digital elevation models (DEMs), HAR maps, and digital cross-sections. The study area boundary for all geomorphic calculations was determined using multiple factors: it includes up to the top of the incised channel for both time periods, capturing slight channel movement between time periods, but excludes government-built levees, bridge abutments, and other large constructed features that would have added unrelated material to the calculations (**Figure 1.3**). In this case, the main channel is different than, and contains, the much smaller baseflow channel.

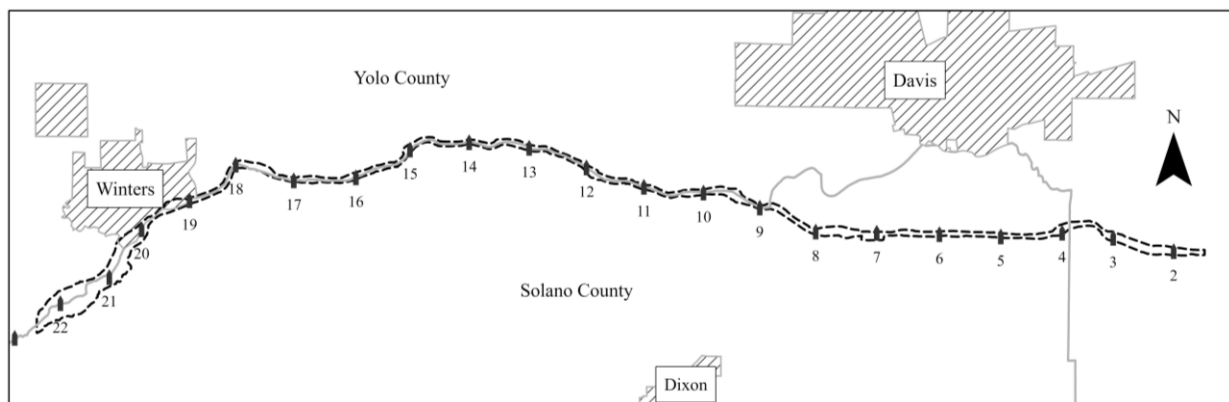


**Figure 1.3.** Study boundary. The study area is indicated by a dashed line, extends from river-mile 1.5 in the east to river-mile 22.5 in the west, and includes up to the top of the main channel of both the 1905 and 2005 DEMs (US Census Bureau, 2023).

The primary data required for geomorphic analyses were DEMs from a 2005 Solano County Water Agency (SCWA) aerial Light Detection and Ranging (LiDAR) survey, and a digitized 1905 USGS topographic survey. The LiDAR flight occurred on September 16<sup>th</sup>-18<sup>th</sup>, 2005, when streamflow was very low (20 cfs) (Bureau of Reclamation, 2023; Solano County Water Agency, 2005). The extent of the original post-dam LiDAR dataset includes the levees where levees exist and 300 feet on either side of the top-of-channel where levees do not exist.

In order to create the pre-dam elevation model, a set of historical 7.5-minute USGS topographic quadrangle maps from a survey in 1905 (**Figure 1.4**) were digitized into contour

lines, then converted into a DEM. The 7.5-minute quadrangles were downloaded as georegistered images (geoTIFFs) from the USGS National Map Viewer for the entire study area. Contour lines were manually digitized using a graphics tablet and converted to a DEM in ArcMap 10.3 (ESRI, 2020). The contour lines, surveyed at a five-foot contour interval, were traced using vector polylines, then converted to a raster, and run through the ArcGIS Focal Statistics tool, which smoothed the output to remove a stairstep surface created as a result of the conversion from contours to a DEM. The Focal Statistics tool settings were: circle sample shape, radius of six feet, and mean statistic. This radius smoothed the resulting elevation contours without noticeably modifying bottom-of-channel topography.

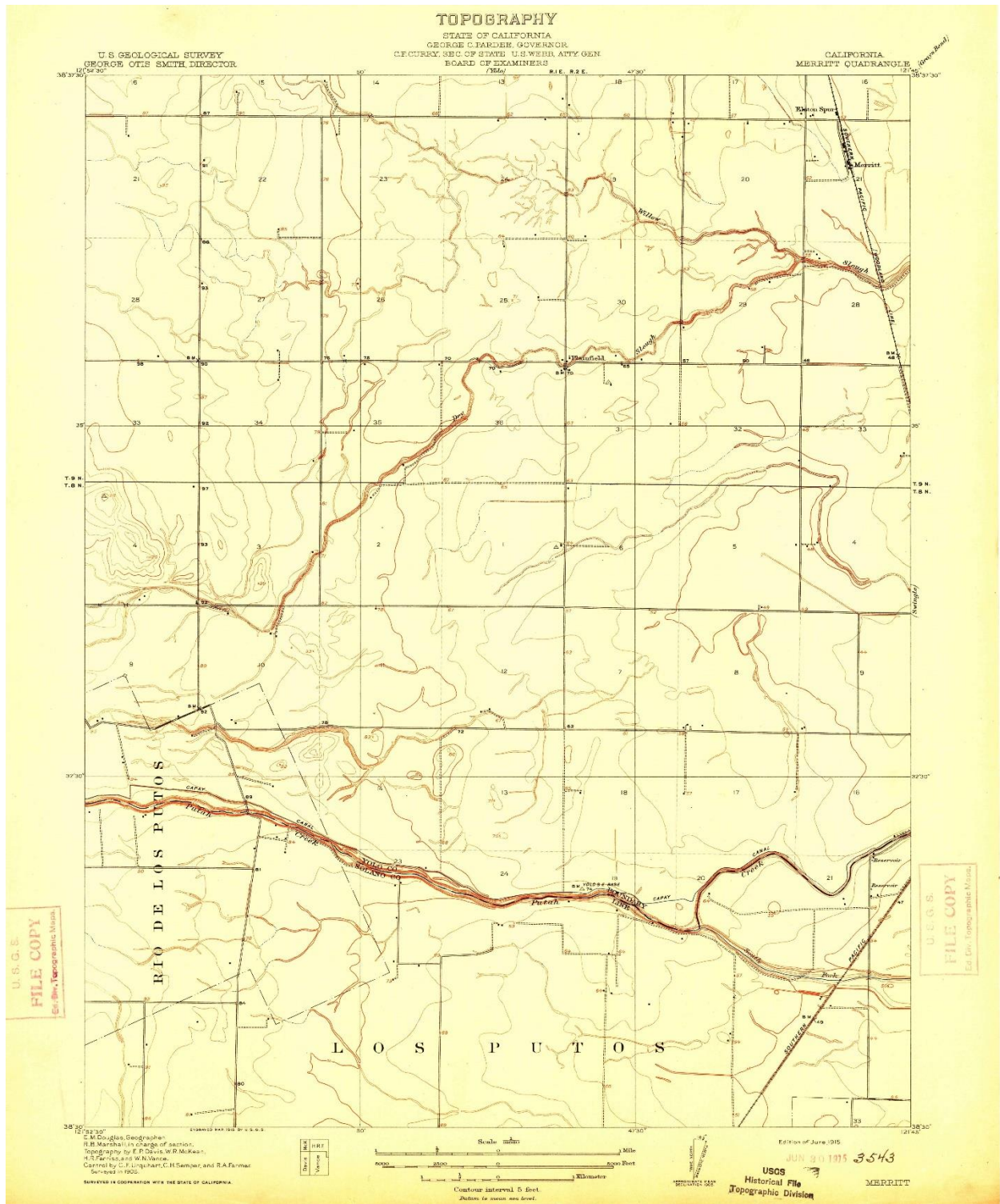


**Figure 1.4.** A 1905 USGS topographic quadrangle, Merritt, used in the study. Putah Creek is in the lower half of the map, and the Putah Creek fork is in the bottom right, showing the new channel (South Fork) breaking off from the old channel (North Fork), which bends north at a 90-degree angle. The contour interval is five feet.

In order to understand how the shape of the channel changed, the 1905 DEM was subtracted from the 2005 DEM in ArcGIS Pro 3.0 using the Spatial Analyst tool Raster Calculator. In order to determine system-wide net change in sediment volume, the ArcGIS Spatial Analyst tool Cut Fill was used to calculate the volume change in each cell between time periods. The Summary Statistics tool was used to sum the values of all cells in the study area.

Additionally, cross-sections were used to examine site-scale changes in geomorphology (i.e., channel incision) and explain larger patterns in the DEM and HAR analyses. These were created by identifying areas that are geomorphologically representative of a reach, as well as where the cross-sections could intersect the streamlines (digitized for the HAR model) at an appropriate perpendicular angle in both time periods. In all, 41 cross-sections were used to represent 22 miles of creek, or an average of 1.9 cross-sections per mile. After cross-sections were drawn as line features in ArcGIS Pro, elevation profiles were created from them using the Exploratory 3D Analysis Workflow, then exported as CSVs in order to create editable cross-sections in MS Excel. All cross-sections are in **Appendix Figure A.1**, with the respective cross-sections for the 1905 and 2005 datasets sharing the same graph, and a representative sample of the cross-section set is in the Results section.

To create the HAR rasters, first a stream raster for each time period was created using the inundation boundary from 1-D HEC-RAS (the Hydrologic Engineering Center's River Analysis System) (U.S. Army Corps of Engineers, 2023a) flow models. The terrain inputs were the 1905 and 2005 DEMs. The flow input for both models was the same (20 cfs), in order to create comparable baseflow river surfaces. While pre-dam Putah Creek was an ephemeral river that periodically dried up in most reaches from August-October, seasonal low-flows were comparable between pre-dam and post-dam flow regimes (Bureau of Reclamation, 2023; Harvey et al.,

1993). The pre-dam model had an average channel slope of 0.086% and used 245 representative digitally-created cross-sections placed an average of 472 ft apart. The post-dam model had an average channel slope of 0.083% and used 257 cross-sections placed an average of 433 ft apart. While cross-section placement is often determined case-by-case from individual surveyor opinion, placement in this study was based on an equation developed by Samuels (1990) and adopted for general use in 2-yr to 100-yr flood modeling (U.S. Army Corps of Engineers, 2023b). Due to the relatively barren channel in 1905, a Manning's  $n$  value of 0.025 was used, representing a clean channel with rocks and gentle turns; in the 2005 model, the Manning's  $n$  was 0.035, equivalent to a winding channel with rocks and some aquatic and riparian plants (England et al., 2019). The inundation boundary maps were converted to raster format for use in creating HAR rasters, though the original shapefiles were used later in the longitudinal analyses. Then, along with the DEM, the stream rasters were used as inputs in the HAR models (Dilts et al., 2010).

As a method, HAR can be accomplished several ways; this study used some of the procedure and the “riparian toolbox” from Tom Dilts’ ArcMap page (Dilts, 2015; Dilts et al., 2010). The respective DEM and stream features were used as inputs to the HAR model from the riparian toolbox in ArcGIS ModelBuilder, which calculates a distance-weighted average of river elevations using a kernel density function, such that cells close to the river receive a greater weight than those farther away. The kernel size (radius) affects the distance from the river that HAR can be mapped at, as well as the smoothness and detail of the output raster. Kernel size for this raster was set to 2,000 ft from the surface edge, since that was the minimum to contain the entire study area. Radii up to 3,000 ft were tested but there was no noticeable effect on the smoothness of the output raster. Next, the weighted average output was subtracted from the input

DEM to create the HAR map. This method can produce negative grid cells, which may or may not be real, depending on the study site. In this area, the negligible number of negative-value cells were converted to 0-ft relative elevation using the ArcGIS Con tool (conditional statement). The resulting rasters were then clipped to the study boundary. A sample of the HAR maps are shown in **Figure 1.5**.

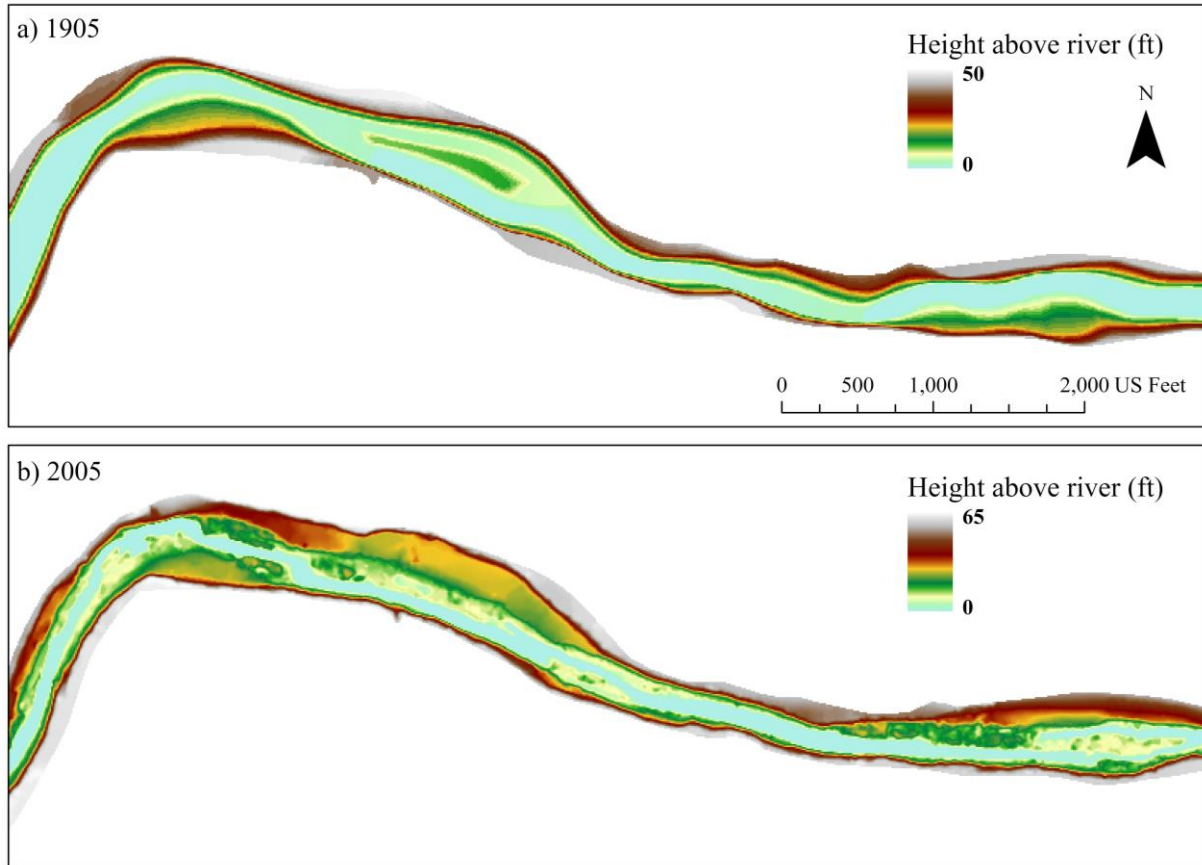


**Figure 1.5.** An example of the HAR maps. These show the HAR models at river-mile 17, just downstream of El Rio Villa, for (a) 1905 and (b) 2005. This comparison demonstrates that, between 1905 and 2005, the baseflow channel narrowed significantly.

In order to analyze geomorphic change along the entire creek without losing site-scale variation, two longitudinal analyses were conducted: width of the baseflow water surface and maximum depth of incision. These analyses used the same cross-sections and baseflow inundation surfaces from the HEC-RAS models used to create the HAR maps, because cross-



section spacing for those models was adequately resolute to capture local variation for baseflow width and incision depth, and they were perpendicular to the stream centerline (perpendicularity is important for calculating baseflow width). For baseflow depth, cross-sections were clipped to the baseflow inundation boundary for each time period, and their length was plotted against river-miles. Note that river-miles were aligned with existing river-mile markers, and that river-miles begin with zero at the mouth of the river. For Putah Creek, the mouth of the river is beyond the eastern end of the study area, where Putah Creek meets the waters of the Yolo Bypass flood control channel (previously known as the Putah Sinks), so river-miles run east-to-west (**Figure 1.1**).

For maximum incision depth, the 1905 channel elevation values were subtracted from the 2005 values, and the output was plotted against river-miles. The cross-sections from the 2005 HEC-RAS model were used (not clipped to the baseflow inundation surface), because maximum incision is not dependent on being perpendicular to the stream centerline, and only representative samples were necessary. The cross-sections were run through the ArcGIS 3D Analyst tool Add Surface Information on both DEMs, to attribute each cross-section with the minimum z value along the cross-section for both time periods. For additional graphical context, the thalweg elevation profiles of the 1905 and 2005 DEMs were extracted using the Exploratory 3D Analysis tool and plotted together against river-miles.

## **4. Results**

### **4.1 Flow frequency**

Annual peak streamflow in the post-dam system is less than the pre-dam system by at least 82% for all recurrence intervals. While the Weibull table outputs are only estimates, the reduction in flow in the post-dam river is relatively consistent across recurrence intervals, from

82-86%, with an exception for 2-year flows, which have been reduced by 96% (**Table 1.1, Figure 1.6**).

The shape of the post-dam Weibull plot is similar to the shape of the pre-dam Log-Pearson plot, although lower in magnitude by at least a factor of five, which accounts for the reduction in annual peak streamflow as a result of the dam (**Figure 1.7**). In the pre-dam flow frequency model, all but four of the 51 data points are within two standard deviations of the curve, (see 5% and 95% confidence bounds in **Figure 1.7a**), and those four are only just outside the second standard deviation. This is an acceptable level of error in flow frequency analyses, especially since most of the error is created by sampling or measurement error of the flow events (England et al., 2019; NRCS, 2015), not the calculations themselves. Also, agency guidance is to retain outliers since they represent real events (Yochum, 2017), though no outliers were detected in the calculations. The curvature of the line, showing a weighted skew coefficient of -0.49, is gentle and can be interpreted as a small amount of regional climatic influence on the size of large peak flow events relative to small events; according to guidance, weighted skew beyond -2.00 or +3.00 indicates the data need revision (Yochum, 2017) or fitting to a different distribution formula. The Weibull plotting formula for the post-dam system has no error estimate since it is a non-parametric formula, and again, most error would lie in measurements rather than calculations.

**Table 1.1.** Flow frequency values for selected recurrence intervals. Post-dam flows are shown as a percentage of pre-dam flows.

Flow Frequency	pre-dam (cfs)	post-dam (cfs)	pre-dam % of pre-dam
1-yr	2,540	368	14%
2-yr	24,548	906	4%
5-yr	46,376	6,580	14%
10-yr	62,398	8,800	14%
22-yr	80,606	14,800	18%
33-yr	90,239	16,300	18%
65-yr	106,284	18,700	18%

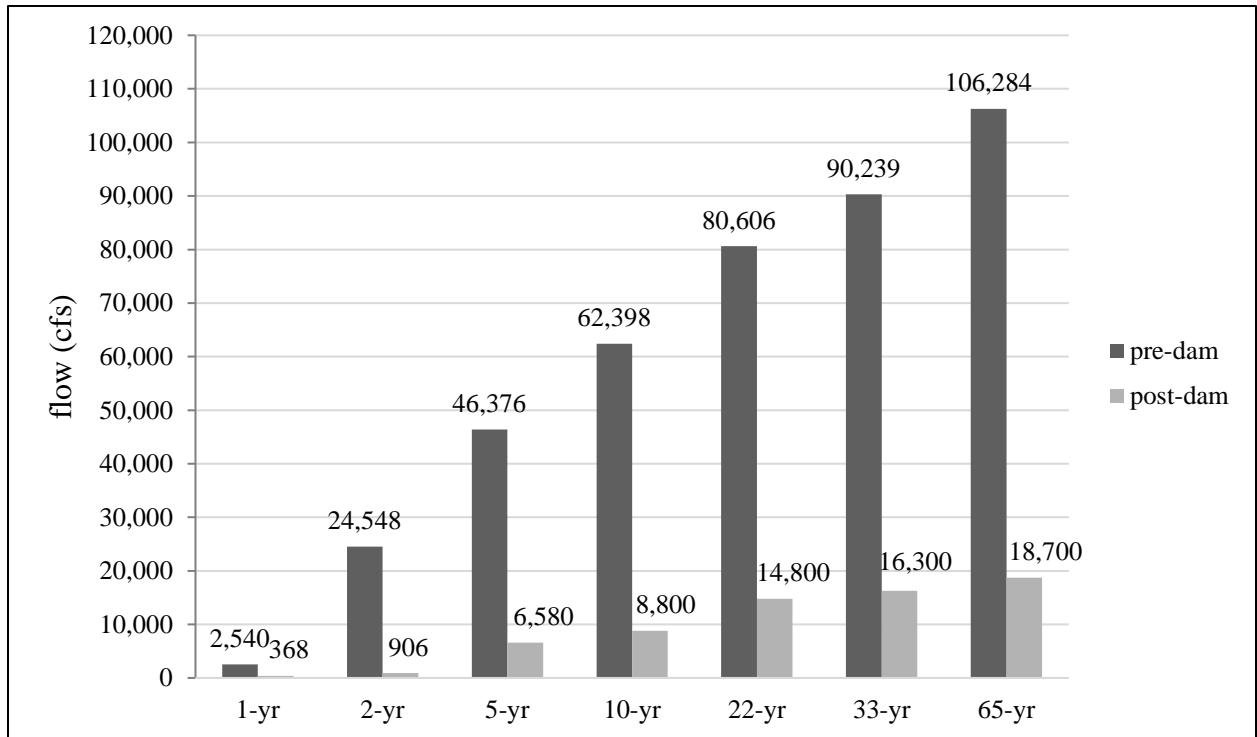


**Figure 1.6.** Flow frequency values for selected recurrence intervals in pre-dam and post-dam. Post-dam peak flows are between five and twenty-five times smaller than pre-dam flows.

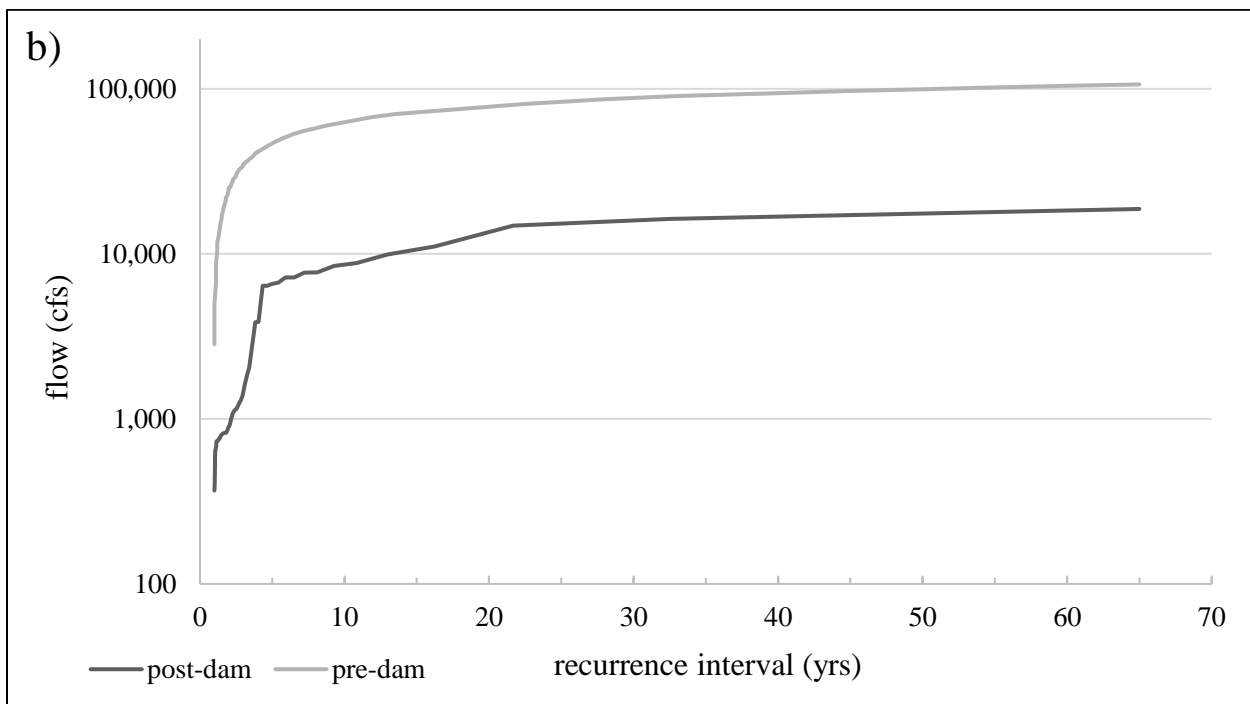
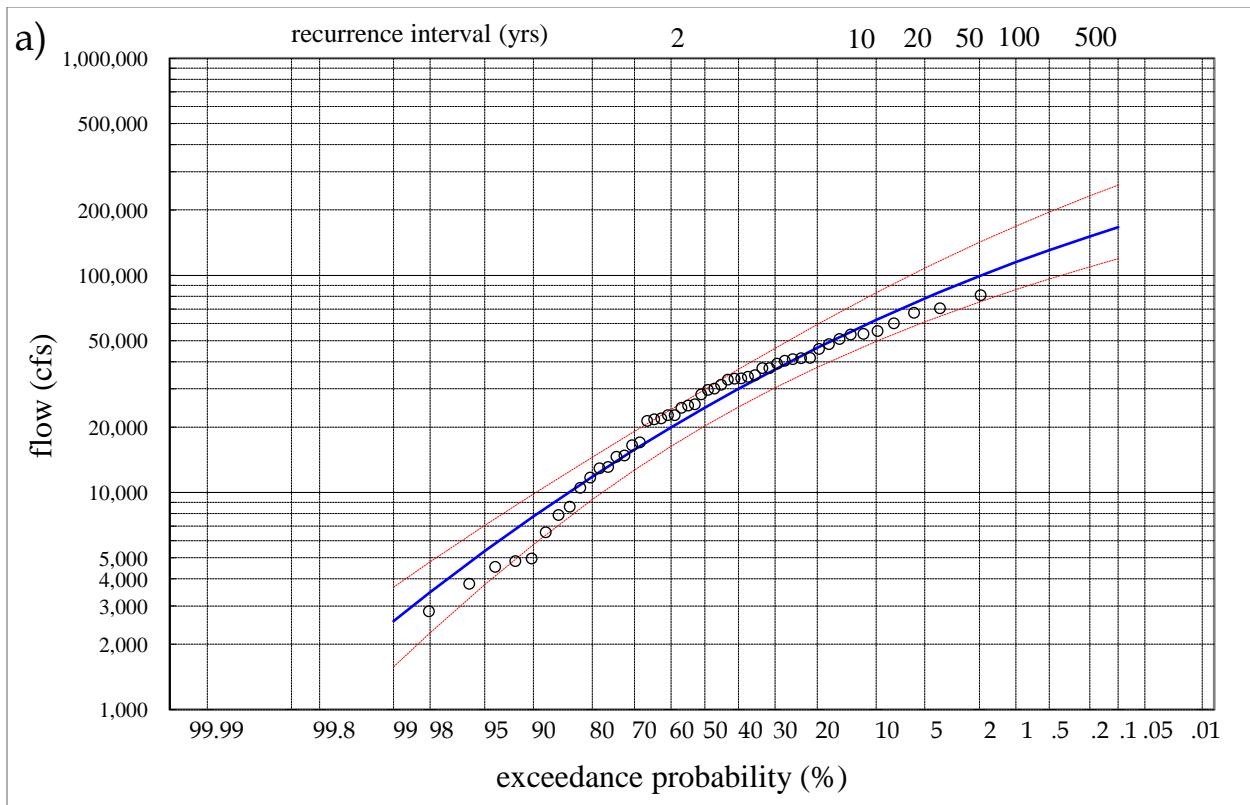


**Figure 1.7.** Flow frequency curves for pre-dam and post-dam. (a) Log-Pearson Type III flow frequency curve for pre-dam, created using the outputs from the NRCS worksheet; and (b) comparison of flow frequency curves for the pre-dam flow regime, created using the Log-Pearson Type III formula, and post-dam flow regime, created using the Weibull plotting formula.

## 4.2 Geomorphology

Visual examination of the DEM subtraction between the two time periods over the 22 miles of Lower Putah Creek reveals most areas of gained material (aggradation) are on the top of the banks, while most areas of lost material (incision or degradation) are in the bottom of the channel, although there was some reach-scale variation (**Figure 1.8**). The output from the cut-fill analysis, which calculated net change in the volume of material, was 470,786 cubic yards of sediment lost between the pre-dam and post-dam systems.

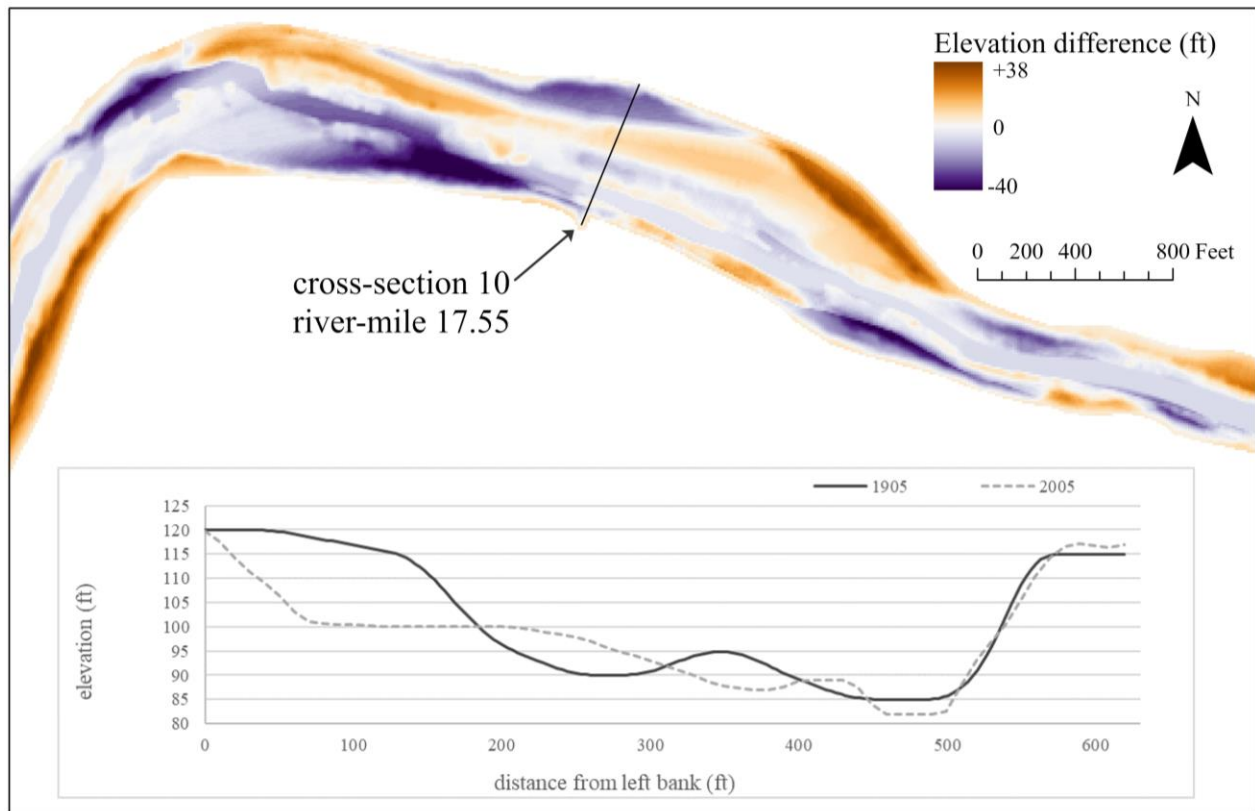


**Figure 1.8.** DEM subtraction map and accompanying 1905 and 2005 cross-sections at river-mile 17. Purple indicates material lost from 1905 to 2005; orange indicates material gained from 1905 to 2005. The cross-section shows exaggeration in the z dimension to characterize local topographic change.

The distribution of area by HAR indicates a generalized picture of change across all 22 miles of creek. Similar to the HAR visual analysis, the histogram shows lost material in the

bottom-of-channel along most of the length of the creek (**Figure 1.9**). This finding is corroborated by the cross-sections (**Figure 1.10**), which show that the 2005 channel is more V-shaped and contains a narrow, deeper baseflow channel, whereas the U-shaped 1905 channel bottom was flat and wide.

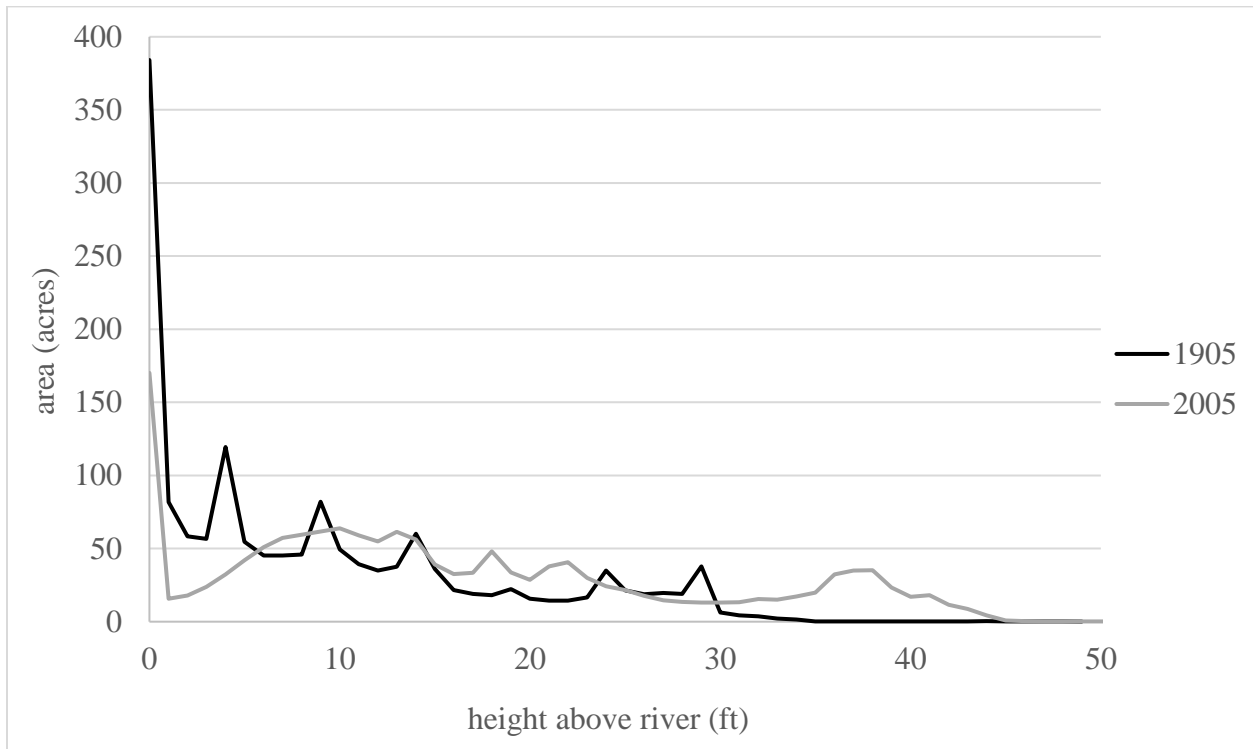


**Figure 1.9.** The distribution of area by HAR for 1905 and 2005. Two significant findings are visible: (1) the 2005 channel has significantly more area above 35-ft HAR, indicating the 1905 channel was much shallower than the 2005 channel; and (2) there is significantly more low-HAR area in 1905 than in 2005, indicating the 1905 channel had a flatter, wider channel bottom. These results indicate significant downward incision and baseflow narrowing.

The longitudinal analysis of baseflow (20 cfs) surface width shows a 49% decrease in average width, from 108 ft in 1905 to 54.8 ft in 2005, and a decrease in width along almost the entire creek, though there is significant site-scale variation in the magnitude and direction of change (**Figure 1.11a**). The resolution of measurements shows some patterns in channel width that may allow for identification of anthropogenic geomorphic modification, including dredging. The longitudinal analysis of maximum incision depth shows an average incision of 8.5 ft and a

maximum of 17 ft, with incision occurring along the entire channel except for a short section from river-mi 17.14 to river-mi 17.21, where the incision was 0 ft (**Figure 1.11b**). Incision was highly variable but patterned by reach, as indicated by local changes in slope, which differed between 1905 and 2005 (**Figure 1.12**). Incision was greatest from approximately river-mi 7.5 to river-mi 15.5, and in general, incision was much greater downstream of river-mi 16 than upstream of that point. The regularly-spaced peaks and valleys in **Figure 1.11b** are explained by the stairstep pattern of the 1905 DEM, an artefact of the 1905 five-foot contour interval (**Figure 1.12**).

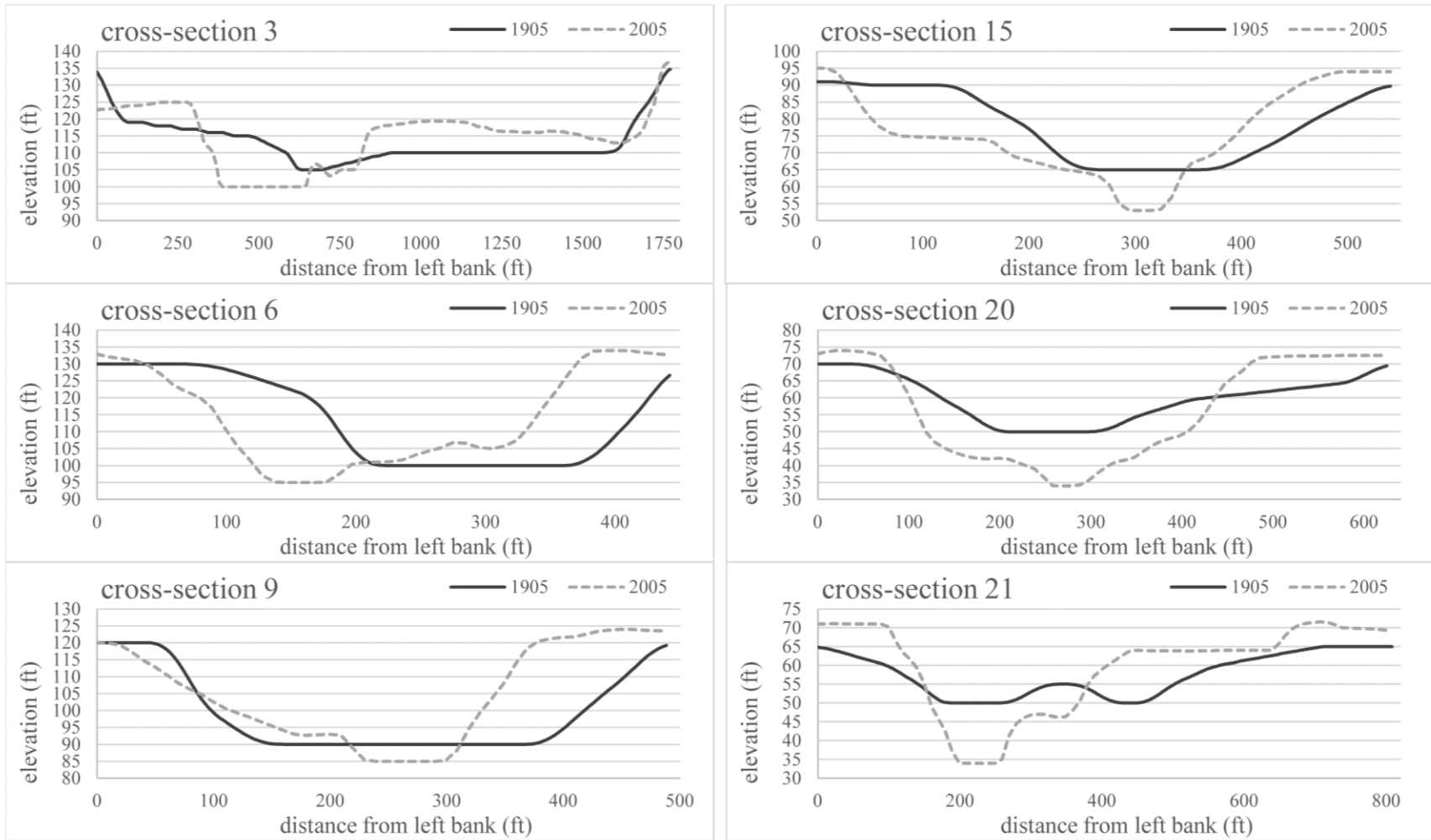


**Figure 1.10.** Cross-sections sampled from the 41 representative cross-sections in **Appendix Figure A.1**. These plots show incision of the baseflow channel along the entire creek, with variable magnitude by location. In general, the 2005 channel banks are steeper and the baseflow channel has narrowed. Figure continued on next page as **Figure 1.10b**.



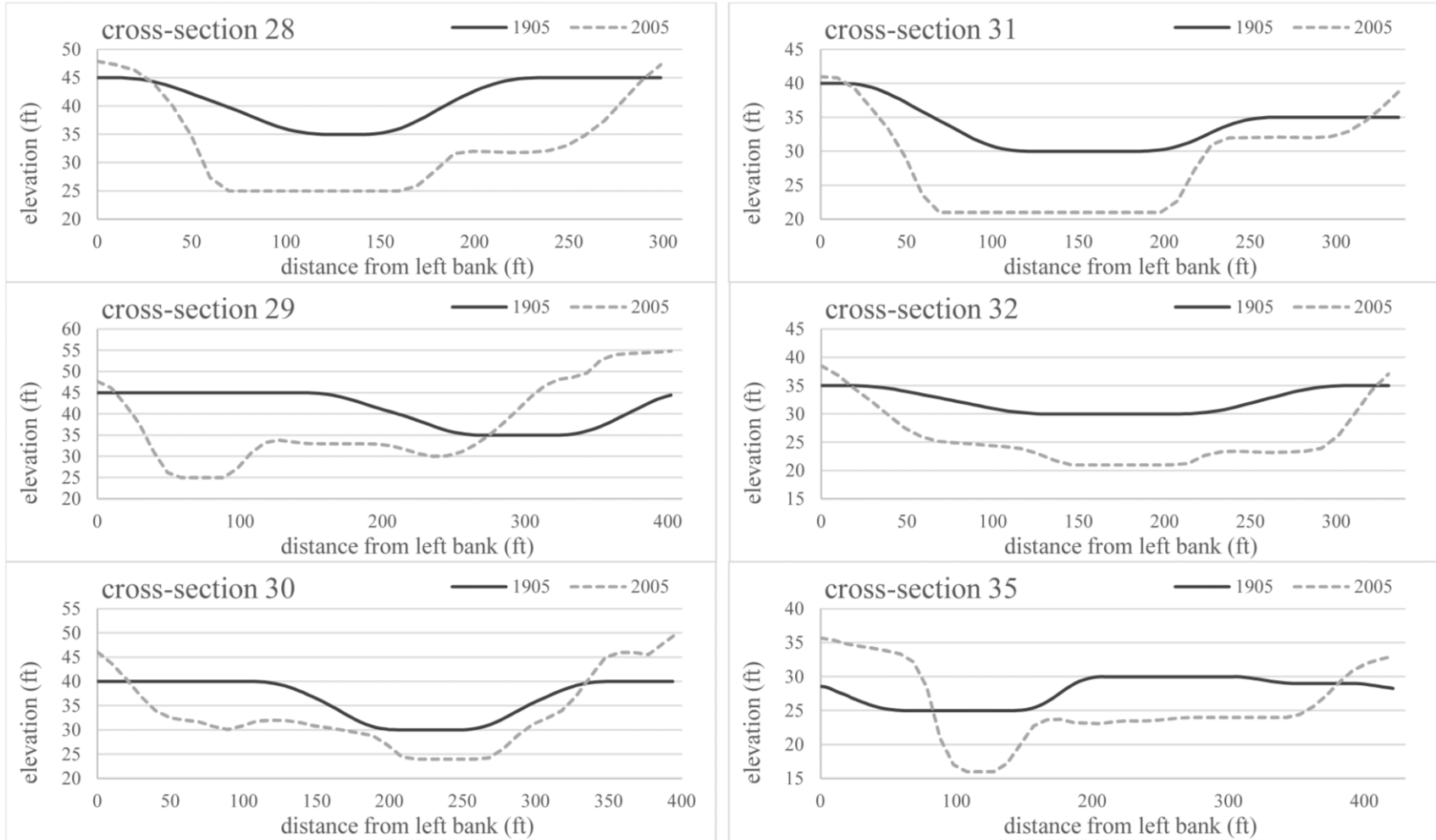


**Figure 1.10b.** Cross-sections sampled from the 41 representative cross-sections in **Appendix Figure A.1**. These plots show incision of the baseflow channel along the entire creek, with variable magnitude by location. In general, the 2005 channel banks are steeper and the baseflow channel has narrowed.

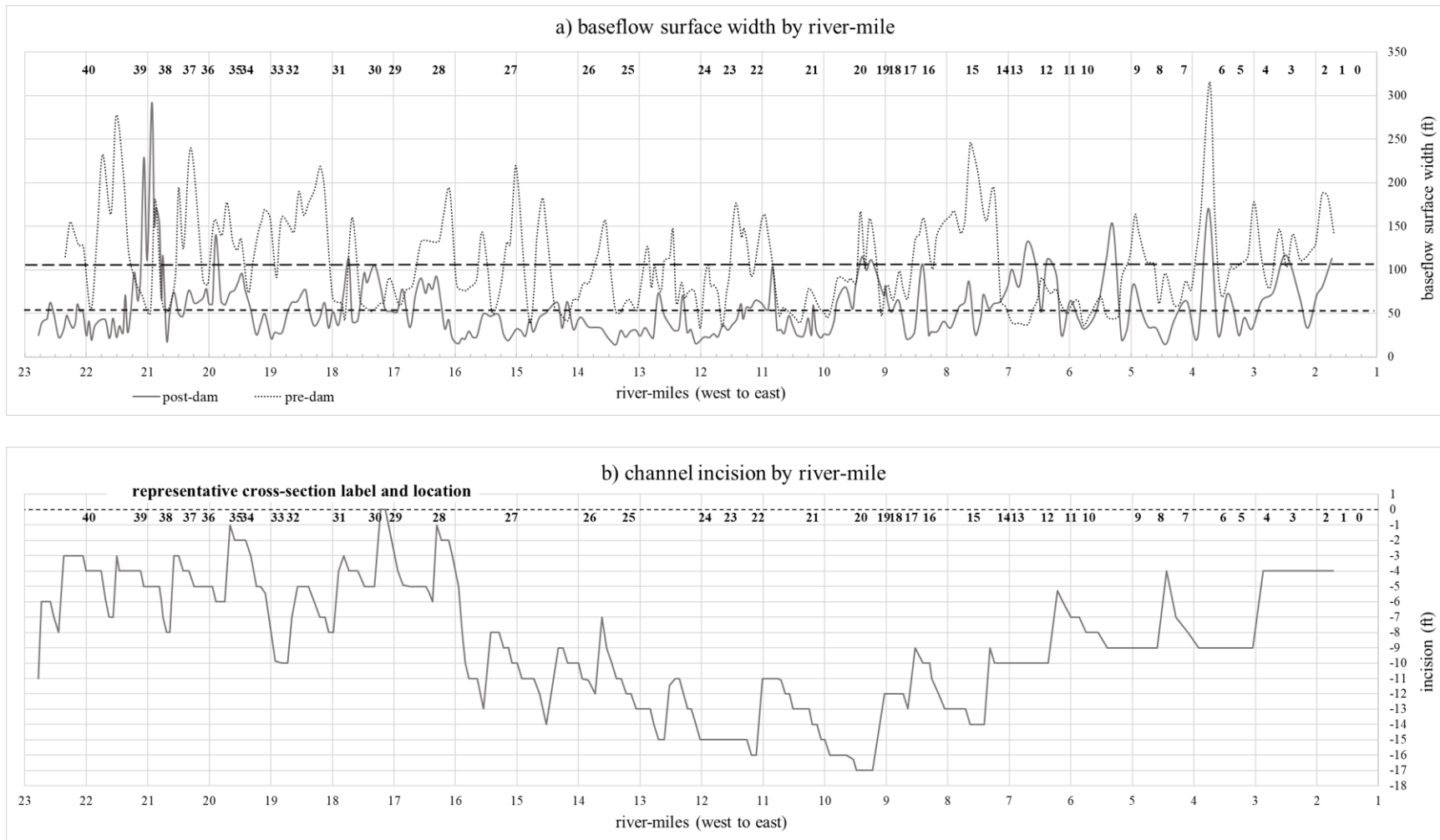


**Figure 1.11.** Longitudinal plots by river-mile. The 41 representative cross-sections are labeled at the top of each plot for reference, indicating: (a) baseflow river surface width for pre-dam and post-dam, as well as mean values for width (dashed lines), and (b) maximum channel incision between pre-dam and post-dam (dotted line indicates zero incision); the dashed line here indicates zero incision.

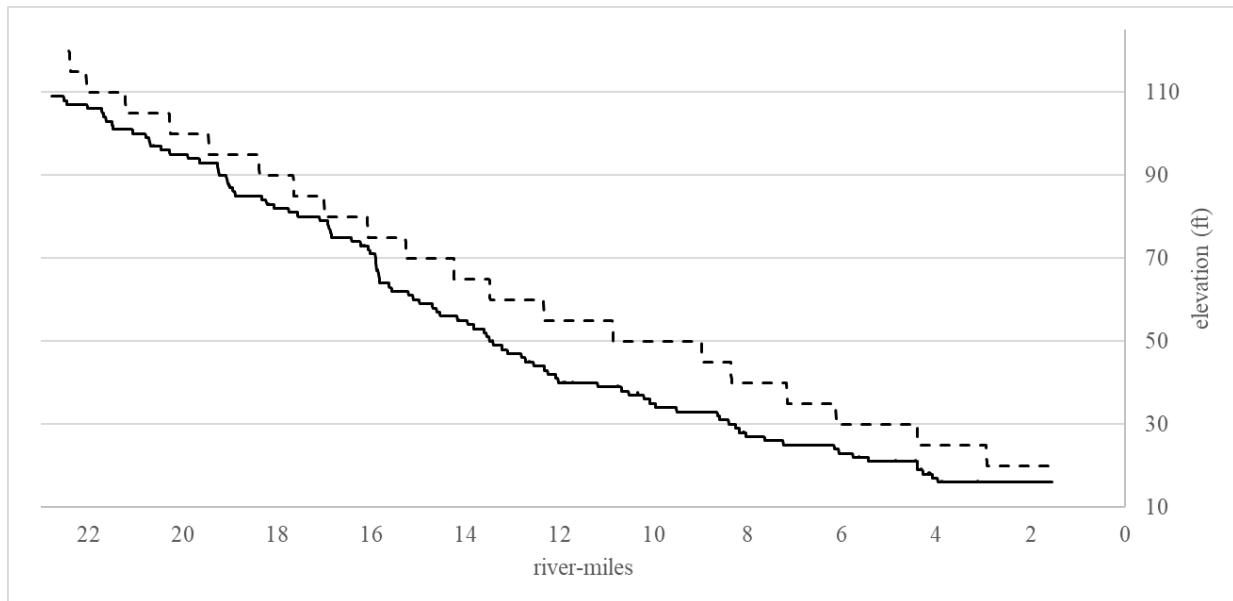


**Figure 1.12.** Thalweg elevation profiles for 1905 (dashed line) and 2005 (solid line). There was incision along the entire creek except for a very short section at river-mile 17.14, where the incision was 0 ft. The staircase pattern in the 1905 profile is an artefact of the 1905 five-foot contour interval.

## 5. Discussion

### 5.1 Flow frequency

Dam construction on Putah Creek caused a predictable reduction in peak streamflows across recurrence interval sizes. While dams are constructed for a variety of reasons and do not always cause a large reduction in peak flow events (Magilligan and Nislow, 2005; Petts and Gurnell, 2005), Monticello Dam and Putah Diversion Dam were built to provide irrigation and drinking water, and it is unsurprising that the dams detain the bulk of water from large storms, providing flood protection to urban and agricultural areas downstream.

In the pre-dam system, the 65-year flow (106,284 cfs) was large enough to flood farms in the floodplains several miles from the banks of the creek (Vaught, 2007). In the post-dam system, the 65-year flow is just 18,700 cfs, and very safely contained within the banks of the incised channel. In fact, the post-dam 65-year flow is smaller than the pre-dam five-year flow of

24,548 cfs; the post-dam five-year flow is just 6,580 cfs. The difference in these flows represents a considerable difference in stream power to shape the channel and transport material (Larsen et al., 2006). In the post-dam system, large, scouring flows are absent, and sediment-transporting flows occur with much less frequency, although the flow regime has apparently been powerful enough to incise over 470,000 cubic yards of material. In Putah Creek, this massive reduction in peak flow may have enabled the encroachment of riparian vegetation within the banks of the channel (Northrup, 1965; Schumm, 1969).

It can be expected that to meet water demands under projected future climate change (Griffin and Anchukaitis, 2014; Ullrich et al., 2018), even a greater peak flow volume and total annual volume will be held back or diverted from Lower Putah Creek. In California, periodic droughts are part of the historical interannual hydrograph, although due to climate change, they have become more common and will continue to worsen (Griffin and Anchukaitis, 2014; Ullrich et al., 2018). In the last twenty years, California has experienced multiple prolonged droughts, where reservoir levels reached critically low levels. During the succeeding normal or wet years, in the absence of required peak flow schedules, reservoir managers are more likely to detain as much water as possible in order to rebuild storage. Smaller peak flows will influence slow but significant cumulative changes to channel dynamics and vegetation communities along the river, and it will be very challenging to predict the extent and pace of those changes.

## **5.1 Geomorphology**

The large net negative change in material between 1905 and 2005 is likely because the Monticello and Putah Diversion dams have cut off any significant sediment supply into Lower Putah Creek (the only remaining source is small, ephemeral Dry Creek), and localized dredging or in-stream gravel mining took place as late as the 1970s (P. Moyle, personal communication,

2018). This sediment load has been documented in aerial imagery studies after large storm events (Sommer et al., 2008). Other studies have confirmed that large dams in the Sacramento River Watershed (Folsom, Oroville, and Englebright dams) have aggraded sediment on the order of many millions of cubic yards from their construction in the mid-1900s to 2000, a factor that has likely contributed to a reduction in sediment yield of 50% from the Sacramento River to the Bay-Delta (Wright and Schoellhamer, 2004). The factors affecting sediment load and deposition in each reservoir are different, and studies (e.g. Harrison et al., 2000; Solano County Water Agency, 2014) have documented large volumes of aggradation in Lake Solano and the Putah South Canal (likely a result of severe downcutting in Pleasants Creek, which occurred as a result of the regulated flow regime on Putah Creek (R. Marovich, personal communication, 2018)), but almost no sediment deposition in Lake Berryessa (Solano County Water Agency, 2014). Between dam construction in 1957 and 2012, approximately 425,000 cubic yards of sediment were aggraded in Lake Solano, reducing the storage capacity of the reservoir by 43%. This suggests that the large volume of material lost in Putah Creek below the dams could be at least partly due to scouring without the historical sediment input, which may have been provided by the historical flow regime.

However, the HAR histogram (**Figure 1.9**) shows a more complicated change in geomorphology than system-wide channel degradation. While bottom-of-channel changes, including deepening and a narrower baseflow channel, are the result of incision and dredging, there is a consistent pattern indicating gained material along the top-of-bank that is most likely the result of agricultural landowners pushing material into the channel to extend field size or create small levees, although it is also possible that dredging or scraping of the channel in the early 1900s (but after 1905) moved material from the bottom of the channel to the top of the

banks (Vaught, 2007). This can be observed in not only the significant increase in area above 32 ft HAR compared to pre-dam, but also in the DEM subtraction in areas shown in orange along the upper banks in **Figure 1.8**, and in most of the cross-sections, as indicated by small mounds in the elevation profile at the top-of-bank in 2005 but not 1905 (**Figure 1.10, Appendix Figure A.1**). It is possible that the net change in channel material was influenced by not only the geomorphic effects of the dam and dredging, but also by creek-side landowner operations, which have been extensive throughout the agricultural development of the area from the 1840s to the present (Grismer, 2018; Lower Putah Creek Coordinating Committee, 2005; Rubin, 1988; Vaught, 2007).

Longitudinal analyses confirmed substantial sediment degradation in the channel and may help identify areas of possible dredging, as well as areas that might be in greatest need of geomorphic restoration. A bathymetric survey from around the same time as the 2005 LiDAR mapping showed significant degradation in the middle reach of the creek (i.e., roughly river-miles 16-6), where there are very few sections of riffle sequences and mostly long, deep pools (Yates, 2003). This reach had significant incision (**Figure 1.11b, Figure 1.12**), and hosts multiple known dredging, or gravel mining, sites (P. Moyle, personal communication, 2018). The average narrowing of the baseflow surface width by 49% corroborates our finding from the HAR analysis, which shows a change from a U-shaped to a V-shaped channel topography. The channel incision also corroborates the HAR findings of significant deepening along nearly the entire creek, and which could account for the large net loss in sediment volume.

Some areas of the baseflow inundation surface (river-miles 3.5-4, 4.5-5.2, 7.5-8.8, 9.5-10.7, 18.5-19.9) seem to have narrowed in a pattern consistent with even degradation laterally across the channel; we hypothesize that this pattern indicates narrowing by flow incision rather

than dredging (**Figure 1.11**). Areas of the surface that widened (river-miles 5.2-5.6, 6.2-7.2, 17.3-17.6, 20.8-21.2), which are inconsistent with the channel becoming V-shaped, we hypothesize indicates a dredged morphology. However, areas of the greatest incision could more strongly indicate dredging, especially since incision was highly variable. When comparing the entire longitudinal incision plot to the entire baseflow surface plot, the reach with the greatest incision (river-miles 7.5-15.5) aligns with the reach where the baseflow surface showed the least change (river-miles 8.5-13.5) (**Figure 1.11**), suggesting an artificial vertical removal of sediment, rather than a more even lateral downcutting. This reach was also known to have been dredged extensively by UC Davis to mine aggregate to construct campus roads and buildings as late as the 1970s (P. Moyle, personal communication, 2018). A more in-depth examination of longitudinal plots and all 257 post-dam cross-sections could identify reaches that might serve as appropriate reference sites for geomorphic restoration or rehabilitation. In rivers of the Central Valley, restoration of the channel and vegetation would likely utilize a topo-sequence of riparian vegetation (e.g. Conard et al., 1980) according to HAR and modeled flow inundation surfaces. On Lower Putah Creek, these would be reaches with shallow sloped channel banks and a wide floodplain, which under the regulated flow regime would increase the riparian zone and be better able to support a more dynamic riparian ecosystem (**Figure 1.13**).

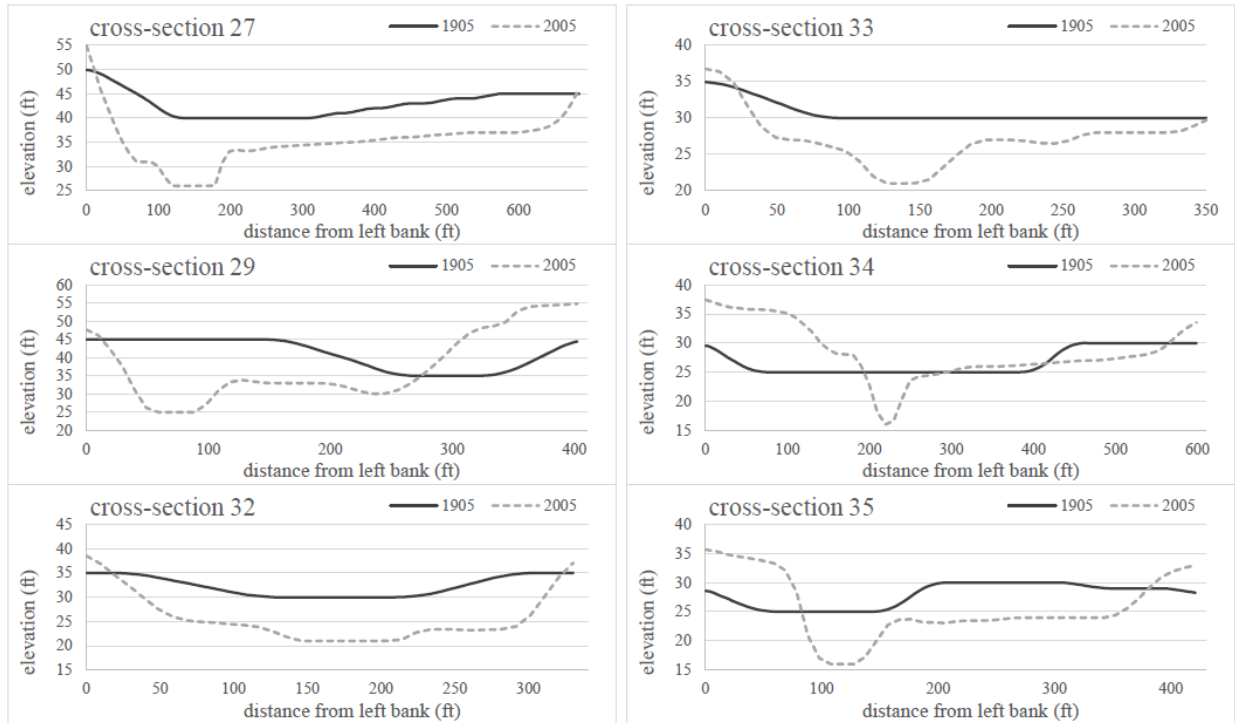


**Figure 1.13.** Cross-sections that could serve as reference sites for geomorphic restoration. While there is significant incision in these cross-sections, they have a relatively narrow (<50 ft.) and shallow (<7 ft.) baseflow channel as well as relatively wide floodplains with gentle gradients, requiring only minor geomorphic modification for restoration compared to other areas.

Finally, an additional geomorphic modification not accounted for in this study is the construction of small check dams along Putah Creek by farmers in the first half of the 1900s, when their irrigated industrial crops rapidly depleted groundwater basins in Solano County. Groundwater depletion was one of the primary motivations for damming Putah Creek (Rubin, 1988). In order to identify dredged sites with greater confidence, individual cross-sections should be reviewed reach-by-reach.

## 6. Conclusion

This study demonstrates the effectiveness of HAR as a tool for analyzing geomorphic change over time in river systems. It provided valuable census statistics and was able to be completed through straightforward GIS workflows. Combined with a DEM subtraction,



representative cross-sections, longitudinal analyses, and flow frequency analyses, HAR characterized multiple types of human-induced geomorphic changes, which are corroborated by historical documentation. Additionally, using multiple analyses in conjunction provides important perspectives into the way Lower Putah Creek changed over a century. This study highlights how challenging it can be to characterize intensely modified rivers, but also the importance of studying modified systems to establish new baseline conditions, identify causes of change, and develop methods for restoration or rehabilitation.

HAR is an underutilized tool in river restoration practice, including for channel and planting design, and the framework now exists for managers to use it (Bair et al., 2021; Greco et al., 2008). It will be important to continue updating and making publicly available reliable HAR workflows, including some that may analyze the relationships between HAR and other variables, for science and industry.

## **Chapter 2 Modeling pre- and post-dam geomorphological drivers of riparian vegetation distribution using machine learning imagery classification on a California coast range river**

### **Highlights**

- Between dam construction in 1957 and 2009, land cover primarily transitioned to woody vegetation with 31% woody cover in 1937 to 69% woody cover in 2009
- Between 1937 and 2009, 57% of the study area shifted cover type, and of that, 75% was a shift from barren and herbaceous to woody vegetation
- Random forest-based classification models on both the pre-dam and post-dam datasets consistently assigned nearly identical importance to the three explanatory variables: height above river, bank slope, and distance to baseflow surface
- The amount of steep bank slopes increased between 1937 and 2009 across the study area due to channel deepening and narrowing through incision; in 1937 the vast majority of the vegetated area was found on bank slopes shallower than 18% (10 degrees) and in 2009 steep slopes >14-18% (8-10 degrees) are dominated by woody cover, indicating compression of the riparian zone
- Support vector machine, a machine learning tool, effectively classified both historical and modern imagery

### **Abstract**

Quantifying land cover change can inform watershed management and stream restoration. Recently, new tools in statistics and geographic information systems (GIS) have made it possible to not only better quantify riparian vegetation change but to more clearly

determine the drivers of change. Machine learning algorithms have been used for several decades to identify the most important explanatory variables in a wide array of sciences, including land cover classification. While some frameworks have recently been proposed for machine learning image classification in riparian systems, no such frameworks exist for studying the downstream effects of flow regulation. In this study, support vector machine (SVM) was used to classify vegetation cover types in the riparian zone of Lower Putah Creek, California, from 1937 aerial photographs taken before the construction of Monticello Dam (1957) and 2009 aerial imagery. Random forest-based classification was used to try to identify the importance of three topographic variables: height above river (HAR); bank slope; and distance to baseflow surface in determining cover type. Classification results support findings from previous studies in post-dam creeks, where a regulated flow regime enables longer-term plant succession and establishment of woody vegetation, though we were not able to determine the extent to which this finding is a result of flow regulation or vegetation recovery following razing of the vegetation in the 1800s. While woody vegetation increased in cover significantly across the site, its downward tracking of channel incision showed compression of the riparian zone. Random forest classification identified each of the three topographic variables as equally important predictors of cover type. Analysis of the distribution of cover types by topography effectively characterized vegetation change and allowed for a useful comparison between pre- and post-dam states, underscoring the importance of basic descriptive metrics in historical ecology when attempting to identify patterns of change.

## **Keywords**

GIS, random forests, image classification, historical aerial photographs, aerial imagery, NAIP, height above river, geomorphology, flow regulation, dams, historical reconstructions, historical ecology, landscape change, machine learning

## **1. Introduction**

Historical reconstructions are critical to the effective management of ecosystems because they can characterize baseline conditions, identify the drivers of change, and inform predictive models of future change (Eitzel et al., 2016; Lydersen and Collins, 2018; Swetnam et al., 1999; Whipple et al., 2011). They often require multiple lines of scientific study, which enhance the usefulness of research findings (Beller et al., 2017; Grossinger and Askevold, 2012; Sanderson, 2009) and cultural awareness (Crumley, 1994). Knowing pre-modification conditions can be essential to restoring any ecosystem, whether by form, function, or evolution. In fact, nearly a quarter of all historical ecology studies have provided recommendations that diverged from existing management prescriptions (Beller et al., 2020), indicating they provide useful context to ecosystem managers.

Until the last 15 years, historical reconstructions were focused on describing historical conditions to inform management and restoration in a more traditional sense (Anderson, 2001; O'Brien, 2001; Swetnam et al., 1999), as well as the direction and magnitude of change over time. Due to several factors, including the urgency of climate change and advancements in statistical tools, researchers have recently focused on identifying the drivers of landscape change (Fertel et al., 2023; Whipple et al., 2011), not just the type of change. This often involves applying statistical tools to identify the most important explanatory variables (Fertel et al., 2023;

Solins et al., 2018) and how scale affects the ecological relationships being studied (Eitzel et al., 2016). Due to this change, there has been a shift from traditional methods in historical ecology, such as field surveying and analysis of written records, to big data and machine learning, including spatially extensive analyses of entire landscapes (Beller et al., 2017, 2020; Crumley, 2021; Salazar Loor and Fdez-Arroyabe, 2019).

The new tools can be useful for land cover classification of historical conditions, where machine learning methods like support vector machine (SVM) or random forests can classify large areas quickly and accurately, especially compared to manual digitizing. Historical aerial photographs and modern aerial imagery together provide an excellent opportunity to analyze change over time across entire landscapes (Rango et al., 2008) using machine learning. Many studies have already used machine learning for image classification (Sheykhmousa et al., 2020), including with historical aerial photos, and there even exist some frameworks for the use of remote sensing to study change in river systems (Huylbroeck et al., 2020; Piégay et al., 2020a; Tomsett and Leyland, 2019). However, there have been few studies using historical and modern image classification to study the downstream effects of flow regulation on riparian vegetation (Greco and Plant, 2003; Han et al., 2020; Poff and Hart, 2002); most studies still rely on field data (Li et al., 2012; Mallik and Richardson, 2009). While there exist powerful, comprehensive tools to study hydrologic alteration (e.g. IHA (Richter et al., 1996)), they usually require extensive datasets on dozens of variables, unavailable in most medium-to-small ecosystems. To date, no studies have yet analyzed landscape-scale vegetation change on Putah Creek, in Northern California, despite its importance to the ecology and human society of the state's Central Valley (Kelley, 1989; Larkey, 1969; Moyle, 2014; Moyle et al., 1998; Vaught, 2007). Since only 8.7% (approximately 226,000 acres as of 2003) of Central Valley riparian forests and

wetlands remain from pre-European settlement (Geographical Information Center, 2003; Roberts et al., 1980; Thompson, 1961), it is important that studies of these systems help inform their conservation.

Information about the type, magnitude, and drivers of vegetation change in rivers can inform their management, such as changes to environmental flow regimes, and both passive and active restoration. Topographic variables affecting vegetation distribution in riparian systems include height above river (HAR) (Dilts, 2015; Fremier and Talley, 2009; Greco et al., 2008; Teversham, 1973; Vaghti et al., 2009), channel geometry (e.g., bank slope and channel slope) (Hupp and Osterkamp, 1985; Parker and Bendix, 1996; Swanson et al., 1988), and distance to baseflow water/surface (Fremier and Talley, 2009; Lite et al., 2005; McCarthy, 2006; Stromberg et al., 1996). HAR and distance to baseflow surface differ in that HAR assumes either a consistent connection with groundwater regardless of the distance from the baseflow surface water and/or that HAR is associated with flow regimes that directly affect vegetation distribution; on the other hand, distance to baseflow surface can be a useful predictor if the groundwater elevation or soil moisture (as represented by HAR) changes with increasing distance from the baseflow surface (Tsheboeng, 2018). Since these three variables (HAR, bank slope, and distance to baseflow surface) were readily available at high resolution for both pre-dam and post-dam, they were chosen here as explanatory variables for land cover type.

In this study, historical and modern topography and imagery datasets were used to address three objectives:

- Characterize the type, magnitude, and distribution of vegetation change between the pre-dam and post-dam states of Lower Putah Creek;

- Use machine learning to identify the possible topographic drivers of vegetation change; and
- Demonstrate the effectiveness of topographic variables, including HAR, bank slope, and distance to baseflow surface, in characterizing vegetation change.

## 2. Study Area

Putah Creek is an ephemeral, semi-arid river and one of the lowest elevation tributaries to the Sacramento River in Northern California. It is situated in a Mediterranean climate, with cool, wet winters and warm, dry summers. While the upper watershed has historically averaged (1980-2010) about 30 inches of precipitation annually, the lower watershed has averaged just 17 inches annually (UC Berkeley GeoData Repository, 2023). Putah Creek is part of the Putah-Cache bioregion (Thayer, 2003) and connects the wetlands of the Yolo Basin with the mountains of the Northern Coast Range. Nearly all of the surrounding landscape in the Central Valley portion of the stream outside of its banks has been converted to agricultural and urban cover (**Figure 1.1** in Chapter 1). Nearly all of the upper watershed, including the inter-dam reach, remains undeveloped and uncultivated.

Before U.S. and Mexican settlers occupied the region starting in the 1800s and forcibly removed or displaced the indigenous inhabitants through disease, a riparian forest two miles wide straddled the banks of Lower Putah Creek (Thompson, 1961; Vaught, 2007), beyond which oak savannahs and dense valley oak woodlands covered the Putah Creek and Cache Creek alluvial plains (Conard et al., 1980; Geographical Information Center, 2003; Holmes and Nelson, 1915; Tuil, 2019). In the lower reaches of Putah Creek, from what is now the South Fork that flows to the Yolo Bypass, which contains the area that used to be the Putah Sinks, vast wetlands

and wet grasslands formed the upper end of the Sacramento-San Joaquin Delta, making year-round human habitation and winter travel impossible (Conard et al., 1980; Griggs, 2009; Lower Putah Creek Coordinating Committee, 2005; Roberts et al., 1980; Vaught, 2007). Indeed, while Native Americans settled much of California starting around 11,000-13,000 years ago, they did not settle the Putah Creek area until about 2,500-1,500 years ago, perhaps due to the challenging and volatile seasons (Vaught, 2007). They managed this landscape, including the riparian forest, sustainably to enhance food and material productivity (Anderson, 1993), until the vast majority of them were forced into missions or died from diseases brought from white settlers, and their traditional way of life ended by the 1830s (Stevens and Ryan, 1997).

The contemporary vegetation along the Putah Creek channel consists of a mix of riparian forest, which can be classified using the California Wildlife Habitat Relationship system (California Department of Fish and Wildlife, 2023) as valley foothill riparian (VRI) on floodplains, willow scrub (also VRI) on sand bars, and valley oak woodland (VOW) and annual grassland/forbland (PGS; also known as California prairie) on upper terraces. These types correspond to the toposequence of Central Valley riparian vegetation characterized by Conard et al. (1980). Putah Creek's extensive riparian forest was largely razed by early European settlers starting in the 1840s, and channelization started in the 1870s (Vaught, 2007), beginning with small-scale damming in the early 1900s and subsequent large-scale damming in 1957. Other geomorphic modifications, such as aggregate dredging, occurred as late as the 1970s (P. Moyle, personal communication, 2018).

Due to the shape of the watershed (**Figure 1.1** in Chapter 1) and the geomorphology of Putah Creek, which is heavily incised (see Chapter 1), 98% of the volume of water received in the watershed is regulated by the dams. Less than 30% of the water that falls in the watershed



flows into Lower Putah Creek. While a legal agreement stipulates minimum regulatory flows and periodic ecological flows for salmon migration (Jacinto et al., 2023; Somach, 2000), there is currently no regulation for floodplain enhancement flows. Flood attenuation in Putah Creek led to not only changes in geomorphology, but also vegetation, which have not yet been characterized.

### **3. Methods**

#### **3.1 Creating imagery mosaics**

Historical aerial photographs for the 1937 flight (**Figure 2.1**) were downloaded from the FrameFinder tool on the University of California, Santa Barbara, library website. This flight took place from August 20-28, 1937, at an altitude of 13,750 ft and a scale of 1:20,000, with front overlap of 60% and side overlap of 20%. Each photograph's scanned resolution is 0.7 cm/pixel. This aerial photography, which documented more than 90% of the agricultural land in the U.S. from 1937-1941, was done by the Works Progress Administration and USDA Farm Service Agency to verify compliance with the way New Deal funds were spent (Monmonier, 2002). Since then, it has been used for land-use and conservation planning (Monmonier, 2002), environmental health assessment (Maxwell et al., 2010), and historical ecology and environmental history research (Ma et al., 2020; Weems, 2011).



**Figure 2.1.** Black and white 1937 aerial photograph for a section of Lower Putah Creek. Here, the river flows freely through the area in the lower left that in 1957 would become impounded by Putah Diversion Dam. The city of Winters, CA, is in the upper right. Surface water is visible in some areas of the channel, including in the mid-lower center and mid-lower center-left of the image, appearing as smooth-edged, dark objects against bright, barren material and more textured, woody vegetation. While surface water was often not visible in the driest months of the year pre-dam, complex connections with groundwater may have helped maintain flow in dry reaches during these months (Grismer, 2018).

The imagery was orthomosaicked in photogrammetry software Pix 4D 4.8 with full keypoints to maximize output integrity, and all other settings on default. Due to the wide variation in contrast between individual photos, Pix 4D created two partial orthomosaics in the output, each with slightly different brightnesses. To correct this, both orthomosaics were georeferenced in ArcGIS Pro 3.1 to current basemap aerial imagery, then color-balanced and

merged in remote sensing software ENVI 5.0, then georeferenced in ArcGIS Pro again as one orthomosaic. To georeference the file, link points were chosen based on common features between the 1937 mosaic and current aerial imagery (basemap), such as old building corners, the center of signature oak trees, old bridges, street corners, and town monuments. The spline method was used for rectification in order to allow the greatest degree of alignment (Tobias et al., 2021). Approximately 100 control points were used in each of two georeferencing processes. The output georeferenced orthomosaic has a pixel resolution of 8.8 ft (**Figure 2.2**) and was clipped to the study area boundary.

Aerial imagery for the post-dam system was downloaded from USGS EarthExplorer and consisted of National Agriculture Imagery Program (NAIP) (USDA, 2023) aerial imagery tiles for June 7, 2009, with a resolution of one meter. This date was chosen because it was the last imagery collected before a one-mile reach of creek was geomorphologically restored and replanted near the city of Winters as Winters Putah Creek Nature Park. Flow on the day of the NAIP imagery was 43 cubic feet per second (cfs), which has a very similar footprint to the flow modeled in the HAR analyses (20 cfs) (see Chapter 1); flow was entirely contained within the banks of the baseflow channel. In ArcGIS Pro, these tiles were color balanced in a mosaic dataset, mosaicked into one raster (**Figure 2.2**), then clipped to the study boundary. This chapter used the same study boundary used in Chapter 1 (**Figure 1.3**): it only includes up to the top-of-channel for both time periods since all of the surrounding land has been converted to agricultural and urban cover. No native plant communities connected to the flowing portion of Lower Putah Creek exist outside of the study boundary except for a 75-acre restored oak woodland adjacent to the channel at river-mile 3.0.



**Figure 2.2.** Mosaicked aerial imagery for 1937 (top) and 2009 (bottom). These maps show the 1937 and 2009 mosaics for the same reach of creek shown in **Figure 2.1**. For the purposes of this study, cover types clipped out of each dataset include: crops, developed areas, and water.

### **3.2 Support vector machine (SVM) imagery classification**

In order to remove irrelevant land classes from the imagery, manually-digitized polygons were used to mask out water, crops, roads, buildings, and any other built-up cover in the imagery rasters. While it is acceptable to use machine learning methods to classify any land cover, developed cover types were removed in order to have a more ecologically appropriate random forest classification later (Eitzel et al., 2016; Fertel et al., 2023; Lydersen and Collins, 2018). This also ensured that both image classification analyses used the same input data. From the 1,550-acre study boundary, 250 acres of water, buildings, roads, and cropland were removed from the 1937 imagery for classification; the final 1937 raster area was 1,300 acres. In the 2009 imagery, 487 acres were removed; the final 2009 raster area was 1,074 acres.

Image classification was performed in ArcGIS Pro using Imagery Classification tools. The Training Samples Manager was used to collect polygon training features across three cover classes: woody, herbaceous, and barren. Due to the low contrast of the 1937 black and white aerial photographs, it was not possible to classify any finer than this. For the 1937 imagery, between 50 and 75 training samples were taken for each class by one person in one sitting to avoid bias. For the 2009 imagery, the same procedure was used but between 50 and 120 samples were used for each class due to the greater variety of colors in the imagery.

In ArcGIS Pro, the machine-learning tool Classify was used to run supervised, pixel-based classifications on both datasets. For both 1937 and 2009 imagery, support vector machine was selected as the classifier used in later geomorphic analyses because it had the highest accuracy over other supervised methods. Two other classifiers, random trees (different from random forests) and maximum likelihood, delivered similar results but slightly under-estimated

woody cover. One other classifier, K-Nearest Neighbor, under-estimated both woody and barren cover, to a greater degree than the next best methods.

Accuracy was assessed in both datasets using a similar method to Eitzel et al. (2016), using ground-truthed random points and a confusion matrix (Congalton and Green, 2008; Olofsson et al., 2014). In ArcGIS Pro, the Create Accuracy Assessment Points tool was used to create 50 random points in each class (150 points total), then ground truth values were entered manually by one person in one sitting to avoid bias. From this table, a confusion matrix was created to calculate accuracy.

To analyze class transitions between the pre-dam and post-dam classifications, the Change Detection workflow was used to create a cover type transition matrix. The output only includes the intersecting areas between 1937 and 2009, since the clipped areas (i.e., water, buildings, etc.) of each classification did not match; the output raster was 975 acres, smaller than both input rasters.

It is important to note that an analysis of just two time periods may only show limited dynamism, and uni-directional shifts are inferred from transitions between cover types. While not within the scope of this study, more time slices could be used to create a detailed transition matrix to characterize the pattern of land cover change since the dam was constructed; this could indicate to what degree the regulated flow regime, versus other factors, caused shifts in cover type. Another factor that would help characterize change is breaking up woody cover into three-to-four cover types, such as: shrub (willow), mixed riparian forest, and valley oak. This level of resolution was not possible with the 1937 imagery, but later aerial imagery sets have better contrast and are available in 15-20-year increments starting in 1957, the year the dam was

constructed. However, our objective was to compare pre- and post-dam vegetation patterns, so we retained the earlier imagery.

### **3.3 Random forest classification**

In addition to the support vector machine classification, which provided a more accurate classified raster output than the random forests classification, a random forest classification was performed to identify the importance of several geomorphological variables in determining vegetation distribution in each time period. While random forests (RF) have been shown to sometimes create superior classifications to SVM due to their ability to avoid overfitting (Ahmed K et al., 2013), SVM has been shown to outperform RF and other forms of decision trees in imagery classification where there are a small number of variables (Adam et al., 2014; Medina and Atehortua, 2019; Thanh Noi and Kappas, 2018). Here, the RF method was only used to identify variable importance.

In ArcGIS Pro, the Forest-based Classification and Regression tool was used with varying parameters to find the most accurate model. Models for both 1937 and 2009 were run with 5, 10, 50, 100, and 500 trees. In every run, 30% of the training data were saved for validation. Since this tool was used only to estimate variable importance, it was set to train only; outputs included a variable importance table and a confusion matrix.

### **3.4 Geomorphic analysis**

Topographic rasters for bank slope and distance to baseflow surface were created in ArcGIS Pro using the same digital elevation models (DEM) used in chapter one, and the HAR rasters from Chapter 1 were used here. The ArcGIS Pro tool Distance Accumulation was used to

create distance to baseflow surface rasters, and used the same 20-cfs baseflow inundation surface used in Chapter 1 for creating the HAR analyses. While HAR represents the vertical distance above the nearest water surface edge, distance to baseflow surface represents the three-dimensional distance, or surface distance. In this way, it might better represent the vegetation's connection to water than HAR since HAR does not account for horizontal distance to water.

To characterize vegetation cover according to geomorphological metrics, the mean and distribution of values in HAR, bank slope, and distance to baseflow surface of each class were calculated in the Zonal Statistics and Zonal Histogram tools in ArcGIS Pro. Outputs from Zonal Histogram were plotted in MS Excel.

### **3.5 Reach-scale analysis**

Land cover transitions and geomorphology were also analyzed by reach. Reaches were determined based on: (1) the extent of cover change (transition) between 1937 and 2009 and (2) significant changes and differences in channel geomorphology. The channel in the reach upstream of the city of Winters is significantly wider than the channel downstream of Winters, the middle reach from Winters to the South Fork is the most horizontally stable as well as the most incised (see Chapter 1), and the South Fork reach is an anthropogenic channel, created from scraping and subsequent downcutting (Vaught, 2007).

## **4. Results**

### **4.1 Creating imagery mosaics**

The 2009 NAIP tiles are a georeferenced product from the USGS, and generally have a georeferencing accuracy concurrent with their resolution; for these data, it is one meter, or a little



over three feet. There is no RMS error to report in creating the 1937 orthomosaic because the spline georectification method maximizes local accuracy; it does not produce RMS error, although georeferencing error may still be present farther away from control points. Within the study boundary, alignment between the 1937 and 2009 imagery was very good on visual inspection, from one foot to three feet. Outside the study boundary, alignment varied from one foot to five feet, depending on the distance from control points.

#### 4.2 Support vector machine (SVM) imagery classification

In the 1937 classification, 31% of the study was woody vegetation, 50% was herbaceous, and 19% was barren (**Table 2.1**). In the 2009 classification, 69% of the area was woody, 26% was herbaceous, and 5% was barren. **Figures 2.3a** and **2.3b** show a sample area of classified land cover in each time period.

**Table 2.1.** Total area in acres of each cover class in 1937 and 2009.

	<b>woody</b>	<b>barren</b>	<b>herbaceous</b>	<b>total (ac)</b>
<b>1937</b>	408.1	242.1	650.0	1300.2
<b>2009</b>	730.5	50.6	292.6	1073.7

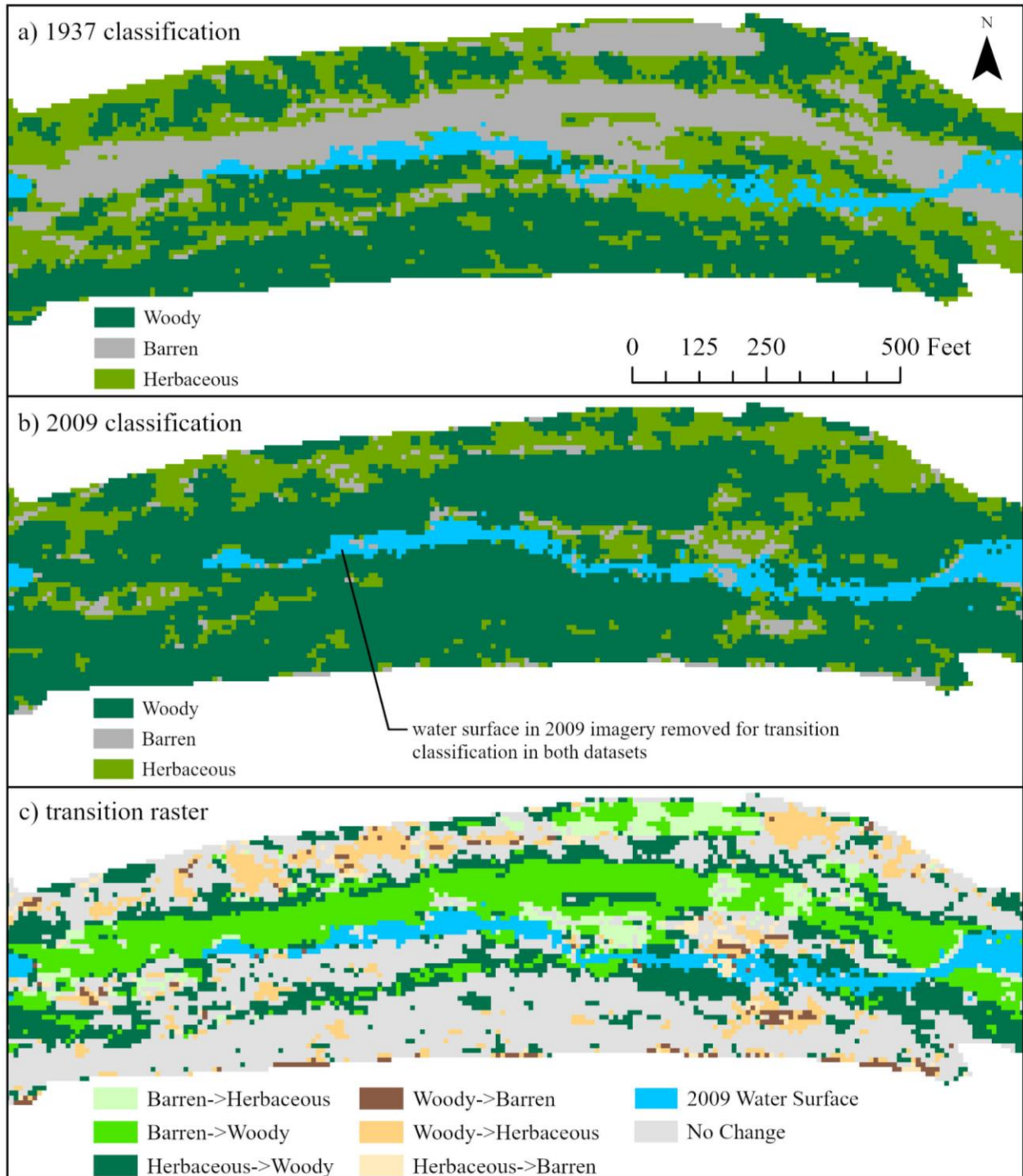


**Figure 2.3.** Classified imagery for 1937 and 2009 and the land cover transition map. At river-mile 10, classified imagery for (a) 1937 and (b) 2009 are distinctly different in the proportion of each cover type. The transition map (c) shows a clearly dominant conversion of barren and herbaceous to woody cover. This site is just east of Pedrick Road.

Transitions between cover types (**Table 2.2**) characterize the change in classes more finely than total change in cover. Woody cover primarily remained woody; a small amount transitioned to barren and a moderate amount to herbaceous. Barren cover was dynamic; it transitioned primarily to vegetation, especially to woody, and areas of barren in post-dam were made up more of transitions from vegetated areas than from originally-barren areas in 1937. Herbaceous cover was also dynamic; it transitioned primarily to woody, and some herbaceous areas became barren. Of the 975 acres in the transition overlay, 420 acres (43%) had no change in cover type. **Figure 2.3c** shows a sample of the class transition raster.

**Table 2.2.** Transition matrix for land cover change between 1937 and 2009. This table shows acres converted to each class using the intersection between 1937 and 2009 rasters. The 1937 classes are listed vertically; 2009 classes are listed horizontally. Of the 975 acres, 420 acres (43%) did not change cover type.

	<b>1937 woody</b>	<b>1937 barren</b>	<b>1937 herbaceous</b>	<b>Total in 1937 (ac)</b>
<b>2009 woody</b>	249.1 (25.5%)	7.9 (0.8%)	57.4 (5.9%)	314.4 (32.2%)
<b>2009 barren</b>	98.3 (10.1%)	5.8 (0.6%)	55.3 (5.7%)	159.4 (16.3%)
<b>2009 herbaceous</b>	314.3 (32.2%)	29.5 (3.0%)	158.0 (16.2%)	501.8 (51.5%)
<b>Total in 2009 (ac)</b>	661.7 (67.9%)	43.2 (4.4%)	270.7 (27.8%)	975.6 (100%)

Accuracy of the imagery classifications was estimated using transition matrices (**Table 2.3**) (Congalton and Green, 2008; Olofsson et al., 2014). In the 1937 analysis, the producer's accuracy (1 - omission error) was 98% for woody, 100% for barren, and 84% for herbaceous. The user's accuracy (1 - commission error) was 100% for woody, 82% for barren, and 98% for herbaceous. Overall accuracy was 93%, and Kappa, which takes into account the sampling distribution of each class, was 0.9. These values indicate a very good classification model, with accuracy typical of other SVM and random forest machine learning models (Sheykhmousa et al.,

2020), although a notable amount of herbaceous values were misclassified as barren, likely because their class ranges overlap in the intermediate bright values. In a grayscale image, a lack of variation can cause this issue.

In the 2009 analysis, the producer's accuracy was 93% for woody, 94% for barren, and 98% for herbaceous. The user's accuracy was 100% for woody, 94% for barren, and 90% for herbaceous. Overall accuracy was 95%, and Kappa was 0.92. These values also indicate a very good classification model, although a small amount of woody was misclassified as herbaceous and barren, and a small amount of woody and barren were misclassified as herbaceous. Likely, there was more mixed classification in this model than in the 1937 model due to the color variation (RGB) in this imagery; intermediate green values appear in all three classes.

**Table 2.3.** Confusion matrices for the SVM imagery classification for 1937 and 2009. For both (a) 1937 and (b) 2009 tables, the producer's accuracy (1 - omission error) is presented vertically and user's accuracy (1 - commission error) is presented horizontally. Kappa is reported in the bottom right.

a) 1937	woody	barren	herbaceous	total	user's accuracy	Kappa
woody	50	0	0	50	1.00	
barren	0	41	9	50	0.82	
herbaceous	1	0	49	50	0.98	
total	51	41	58	150		
producer's accuracy	0.98	1.00	0.84		0.93	
Kappa						

b) 2009	woody	barren	herbaceous	total	user's accuracy	Kappa
woody	50	0	0	50	1.00	
barren	2	47	1	50	0.94	
herbaceous	2	3	45	50	0.90	
total	54	50	46	150		
producer's accuracy	0.93	1.00	0.84		0.95	
Kappa						

### 4.3 Random forest classification

All random forest classification models on both the pre-dam and post-dam datasets consistently assigned nearly identical importance to the three explanatory variables (HAR, bank slope, and distance to baseflow surface), ranging from 33.1% to 33.5% each, indicating all variables had a nearly-equal influence on model accuracy when included or excluded from a decision tree.

Validation accuracy of the 1937 random forests imagery classification was very low to low, ranging from an average class accuracy of 47% with five trees to 65% with 500 trees. Accuracy of each class was within 2-5% of the average accuracy in each run. Because the SVM classification had much higher accuracy, it was used as the classified land cover raster in the geomorphic analysis.

#### **4.4 Geomorphic analysis**

The distribution of acreage of each land cover class in each time period was analyzed by height above river (**Figures 2.4, 2.5, and 2.6**), bank slope (**Figures 2.7 and 2.8**), and distance to baseflow surface (**Figures 2.9 and 2.10**). The distribution of vegetation by HAR changed only slightly between time periods. The mean HAR value of woody cover (**Table 2.4**), 7.7 ft, remained the same between time periods, barren cover barely changed, decreasing from 8.8 ft to 8.7 ft, and herbaceous cover increased slightly from 7.2 ft to 8.3 ft. It is important to note that HAR analyses from Chapter 1 found stream-wide incision between 1905 and 2005; since HAR is relative to the baseflow surface and not a fixed value (like elevation above mean sea level), a lack of significant change in vegetation distribution by HAR is not necessarily a sign of no change. Rather, it could mean the vegetation tracked, or filled in, area along the channel banks as the channel deepened.

The average bank slope of the three land cover types (**Table 2.4**) increased significantly between time periods, reducing the area in recruitment zones (i.e., Mahoney and Rood, 1998) and thus compressing habitat for some riparian vegetation (in low HAR zones). Woody cover increased in bank slope from 9.5% to 19.1% (5.4 degrees to 10.8 degrees), barren cover increased from 4.0% to 6.1% (2.3 degrees to 3.5 degrees), and herbaceous cover increased from

5.1% to 11.4% (2.9 degrees to 6.5 degrees). Distance to baseflow surface changed notably between time periods. The average distance to baseflow surface edge for woody cover increased from 107 ft to 134 ft, barren cover decreased from 235 ft to 233 ft, and herbaceous increased from 160 ft to 216 ft.

The standard deviation (SD) for all values is large, representing a wide dispersion in values from the means. For most metrics, when the standard deviation is larger than the mean there is large dispersion in one direction (i.e., larger HAR, greater distance, steeper slope); the data are generally right-skewed but the bulk of values are found closer to the channel (horizontally and vertically) on shallower slopes.

**Table 2.4.** Mean and standard deviation of each geomorphic variable for each cover type in 1937 and 2009. Standard deviation is shown in parentheses. Units are reported in feet.

	<b>1937 barren</b>	<b>2009 barren</b>	<b>1937 herb.</b>	<b>2009 herb.</b>	<b>1937 woody</b>	<b>2009 woody</b>
<b>HAR mean (SD)</b>	8.8 (7.8)	8.7 (12.5)	7.2 (7.7)	8.3 (11.3)	7.7 (9.2)	7.7 (10.3)
<b>Slope mean in degrees (SD)</b>	2.3 (3.7)	3.5 (4.9)	2.9 (4.6)	6.5 (8.2)	5.4 (6.5)	10.8 (9.8)
<b>Distance to baseflow surface mean (SD)</b>	235 (254)	233 (168)	160 (177)	216 (160)	107 (142)	134 (142)

Plotted alongside the distribution of HAR values for context, there are significant differences in the spatial patterns and extents of vegetation pre- and post-dam. Herbaceous cover dominates in pre-dam, while woody cover dominates in post-dam, however, woody cover is distributed much less evenly post-dam compared to pre-dam, primarily occupying zones from two ft HAR to 20 ft HAR. Finally, there is much less barren cover across the entire HAR gradient post-dam.

There are also some similarities between periods: woody cover is distributed in noticeable amounts along the entire HAR gradient in both time periods, and there is a notable

amount of vegetation cover in the 0-ft HAR zone in both time periods (though the proportion of classes varies between periods), showing vegetation occupying areas at baseflow surface level outside the channel or—in the case of woody cover—hanging over the water surface. While this finding seems to contradict the fact that woody cover increased in distance to baseflow surface, it might be explained by two facts: woody vegetation filled in across the entire study area, not just in low HAR and distance to baseflow areas, and the values of distance to baseflow surface (values in the distance raster itself) increased post-dam because the channel deepened (Chapter 1), essentially increasing the actual distance (x-y-z) from the water of most values in the study area.

Proportional cover of each class by HAR differed significantly between time periods, and relationships plotted in **Figure 2.4** and **Figure 2.5** help characterize the zonation or gradient of each class. In 1937, the distribution of each cover type was much more evenly apportioned in low HAR areas than in 2009, though it is clear that in 1937 herbaceous dominated zones below 15 ft HAR and woody dominated zones above 15 ft HAR. In 2009, woody cover dominates all but the highest (i.e., above 44 ft) HAR zones, and especially those in the first 15 ft HAR.



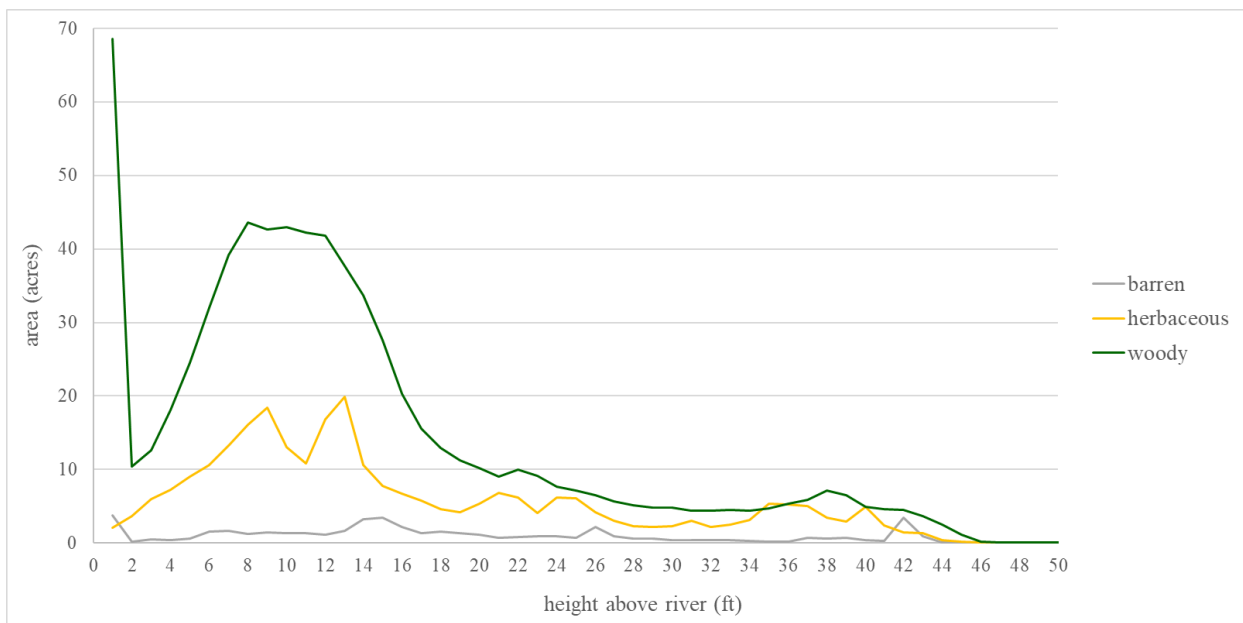
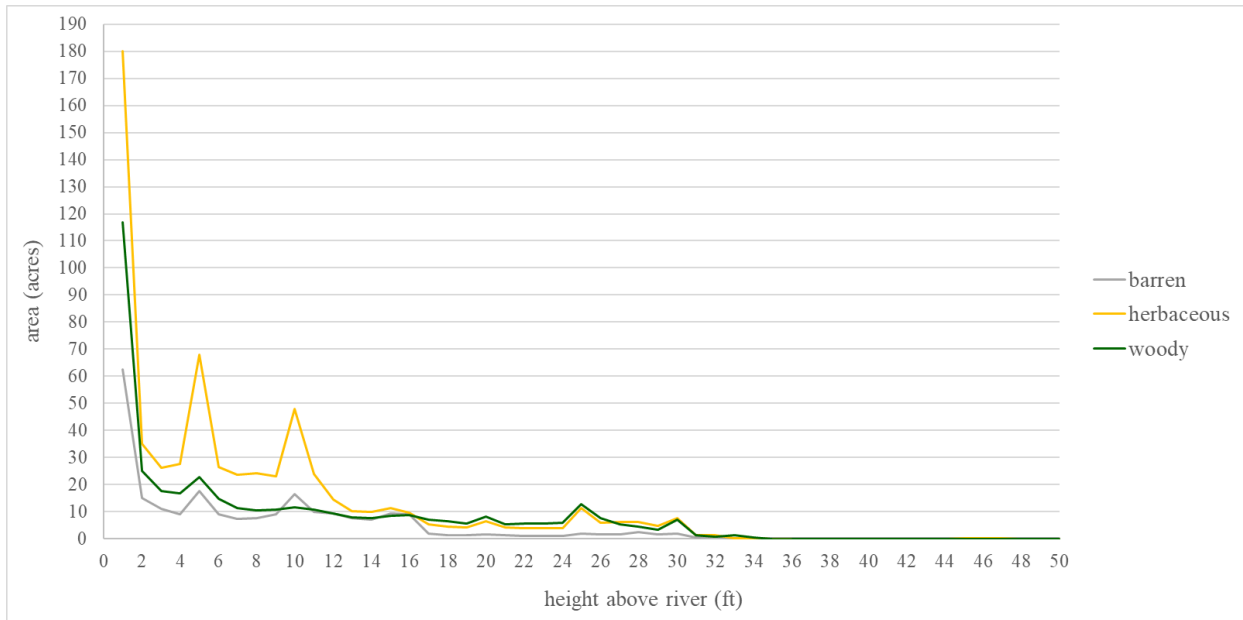


**Figure 2.4.** The distribution of land cover type by HAR for 1937 (top) and 2009 (bottom). In 1937, note that the cover drops to near zero above 30 ft HAR; this is because the channel was much shallower in 1905 than in 2005 (Chapter 1). The distribution of values changes significantly between time periods, with the peak in 1937 at 0 ft HAR and the peak in 2009 around 6-14 ft HAR.

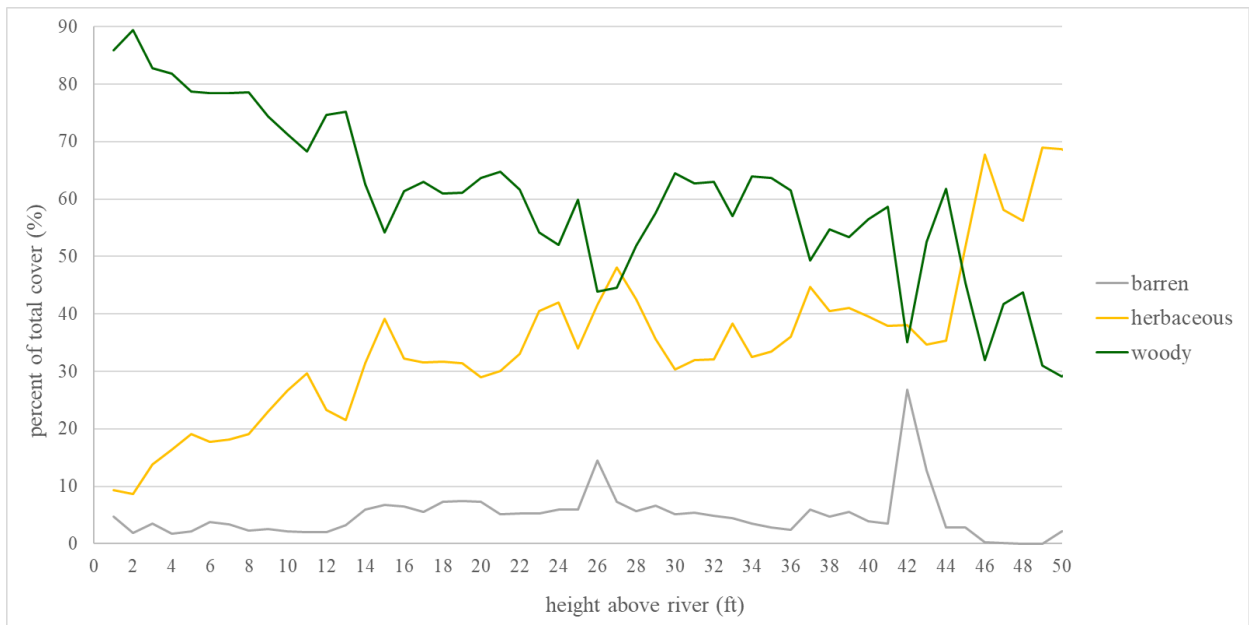
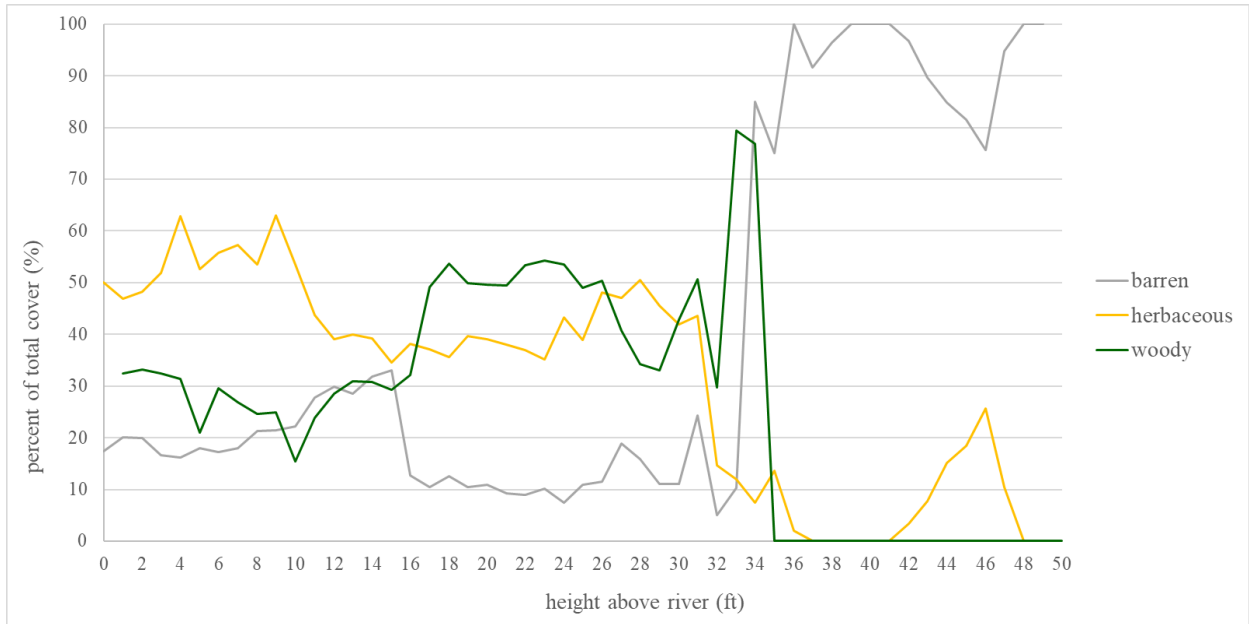


**Figure 2.5.** Proportional cover of each class by HAR in 1937 (top) and 2009 (bottom). In 1937, values become skewed above 30 ft HAR due to the shallower channel in 1905. Again, there is a significant change in the distribution of land cover type, with herbaceous dominating low HAR in 1937 and woody dominating low HAR (and nearly all the entire study area) in 2009.

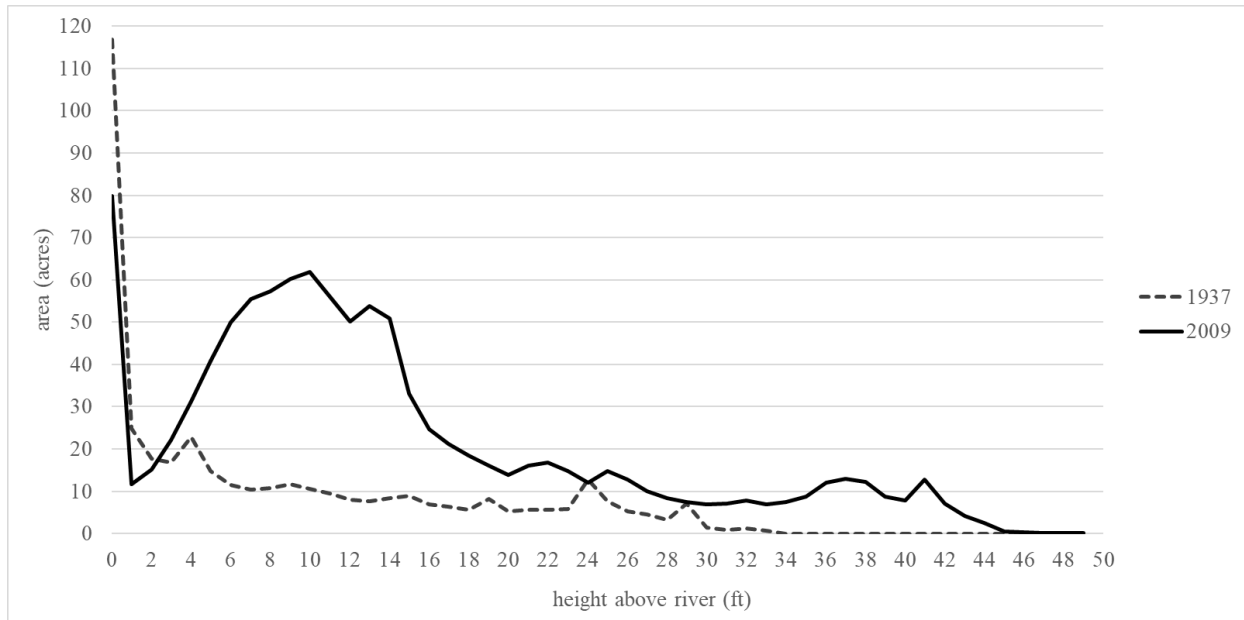


**Figure 2.6.** Distribution of woody vegetation by HAR in 1937 and 2009. This plot demonstrates well both the change in distribution of woody vegetation and the change in dominance of woody vegetation between 1937 (dashed line) and 2009 (solid line).

The amount of steep bank slopes increased between 1937 and 2009 across the study area due to channel deepening and narrowing (i.e., incision; Chapter 1), and the distribution of all three cover types by bank slope reflects that finding (**Figure 2.7**). In 1937, very little cover of any kind was found on bank slopes steeper than 26.8% (15 degrees), and the vast majority of the vegetated area was found on bank slopes shallower than 17.6% (10 degrees). In 2009, around half of the study area has a bank slope greater than 17.6% (10 degrees), steep slopes (those greater than 14.1-17.6% (8-10 degrees)) are dominated by woody cover, and barren cover is only found on the shallowest slopes.

The proportion of cover type by bank slope (**Figure 2.8**) changed significantly between time periods. The results indicate that vegetated bank slope increased from a maximum of 36 degrees (72.7% slope) in 1937 to a maximum of 56 degrees (148.3% slope) in 2009. While woody cover dominated the steepest slopes in both 1937 and 2009, it dominates steep slopes

notably more in 2009. Woody cover also shifted to dominate the shallowest slopes, replacing herbaceous cover evenly across all slope values and barren across all but the shallowest slopes.

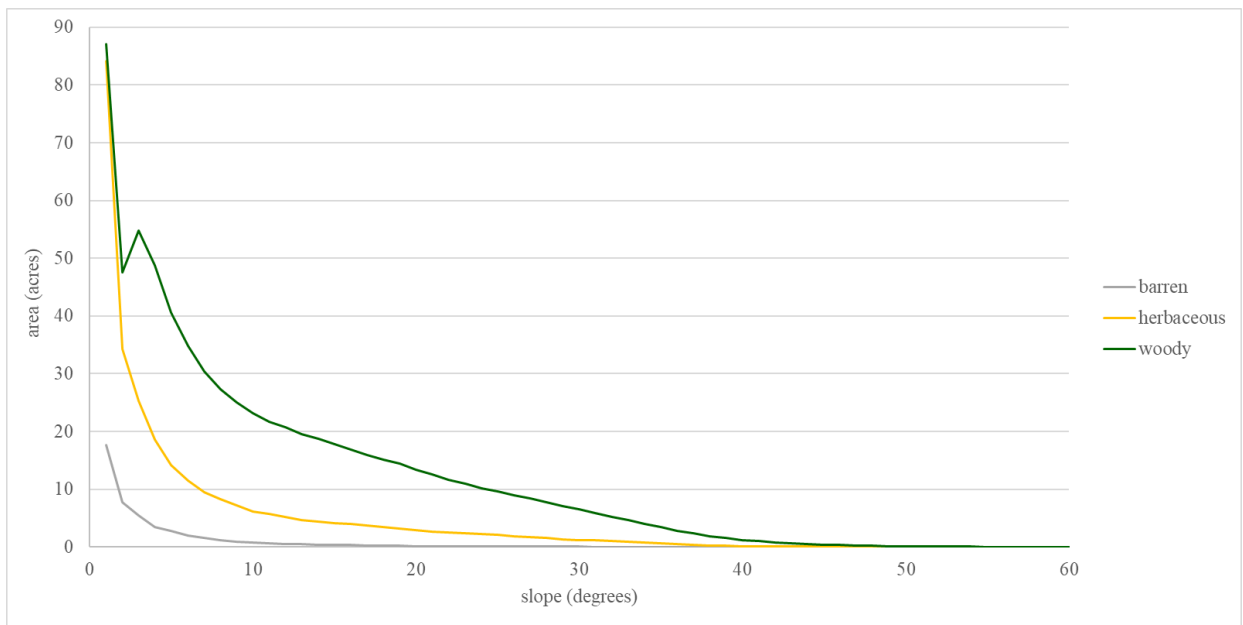
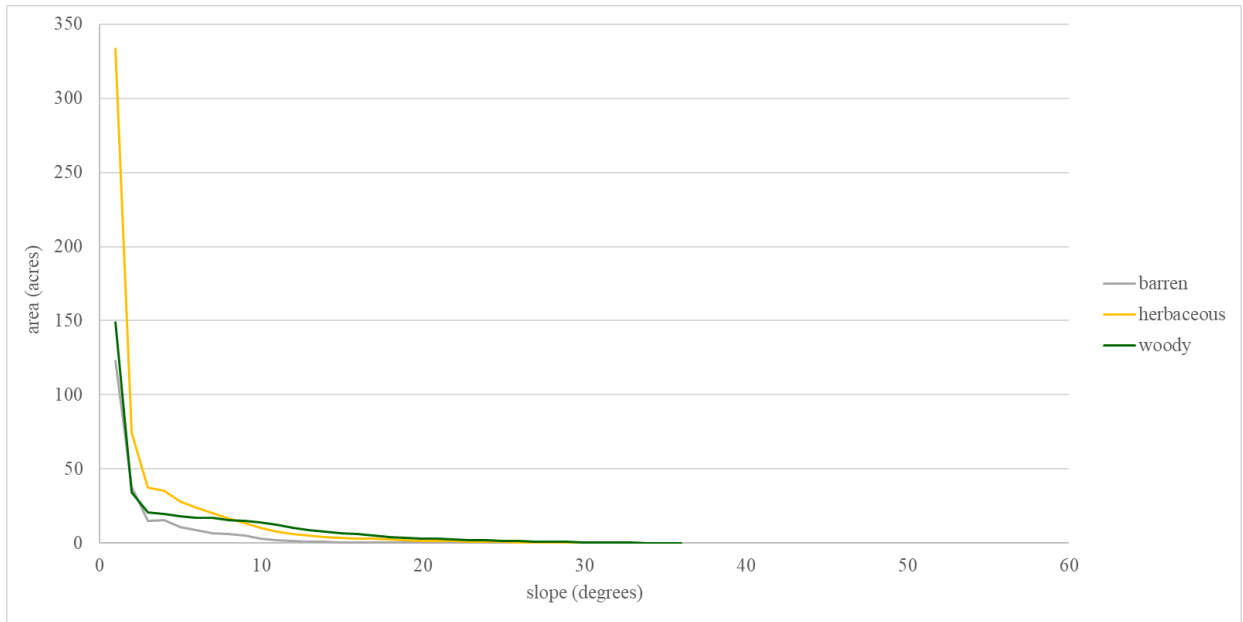


**Figure 2.7.** The distribution of land cover type by bank slope for 1937 (top) and 2009 (bottom). The 1937 plot shows in general much shallower slopes than the 2009 plot. Also, in 1937 herbaceous cover dominated the shallowest slopes (<8 degrees), whereas in 2009 woody cover dominated all slopes, and the distribution across slope values was relatively even compared to the distribution in 1937.

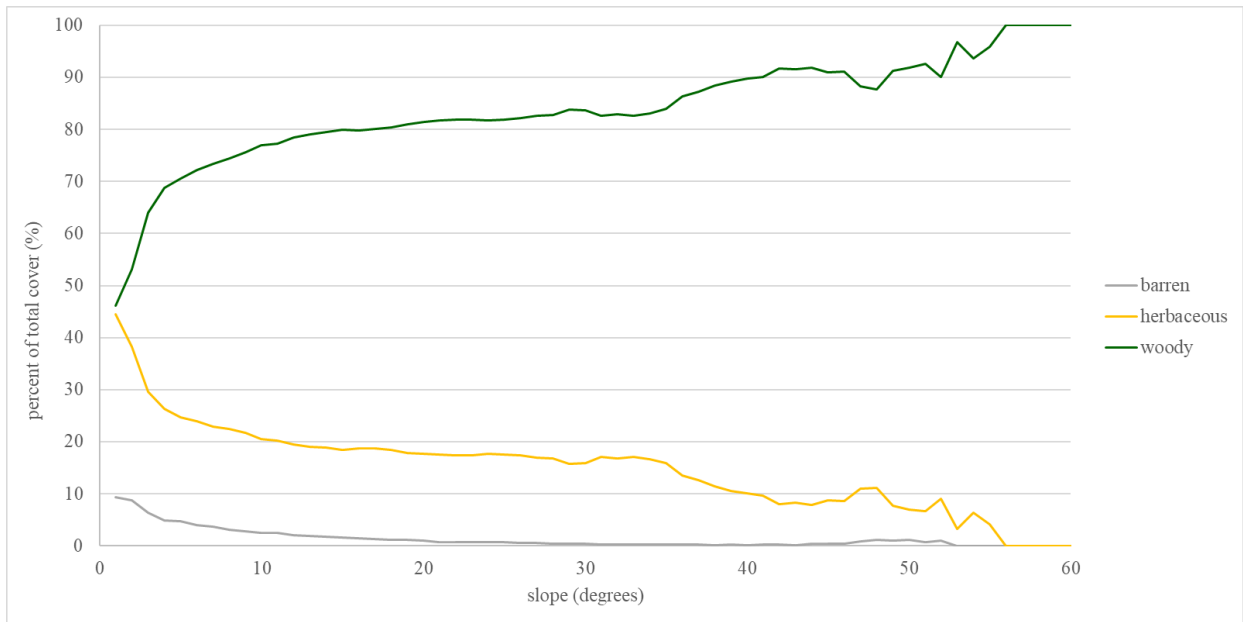


**Figure 2.8.** Proportional cover of each class by bank slope in 1937 (top) and 2009 (bottom). Comparing the maximum bank slope values in 1937 and 2009, it is clear that the 2009 channel is significantly deeper than the 1937 channel, due to the steeper banks. The skew of the 1937 curve above 35 degrees and the skew of the 2009 curve above 53 degrees are due to the low number of cells with that steepness.

Charts of the distance to baseflow surface values for each cover class show significant changes to vegetation distribution (**Figure 2.9**). Woody cover and herbaceous cover both peak farther from the baseflow surface in post-dam than in pre-dam. Woody cover, which forms the vast majority of cover in post-dam, shifted from consistently decreasing cover away from the water to a peak around 50 ft from the water, and values overhanging the water surface decreased. All three land cover types showed similar pre-dam distribution. Post-dam, herbaceous cover was found in only small amounts near the baseflow surface, peaking about 150 ft from the water. Barren cover in the post-dam was found in small extents throughout the study area, and peaked around 210 feet from the water.

There are some similarities in distance to baseflow surface between time periods: the bulk of woody and herbaceous cover is still found within 300 feet of the channel, and similar to findings from the HAR zonation, all three cover classes are found in significant amounts in the 0-ft HAR zone. This second point can be explained by two phenomena: (1) in the pre-dam model, there was an exceptionally low baseflow present in the aerial photography, showing up as only a few pools that were removed from the imagery manually, so the image classification was conducted in much of the area that would be considered the baseflow surface during slightly wetter months (this point applies to the post-dam model to a lesser degree due to the larger baseflow present in the imagery); and (2) as seen in the HAR distribution, woody vegetation hung over the baseflow water surface.

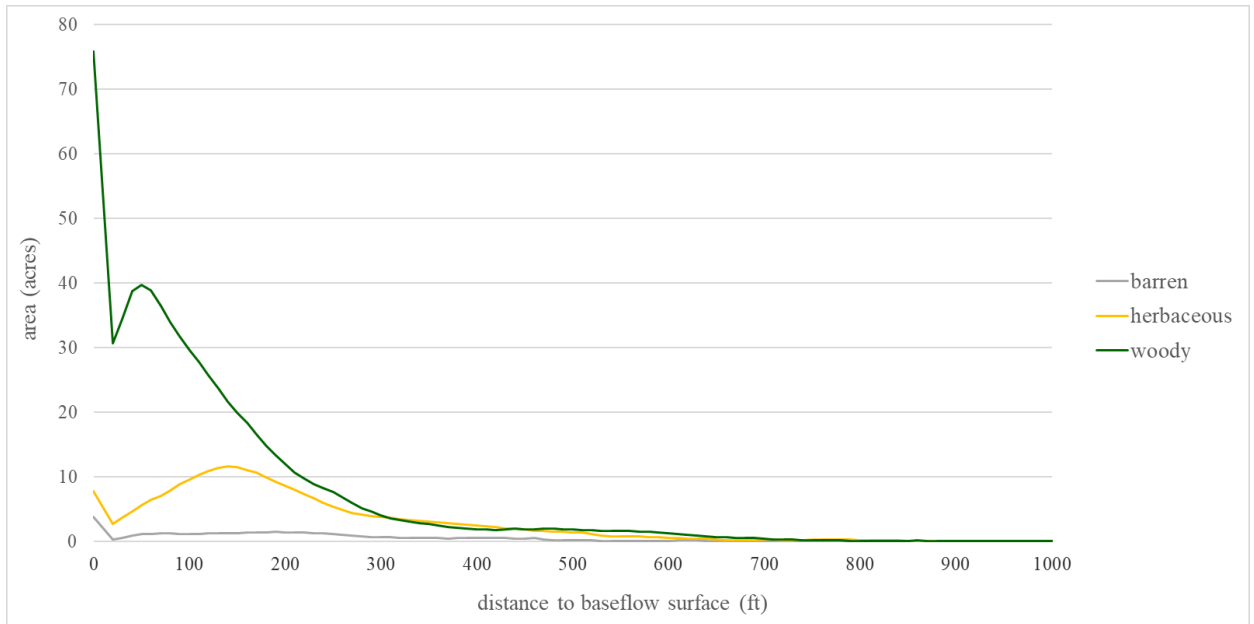
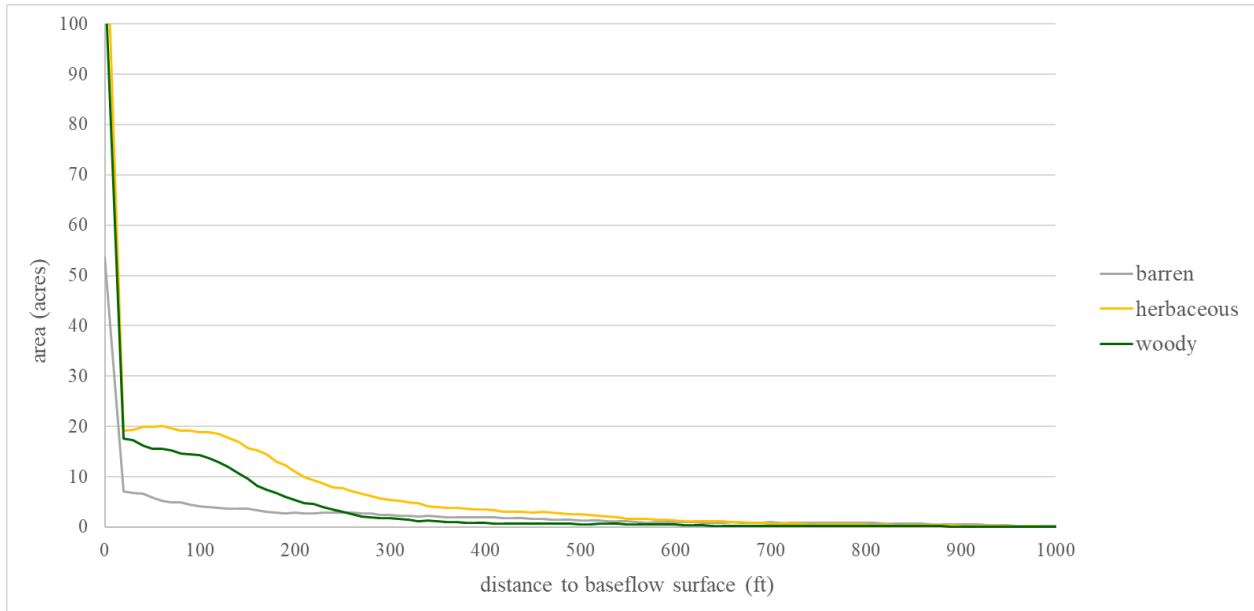


**Figure 2.9.** Distribution of cover type by distance to baseflow surface for 1937 (top) and 2009 (bottom). In 1937, herbaceous cover dominates almost all values, whereas in 2009, woody cover dominates almost all values. There is also a shift in the peak distribution of all cover types between time periods: in 1937, there are more values at zero ft from the baseflow surface because the channel bottom was wider and flatter than in 2009.





**Figure 2.10.** Proportional cover of each class by distance to baseflow surface in 1937 (top) and 2009 (bottom). In 1937, herbaceous cover dominates all but the farthest areas from the channel, but in 2009 (bottom), woody cover dominates in most areas, especially in areas within 300 ft of the baseflow surface; this indicates filling in of woody vegetation across the study area but especially in the riparian zone.

Proportional cover of each class by distance to baseflow also differed significantly between time periods (**Figure 2.10**). In 1937, the distance gradient of each cover type was smoother and gentler than in 2009. In 1937, each cover type appears to have an optimal range: for barren, it is the farther distances; for herbaceous, it is the moderate distances; and for woody it is the areas closest to the channel. In 2009, optimal ranges are much less clear: woody and herbaceous both have two peaks, and barren is found in small amounts along the distance gradient. Two reasons might explain this phenomenon: (1) there is little total area at the greatest distances (>700 ft), leading to skewing of the right end of the curve; and (2) woody cover is a broad class and may not represent the distributions of all types of vegetation it represents (e.g., riparian forest and shrub cover would dominate close to the channel but valley oak woodland (including grass/herbaceous) would dominate at farther distances, such as on terraces).

#### **4.5 Reach-scale analysis**

The amount and type of cover change varied considerably by reach (**Tables 2.5, 2.6, and 2.7; Figure 2.11**). In the South Fork reach, which is moderately incised (mean 7.8 ft) and has the shallowest channel and bank slope (**Table 2.8**), 65.4% of the area changed cover type. The middle reach, which is the most incised (mean 10.7 ft) and has the steepest bank slope, experienced by far the least change, with only 43.3% of the intersected area between 1937 and 2009 changing cover type. In the Winters reach, which is the least incised (mean 5.0 ft) and has moderate bank slope, 72.9% of the area changed cover type.

The proportion of each cover type also varied considerably between reaches in both time periods. In 1937, the middle reach had significantly greater relative cover of woody vegetation (57.8%) than the Winters (21.6%) or South Fork (9.4%) reaches. In 2009, the Winters and

middle reaches had similar high proportions of woody cover (74.8% and 76.8%), while the South Fork had much less woody cover (51.9%) and much more herbaceous cover. In all three reaches, the Herbaceous→Woody transition was the largest active transition type. The Barren→Woody and Barren→Herbaceous transition types were also notable for the Winters and South Fork reaches but not for the middle reach.

**Table 2.5.** Transition cover (in acres and percent) for the Winters upstream reach. Of the total area, 27.1% (58.3 ac) remained the same cover type between 1937 and 2009.

	<b>1937 woody</b>	<b>1937 barren</b>	<b>1937 herbaceous</b>	<b>total in 1937 (ac)</b>
<b>2009 woody</b>	36.0 (16.7%)	0.9 (0.4%)	8.9 (4.1%)	46.4 (21.6%)
<b>2009 barren</b>	37.4 (17.4%)	1.8 (0.8%)	19.3 (8.9%)	58.5 (27.2%)
<b>2009 herbaceous</b>	87.5 (40.7%)	2.9 (1.3%)	19.7 (9.2%)	110.4 (51.3%)
<b>total in 2009 (ac)</b>	160.9 (74.8%)	5.6 (2.6%)	47.9 (22.3%)	215.2

**Table 2.6.** Transition cover (in acres and percent) for the middle reach. Of the total area, 56.7% (234.3 ac) remained the same cover type between 1937 and 2009.

	<b>1937 woody</b>	<b>1937 barren</b>	<b>1937 herbaceous</b>	<b>total in 1937 (ac)</b>
<b>2009 woody</b>	194.8 (47.1%)	4.4 (1.1%)	37.3 (9.0%)	238.9 (57.8%)
<b>2009 barren</b>	19.1 (4.6%)	0.7 (0.2%)	5.1 (1.2%)	25.2 (6.1%)
<b>2009 herbaceous</b>	103.4 (25.0%)	7.7 (1.9%)	38.8 (9.4%)	149.3 (36.1%)
<b>total in 2009 (ac)</b>	317.3 (76.8%)	12.8 (3.1%)	80.2 (19.4%)	413.4

**Table 2.7.** Transition cover (in acres and percent) for the South Fork reach. Of the total area, 34.6% (122.4 ac) remained the same cover type between 1937 and 2009.

	<b>1937 woody</b>	<b>1937 barren</b>	<b>1937 herbaceous</b>	<b>total in 1937 (ac)</b>
<b>2009 woody</b>	18.3 (5.2%)	2.6 (0.7%)	11.1 (3.1%)	33.2 (9.4%)
<b>2009 barren</b>	41.8 (11.8%)	3.5 (1.0%)	30.9 (8.7%)	76.9 (21.8%)
<b>2009 herbaceous</b>	123.4 (34.9%)	18.7 (5.3%)	100.6 (28.5%)	243.4 (68.9%)
<b>total in 2009 (ac)</b>	183.5 (51.9%)	24.8 (7.0%)	142.6 (40.3%)	353.5

**Table 2.8.** Reach-scale geomorphology in 1905 and 2005, including channel slope and bank slope, and incision between 1905 and 2005.

	<b>Upstream of Winters</b>	<b>Middle</b>	<b>South Fork</b>
<b>River-miles</b>	21.23-18.56	18.56-7.41	7.41-1.54
<b>Channel slope mean 1905 (degrees)</b>	0.14	0.09	0.07
<b>Channel slope mean 2005 (degrees)</b>	0.1	0.11	0.04
<b>Incision mean (1905-2005) (ft)</b>	5.0	10.7	7.8
<b>Incision std. dev. (1905-2005) (ft)</b>	2.0	4.1	2.2
<b>Bank slope mean 1905 (degrees)</b>	2.34	6.28	1.49
<b>Bank slope std. dev. 1905 (degrees)</b>	3.89	6.8	2.35
<b>Bank slope mean 2005 (degrees)</b>	4.76	10.2	5.9
<b>Bank slope std. dev. 2005 (degrees)</b>	6.48	10.38	7.57

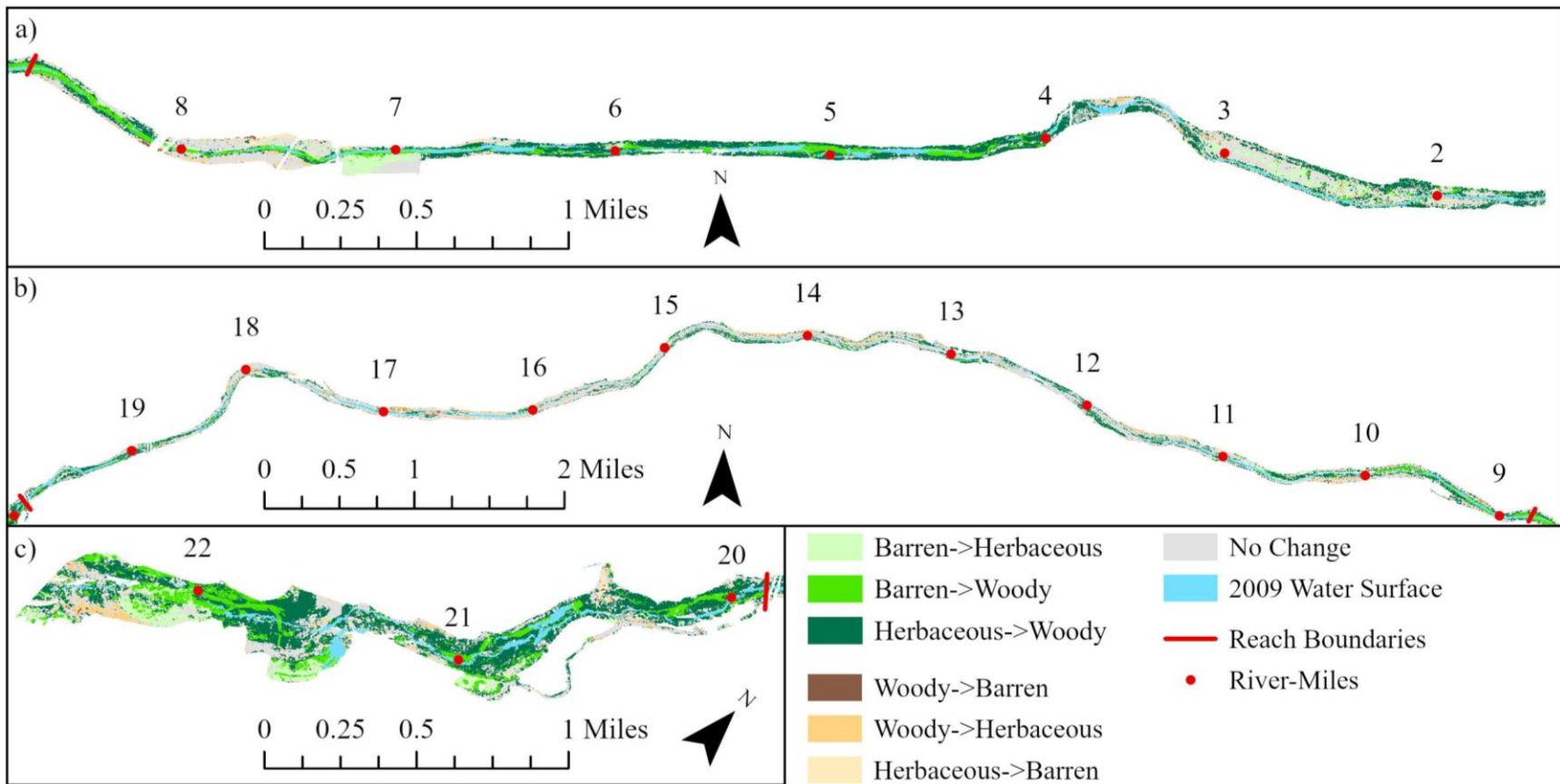


**Figure 2.11.** Land cover transition map for the reach-scale analysis. From low-to-high river-miles are (a) the South Fork reach, (b) the middle reach, and (c) the Winters upstream reach. The middle reach showed by far the least amount of change (56.7%), a pattern that is clearly visible on the map and which helped define each “reach” for this analysis.

## 5. Discussion

Land cover in the study area changed significantly pre-dam to post-dam, even after accounting for agricultural and urban cover types. Between 1937 and 2009, 57% of the study area shifted cover type, and of that, 75% was a shift from barren and herbaceous to woody vegetation. While the pre-dam channel was dominated by herbaceous cover, the post-dam channel is overwhelmingly dominated by woody cover. These results are consistent with riparian forest succession following damming and subsequent flow regulation, where a lack of geomorphological disturbance, in this case large flows, and heightened baseflow created competitive conditions for woody species establishment (Han et al., 2020; Kondolf, 1997; Poff and Zimmerman, 2010). In the new flow regime, a perennial baseflow made more surface and groundwater available in summer months, and reduced scouring flows in the winter (see Chapter 1). Since this regime is permanent for Lower Putah Creek, remaining herbaceous cover will likely continue to fill in with woody vegetation. In 2009, barren cover already occupied what could be a minimum total area, restricted to areas in and near the baseflow channel (i.e., sandbars) and near the top of the channel banks where some areas of bare soil or gravel from farm roads may not have been clipped out entirely from the 2009 imagery.

Pre-dam, the HAR distribution of woody vegetation was relatively even (i.e., wider elevational distribution); post-dam, the HAR distribution of woody vegetation became restricted to the lowest 20 ft HAR (**Figures 2.4 and 2.5**) (i.e., narrower in elevational distribution). This indicates that the woody cover tracked (i.e., filled in) channel deepening/incision (see Chapter 1), although the narrowing and deepening of the baseflow channel also reduced recruitment space (i.e., compression of the floodplain) for riparian vegetation on the channel banks by increasing bank slope. While this reduced gradient may affect riparian vegetation in particular, the shift in

cover distribution by bank slope indicates that woody vegetation (a very coarse class) did not have trouble establishing on the steepening slopes. However, a finer-resolution vegetation classification, that separates hydro-riparian plant communities from meso- and xero-riparian communities (other woody riparian classes; see (Johnson et al., 1984)), may provide important nuances to these findings. It is hypothesized for future studies that recruitment space (i.e., lower HAR values) for willow (*Salix* spp.) and cottonwood (*Populus fremontii*) are highly limited, while valley oak (*Quercus lobata*) and other terrace woody plant species (occupying higher HAR values) is relatively more abundant.

The fact that land cover change varied significantly by reach indicates that, either pre- or post-dam, not all areas of the channel experienced the same geomorphological conditions. The wide, mostly-barren reach upstream of Winters in 1937 filled in with woody vegetation by 2009, perhaps because of a lack of scouring flows. The Winters reach also experienced the greatest transition in cover type despite experiencing the least incision and moderate bank slope; this might be due to the fact that a significant amount of earth-moving activity occurred there during the construction of the Putah Diversion Dam (1955-1959), affecting vegetation growth and distribution. The shallow, mostly herbaceous and barren South Fork reach in 1937 also filled in with woody vegetation by 2009, likely because of a lack of scouring flows and increased perennial baseflow, which enhanced soil moisture and stimulated riparian vegetation growth. However, in 2009 the South Fork also had the least woody cover of all three reaches, likely due to a few places in the study area of high distance to baseflow surface (see **Figure 2.11**), where the increased perennial baseflow had little-to-no effect on soil moisture. Additionally, the far eastern South Fork was, and still is, very shallow compared to the rest of Lower Putah Creek (Chapter 1); it became inundated with floods for weeks or months at a time nearly every year

before the construction of the Putah Creek dams and Sacramento Valley flood control levees (Kelley, 1989; Lower Putah Creek Coordinating Committee, 2005; Vaught, 2007). The middle reach, which experienced the least amount of cover change and is the most incised, appears to be the section of creek with the most stable banks. This stability enabled established woody vegetation to remain intact and succession of barren and herbaceous to woody cover.

A limitation of this study is that, while the 1937 imagery is referred to here as “pre-dam,” and is the earliest aerial imagery available for the area, it is not entirely representative of pre-settlement conditions and shows a heavily-modified state. Likewise, the 1905 DEM used here is also not entirely representative of pre-settlement conditions, despite it being the only and earliest topographic dataset available. Both datasets are only a snapshot in time, an inherent limitation to historical ecology (O’Brien, 2001). The sparser woody vegetation and larger total area of barren cover in 1937 appears to match the geomorphological conditions of a more powerful, scouring creek with a wider channel bottom, when the vast riparian forest was periodically flooded by large flows (i.e., the 30-year recurrence interval and above) (Vaught, 2007); it is possible that the 1937 imagery shows an earlier stage of the recovery of woody vegetation. Since cattle ranchers in the 1800s razed nearly the entire riparian forest for fencing and fuel (Vaught, 2007), it is possible that the 1937 imagery only shows the middle stages of recovery of the native riparian forest. Indeed, since the vegetation was cleared in the 1800s, flows could increase in velocity; this could have contributed to channel incision by the time of the 1905 USGS topographic survey.

HAR has been shown many times to be a useful and reliable predictor of vegetation cover in riparian ecosystems (Bendix and Hupp, 2000; Politti et al., 2018; Shafroth et al., 1998; Stromberg et al., 1996). While random forest classification indicated an unlikely result (all three



variables had identical importance in determining cover type), it is possible that several factors are confounding results here: (1) classification resolution (i.e. number of classes) was very coarse, and since HAR is species-specific or at least alliance-specific (i.e., based on recruitment zones (Mahoney and Rood, 1998; Politti et al., 2018; Shafroth et al., 1998)), it could be that classifying all woody vegetation together made it impossible to determine HAR's influence; and (2) HAR works along gradients, often most strongly related to groundwater (Greco et al., 2008) and inundation (e.g. flow frequency; Friedman et al., 2006; Hupp and Osterkamp, 1996), but elevational gradients in much of Lower Putah Creek are steep and a HAR-vegetation relationship might not show up in the data in such a small study area.

Distance-to-baseflow surface is related to HAR and may have been affected by some of the same issues. Bank slope is somewhat related to HAR in that it can affect recruitment zones and vegetation feedbacks (Politti et al., 2018), but its contribution to the dynamics of ecological gradients may only appear at larger spatial scales (i.e., larger areas) (Cheng et al., 2023; Nüchel et al., 2019; Pinder et al., 1997). Average bank slope across the study site increased due to the channel deepening after major dam construction (Chapter 1) and while there is significant topographic variation in Lower Putah Creek, the banks are stable. It could simply be that none of the land cover types used here are sensitive to bank slope, especially in the context of other variables affecting vegetation establishment.

While the random forest classification may not have produced a useful map, the geomorphic analyses using those variables effectively characterized vegetation distribution and helped form inferences about how flow regulation may have affected the vegetation. The only cover that shifted in average HAR was barren, indicative of vegetation filling in near the channel bottom. Unsurprisingly, the bank slope of all land cover classes increased, an effect of the entire

channel deepening and narrowing (Chapter 1). The distance to baseflow surface increased for both woody and herbaceous classes, showing the study area filled with vegetation. The distribution of each land cover class by HAR and distance to baseflow surface corroborated these findings, showing woody vegetation replacing herbaceous and barren across the study area. Peaks in cover at lower HAR and distance to baseflow surface indicate that woody vegetation filled into newly incised area as the channel deepened.

While the findings in this study have limited application in designing planting zones for restoration or managing flow regimes (because of the lack of differentiation of woody plant communities in this study), they help characterize a broader pattern of change across all of Lower Putah Creek: since 1937, more woody vegetation has established in all areas of the channel, though significant reach-scale variation seems tied to major local differences in the channel's geomorphology, including incision and bank slope. It is also possible that some planting restoration projects in the channel (e.g., South Fork Preserve, Restoria (Gardner, 2019; University of California, Davis, 2005)) or invasive species (Lower Putah Creek Coordinating Committee, 2005) have contributed to modern vegetation patterns to a degree we could not account for in this study. More fine-scale classification is necessary to break down how individual woody vegetation types (e.g., willow, cottonwood, mixed riparian forest, valley oak) relate to HAR in the post-dam system; this level of analysis would enable a geomorphological restoration design based on maximizing a specific cover type, such as riparian forest, or balancing a suite of restoration priorities.

## 6. Conclusion

This study demonstrates the value of historical and modern imagery datasets, the potential effects of flow regulation on riparian vegetation, and the complications with using machine learning to create predictive models of land cover. Image classification and geomorphic analysis effectively characterized the magnitude, direction, and distribution of change between time periods, and corroborated existing findings that show flow regulation enhances the establishment of woody vegetation (Poff and Zimmerman, 2010). Both forest-based classification and geomorphic analysis indicated that woody cover was not strongly linked to HAR, bank slope, or distance to baseflow surface, though examination of reach-scale variation showed how vegetation may be strongly tied to local geomorphology. A more resolute riparian vegetation classification system may clarify these results.

These geomorphological metrics, especially HAR, are still an underutilized tool in applied historical ecology (Morris et al., 2022) and topography-based restoration design (Bair et al., 2021). Here, we demonstrated their utility for tracking change on a heavily-modified river and their potential to be incorporated into predictive machine learning models to inform management and ecological restoration.

### **Chapter 3 Assessing reach-scale geomorphology using height above river zones to prioritize riparian restoration sites and inform restoration design on an incised and regulated California coast range river**

#### **Highlights**

- Height above river (HAR) represents the spatial extent of inundation according to flow frequency
- HAR accurately predicted the distribution of riparian land cover types in a random forest classification, where riparian vegetation dominates the lowest HAR areas
- Vegetation-based HAR zones were effectively used to assess reach-scale geomorphology
- Eighty-five percent of flow-regulated Lower Putah Creek qualifies as “geomorphologically degraded,” but there is significant potential to create riparian habitat (e.g., double the riparian zone) through HAR-based floodplain lowering and baseflow narrowing
- One half of Lower Putah Creek qualifies for floodplain lowering, one third qualifies for baseflow narrowing, and one seventh qualifies for both

#### **Abstract**

Predicting vegetation distribution using physical variables can be a useful tool in planning river restoration projects. One geomorphological metric, height above river (HAR), has been shown to be correlated to riparian vegetation distribution through several relationships, including depth to groundwater, discharge frequency, and soil moisture. HAR has even been used to identify areas suitable for riparian restoration according to inundation frequency and to

create appropriate planting zones after geomorphological restoration. There are also many frameworks and methods for prioritizing and planning riparian restoration projects. However, no studies have used a HAR-classified land cover model to assess geomorphology, quantify restoration potential, and plan restoration design.

In a study on Lower Putah Creek, California, USA, we first establish that HAR is well-correlated to vegetation and discharge using 1-D inundation modeling and support vector machine (SVM) image classification. Riparian forest was found to dominate the lowest HAR zones. Next, we used HAR to predict land cover types using a random forest classification, then created HAR zones relevant for restoration planning, and ranked each reach of the river by the sum two independent rankings: (1) the in-channel relative area of their combined core riparian and marginal riparian zones; and (2) the in-channel relative area of their combined aquatic and transition zones. Of the 21.22 river-miles examined, only 3.22 river-miles qualified as “reference”; the rest qualified as “degraded,” including 6.42 river-miles that are “severely degraded,” indicating a significant opportunity to create riparian forest in the Central Valley. Finally, we used the relative area of aquatic and transition zones and the mean baseflow width of each reach to prescribe either baseflow narrowing or floodplain lowering as a geomorphological restoration action. Most of the creek qualifies for floodplain lowering, while a third qualifies for baseflow narrowing and several reaches qualify for both. These methods can be used in other river systems to plan restoration, and the HAR zones created here can be directly incorporated into existing restoration design software for future projects on Lower Putah Creek.

## **Keywords**

Height above river (HAR), geographic information systems (GIS), ecological restoration, restoration ecology, restoration prioritization, random forests, machine learning, NAIP, regulated river, dams, suitability analysis

## **1. Introduction**

Geomorphological assessment can be an important first step in planning and prioritizing ecological restoration in rivers. Assessments are usually field-based and include reach-scale data collection for dozens of geomorphological and biological variables (Bauman et al., 2006; Dunn et al., 2014; Inter-Fluve, 2018; Iowa Department of Natural Resources, 2018; Pagliuco et al., 2023; Worley et al., 2023). There are many peer-reviewed frameworks for prioritizing restoration sites based off of collected geomorphic data (Beechie et al., 2011; Harris and Olson, 1997; Hauer and Lorang, 2004; Perry et al., 2015; Rosgen, 1996; Stanford et al., 1996; Trabucchi et al., 2014), but practitioners often develop their own assessment, prioritization, and monitoring criteria according to agency policies, restoration objectives and stakeholder input (Bauman et al., 2006; Beechie et al., 2011; Cody, 2019; Dunn et al., 2014; Pagliuco et al., 2023). Also, even when an abundance of data are available, it can be challenging to comprehensively assess an entire river landscape and choose one or two sites to restore among many worthy candidate reaches (Worley et al., 2023), especially with conflicting restoration objectives (Schmidt et al., 1998). The challenge is not just in balancing restoration priorities, but also in determining which sites would have the greatest restoration “value” for the money spent.

The availability of a single metric to estimate the restoration potential of multiple sites could help make the assessment and prioritization process more efficient. Field-based

geomorphological assessments, such as transect sampling, are time-intensive and can only provide estimates of system-wide topography. Cell-based geographic information system (GIS) analysis, on the other hand, allows for high-resolution, near-census analysis of continuous surfaces and discrete objects across wide and extensive spatial scales. Recently, the integration of machine learning into GIS has enabled the association of geomorphic variables with vegetation distribution, where the modeled output can be used as a predictor variable in river assessment and restoration planning (Bair et al., 2021; Huylenbroeck et al., 2020; Piégay et al., 2020b). A geographic variable, height above river (HAR), has been shown to be particularly effective in assessing riverscape topography and designing geomorphological restoration.

HAR is useful because it represents a critical gradient in geomorphology: relative elevation. Elevation can be mapped based on a single baseline datum as with elevation above mean sea level (e.g., all the USGS topographic map series) or it can be mapped based on a series of baseline datums such as the nearest low-flow (baseflow) channel edge (or thalweg line) as is the case with HAR models. HAR can be used to model the distribution of riparian vegetation on a floodplain (Fremier and Talley, 2009; Friedman et al., 2006; Greco et al., 2008; Mahoney and Rood, 1998; Vaghti et al., 2009), the extent and depth of flow inundation (Bair et al., 2021; Greco et al., 2008; Sagers et al., 1996; Vondrasek, 2015), and depth to groundwater (Greco et al., 2008; Grismer, 2018). In applied research and practice, it has been used to model an entire watershed to identify sites for hydric restoration (Benda et al., 2011), design riparian revegetation zones (Bair et al., 2021), identify sites for floodplain lowering according to HAR's association with flow frequency (California Department of Water Resources, 2017; cbec, 2023), and design river channels for optimal riparian conditions (e.g., landform longevity) (Brown et al., 2014; Brown and Pasternack, 2019).

It is important to characterize physical relationships relating to flow frequency because, in planning geomorphological modifications, designers often take into account the discharge (flow and duration) that most strongly determines channel form and build projects according to that discharge. Research suggests that appropriate discharge modeling and design can help projects reach their reference, or target, state as quickly as possible (Tranmer et al., 2022). Most studies indicate this discharge is in the 1-2-yr recurrence interval (RI) range for large floodplain rivers and 5-7-yr RI range for incised rivers (Bray, 1975; Cody, 2019; Soar and Thorne, 2011; West and Niezgod, 2006), but the methods by which the dominant discharge is calculated vary. For example, Perry et al., (2015) suggest using a suite of discharges to design geomorphology, rather than a single discharge. As with many regulated rivers, the flow frequency-to-discharge curve for Lower Putah Creek is uneven (Chapter 1), so it may be more useful to identify the discharges associated with important physical processes than the inundation frequency; this is the reason why many studies recommend using “effective discharge” to design restoration terrains instead of “recurrence interval discharge” (Doyle et al., 2007; Perry et al., 2015; Shields et al., 2003; Soar and Thorne, 2011; Tranmer et al., 2022). Here, we associate flow frequency with HAR, which has already been shown to be a useful proxy for dynamism (California Department of Water Resources, 2017).

In this study, we first tested the ability of HAR to represent key geomorphological processes on Lower Putah Creek, including inundation frequency and vegetation distribution. We then used a random forest classification (Breiman, 2001), which is a machine-learning predictive model, to create a land cover surface, in order to characterize HAR zones relevant to restoration planning and design. Broad categories of interest included aquatic, riparian, and upland vegetation zones. We analyzed the system-wide and reach-scale distribution of the HAR zones,



and ranked the reaches based on their relative level of geomorphological degradation, representing the potential of restoring the site. Finally, we prescribed either baseflow narrowing or floodplain lowering to each reach based on relative area of aquatic and transition zones and mean baseflow width.

The research questions of this study are:

- Can the spatial distribution of HAR zones be used to characterize reaches and identify which reaches have functional riparian morphology?;
- Can height above river methods to be used to predict riparian vegetation zones?;
- Can scoring each reach by its HAR zonal area identify the nature of geomorphological restoration required in each reach to produce a functional riparian floodplain morphology, as well as the potential riparian area that could be gained through geomorphological restoration?; and
- Can the relative area of HAR zones be used to prescribe reach-scale geomorphological restoration actions?

## 2. Study Area

Lower Putah Creek is a regulated river in the Coast Range of Northern California, USA (**Figure 1.1**). It experienced dramatic geomorphological and biological change after U.S. and Mexican settlement in the 1830s, including razing of its riparian forest, channel realignment (Vaught, 2007), significant channel incision and narrowing (Chapter 1), dam-induced reduction in peak flows and heightened perennial baseflow (Chapter 1), and subsequent recovery of woody vegetation that only partially resembles the historical plant communities (Chapter 2; Conard et al., 1980). Pre-settlement Putah Creek flooded its natural levees regularly and sustained a

20,000-acre riparian forest that spread 1-2 miles on either bank (Geographical Information Center, 2003; Roberts et al., 1980; Tuil, 2019; Vaught, 2007). It currently passes through a 1,700-acre mix of valley oak woodland, riparian forest, and wetlands (8.7% of the original extent (Geographical Information Center, 2003)). No studies have analyzed the relationship between Lower Putah Creek's geomorphology and riparian vegetation, nor have restoration projects on Lower Putah Creek attempted to incorporate HAR as a design metric.

Four reach-scale restoration projects have been completed on Lower Putah Creek in the last 25 years, only two of which modified geomorphology. The South Fork Preserve project in 1997 (both sides of the channel, river-miles 3.3-3.8) planted the active riparian zone in low HAR areas and planted tens of acres of oak woodland and grassland in upland areas (Gardner, 2019) (**Figure 3.#**). The Restoria project in 2001 (north side of the channel, river-miles 7.3-8.0) planted oaks and other upland species in high HAR areas (Parker, 2003; University of California, Davis, 2005). Only the Winters Putah Creek Nature Park project in 2020 (both sides of the channel, river-miles 18.9-20.0) and the Nishikawa project in 2023 (both sides of the channel, river-miles 10.7-11.2) modified the geomorphology, doing so by lowering the floodplain and narrowing the baseflow channel, in addition to planting (City of Winters, 2008; LSA, 2023). While findings from Chapters 1 and 2 could help identify suitable areas for restoration on Lower Putah Creek, more information is needed about the relationship between riparian vegetation and HAR, and about local variation since the reach scale is where restoration efforts are most often implemented (Bair et al., 2021; Brown and Pasternack, 2019; California Department of Water Resources, 2017; cbec, 2023; Iowa Department of Natural Resources, 2018; LSA, 2023; Worley et al., 2023).

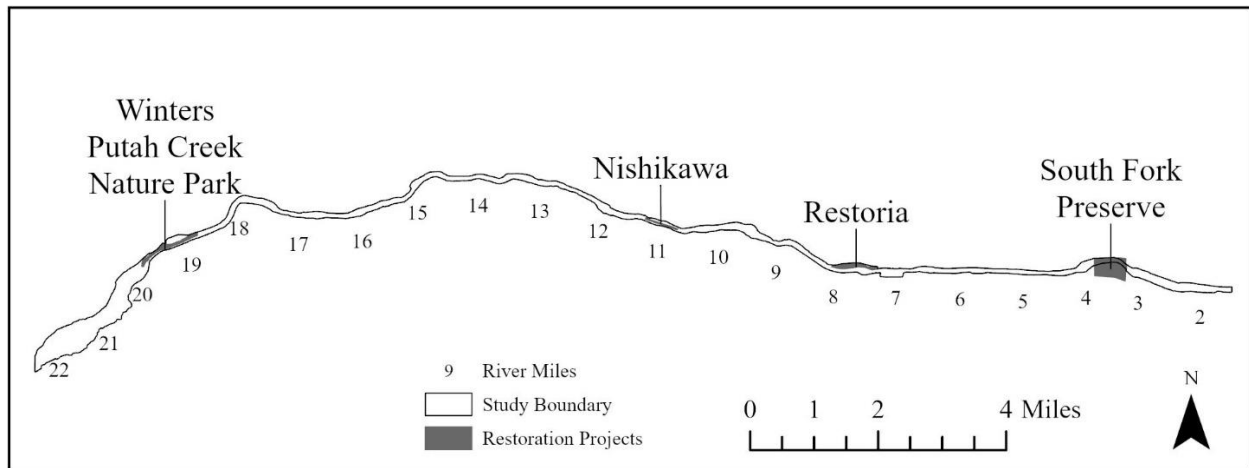


**Figure 3.1.** Locations and extents of major restoration projects on Lower Putah Creek in relation to the study boundary and river-miles. The Winters Putah Creek Nature Park and Nishikawa projects modified channel morphology by lowering the floodplains and narrowing the baseflow channel, in addition to planting. The Restoria and South Fork Preserve projects only included planting.

### 3. Methods

Methods in this study are summarized as a flowchart in **Figure 3.2**. In section 3.1, recurrence interval discharges are used to create inundation areas, and both the mean HAR of inundation area edge and total inundated area are plotted against discharge. In section 3.2, NAIP imagery is used to create training samples for image classification, a support vector machine (SVM) image classification is performed, and SVM-classified land cover distributions are plotted against HAR and discharge. In section 3.3, HAR and training samples are used in a random forest classification, random forest-classified land cover distributions are plotted against HAR, and the total area of each cover type is compared between the SVM classification (“actual cover”) and the random forest classification (“predicted cover”). In section 3.4, land cover distributions are used to reclassify the HAR raster into zones relevant for geomorphological assessment and restoration planning, reaches are delineated based on geomorphological uniformity, and reaches are ranked according to their relative area of certain HAR zones. In

section 3.5, reaches are prescribed one of two restoration actions according to their relative areas of aquatic and transition zones and mean baseflow width.

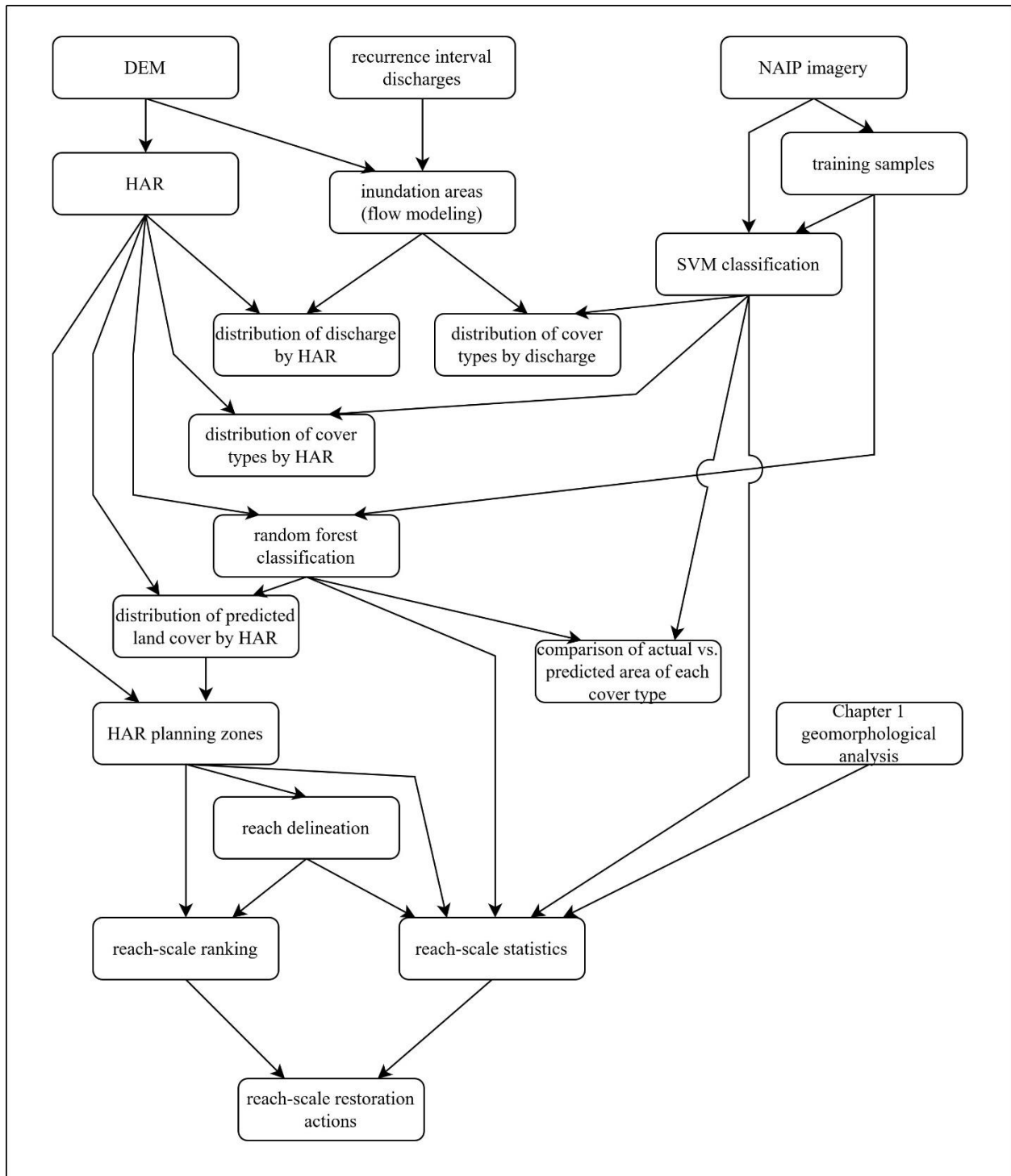


**Figure 3.2.** Flowchart of study methods, including input and output datasets for each step. Raw input datasets included the LiDAR-generated 2005 DEM, recurrence interval discharges from the Chapter 1 flow frequency analysis, and 2020 NAIP aerial imagery. Final outputs included reach-scale statistics, a reach-scale ranking by relative area of HAR zones, and assignment of reach-scale geomorphic restoration actions according to several metrics.

### 3.1. 1-D flow modeling

Steady-state 1-D flow models were created in HEC-RAS (U.S. Army Corps of Engineers, 2023a) following standard guidance (England et al., 2019) and the same procedures outlined in Chapter 1, except that Manning's n values were changed to 0.035 in the channel and 0.1 out of the channel to better reflect the entire cross-sectional roughness of the study area, which is mostly vegetated by riparian forest and valley oak woodland from the banks of the baseflow channel up the banks of the main channel in the area inundated by all modeled flows. Inundation polygons in both time periods were created for flow frequencies 1-yr through 9-yr, as well as 11-yr, 13-yr, 16-yr, 22-yr, 33-yr, 65-yr, and 100-yr flows (**Table 3.1**), since those were all the relevant discharges available for the post-dam period (see Chapter 1). The 100-yr flow was not modeled in Chapter 1, but was estimated using similar methods in another study (Jones and Stokes, 1992). Inundation polygons were exported as shapefiles from HEC-RAS, converted to rasters in ArcGIS Pro, and clipped to the study boundary (**Figure 1.3**).

**Table 3.1.** Recurrence interval flows used for creating flood inundation polygons. Note: The 100-yr flow was not modeled in Chapter 1, but was estimated in another study using similar methods (Jones and Stokes, 1992).

<b>recurrence interval</b>	<b>flow (cfs)</b>
baseflow	20
1-yr	368
2-yr	906
3-yr	1,380
4-yr	3,870
5-yr	6,580
6-yr	7,180
7-yr	7,700
8-yr	7,740
9-yr	8,460
11-yr	8,800
13-yr	9,930
16-yr	11,100
22-yr	14,800
33-yr	16,300
65-yr	18,700
100-yr	30,269

In ArcGIS Pro 3.1, Zonal Histogram was used to calculate the spatial extent of inundation at each HAR level. The inundation areas were converted to rasters and run through the Zonal Statistics tool to calculate the mean HAR value of the edge of each inundation area. Inundation areas were also combined into multipart polygons using Union, and the output was then converted to a raster to create inundation zones.

### **3.2 Support vector machine imagery classification and geomorphic distribution**

Land cover classification was performed on a 1-m resolution 2020 National Agriculture Inventory Program (NAIP) (USDA, 2023) mosaic using the same machine methods outlined in Chapter 2. However, we used object-based classification because it was able to correctly classify

dark cover, including valley oak canopies and trees with shadows. Support vector machine (SVM) was used as the classifier because it had the highest accuracy of available classifiers. Developed land use classes, including agriculture and urban areas, were removed, but water was able to be retained. The following cover classes were defined in a supervised classification schema: water, barren, herbaceous, shrub, riparian forest, and valley oak. Herbaceous represents dry grassland, and could be considered part of the California Wildlife Habitat Relationships (CWHR) type perennial grassland (PGS) or valley oak woodland (VOW), since it is distributed similarly to, and among, valley oak trees (California Department of Fish and Wildlife, 2023). Another study, where researchers manually digitized land cover from aerial infrared imagery, used similar classifications along Lower Putah Creek (parentheses indicate our cover type names): open water (water), bare ground (barren), shrub/scrub (shrub), grassland (herbaceous), riparian forest (riparian forest), and oak woodland (valley oak) (U.S. Fish and Wildlife Service, 1992).

Shrub was classified using samples taken on sandbar willow (*Salix exigua*), the main shrub cover on Lower Putah Creek; the shrub cover type qualifies in CWHR as valley foothill riparian (VRI), along with the riparian forest VRI cover type (California Department of Fish and Wildlife, 2023). VRI canopy species on Lower Putah Creek primarily include: Fremont's cottonwood (*Populus fremontii*), white alder (*Alnus rhombifolia*), box elder (*Acer negundo*), Goodding's willow (*Salix gooddingii*), Oregon ash (*Fraxinus latifolia*), and red willow (*Salix laevigata*). Also, while valley oak (*Quercus lobata*) can be found in California riparian forests, it tends to be distributed mostly at relatively higher relative elevations, like riverbank terraces. Since valley oak also has the darkest leaves of the tree species in the study area, it was possible to distinguish valley oak from the lighter-colored riparian forest species. In this study system,



elevational gradients were steep and hard to distinguish, but the “valley oak” cover type qualifies in CWHR as valley oak woodland (VOW) (California Department of Fish and Wildlife, 2023). An accuracy assessment was performed using the same methods outlined in Chapter 2, with 50 assessment points per class.

The distribution of each class was characterized by HAR using methods outlined in Chapter 2 in order to identify potential vegetation zonation. The mean and distribution of HAR values of each land cover type were calculated in the Zonal Statistics and Zonal Histogram tools. Outputs from Zonal Histogram were plotted in MS Excel.

### **3.3 Random forest imagery classification using height above river**

In ArcGIS Pro, the Forest-based Classification and Regression tool was used to create a classified raster surface, predicted according to HAR, using the same training samples as the SVM classification. While other types of machine learning classification methods, such as SVM, use pixel color and grouping (in the case of object-based classification) to classify an image, random forest classification is predictive; the inputs are the same training samples used in the SVM classification, but the surface (or surfaces) on which classified values are predicted is the explanatory variable, not the imagery. In this study, the only explanatory variable is HAR. Models were run using 5-100 trees, and 10% of the training samples were saved for validation. The model with 100 trees predicted with the greatest accuracy, although all models had similar accuracy and nearly identical classification outputs.

To compare the total area of each cover type actually in the study area to what was predicted to be there based on HAR, the random forest classified surface was clipped to the SVM

classified surface. The area of each cover type in the clipped area was compared between the SVM-classified model and the HAR-based model.

### **3.4 Identifying potential restoration sites**

Graphical outputs from the random forest land cover classification, as well as visual analysis of the classified raster, were used to create six vegetation zones based on their predictive relationship to HAR, from: aquatic, core riparian, marginal riparian, transition, valley oak, to out-of-channel. Stream reaches were then defined by visual analysis of the six HAR zones, where each reach had relatively uniform geomorphology throughout its length. In all, 25 reaches were delineated and table-joined with their geomorphological (e.g., channel slope, bank slope), zonal HAR, and vegetation values (**Appendix Tables A.3-A.7**). Reaches were scored by the sum of two independent rankings: (1) the in-channel (<30-ft HAR) relative area of their combined core riparian and marginal riparian zones; and (2) the in-channel relative area of their combined aquatic and transition zones.

Significant reach-scale variation in the relative area of HAR zones enabled quantification of each reach by degree of degradation. Reaches were ranked by the sum of two independent rankings: (1) the in-channel relative area of their combined core riparian and marginal riparian zones; and (2) the in-channel relative area of their combined aquatic and transition zones (**Table 3.8**). They were then placed into four broad degradation categories based on close visual examination of the HAR classification raster. While the differences between reaches are continuous, this discrete categorization is only intended as a planning tool:

- Reference: large relative area of riparian, small relative area of aquatic and transition, little-to-no geomorphological restoration required (sum ranking: 4-10)

- Somewhat degraded: moderate area of riparian, moderate area of aquatic and transition, some geomorphological restoration required to narrow the baseflow channel and/or lower the floodplain (sum ranking:12-22)
- Moderately degraded: small area of riparian, moderate-to-large area of aquatic and transition, major geomorphological restoration required to narrow the baseflow channel and/or lower the floodplain (sum ranking: 29-36)
- Severely degraded: small area of riparian, large area of aquatic and/or transition, radical geomorphological restoration required to narrow the baseflow channel and/or lower the floodplain channel (sum ranking: 40-43)

### **3.5 Prescribing restoration actions**

Using outputs from the reach-scale ranking as well as reach-scale statistics, degraded reaches were prescribed one of two geomorphological restoration actions: baseflow narrowing or floodplain lowering. Reaches with greater than 20% aquatic zone were prescribed baseflow narrowing, and reaches with greater than 24% transition zone were prescribed floodplain lowering. Additionally, reaches could qualify for baseflow narrowing if their mean baseflow width was greater than 60 feet; this ensured that reaches with atypical geomorphology were still prescribed the correct restoration action. Reaches were visually examined to ensure these criteria appropriately determined restoration actions.

## 4. Results

### 4.1 1-D flow modeling

Inundation polygons are shown in **Figure 3.3**. In **Figure 3.4**, a trendline indicates a linear relationship between discharge (cfs) and inundated area (acres), although there is a non-linear relationship between recurrence interval and discharge (**Figure 1.6b**). The smoothness of the relationship indicates that, across the entire creek, there is not a discharge contributing significantly to floodplain dynamics, relative to other discharges. To a certain extent, the 1-yr flow breaks out of the baseflow channel, but it only adds 31 acres of inundated area, or 23% more area, above the baseflow. Around a discharge of 16,000 cfs, the area gained by increasing flow diminishes, perhaps due to increased bank steepness beginning at that HAR level (11 ft HAR). These results indicate Lower Putah Creek may not have a clear dominant discharge, or a channel-forming discharge, like alluvial and gravel-bed rivers (Bray, 1975; Doyle et al., 2007; Perry et al., 2015; West and Niezgoda, 2006).

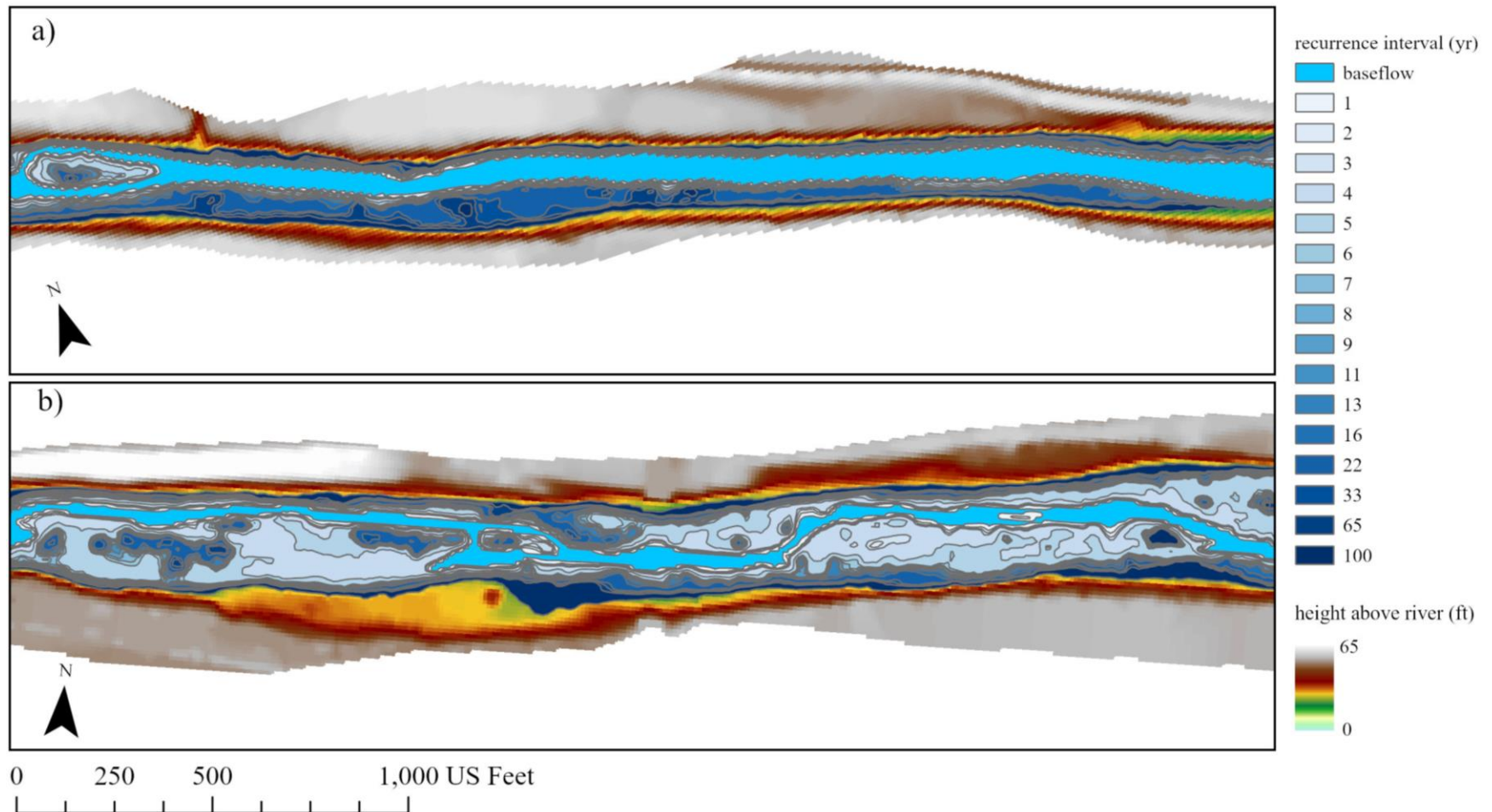


**Figure 3.3.** Inundation areas for all modeled recurrence intervals, overlaid on the HAR (ft) raster. (a) River-miles 11 and (b) 10 experience very different flow dynamics due to their geomorphology; the steep banks and wide baseflow channel at river-mile 11 has essentially no regularly active floodplain, whereas the shallower banks and narrow baseflow channel at river-mile 10 supports a large and frequently-inundated floodplain.

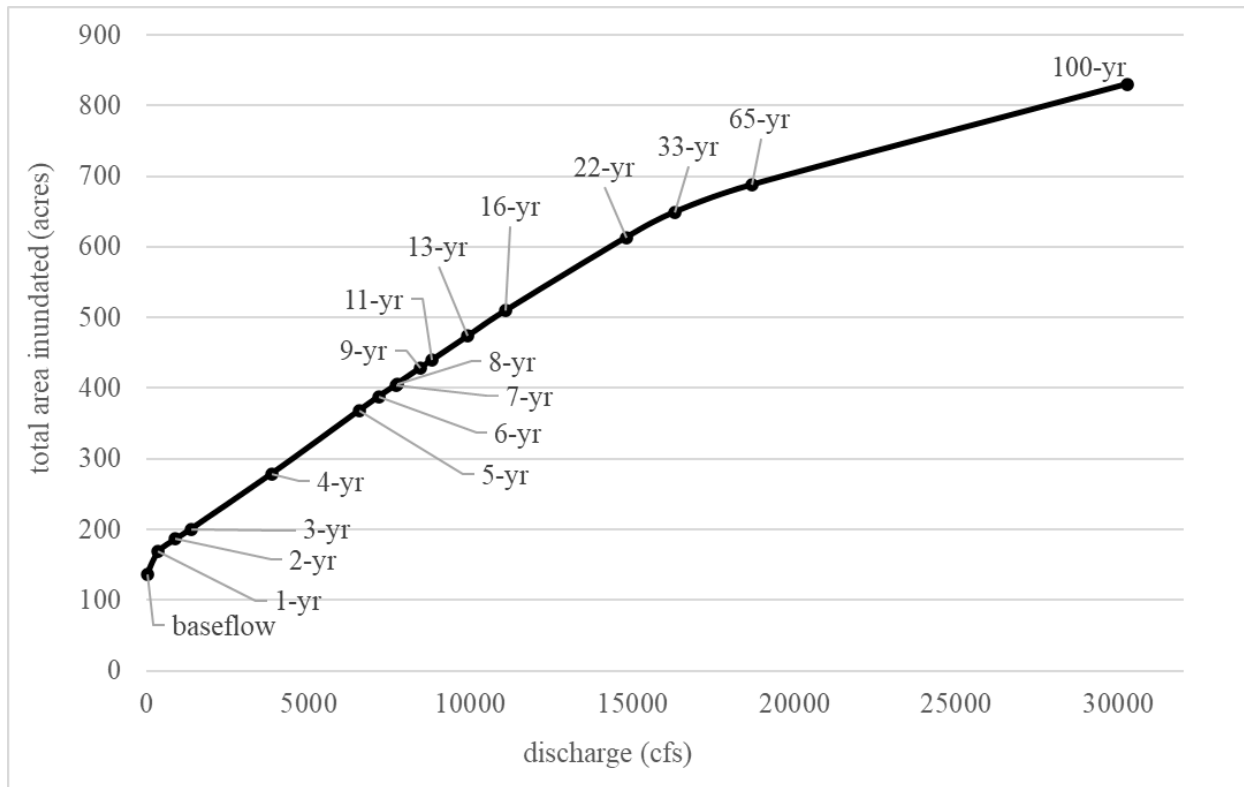


**Figure 3.4.** Total inundated area by discharge. Modeled recurrence interval flows are indicated with leader lines. Across the study area, channel surface area is inundated in a predictable way according to discharge, but not according to recurrence interval.

There is a logarithmic relationship between discharge and the mean HAR of inundation surface edge (**Figure 3.5**), although the curve is most apparent with flows smaller than 7,000 cfs. Logically, this corroborates the linear relationship in **Figure 3.3** and is based on the cross-sectional area of the channel. As water rises in a V-shaped channel (see Chapter 1), an incremental increase in flow is spread over a larger X-Y plane than the same volume increment before it, so the rise in Z is less than the one before it. Since HAR appears to be strongly correlated to discharge on Lower Putah Creek, even if there is not a clear dominant discharge, it can be used as a representation of inundation frequency.

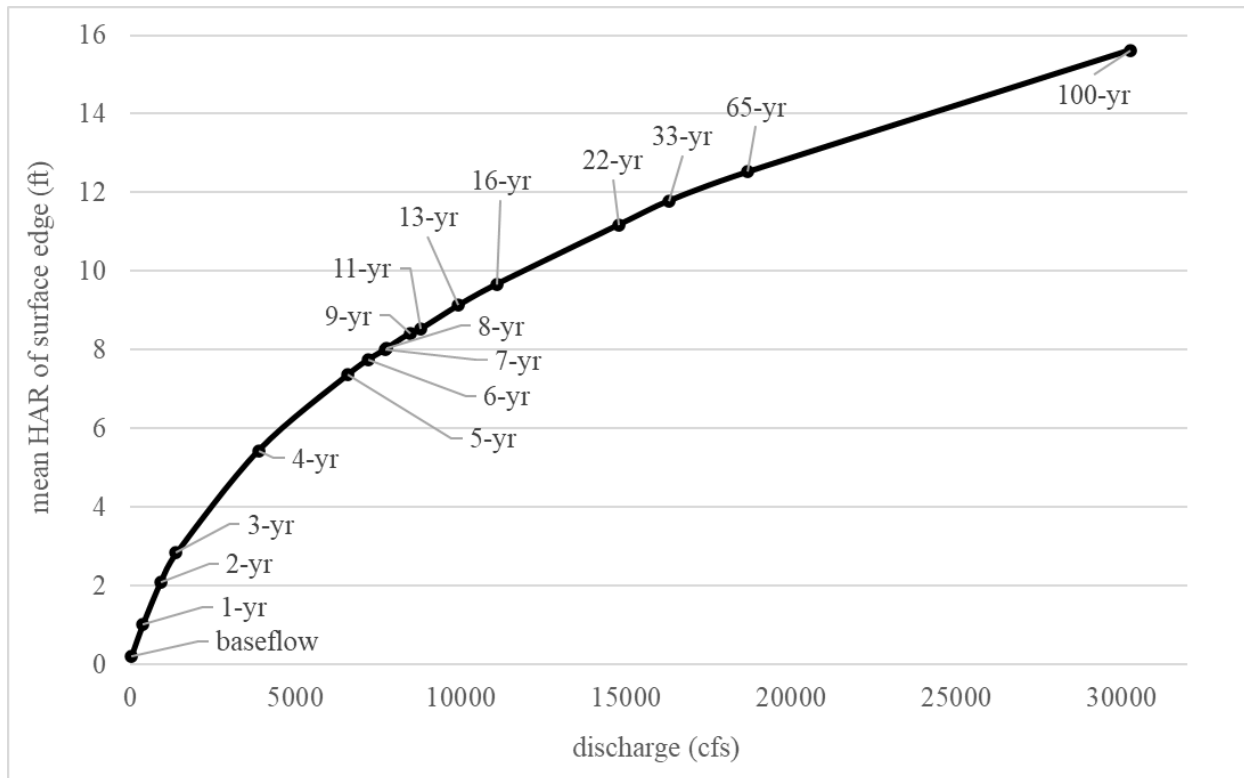


**Figure 3.5.** Mean HAR of inundation surface edge by discharge. Recurrence interval flows are indicated with leader lines. Across the study area, the HAR value of discharge is predictable according to the size of the flow, and vice versa.

#### 4.2 Support vector machine imagery classification and geomorphic distribution

Of the 1,146 acres of SVM-classified imagery, 995 acres (86.8%) were classified as vegetated (**Table 3.2**); the other 151 acres (13.2%) were classified relatively evenly between water and barren. The baseflow water surface (**Figure 3.3**) is 136.8 acres, but because vegetation hangs over the water's surface and thus hides much of the water from aerial imagery, it constituted only 77.2 acres (6.7%) of the classified output.

Of the total vegetated area (excluding water and barren), herbaceous covered 309.4 acres (31.1%), shrub covered 88.6 acres (8.9%), riparian forest covered 257.2 acres (25.9%), and valley oak covered 339.5 acres (34.1%). Riparian forest and shrub are effectively the same CWHR classification (VRI) (California Department of Fish and Wildlife, 2023) and together

constitute 34.8% of the vegetated area. A sample of the classified land cover is shown in **Figure 3.6**.

**Table 3.2.** SVM-classified land cover area and proportional cover, including absolute cover (% of total area) and relative cover (% of vegetative cover).

<b>land cover</b>	<b>water</b>	<b>barren</b>	<b>herbaceous</b>	<b>shrub</b>	<b>rip. forest</b>	<b>valley oak</b>	<b>total</b>	<b>total veg.</b>
<b>area (ac)</b>	77.2	73.8	309.4	88.6	257.2	339.5	1,146	995
<b>absolute cover (%)</b>	6.7	6.4	27.0	7.7	22.4	29.6	100	86.8
<b>relative vegetation cover (%)</b>			31.1	8.9	25.9	34.1	100	



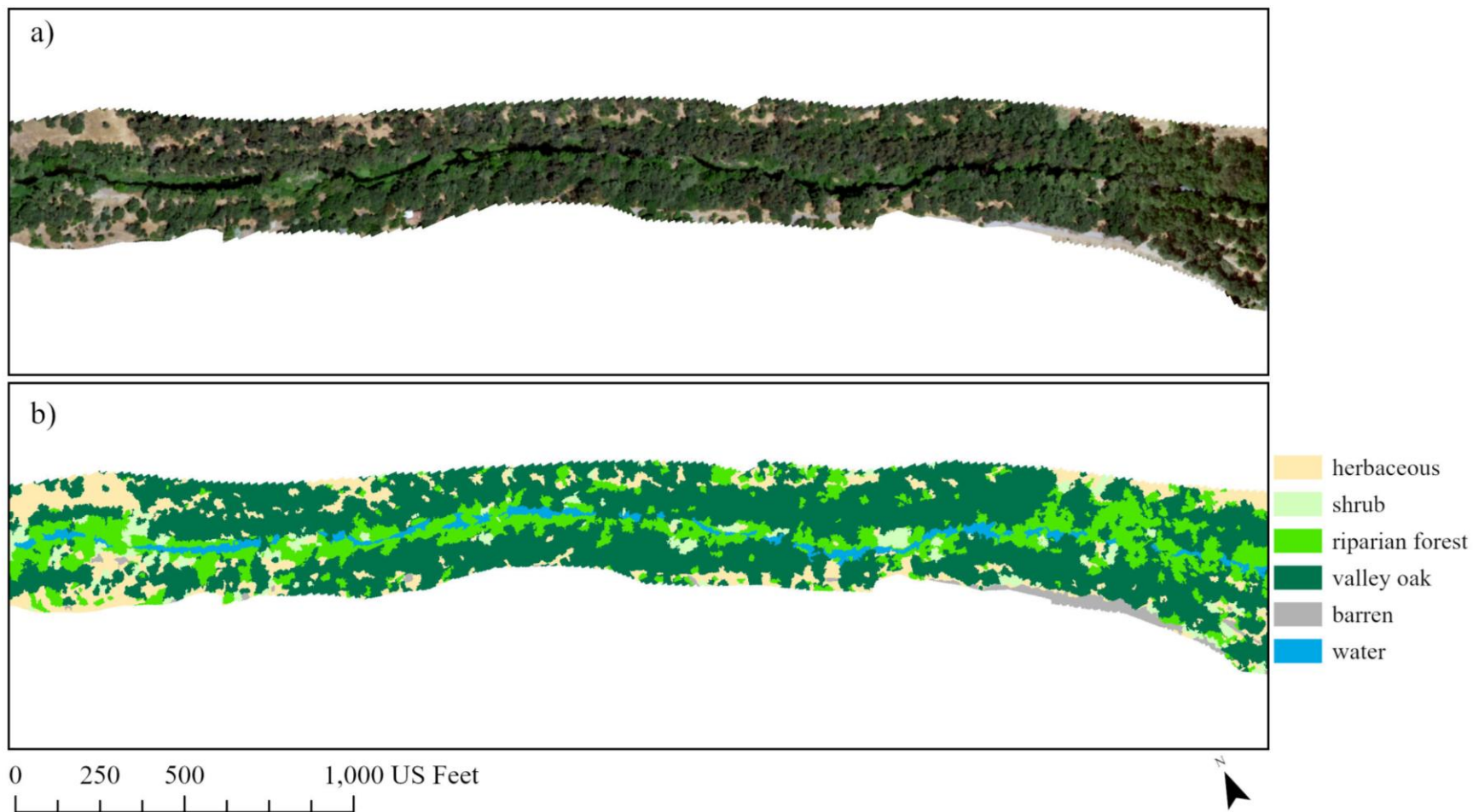


**Figure 3.6.** (a) Aerial imagery and (b) SVM land cover classification. The darkest foliage in the aerial imagery (2020 NAIP) is classified as valley oak. This site is from river-miles 12-13, just downstream, or east, of Stevenson Bridge.

Accuracy of the imagery classification was estimated using a transition matrix (**Table 3.3**) (Congalton and Green, 2008; Olofsson et al., 2014). Producer’s accuracy (1 - omission error) was 91% for water, 100% for barren, 89% for herbaceous, 95% for shrub, 88% for riparian forest, and 96% for valley oak. User’s accuracy (1 - commission error) was 100% for water, 96% for barren, 98% for herbaceous, 82% for shrub, 92% for riparian forest, and 90% for valley oak. Overall accuracy was 93%, and Kappa, which accounts for uneven sampling distribution, was 0.92. These values indicate an excellent classification model, with accuracy typical of other SVM machine learning models (Sheykhmousa et al., 2020).

**Table 3.3.** Confusion matrix for the SVM imagery classification accuracy assessment. Producer’s accuracy (1 - omission error) is presented vertically and user’s accuracy (1 - commission error) is presented horizontally. Kappa is in the bottom right.

	water	barren	herbaceous	shrub	rip. forest	valley oak	total	user's accuracy	Kappa
water	50	0	0	0	0	0	50	1.00	
barren	1	48	1	0	0	0	50	0.96	
herbaceous	0	0	49	1	0	0	50	0.98	
shrub	0	0	3	41	5	1	50	0.82	
rip. forest	2	0	0	1	46	1	50	0.92	
valley oak	2	0	2	0	1	45	50	0.90	
total	55	48	55	43	52	47	300		
producer's accuracy	0.91	1.00	0.89	0.95	0.88	0.96		0.93	
Kappa									0.92

Each cover type was distributed unevenly according to HAR (**Figure 3.7**). Barren cover is found in the lowest zones (<17-ft HAR), but its uneven distribution curve suggests there is a

disturbed area somewhere in the channel in the 12-17-ft HAR zone, possibly from landowner operations. The mean HAR of barren cover is 15.4 ft (SD = 8.4 ft) (**Table 3.4**). Herbaceous cover peaks at 11-ft HAR but is found in significant amounts across the study area above 2-ft HAR. The mean HAR of herbaceous cover is 16.5 ft (SD = 8.8 ft). Except for the 0-1-ft HAR spike, shrub cover peaks between 7-ft and 12-ft HAR and is not found in notable amounts above 16-ft HAR. The mean HAR of shrub cover is 9.2 ft (SD = 11.0 ft). Except for the 0-1-ft HAR spike, riparian forest cover peaks at 8-ft HAR and is not distributed in notable amounts above 17-ft HAR. The mean HAR of riparian forest cover is 8.6 ft (SD = 10.9 ft). Valley oak cover peaks between 10 and 12-ft HAR but is distributed in large amounts across the study site above 4-ft HAR. The mean HAR of valley oak cover is 15.8 ft (SD = 11.3 ft). The spike in all cover types at 0-1-ft HAR (0-ft and 1-ft are grouped together here) represents not just the area of vegetation from 0-ft HAR to 1-ft HAR, but also the large amount of vegetation (59.6 acres) hanging over the 0-ft HAR baseflow surface. The large standard deviation (SD) in HAR for all cover types indicates a wide dispersion in values, mostly due to a large right-hand skew (higher relative elevations).

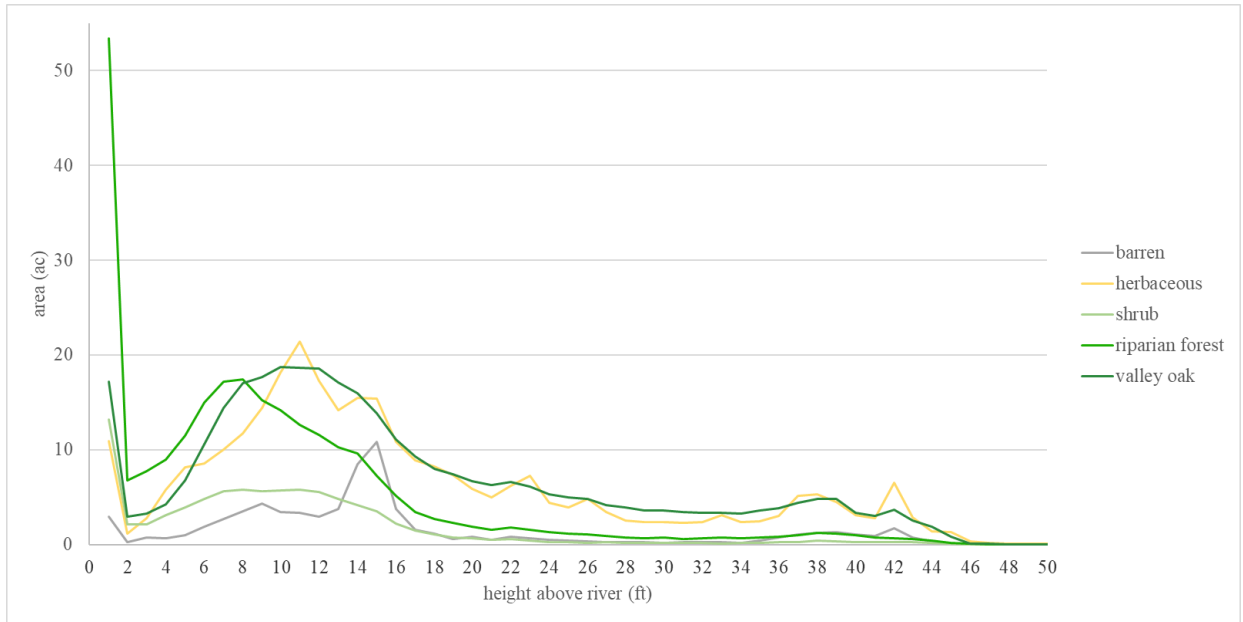


**Figure 3.7.** Distribution of each SVM-classified cover type by HAR. There is significant variation between cover types: riparian forest dominates, and peaks in, the lowest HAR areas. Shrub peaks higher than riparian forest, but tapers to near-zero around 19-ft HAR. Valley oak and herbaceous have similar distributions, although valley oak is found in higher density below 10 ft HAR.

**Table 3.4.** Mean and standard deviation (SD) of the HAR values (ft) of each land cover type in the SVM classification.

	barren	herbaceous	shrub	riparian forest	valley oak
<b>HAR mean (SD)</b>	15.4 (8.4)	16.5 (8.8)	9.2 (11.0)	8.6 (10.9)	15.8 (11.3)

Of the vegetation cover types, riparian forest dominates below 8-ft HAR, and shrub follows a very similar curve, although shrub is less prevalent in the lowest HAR zones (**Figure 3.8**). While both these types should be found in the lowest HAR zones only, they constitute a measurable amount of cover above 19-ft HAR; this may be due to the misclassification of several species. On Lower Putah Creek, black walnut (*Juglans hindsii*) and elderberry (*Sambucus* spp.) are distributed similarly to valley oak, but in much lower abundance, and have lighter-colored foliage; this might have been classified as riparian forest. Also, tamarisk

(*Tamarix* spp.), an invasive shrub, is found in small amounts on Lower Putah Creek, but its shading in the 2020 NAIP imagery is similar to sandbar willow and it can be found in mesic and xeric areas, above the lowest riparian zones; it might have been classified as shrub.

Valley oak and herbaceous cover somewhat equally dominate areas above 8-ft HAR, and are found in lesser, relatively equal, abundance below 8-ft HAR, indicating herbaceous cover is primarily dry grassland associated with valley oak, which can be considered valley oak woodland (VOW) (California Department of Fish and Wildlife, 2023).

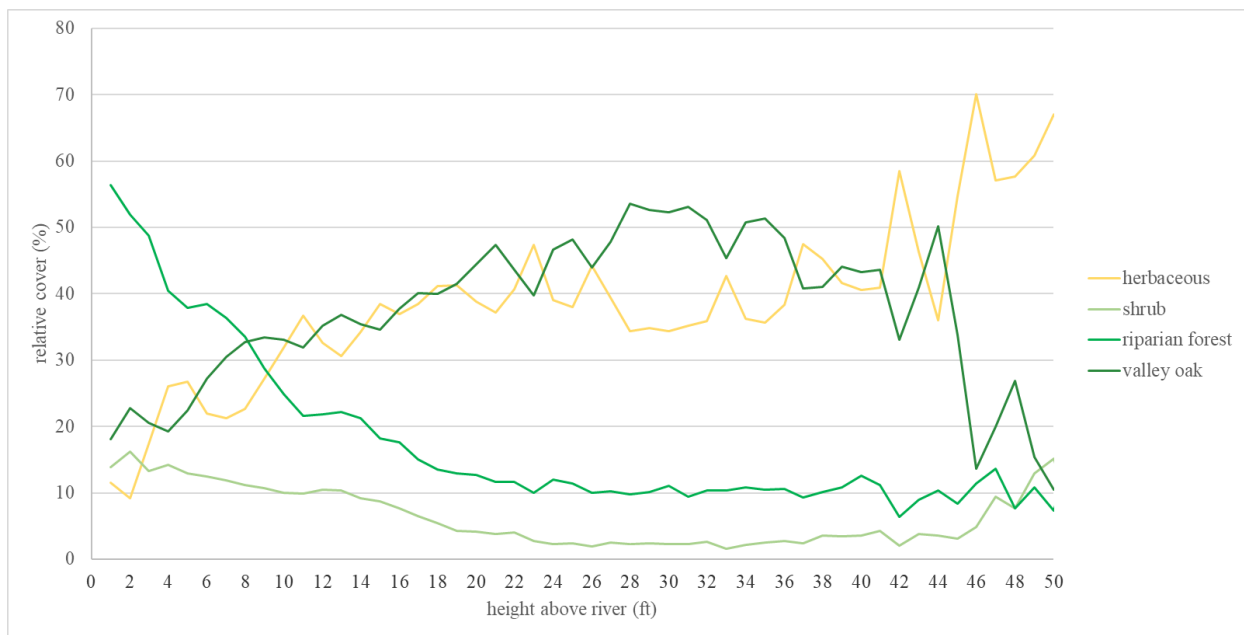


**Figure 3.8.** Relative cover of each vegetation cover type by HAR. Relative cover excludes barren and water from the total area. Riparian forest dominates below 8-ft HAR, and shrub follows a very similar distribution to riparian forest. Valley oak and herbaceous follow similar distributions. Values above 44 ft HAR are skewed due to the small amount of area of that relative elevation.

Riparian forest dominates in areas inundated by all modeled flow frequencies, although its dominance diminishes significantly in flows larger than 17,000 cfs (**Figure 3.9**). This curve could indicate a relationship between flow frequency and riparian cover, where high flow frequencies areas (low floodplains) are most suitable for riparian vegetation (Auble et al., 1994), or it could simply be a reflection of the broader relationship between HAR and riparian cover

(which could be more strongly based on depth to groundwater or soil moisture than flow frequency (Bair et al., 2021; Greco et al., 2008; Sagers et al., 1996; Vondrasek, 2015)). Shrub cover, another riparian cover type, is also primarily found where inundation surfaces are smaller than the 17,000-cfs flow, although because its curve is gentle, it does not appear to be as strongly tied as riparian forest cover to the lowest flow frequencies.

Valley oak and herbaceous cover follow curves very similar to the total inundated area curve (black line and secondary y-axis in **Figure 3.9**), perhaps indicating they are not affected by flow frequency, especially in low HAR areas of the channel (i.e., the 100-yr flow only reaches partway up the channel banks along most of Lower Putah Creek, and the vast majority of area above the 100-yr flow (15.5 ft HAR) is dominated by valley oak and herbaceous cover). Barren cover is spread evenly throughout all modeled flow frequency inundation surfaces, even up to the 100-yr flow, suggesting that any barren cover in the channel is not caused by flow dynamics but by other factors, such as landowner operations. Based on the significant vegetation succession—or recovery—found between 1937 and 2009 (Chapter 2), it would be expected that any barren areas caused by flow dynamics, such as floodplain sedimentation or scour outside of the baseflow channel, would fill in with woody vegetation. However, it appears there are very few places of “natural” barren cover, and/or that the barren cover that exists is entirely unrelated to flow frequency.

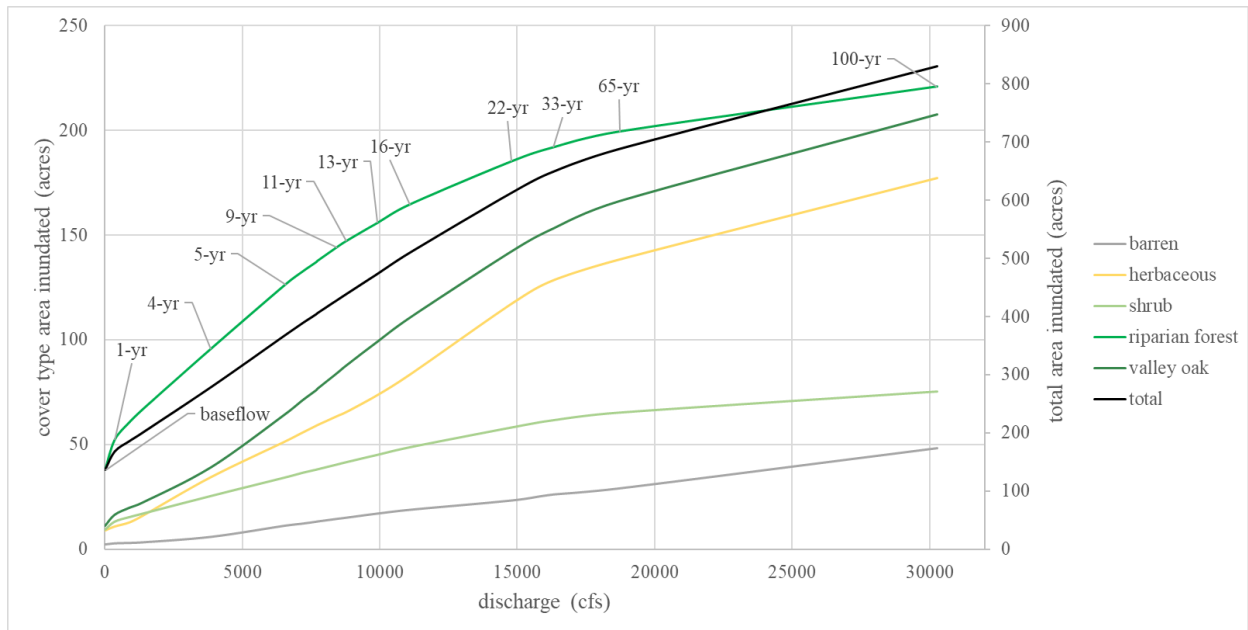


**Figure 3.9.** Inundated area of each cover type by discharge (cfs). Total inundated acreage of the study area (black line) is plotted on the secondary (right-hand) y-axis. Riparian forest and shrub follow markedly different curves than valley oak and herbaceous. Riparian forest dominates the smallest discharges but tapers off quickly in distribution starting around 9,000 cfs, more quickly than valley oak and herbaceous, whose curves continue rising in accordance with total available area. Shrub is somewhat less tied to the lowest discharges, beginning its taper around 15,000 cfs, but adds very little acreage above roughly 17,000 cfs.

#### 4.3 Random forest imagery classification using height above river

The random forest imagery classification covers the entire 1,551-acre study area (**Figure 1.3**) because it was predicted using the maximum HAR surface (**Figure 3.10a**), which covers the entire study area. This is in contrast to the SVM-classified surface, which excluded agricultural and urban areas and only totaled 1,146 acres. In the random forest model, water covered the same area as the baseflow water surface (136.9 acres), barren covered 65.4 acres, herbaceous covered 400.1 acres (29.7% of the vegetated cover), shrub covered 96.9 acres (7.2% of the vegetated cover), riparian forest covered 348.5 acres (25.8% of the vegetated cover), and valley oak covered 503.6 acres (37.3% of the vegetated cover) (**Table 3.5**). A sample of the classified surface is shown in **Figure 3.10b**.

**Table 3.5.** Random forest-classified land cover area (ac) and proportional cover (%) across the entire 1,551-acre study area.

<b>predicted land cover</b>	<b>water</b>	<b>barren</b>	<b>herbaceous</b>	<b>shrub</b>	<b>rip. forest</b>	<b>valley oak</b>	<b>total</b>	<b>total veg.</b>
<b>area (ac)</b>	136.9	65.4	400.1	96.9	348.5	503.6	1,551	1,349
<b>absolute cover (%)</b>	8.8	4.2	25.8	6.2	22.5	32.5	100	87.0
<b>relative cover (%)</b>			29.7	7.2	25.8	37.3	100	



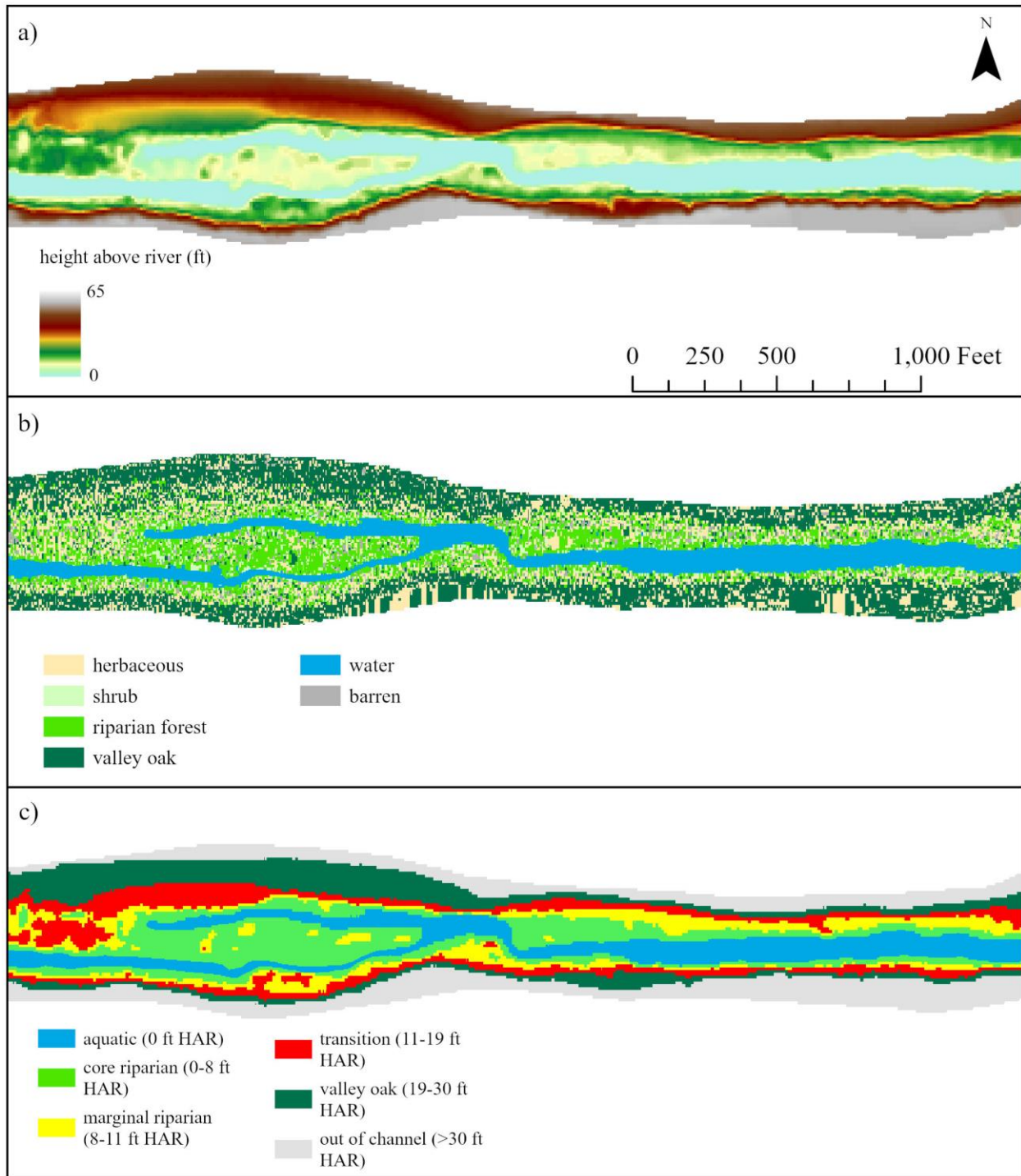


**Figure 3.10.** Maps showing (a) HAR, (b) the random forest classification, and (c) the reclassified HAR zones. The HAR surface shows height of the topography above the baseflow surface, the random forest classification shows clear boundaries in cover type distribution, and the HAR zones classify the topography for planning purposes. At this site (river-mile 16.5, upstream of Walnut Bayou Lane), there is a mix of functional and dysfunctional topography. On the left, there is a relatively functional riparian area with a narrow baseflow channel and large core riparian zone. On the right, there is a wide baseflow channel and very little riparian zone.

The relative cover of herbaceous and shrub is very similar between the SVM and random forest classifications, but the relative cover of riparian forest is noticeably higher under the random forest classification and valley oak is noticeably lower, suggesting that the random forest predictive model could be overestimating the dominance of riparian forest in the masked study area (**Table 3.6**).

**Table 3.6.** Random forest classification of land cover area masked to the same coverage as the SVM classified output. This includes absolute cover (% of total area) and relative cover (% of vegetative cover).

<b>predicted land cover</b>	<b>water</b>	<b>barren</b>	<b>herbaceous</b>	<b>shrub</b>	<b>rip. forest</b>	<b>valley oak</b>	<b>total</b>	<b>total veg.</b>
<b>area (ac)</b>	77.2	56.2	278.8	84.9	301.8	266.5	1,065	932
<b>absolute cover (%)</b>	7.2	5.3	26.2	8.0	28.4	25.0	100	87.6
<b>relative cover (%)</b>			29.9	9.1	32.4	28.6	100	

In order to create an appropriate comparison between the SVM (“true cover”) and random forest classification (“predicted cover”), we assumed that the predicted water cover from the random forest classification, found exclusively in 0-ft HAR areas but not removed during the intersection with the SVM classified raster, would otherwise be covered by vegetation hanging over the water surface (this counts as cover only, not planting area). The proportion of each class predicted in this zone (<1-ft HAR) is 69% riparian forest, 27% shrub, and 4% valley oak. After extraction using the SVM classification surface as a mask (which removed areas of water in both SVM and random forest outputs), the random forest classification surface still contains 76.1 acres of water; this area can be assumed to be 52.5 acres of riparian forest, 20.5 acres of shrub, and 3.0 acres of valley oak. With the addition of this vegetation cover, the relative cover of each

type in the random forest classification would change (**Table 3.7**), increasing the relative cover of riparian types (shrub, riparian forest) and decreasing the relative cover of barren, herbaceous, and valley oak. In this case, the random forest classification overestimates riparian forest by nearly 10%, and underestimates other vegetative cover types.

**Table 3.7.** Random forest classification of land cover area masked to the same coverage as the SVM classified output, and with excess water converted back to vegetative cover.

<b>predicted land cover</b>	<b>water</b>	<b>barren</b>	<b>herbaceous</b>	<b>shrub</b>	<b>rip. forest</b>	<b>valley oak</b>	<b>total</b>	<b>total veg.</b>
<b>area (ac)</b>	76.1	56.2	278.8	105.4	354.3	269.5	1,140	1,008
<b>absolute cover (%)</b>	6.7	4.9	24.4	9.2	31.1	23.6	100	88.4
<b>relative cover (%)</b>			27.7	10.5	35.1	26.7	100	

Accuracy of the random forest classification was estimated using a transition matrix (**Table 3.8**) (Congalton and Green, 2008; Olofsson et al., 2014). Producer’s accuracy (1 - omission error) was 80% for water, 87% for barren, 93% for herbaceous, 87% for shrub, 83% for riparian forest, and 92% for valley oak. User’s accuracy (1 - commission error) was 99% for water, 87% for barren, 91% for herbaceous, 79% for shrub, 68% for riparian forest, and 91% for valley oak. Overall accuracy was 88%, and Kappa, which accounts for uneven sampling distribution, was 0.76. These values indicate a very good classification model, with accuracy typical of other random forest classification models (Sheykhmousa et al., 2020). Low user’s accuracy for riparian forest is in large part due to misclassification of riparian forest as shrub; however, in this study, shrub and riparian forest both represent the same CWHR habitat type (VRI) (California Department of Fish and Wildlife, 2023), so the low accuracy here is not of technical concern. If the misclassifications of riparian forest as shrub were corrected, riparian

forest user’s accuracy would increase to 79%. However, because riparian forest had low accuracy relative to other classes, and because the relative area of riparian forest in the clipped area is significantly higher (**Table 3.7**) than in the SVM classification (**Table 3.2**), it should be noted that it is the least-reliably predicted cover among the vegetation cover types, but still acceptable at 0.83 producer’s accuracy and 0.68 user’s accuracy (**Table 3.8**).

**Table 3.8.** Confusion matrix for the random forest classification validation (stratified random validation sampling). Producer’s accuracy (1 - omission error) is presented vertically and user’s accuracy (1 - commission error) is presented horizontally. Kappa is in the bottom right.

100 trees	water	barren	herbaceous	shrub	rip. forest	valley oak	total	user's accuracy	Kappa
water	1079	0	1	9	5	0	1094	0.99	
barren	2	324	16	21	2	8	373	0.87	
herbaceous	25	21	2033	62	15	68	2224	0.91	
shrub	163	19	60	1174	35	30	1481	0.79	
rip. forest	67	3	13	47	301	11	442	0.68	
valley oak	15	6	67	36	5	1304	1433	0.91	
total	1351	373	2190	1349	363	1421	7047		
producer's accuracy	0.80	0.87	0.93	0.87	0.83	0.92		0.88	
Kappa									0.76

In the random forest imagery classification, cover types were classified into relatively distinct HAR zones (**Figure 3.11**), especially compared to their distribution in the SVM classification, supporting existing studies that show HAR is a strong predictor of vegetation type in riparian areas (Friedman et al., 2006; Greco et al., 2008; Ibarra et al., 2019). Barren, shrub, and riparian forest were classified almost exclusively into areas from 0-ft to 17-ft HAR. Herbaceous was distributed mostly between 7 ft HAR and 27 ft HAR, although it was distributed

in notable amounts up to 43 ft HAR. Valley oak was found as low as 0 ft HAR but was distributed in increasing amounts above 3 ft HAR, becoming the dominant cover type above 17 ft HAR (**Figure 3.12**). Riparian forest clearly dominates below 8 ft HAR, accompanied by shrub, and together riparian forest and shrub have a dominant role up to about 12-16 ft HAR.

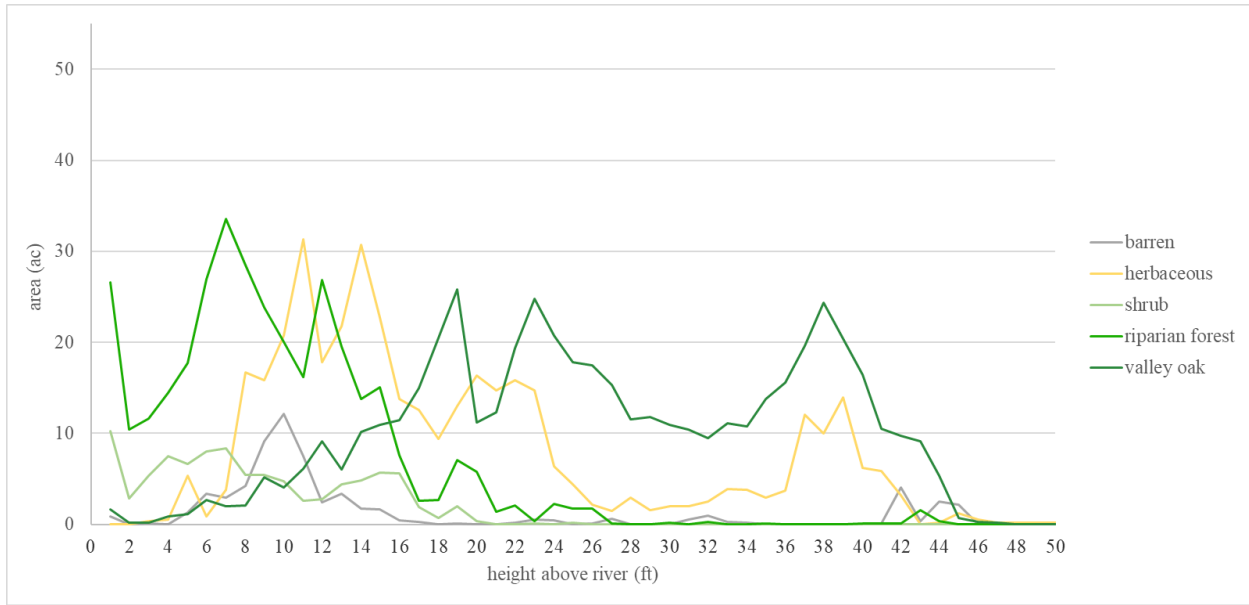


**Figure 3.11.** Distribution of each cover type by HAR in the random forest classification. In this model, riparian forest very strongly dominates the lowest HAR zones, in alliance with shrub. Valley oak slowly increases in density to around 17-ft HAR, above which it dominates in cover. Herbaceous distribution is variable, peaking at 10-14-ft HAR, but does not clearly dominate any one area. Barren cover peaks at relatively low HAR and tapers to near zero around 16-ft HAR.

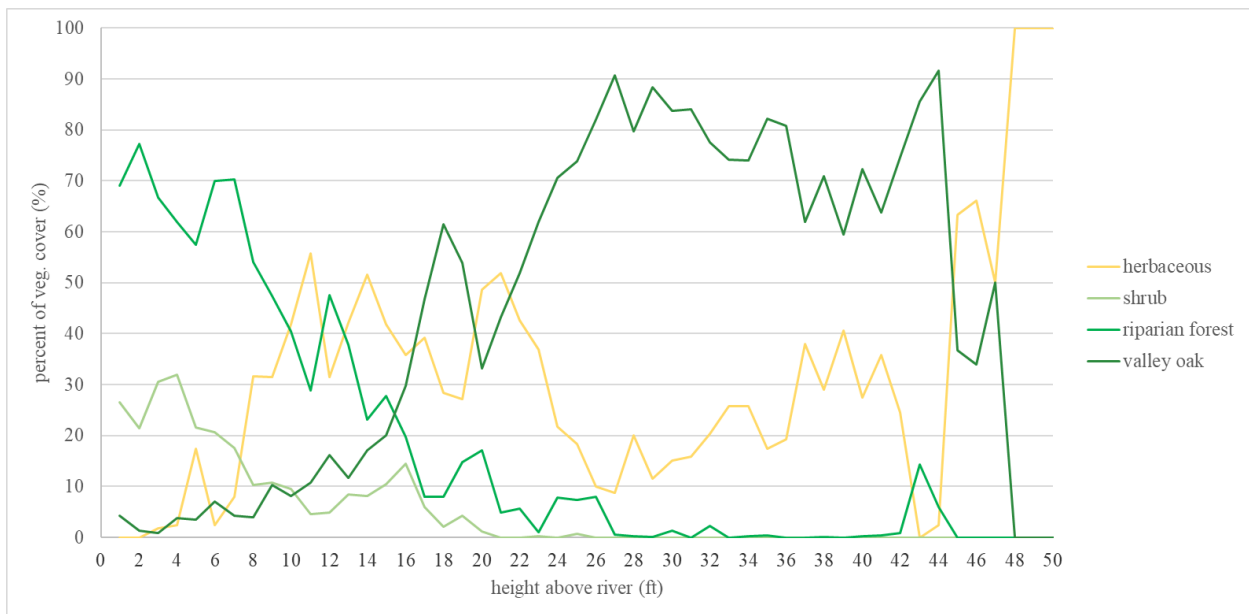


**Figure 3.12.** Relative cover of each vegetative type by HAR in the random forest classification. Here, the dominance of each cover type is even clearer than in **Figure 3.9**. Riparian forest and shrub dominate the lowest HAR zones, and valley oak dominates the high HAR zones. Herbaceous more clearly peaks in this graph at moderate HAR elevations (transition zone), where neither riparian forest nor valley oak clearly dominate. The distributions become erratic above 44 ft HAR because there are so few cells with values greater than 44 ft HAR.

#### 4.4 Identifying potential restoration sites

Based on the elevational distribution of cover types in the random forest classification, six HAR zones were developed for reach-scale geomorphological assessment and restoration planning: aquatic (0 ft HAR), core riparian (0-8 ft HAR), marginal riparian (8-11 ft HAR), transition (11-19 ft HAR), valley oak (19-30 ft HAR), and out-of-channel (>30 ft HAR) (**Table 3.9** and **Figure 3.10c**). The riparian zones are intended for restoration planning, so they were delineated conservatively into the lowest HAR, where riparian forest and shrub both dominate over valley oak. For ranking, the core riparian and marginal riparian zones were combined into one riparian zone, but if planners wanted to be even more conservative, they could only consider the core riparian zone. While the transition zone is relatively wide, it was delineated with the purpose of identifying the area available for geomorphic modification (i.e., areas most suitable for floodplain lowering), including areas to source fill material for nearby channel-forming restoration. Out-of-channel was delineated as a zone because, along nearly the entire study area, places that are >30 ft HAR are at or beyond the top of the channel banks (as explained in Chapter 1, the study area was originally delineated in order to capture up to the top-of-bank in both the 1905 and 2005 DEMs, so there is some area captured here that is irrelevant for planning channel modifications). The out-of-channel zone accounted for 284.9 acres, or 18.4% of the study area. If considered relevant for restoration, it could be justifiably lumped into the valley oak zone or reclassified as upland (e.g., perennial grassland (PGS) (California Department of Fish and Wildlife, 2023)).

Across the entire study area, the aquatic zone totaled 152.5 acres (12% of the in-channel area), which is larger than the area of the actual baseflow surface (137 acres) due to some areas of 0-ft HAR that are physically separate from the baseflow channel (e.g., ponds). The core

riparian zone totaled 261.8 acres (20.7% of the in-channel area), marginal riparian totaled 186.8 acres (14.7% of the in-channel area), transition totaled 388.2 acres (30.6% of the in-channel area), and valley oak totaled 277.3 acres (21.9% of the in-channel area).

**Table 3.9.** Total area (ac) of each HAR zone across the study area (study area delineated in **Figure 1.3**).

<b>HAR zone</b>	<b>HAR (ft)</b>	<b>area (ac)</b>	<b>total proportional area (%)</b>	<b>proportional area in channel (&lt;30 ft) (%)</b>
<b>aquatic</b>	0	152.5	9.8	12.0
<b>core riparian</b>	0-8	261.8	16.9	20.7
<b>marginal riparian</b>	8-11	186.8	12.0	14.7
<b>transition</b>	11-19	388.2	25.0	30.6
<b>valley oak</b>	19-30	277.3	17.9	21.9
<b>out-of-channel</b>	30+	284.9	18.4	

The 25 delineated reaches, where each reach has a relatively uniform geomorphology from the reaches immediately upstream and downstream from it, are shown in **Figure 3.13**, and contextual reach locations in relation to river-miles and place names are shown in **Figure 3.14**. Statistics and place names near the reaches are in **Appendix Tables A.3-A.8**, and include the following values: river-miles, upstream and downstream thalweg elevations (ft), channel slope (% slope), bank slope (% slope), mean baseflow width (ft), area (ac) of each HAR zone, relative area (%) of each HAR zone in-channel, area (ac) of current land cover types, relative area (%) of current land cover types, and rankings.



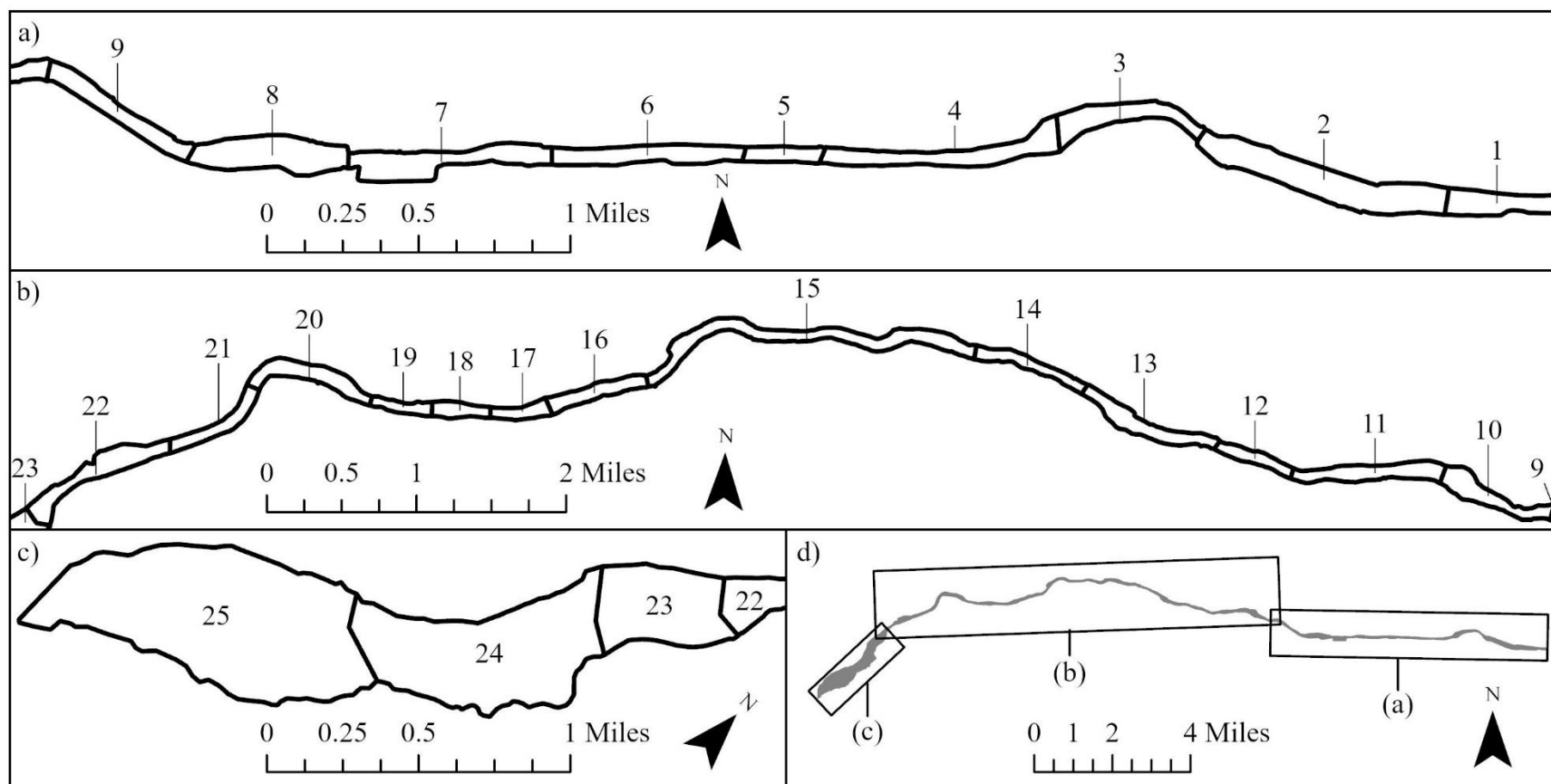


**Figure 3.13.** Boundaries of the 25 planning reaches, numbered from downstream (east) to upstream (west). Reach numbers are unrelated to river-miles. The (a) section is the South Fork from river-mile 1.54 near the Yolo Bypass to the fork, the (b) section is from the fork to Winters, and the (c) section is upstream of Winters. The placements of (a), (b), and (c) across the study area are shown in (d). Place names associated with reach numbers and river-miles are in **Figure 3.14** and **Appendix Table A.8**.

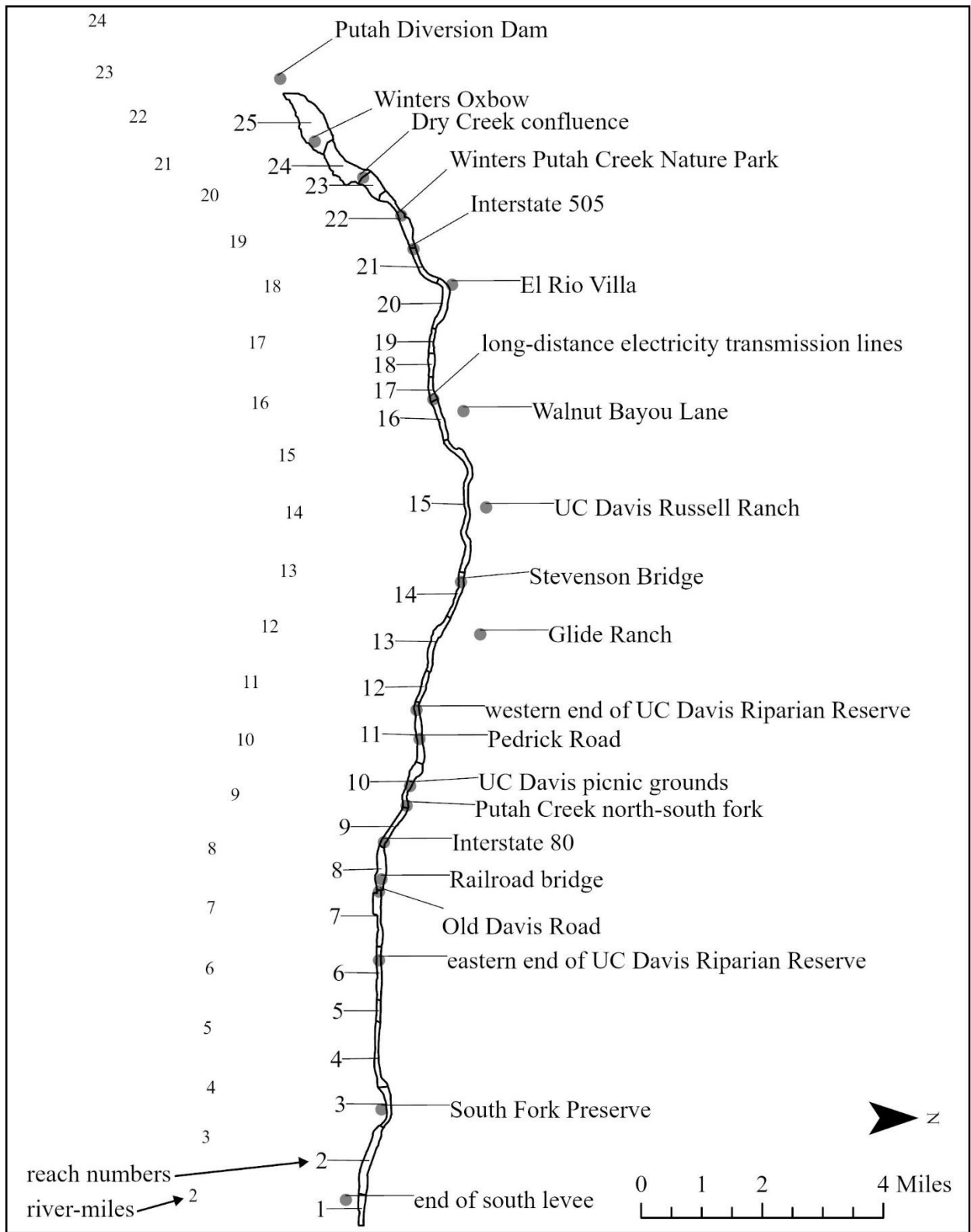


**Figure 3.14.** Reaches in relation to river-miles and place names (see Appendix Table A.8).

In total, 3.22 river-miles of creek qualify as “reference,” 7.46 river-miles qualify as “somewhat degraded,” 4.12 river-miles qualify as “moderately degraded,” and 6.42 river-miles qualify as “severely degraded” (**Table 3.10**). Examples of each reach type are shown in **Figure 3.15**, and the HAR zones map is shown by reach in **Appendix Figure A.2**. It is important to note that two areas of creek have been geomorphologically restored since the 2005 LiDAR was collected, and should be reanalyzed with current elevation models using the criteria in this study. The Winters Putah Creek Nature Park project restored all of reach #22 (somewhat degraded), and the Nishikawa project restored most of reach #12 (severely degraded). If these reaches were restored to “reference” conditions, then 4.85 river-miles of creek would qualify as “reference,” 6.32 river-miles would qualify as “somewhat degraded,” 4.12 river-miles would qualify as “moderately degraded,” and 5.91 river-miles would qualify as “severely degraded.”

**Table 3.10.** Sum ranking of reaches by HAR zones. Reaches were ranked by the sum of two independent rankings: (1) the in-channel relative area of their combined core riparian and marginal riparian zones; and (2) the in-channel relative area of their combined aquatic and transition zones. Green = “reference,” yellow = “somewhat degraded,” orange = “moderately degraded,” red = “severely degraded.” \*Note: In reaches 3, 23, and 24, some of the transition area currently hosts active cropland, so the reaches may have scored slightly higher if cropland areas were excluded.

Reach	downstream river-mile	upstream river-mile	aquatic (%)	core riparian (%)	marginal riparian (%)	transition (%)	combined riparian (%)	combined transition + aquatic (%)	riparian ranking (high % = high score (e.g. 1))	aquatic + transition ranking (high % = low score (e.g. 25))	sum ranking
6	5.56	6.46	14.6	42.4	7.1	12.5	49.4	27.1	3	1	4
9	8.15	8.93	11.3	31.9	13.7	18.5	45.5	29.8	4	2	6
4	4.07	5.2	10.1	46.3	14.3	29	60.7	39.1	1	9	10
18	16.65	17.06	15.6	29.6	13.3	17.1	43	32.7	7	3	10
1	1.54	2.05	16.7	36.1	24.3	22.9	60.4	39.6	2	10	12
11	9.73	10.78	13	25.4	17.7	24	43.1	37	6	6	12
22	19.13	20.27	21	27	16.9	17.3	43.8	38.3	5	8	13
25	21.65	22.75	2.9	22	19	32.1	41	35	10	5	15
*24	20.71	21.65	8	18.3	10.4	25.7	28.7	33.7	17	4	21
7	6.46	7.4	18.3	11.5	29.6	26	41.1	44.3	9	13	22
16	15.55	16.25	8.4	19.7	13.9	29	33.6	37.4	15	7	22
21	18.41	19.13	21	24.6	16	19.2	40.6	40.2	11	11	22
5	5.2	5.56	29	23.2	18.9	22.7	42.1	51.7	8	21	29
14	12.31	13.1	17.1	18	15.9	29.7	33.9	46.8	14	17	31
20	17.47	18.41	14.1	23.8	11.2	32.9	35	47	13	18	31
17	16.25	16.65	28	12.2	13.7	17.2	25.9	45.2	20	14	34
*3	3.28	4.07	17.7	19.9	18.8	40	38.7	57.7	12	24	36
8	7.4	8.15	7.6	9.7	7.2	33.7	16.9	41.3	24	12	36
*23	20.27	20.71	6.9	13.2	12.1	39.1	25.3	46	21	15	36
19	17.06	17.47	29	13.7	13.1	24.1	26.9	53.1	18	22	40
2	2.05	3.28	10	15.1	14.2	60.6	29.3	70.6	16	25	41
10	8.93	9.73	26.8	9.2	7	19.7	16.2	46.5	25	16	41
15	13.1	15.55	14.1	11.2	11.6	33.7	22.9	47.8	22	19	41
12	10.78	11.32	29	13.1	12.9	26.1	26	55.1	19	23	42
13	11.32	12.31	12.8	11.4	11.3	35.5	22.7	48.3	23	20	43

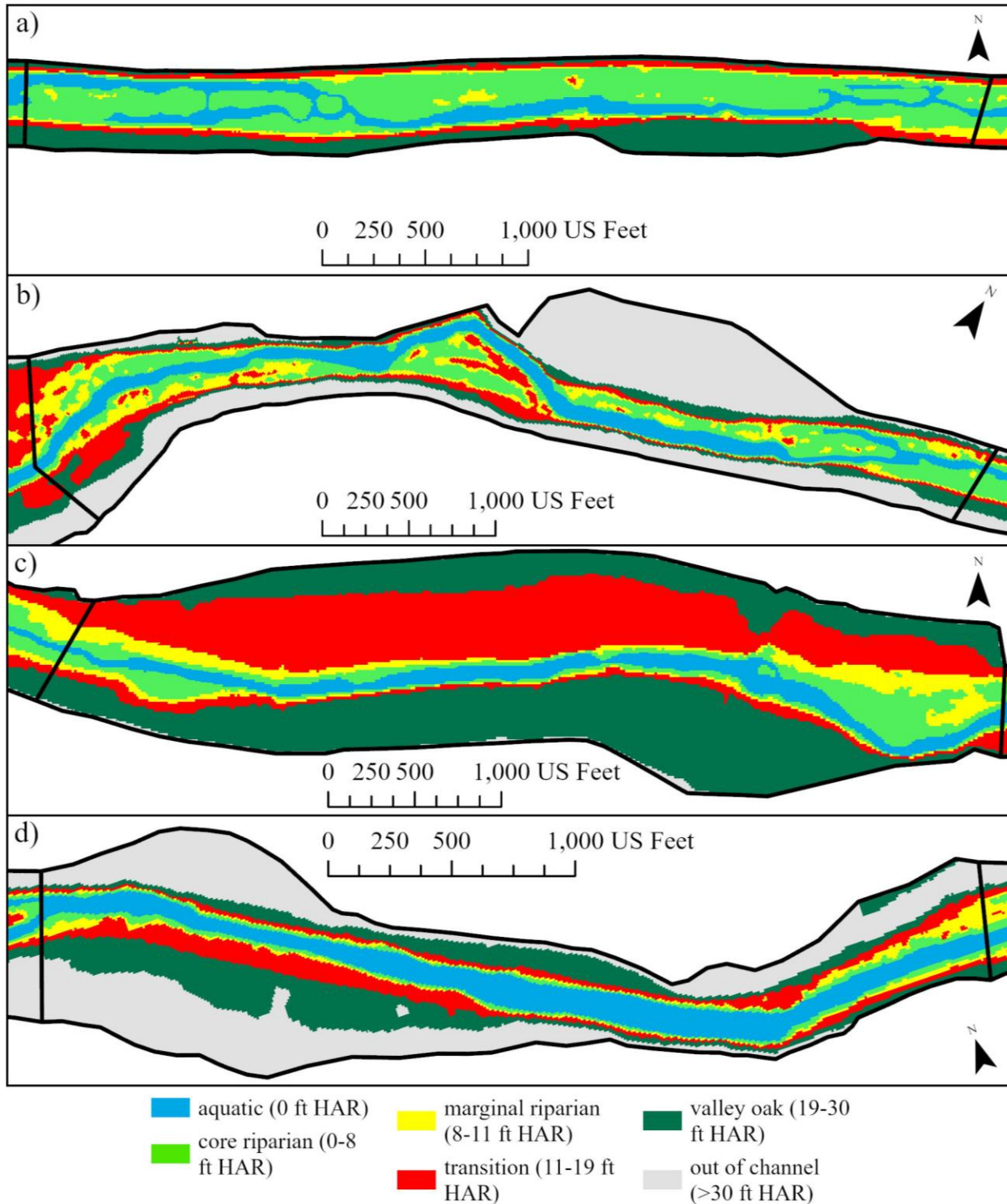


**Figure 3.15.** Examples of the four reach types, ranked by relative area of riparian zone and relative area of transition and aquatic zones. (a) The reference (reach 6) has a large area of riparian and very little aquatic and transition area; (b) the somewhat degraded reach (reach 22) has some functional riparian area but a moderate area of transition and aquatic; (c) the moderately degraded reach (reach 8) has a small riparian zone and large area of aquatic and transition; and (d) the severely degraded reach (reach 10) has almost no riparian area and a very large amount of aquatic and transition zone.

The spatial distribution of degradation is highly variable (**Figure 3.16**). However, some general patterns by large-scale sections of creek are apparent. The South Fork contains three of the four reference reaches, but the reference reaches are separated by moderately degraded reaches (**Figure 3.16a**). The most degraded stretch of creek is the canyon-like section from the fork to just downstream of Winters (**Figure 3.16b**), which has steepest banks and experienced the greatest incision along Lower Putah Creek since 1905 (Chapter 1, **Figure 1.12**). The Winters section, which contains only three reaches but is significantly wider than the rest of Lower Putah Creek (**Figure 3.16c**), is not severely degraded but might otherwise be a high-priority candidate for restoration because it has the potential to host a large total area of riparian zone compared to the narrower reaches of the creek (see area of each zone by reach in **Appendix Table A.3**).

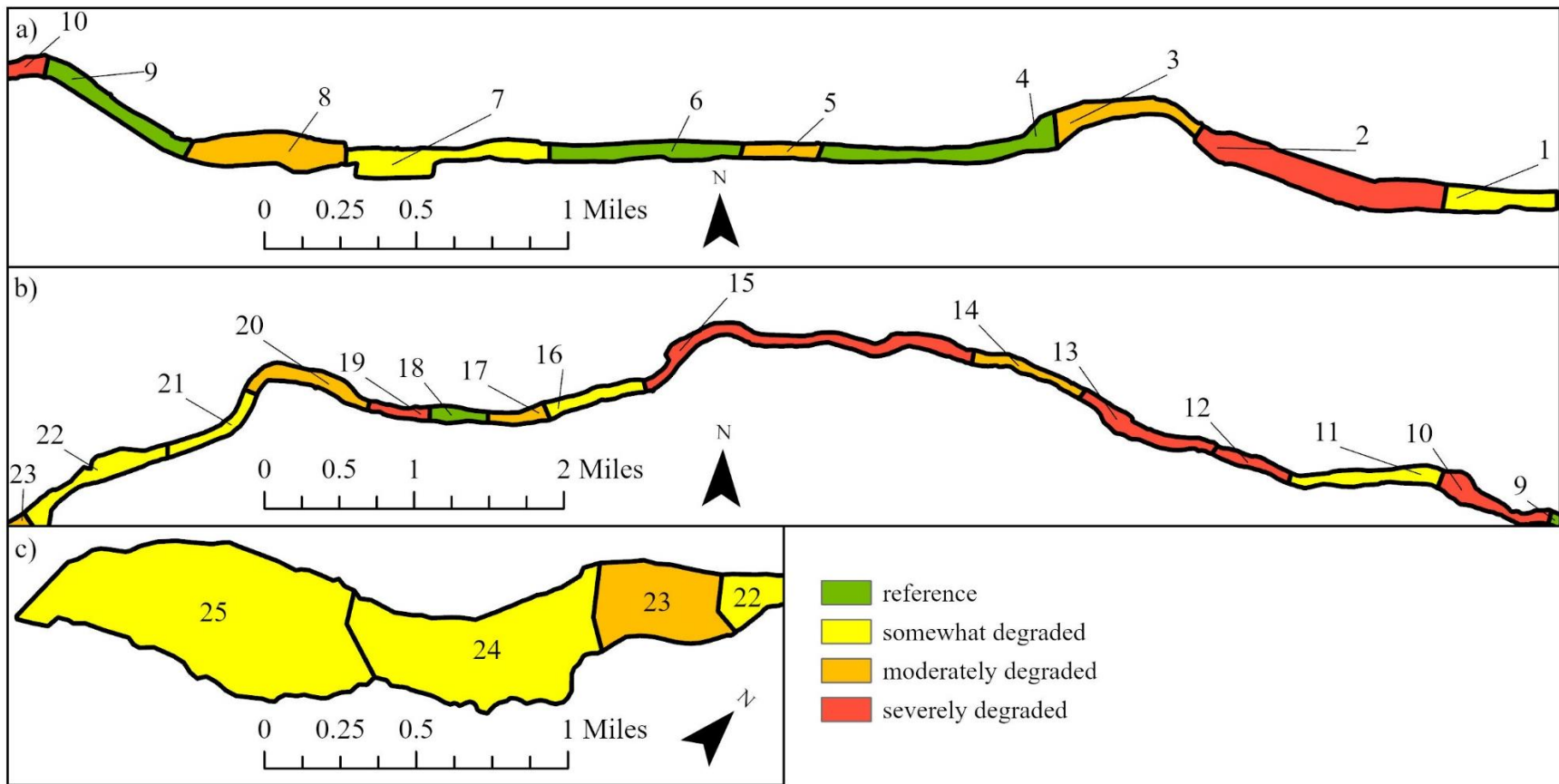


**Figure 3.16.** Reach-scale rankings by larger-scale reach, or section. While reach-scale geomorphology is highly variable, (a) the South Fork is generally the least degraded, (b) the middle section is the most degraded, and (c) the Winters section is in between.

#### **4.5 Prescribing restoration actions**

Of the 18 miles of degraded creek sections, 7.05 miles qualify for baseflow narrowing, 13.64 miles qualify for floodplain lowering, and 3.21 miles qualify for both actions (**Table 3.11**). Reach 1 was excluded from prescriptions because it is part of a larger reach (continues to the east 0.25 miles) that contains a functional weir for flow management. Other reaches that have considerations relevant to this analysis include reach 7, which is undergoing restoration design now; reaches 12 and 22, which were recently geomorphologically restored using baseflow narrowing and floodplain lowering and should be reanalyzed with the criteria in this study using an updated DEM; and reaches 3, 23, and 24, which contain active cropland in the transition zone and thus may not qualify for riparian restoration.



**Table 3.11.** Restoration method according to the relative area of aquatic and transition zones (X) and baseflow width (W). Reaches with greater than 20% aquatic zone may require baseflow narrowing, and reaches with greater than 24% transition zone may require floodplain narrowing. Additionally, reaches with a mean baseflow width greater than 60 feet qualified for baseflow narrowing. In the Reach # field, color indicates degree of degradation.

Reach #	downstream river-mile	upstream river-mile	aquatic (%)	transition (%)	baseflow narrowing	floodplain lowering	mean baseflow width (ft)	notes
1	1.54	2.05	16.7	22.9	*N/A	*N/A	88.36	*no restoration actions prescribed due to existing functional weir
2	2.05	3.28	10.0	60.6		X	57.62	
3	3.28	4.07	17.7	40.0	W	X	69.74	transition zone contains cropland
4	4.07	5.20	10.1	29.0	N/A	N/A	42.13	
5	5.20	5.56	29.0	22.7	X		130.66	
6	5.56	6.46	14.6	12.5	N/A	N/A	60.71	
7	6.46	7.40	18.3	26.0	W	X	81.07	land use issues, undergoing current restoration design
8	7.40	8.15	7.6	33.7		X	50.88	
9	8.15	8.93	11.3	18.5	N/A	N/A	44.78	
10	8.93	9.73	26.8	19.7	X		84.18	
11	9.73	10.78	13.0	24.0		X	34.37	
12	10.78	11.32	29.0	26.1	X	X	63.07	must be reanalyzed; restored in 2023
13	11.32	12.31	12.8	35.5		X	33.50	
14	12.31	13.10	17.1	29.7		X	35.34	
15	13.10	15.55	14.1	33.7		X	35.43	
16	15.55	16.25	8.4	29.0		X	29.20	
17	16.25	16.65	28.0	17.2	X		81.79	
18	16.65	17.06	15.6	17.1	N/A	N/A	54.08	
19	17.06	17.47	29.0	24.1	X		81.69	
20	17.47	18.41	14.1	32.9		X	57.31	
21	18.41	19.13	21.0	19.2	X		47.64	
22	19.13	20.27	21.0	17.3	X		69.89	must be reanalyzed; restored in 2020
23	20.27	20.71	6.9	39.1		X	52.75	transition zone contains cropland
24	20.71	21.65	8.0	25.7	W	X	93.59	transition zone contains cropland
25	21.65	22.75	2.9	32.1		X	40.27	

## 5. Discussion

The results of this study show that the HAR method has great potential for riparian ecosystem analysis, planning, and design (Benda et al., 2011; Brown et al., 2014; California Department of Water Resources, 2017; cbec, 2023). A key use of HAR is to identify segments of a river channel of more or less homogeneous characteristics to allow for reach classification, as was done in this study. On highly degraded creeks (e.g., incised or dredged or flow impaired) the HAR technique can reveal a lack of floodplains (i.e. low HAR areas) for riparian vegetation to colonize (lacking zonation for diverse plant communities), as is evident in Lower Putah Creek. At the same time, it can also show where the creek is most intact (i.e. with floodplains, or low HAR areas) to identify reference sites that can be used as a baseline for restoring the creek. A particularly valuable aspect of HAR methodology is its potential use in site prioritization when funds for restoring creeks are limited, and in prescribing restoration actions at the reach scale.

The flood inundation modeling of Lower Putah Creek indicated that flood flows (from the 1-yr to the 100-yr) are distributed in a predictable way based on discharge, likely due to the shape of the channel. The mean HAR of the inundation surface edge is also predictable based on flow size, suggesting it could be used as a flood zone proxy when actual flow frequency modeling is not feasible (California Department of Water Resources, 2017; cbec, 2023; Ureta et al., 2020; Vondrasek, 2015). If a large and active riparian zone were the goal for all of Lower Putah Creek, high-frequency flows (i.e., <5-yr) would need to inundate a disproportionately large area (more acres) in order to create floodplain dynamism (Doyle et al., 2007; Perry et al., 2015; Shields et al., 2003; West and Niezgodá, 2006). While a few reaches of the channel do experience this sort of dynamism (e.g., reach #9, **Figure 3.3b**), most reaches have very little riparian zone dynamism and are not well-inundated by high-frequency flows (i.e., <5-yr) (e.g.,

reach #12, **Figure 3.3a**). In short, a V-shaped incised channel is not conducive to a dynamic floodplain with shallow gradients to allow diverse riparian zonation, and restoration could increase this dynamism by lowering the banks to nearer the level of the baseflow surface (i.e., 0-11 feet HAR on Lower Putah Creek). This strategy is used for both flood protection in low-lying landscapes (Nienhuis and Leuven, 1998; Van de Steeg and Blom, 1998) and habitat restoration in incised rivers (Fischenich and Morrow, 2000; Maaß and Schüttrumpf, 2019; Rosgen, 1997; Villada Arroyave and Crosato, 2010; Wohl et al., 2015). Some approaches suggest incorporating a variety of design flows into restoration plans (Doyle et al., 2007; Perry et al., 2015), but on a regulated river, if design discharge is an important variable in restoration planning, such flow regulation would also have to be an integral part of reservoir management.

The distributions of current cover types (SVM-classified) indicate relationships between vegetation and HAR and between vegetation and inundation (flow size) on Lower Putah Creek, supporting findings from other studies that show vegetation type in riparian systems is reliably based on topography and hydrology (Bair et al., 2021; Greco et al., 2008; Sagers et al., 1996; Vondrasek, 2015). These findings are also encouraging in that there is enough floodplain, or low HAR area, in some places along Lower Putah Creek to support the kind of riparian habitat that badly needs to be restored in the Central Valley.

The random forest classification found HAR to be a very accurate predictor of cover type (88% overall accuracy), though the model may be over-predicting the relative cover of riparian forest compared to other vegetation cover types. The spatial distribution of each vegetation class enabled the identification of HAR zones relevant for reach-scale geomorphological assessment and restoration planning. The area zoned as core riparian according to HAR (261.8 acres) is less than the area classified as riparian land cover in current imagery (SVM classified 345.8 acres as

shrub and riparian forest), likely due to the conservative delineation of the core riparian HAR zone. After adding the marginal riparian zone (186.8 acres) to the core zone, there is more “potential” riparian zone (448.6 acres) than there is actual riparian forest cover currently (345.8 acres), possibly because succession to woody vegetation is still occurring along the creek (Chapter 2). It is recommended that managers primarily use the core riparian zone to create suitable geomorphology for hydric riparian species (e.g., willows, cottonwood), and reserve the marginal riparian zone for mesic or xeric riparian species (e.g., elderberry, black walnut, valley oak). This point is especially important as warming under projected climate change will increase riparian plant species’ climatic water deficit (Perry et al., 2015; Thorne et al., 2015), and because some riparian tree species (e.g., cottonwood) rely directly on the terrestrial inundation of the lowest floodplains (Mahoney and Rood, 1998). Since some riparian trees on Lower Putah Creek, including cottonwood, are already stressed by groundwater drawdown as well (Grismer, 2018), the soil moisture effects of perennial baseflow will become more important to ecosystem integrity in the coming decades.

Reference reaches were broadly defined based on idealized geomorphological conditions, or optimal conditions (Bauman et al., 2006), according to their relative area and distribution of HAR zones, rather than the narrow definition used by Rosgen (1996), which states that a reference reach is a stable, self-maintaining stretch of river. Rosgen’s definition relies on more data (i.e., more variables, finer spatial resolution, and multiple time periods) than were examined in this study. However, practitioners’ actual restoration planning should take into account all available data when determining what qualifies as “reference conditions” and “optimal (target) conditions.” For example, channel slope (listed by reach in **Appendix Table A.3**) is used to determine pool-riffle sequences (Dunn et al., 2014).

This analysis also identified the nature of degradation (i.e., large aquatic area = baseflow narrowing required; large transition area = floodplain lowering required) and the potential to create a functional riparian zone on Lower Putah Creek. Across all of Lower Putah Creek, there is the opportunity to restore a significant area of riparian forest. Currently, the riparian forest and shrub cover on the stretch of Putah Creek below Putah Diversion Dam constitute 0.4% (345.8 acres) of the 95,645 acres of riparian woody habitat remaining in the Sacramento Valley (Geographical Information Center, 2003; Roberts et al., 1980), but if half of the transition HAR zone were lowered to riparian (by lowering the floodplain) (Fischenich and Morrow, 2000; Maaß and Schüttrumpf, 2019; Rosgen, 1997; Villada Arroyave and Crosato, 2010; Wohl et al., 2015) and appropriately planted, Lower Putah Creek could host nearly double the riparian zone (642.7 acres) than currently exists. If the baseflow channel was narrowed (by filling in the channel, as was done at the Winters Nature Park site (City of Winters, 2008)), on average, to half its current width, an additional 70 acres of riparian habitat could be gained; this change would also enhance flow velocity and improve native fish habitat (Jacinto et al., 2023; Kiernan et al., 2012; Marchetti and Moyle, 2001). Effective restoration of baseflow channel bathymetry, such as filling in deep pools, and flow management could add dynamism and further enhance habitat.

Reach-scale analysis quantified degradation and restoration potential at the site scale. Of the 25 reaches identified, only four qualified as “reference,” indicating significant opportunity for restoration or enhancement along Lower Putah Creek. In this system, the most severely degraded reaches represent the worst geomorphological conditions and/or the greatest potential to lower the floodplain, narrow the channel, and gain significant riparian area. The benefit to using a ranking system based on relative area (%), rather than area (ac), is that all reaches are considered equally; the ranking is based on the proportional area available in each zone, not the

actual area of each zone compared to other reaches. The downside is that it does not account for the proportional area of potential restored habitat between similarly-ranked reaches. For example, narrow, relatively small reaches with already-steep banks (e.g., reach #14) may only accommodate minimal floodplain lowering, whereas wide, relatively large reaches with very shallow banks (e.g., reach #20) could accommodate significant floodplain lowering and host a large area of riparian zone. Due to this, it is important to consider additional variables in choosing actual restoration sites. For a more nuanced approach, other reach-scale variables could be added to this prioritization scheme depending on project goals: detailed bathymetry (e.g., substrate, pool-riffle sequences) (Yates, 2003), sedimentation models (Hauer and Lorang, 2004; Shields et al., 2003), aquatic habitat (Jacinto et al., 2023; Kiernan et al., 2012; Moyle, 2014) and understory plant communities (McClain et al., 2011; Moore et al., 2011).

It is not surprising that most of Lower Putah Creek (13.64 miles) requires floodplain lowering, because the most significant effect of channel modifications over the last 170 years has been incision (Chapter 1), with subsequent change in the shape of the channel from shallow and U-shaped to deep and V-shaped (Chapter 1). While the current mean baseflow width (55 ft) is narrower than the historical mean baseflow width (108 ft), it is still important to narrow the baseflow channel along much of the creek (7.05 miles) to (1) optimize aquatic habitat for native fish (Jacinto et al., 2023) and (2) gain floodplain area suitable for restoring lost riparian forest. It is important to note that while baseflow narrowing and floodplain lowering are presented in this study as distinct actions, they may be implemented together at any given site because they are both radical steps, and a restoration project would likely aim to maximize the restored area. However, it might be advantageous to implement only one action on a reach in order to avoid

disturbing intact, high-quality habitat; in these cases, the prescriptions presented here could be an even more valuable tool for restoration planning.

Finally, riparian HAR zones identified in this study can be directly incorporated into existing channel design tools, such as the ModifyTerrain and RiverBuilder modules of *RiverArchitect* or the HAR tool in the Ecological Floodplain Inundation Potential (EcoFIP) toolset, which identify candidate pixels on a HAR surface for terraforming and designing optimal channel terrains (elevation surfaces) based on input criteria (i.e., HAR zones as developed in this study) (Brown et al., 2014; Brown and Pasternack, 2019; California Department of Water Resources, 2017; cbec, 2023; Pasternack, 2023). These kinds of tools help automate the process of channel design, which can make the process more efficient and, most importantly, more effective at achieving quantitative design objectives.

## **6. Conclusion**

This study presents a practical and straightforward method for assessing reach- and river-scale geomorphological conditions and evaluating restoration potential using HAR. Inundation modeling showed that, on Lower Putah Creek, HAR has a predictable relationship with discharge, and land cover types have a predictable relationship with discharge, indicating HAR could be used as a proxy for inundation frequency in restoration planning. SVM classification modeling showed that, creek-wide, land cover types are distributed, at least in part, according to HAR, with riparian forest and shrub occupying the lowest zones and valley oak and herbaceous occupying the highest zones. Random forest classification accurately predicted land cover types using HAR, and the distribution of each cover type was used to classify HAR into zones relevant for restoration planning. The HAR method was used to identify 25 reaches of creek that were

ranked by their relative area of riparian zone and aquatic/transition zones, and then classed into four broad categories, representing degrees of degradation. Only 3.22 miles of creek met “reference” conditions, out of the 21.22 miles examined, indicating significant opportunity to create and enhance riparian forest in this system. Of the degraded sections, 13.64 miles qualify for floodplain lowering, 7.05 miles qualify for baseflow narrowing, and 3.21 miles qualify for both, indicating that radical geomorphological change is needed to maximize the riparian habitat potential of Lower Putah Creek.

While many dozens of variables are usually used in prioritizing areas for restoration (Beechie et al., 2011; Trabucchi et al., 2014; Worley et al., 2023), this study created a useful geographical metric to evaluate degradation and restoration potential both at the river and reach scales, and assign restoration actions. The zones created here can be directly incorporated into existing restoration design software for future projects on Lower Putah Creek. Future research could examine if other physical variables could be used to predict vegetation distribution on Lower Putah Creek (e.g., bank slope, distance to baseflow surface) (Chapter 2; Fremier and Talley, 2009; Greco et al., 2008) and how the relationship between HAR and riparian vegetation differs by study system. It could also be valuable to compare the effectiveness of different HAR-based methods for identifying candidate sites for floodplain lowering: (1) the inundation frequency/duration method (California Department of Water Resources, 2017), (2) the fine-scale plant-soil interactions method (Bair et al., 2021), and (3) the HAR-predicted vegetation classification method presented in this study.



## **Intellectual Merit**

This dissertation makes the following novel contributions to the literature in geomorphology, historical ecology, and restoration ecology:

1. Height above river (HAR) was used to analyze change over time (Chapter 1).
2. Machine learning classification of aerial imagery and three geomorphological variables (including HAR) were used to characterize change in woody vegetation over time before and after damming (Chapter 2).
3. Forest-based classification of aerial imagery was used to identify HAR zones relevant to geomorphological assessment and restoration planning, and these zones effectively characterized reaches according to their degradation and restoration potential (Chapter 3).
4. Vegetation-based HAR zones were used to prescribe restoration actions at the reach scale (Chapter 3).

## Bibliography

- Adam, E., Mutanga, O., Odindi, J., Abdel-Rahman, E.M., 2014. Land-use/cover classification in a heterogeneous coastal landscape using RapidEye imagery: evaluating the performance of random forest and support vector machines classifiers. *International Journal of Remote Sensing* 35, 3440–3458. <https://doi.org/10.1080/01431161.2014.903435>
- Ahmed K, A., Aljahdali, S., Naimatullah Hussain, S., 2013. Comparative Prediction Performance with Support Vector Machine and Random Forest Classification Techniques. *IJCA* 69, 12–16. <https://doi.org/10.5120/11885-7922>
- Anderson, K., 1993. *The Experimental Approach to Assessment of the Potential Ecological Effects of Horticultural Practices by Indigenous Peoples on California Wildland* (Dissertation). University of California, Berkeley.
- Anderson, M.K., 2001. The Contribution of Ethnobiology to the Reconstruction and Restoration of Historic Ecosystems, in: *The Historical Ecology Handbook*. Island Press.
- Auble, G.T., Friedman, J.M., Scott, M.L., 1994. Relating Riparian Vegetation to Present and Future Streamflows. *Ecological Applications* 4, 544–554. <https://doi.org/10.2307/1941956>
- Ayalew, T.B., Krajewski, W.F., Mantilla, R., 2013. Exploring the Effect of Reservoir Storage on Peak Discharge Frequency. *Journal of Hydrologic Engineering* 18, 1697–1708. [https://doi.org/10.1061/\(ASCE\)HE.1943-5584.0000721](https://doi.org/10.1061/(ASCE)HE.1943-5584.0000721)
- Bair, J.H., Loya, S., Powell, B., Lee, J.C., 2021. A new data-driven riparian revegetation design method. *Ecosphere* 12, e03718. <https://doi.org/10.1002/ecs2.3718>
- Bauman, K., Devine, M., Heyduk, R., Kahan, J., Landau, B., Perkins, S., 2006. *Middle Green River Restoration Blueprint*. King County Department of Natural Resources and Parks.
- Beechie, T., Pess, G., Roni, P., Giannico, G., 2011. Setting River Restoration Priorities: A Review of Approaches and a General Protocol for Identifying and Prioritizing Actions. *North American Journal of Fisheries Management* 28, 891–905. <https://doi.org/10.1577/M06-174.1>
- Beller, E., McClenachan, L., Trant, A., Sanderson, E.W., Rhemtulla, J., Guerrini, A., Grossinger, R., Higgs, E., 2017. Toward principles of historical ecology. *American Journal of Botany* 104, 645–648. <https://doi.org/10.3732/ajb.1700070>
- Beller, E.E., McClenachan, L., Zavaleta, E.S., Larsen, L.G., 2020. Past forward: Recommendations from historical ecology for ecosystem management. *Global Ecology and Conservation* 21, e00836. <https://doi.org/10.1016/j.gecco.2019.e00836>
- Benda, L., Miller, D., Barquín, J., 2011. Creating a catchment scale perspective for river restoration. *Hydrology and Earth System Sciences* 15, 2995–3015. <https://doi.org/10.5194/hess-15-2995-2011>
- Bendix, J., Hupp, C.R., 2000. Hydrological and geomorphological impacts on riparian plant communities. *Hydrological Processes* 14, 2977–2990. [https://doi.org/10.1002/1099-1085\(200011/12\)14:16/17<2977::AID-HYP130>3.0.CO;2-4](https://doi.org/10.1002/1099-1085(200011/12)14:16/17<2977::AID-HYP130>3.0.CO;2-4)
- Best, J., 2019. Anthropogenic stresses on the world’s big rivers. *Nature Geosci* 12, 7–21. <https://doi.org/10.1038/s41561-018-0262-x>
- Bray, D.I., 1975. Representative discharges for gravel-bed rivers in Alberta, Canada. *Journal of Hydrology* 27, 143–153. [https://doi.org/10.1016/0022-1694\(75\)90103-1](https://doi.org/10.1016/0022-1694(75)90103-1)
- Breiman, L., 2001. Random Forests. *Machine Learning* 45, 5–32. <https://doi.org/10.1023/A:1010933404324>

- Brown, R.A., Pasternack, G.B., 2019. How to build a digital river. *Earth-Science Reviews* 194, 283–305. <https://doi.org/10.1016/j.earscirev.2019.04.028>
- Brown, R.A., Pasternack, G.B., Wallender, W.W., 2014. Synthetic river valleys: Creating prescribed topography for form–process inquiry and river rehabilitation design. *Geomorphology* 214, 40–55. <https://doi.org/10.1016/j.geomorph.2014.02.025>
- Buchberger, S.G., 1980. Flood Frequency Analysis for Regulated Rivers. Presented at the 60th annual meeting of the Transportation Research Board.
- Bureau of Reclamation, 2023. CVO 2021 Reservoir Operations Reports [WWW Document]. URL [https://www.usbr.gov/mp/cvo/rpt\\_21.html](https://www.usbr.gov/mp/cvo/rpt_21.html) (accessed 8.2.23).
- Bureau of Reclamation, 2013. Final Riparian Habitat Mapping, Monitoring, and Mitigation Plan: Technical Implementation and Planning Approach Report: San Joaquin River Restoration Program.
- California Department of Fish and Game, 2008. Yolo Bypass Wildlife Area Land Management Plan.
- California Department of Fish and Wildlife, 2023. California Wildlife Habitat Relationships [WWW Document]. URL <https://wildlife.ca.gov/Data/CWHR> (accessed 11.6.23).
- California Department of Water Resources, 2017. Central Valley Flood Protection and Plan (CVFPP) Conservation Strategy - Appendix I. Floodplain Restoration Opportunity Analysis. State of California Natural Resources Agency.
- cbec, 2023. ecological floodplain inundation potential (EcoFIP) [WWW Document]. cbec. URL <https://www.cbecoeng.com/service-area/ecological-floodplain-inundation-potential/> (accessed 12.3.23).
- Cheng, Z., Aakala, T., Larjavaara, M., 2023. Elevation, aspect, and slope influence woody vegetation structure and composition but not species richness in a human-influenced landscape in northwestern Yunnan, China. *Frontiers in Forests and Global Change* 6.
- City of Winters, 2008. Winters Putah Creek Nature Park / Floodplain Restoration and Recreational Access Project - INITIAL STUDY and MITIGATED NEGATIVE DECLARATION.
- Cody, T., 2019. Upper Truckee River Reach 5 Restoration Project Effectiveness Monitoring Report. U.S. Forest Service.
- Conard, S.G., MacDonald, R.L., Holland, R.F., 1980. Riparian Vegetation and Flora of the Sacramento Valley, in: *Riparian Forests in California: Their Ecology and Conservation: A Symposium*. University of California, Davis.
- Congalton, R.G., Green, K., 2008. *Assessing the accuracy of remotely sensed data: principles and practices*. CRC Press.
- Crumley, C., 1994. Historical Ecology: Cultural Knowledge and Changing Landscapes, *The Journal of the Royal Anthropological Institute*. <https://doi.org/10.2307/3034651>
- Crumley, C.L., 2021. Historical Ecology: A Robust Bridge between Archaeology and Ecology. *Sustainability* 13, 8210. <https://doi.org/10.3390/su13158210>
- Daniel, J., 2012. *Sampling Essentials: Practical Guidelines for Making Sampling Choices*. SAGE Publications, Inc. <https://doi.org/10.4135/9781452272047>
- Dilts, T.E., 2015. Topography Tools for ArcGIS 10.3 and earlier - Overview [WWW Document]. URL <https://www.arcgis.com/home/item.html?id=b13b3b40fa3c43d4a23a1a09c5fe96b9> (accessed 7.19.23).

- Dilts, T.E., Yang, J., Weisberg, P.J., 2010. Mapping Riparian Vegetation with Lidar Data [WWW Document]. URL <https://www.esri.com/news/arcuser/0110/mapping-with-lidar.html> (accessed 7.4.23).
- Doyle, M.W., Shields, D., Boyd, K.F., Skidmore, P.B., Dominick, D., 2007. Channel-Forming Discharge Selection in River Restoration Design. *Journal of Hydraulic Engineering* 133, 831–837. [https://doi.org/10.1061/\(ASCE\)0733-9429\(2007\)133:7\(831\)](https://doi.org/10.1061/(ASCE)0733-9429(2007)133:7(831))
- Dunn, J., Rotar, M., Collins, Z., 2014. Clark Fork River Plains Reach Assessment & Restoration Prioritization. Middle Clark Fork River Plains Reach Recovery Committee.
- Dybala, K., Jr, A., Trochet, J., Engilis, I., Truan, M., 2018. Evaluating Riparian Restoration Success: Long-Term Responses of the Breeding Bird Community in California’s Lower Putah Creek Watershed. *Ecological Restoration* 36. <https://doi.org/10.3368/er.36.1.76>
- Eitzel, M.V., Kelly, M., Dronova, I., Valachovic, Y., Quinn-Davidson, L., Solera, J., de Valpine, P., 2016. Challenges and opportunities in synthesizing historical geospatial data using statistical models. *Ecological Informatics* 31, 100–111. <https://doi.org/10.1016/j.ecoinf.2015.11.011>
- England, J.F.Jr., Cohn, T.A., Faber, B.A., Stedinger, J.R., Thomas, W.O.Jr., Veilleux, A.G., Kiang, J.E., Mason, R.R., 2019. Guidelines for Determining Flood Flow Frequency—Bulletin 17C, in: *Survey Techniques and Methods, Book 4, Chap B5, Techniques and Methods*. U.S. Geological Survey, p. 148.
- Ergish, N.J., 2010. Flood frequency analysis for regulated watersheds (M.S.). ProQuest Dissertations and Theses. University of California, Davis, United States -- California.
- Escriva-Bou, A., Mount, J., Jezdimirovic, J., 2019. Dams in California.
- ESRI, 2020. ArcMap.
- Fertel, H.M., Collins, B.M., Lydersen, J.M., Stephens, S.L., 2023. Vegetation type change in California’s Northern Bay Area: A comparison of contemporary and historical aerial imagery. *Forest Ecology and Management* 542, 121102. <https://doi.org/10.1016/j.foreco.2023.121102>
- Fischenich, C., Morrow, J.V.Jr., 2000. Reconnection of Floodplains with Incised Channels (Ecosystem Management and Restoration Research Program Technical Notes Collection No. EMRRP SR-09). U.S. Army Corps of Engineers, Vicksburg, MS.
- Fremier, A.K., Talley, T.S., 2009. Scaling riparian conservation with river hydrology: Lessons from blue elderberry along four California rivers. *Wetlands* 29, 150–162. <https://doi.org/10.1672/07-243.1>
- Friedman, J.M., Auble, G.T., Andrews, E.D., Kittel, G., Madole, R.F., Griffin, E.R., Allred, T.M., 2006. Transverse and Longitudinal Variation in Woody Riparian Vegetation Along a Montane River. *Western North American Naturalist* 66, 78–91.
- Gardner, C., 2019. City of Davis South Fork Preserve. Grasslands.
- Geographical Information Center, 2003. The Central Valley Historic Mapping Project. California State University, Chico, Chico, CA.
- Greco, S.E., Girvetz, E.H., Larsen, E.W., Mann, J.P., Tuil, J.L., Lowney, C., 2008. Relative Elevation Topographic Surface Modelling of a Large Alluvial River Floodplain and Applications for the Study and Management of Riparian Landscapes. *Landscape Research* 33, 461–486. <https://doi.org/10.1080/01426390801949149>
- Greco, S.E., Plant, R.E., 2003. Temporal mapping of riparian landscape change on the Sacramento river, miles 196–218, California, USA. *Landscape Research* 28, 405–426. <https://doi.org/10.1080/0142639032000150149>

- Griffin, D., Anchukaitis, K.J., 2014. How unusual is the 2012–2014 California drought? *Geophysical Research Letters* 41, 9017–9023. <https://doi.org/10.1002/2014GL062433>
- Griggs, F.T., 2009. California Riparian Habitat Restoration Handbook, Second. ed. River Partners.
- Grill, G., Lehner, B., Thieme, M., Geenen, B., Tickner, D., Antonelli, F., Babu, S., Borrelli, P., Cheng, L., Crochetiere, H., Ehalt Macedo, H., Filgueiras, R., Goichot, M., Higgins, J., Hogan, Z., Lip, B., McClain, M.E., Meng, J., Mulligan, M., Nilsson, C., Olden, J.D., Opperman, J.J., Petry, P., Reidy Liermann, C., Sáenz, L., Salinas-Rodríguez, S., Schelle, P., Schmitt, R.J.P., Snider, J., Tan, F., Tockner, K., Valdujo, P.H., van Soesbergen, A., Zarfl, C., 2019. Mapping the world’s free-flowing rivers. *Nature* 569, 215–221. <https://doi.org/10.1038/s41586-019-1111-9>
- Grismer, M.E., 2018. Putah Creek hydrology affecting riparian cottonwood and willow tree survival. *Environ Monit Assess* 190, 458. <https://doi.org/10.1007/s10661-018-6841-x>
- Grossinger, R., Askevold, R., 2012. Napa Valley historical ecology atlas: exploring a hidden landscape of transformation and resilience. University of California Press.
- Hammond, T., 1989. Portions of Putah Creek parched. *The Davis Enterprise*.
- Han, M., Brierley, G., Li, B., Li, Z., Li, X., 2020. Impacts of flow regulation on geomorphic adjustment and riparian vegetation succession along an anabranching reach of the Upper Yellow River. *CATENA* 190, 104561. <https://doi.org/10.1016/j.catena.2020.104561>
- Harris, R., Olson, C., 1997. Two-Stage System for Prioritizing Riparian Restoration at the Stream Reach and Community Scales. *Restoration Ecology* 5, 34–42. <https://doi.org/10.1111/j.1526-100X.1997.tb00203.x>
- Harrison, L.L., MacArthur, R.C., Sanford, R.A., 2000. Lake Solano Sediment Management Study. *Watershed Management* 1–10. [https://doi.org/10.1061/40499\(2000\)167](https://doi.org/10.1061/40499(2000)167)
- Harvey, T.E., Macoubrie, M., Marchetti, M., Winkel, J., 1993. Reconnaissance Planning Report: Fish and Wildlife Resource Management Options for Lower Putah Creek, California (Report to Congress). U.S. Fish and Wildlife Service.
- Hauer, F.R., Lorang, M.S., 2004. River regulation, decline of ecological resources, and potential for restoration in a semi-arid lands river in the western USA. *Aquat. Sci.* 66, 388–401. <https://doi.org/10.1007/s00027-004-0724-7>
- Hobbs, R.J., Higgs, E., Harris, J.A., 2009. Novel ecosystems: implications for conservation and restoration. *Trends in Ecology & Evolution* 24, 599–605. <https://doi.org/10.1016/j.tree.2009.05.012>
- Holmes, L.C., Nelson, J.W., 1915. Reconnaissance soil survey of the Sacramento Valley, California. Bureau of Soils.
- Hosking, J., Wallis, J., 1997. Regional Frequency Analysis. Cambridge University Press, New York.
- Huberty, M.R., Johnston, C.N., 1941. Hydrologic studies of the Putah Creek area in the Sacramento Valley, California. *Hilg* 14, 119–146. <https://doi.org/10.3733/hilg.v14n03p119>
- Hupp, C.R., Osterkamp, W.R., 1996. Riparian vegetation and fluvial geomorphic processes. *Geomorphology, Fluvial Geomorphology and Vegetation* 14, 277–295. [https://doi.org/10.1016/0169-555X\(95\)00042-4](https://doi.org/10.1016/0169-555X(95)00042-4)
- Hupp, C.R., Osterkamp, W.R., 1985. Bottomland Vegetation Distribution along Passage Creek, Virginia, in Relation to Fluvial Landforms. *Ecology* 66, 670–681. <https://doi.org/10.2307/1940528>

- Huylenbroeck, L., Laslier, M., Dufour, S., Georges, B., Lejeune, P., Michez, A., 2020. Using remote sensing to characterize riparian vegetation: A review of available tools and perspectives for managers. *Journal of Environmental Management* 267, 110652. <https://doi.org/10.1016/j.jenvman.2020.110652>
- Hydrologic Frequency Analysis: EM 110-2-1415, 1993.
- Ibarra, A.D.L., Mariano, N.A., Sorani, V., Flores-Franco, G., Alquicira, E.R., Wehncke, E.V., 2019. Physical environmental conditions determine ubiquitous spatial differentiation of standing plants and seedbanks in Neotropical riparian dry forests. *PLOS ONE* 14, e0212185. <https://doi.org/10.1371/journal.pone.0212185>
- Interagency Committee on Water Data (IACWD), 1981. Guidelines for determining flood flow frequency, Bulletin 17B. U.S. Geological Survey, Reston, VA.
- Inter-Fluve, 2018. Lower Mad River Reach Assessment & Restoration Strategy Report. Yakama Nation Fisheries.
- Iowa Department of Natural Resources, 2018. River Restoration Toolbox - Practice Guide 5 (Geomorphic Channel Design).
- Jacinto, E., Fangué, N.A., Cocherell, D.E., Kiernan, J.D., Moyle, P.B., Rypel, A.L., 2023. Increasing stability of a native freshwater fish assemblage following flow rehabilitation. *Ecological Applications* 33, e2868. <https://doi.org/10.1002/eap.2868>
- Johnson, R.R., Carothers, S.W., Simpson, J.M., 1984. A Riparian Classification System, in: *California Riparian Ecosystems: Ecology, Conservation and Productive Management*. University of California Press, Berkeley, California, pp. 375–382.
- Jones and Stokes, 1992. Final Hydraulic, Hydrologic, Vegetation, and Fisheries Analysis for the U.S. Fish and Wildlife Service Putah Creek Resource Management Plan.
- Kelley, R., 1989. *Battling the Inland Sea: American Political Culture, Public Policy & the Sacramento Valley, 1850-1986*. University of California Press.
- Kiernan, J.D., Moyle, P.B., Crain, P.K., 2012. Restoring native fish assemblages to a regulated California stream using the natural flow regime concept. *Ecological Applications* 22, 1472–1482. <https://doi.org/10.1890/11-0480.1>
- Kondolf, G.M., 1997. PROFILE: Hungry Water: Effects of Dams and Gravel Mining on River Channels. *Environmental Management* 21, 533–551. <https://doi.org/10.1007/s002679900048>
- Larkey, J.L., 1969. *Davisville '68: The history and Heritage of the City of Davis*. Davis Historical Landmarks Commission.
- Larsen, E.W., Fremier, A.K., Greco, S.E., 2006. Cumulative Effective Stream Power and Bank Erosion on the Sacramento River, California, Usa1. *JAWRA Journal of the American Water Resources Association* 42, 1077–1097. <https://doi.org/10.1111/j.1752-1688.2006.tb04515.x>
- Lee, J.E., Heo, J.-H., Lee, J., Kim, N.W., 2017. Assessment of Flood Frequency Alteration by Dam Construction via SWAT Simulation. *Water* 9, 264. <https://doi.org/10.3390/w9040264>
- Li, J., Dong, S., Yang, Z., Peng, M., Liu, S., Li, X., 2012. Effects of cascade hydropower dams on the structure and distribution of riparian and upland vegetation along the middle-lower Lancang-Mekong River. *Forest Ecology and Management* 284, 251–259. <https://doi.org/10.1016/j.foreco.2012.07.050>

- Lin, J., Harris, L.S., Truan, M.L., Engilis, A., Jr., Kelt, D.A., 2022. Spatiotemporal patterns of riparian bat assemblages in a novel riparian ecosystem. *Journal of Mammalogy* 103, 512–527. <https://doi.org/10.1093/jmammal/gyab170>
- Lite, S.J., Bagstad, K.J., Stromberg, J.C., 2005. Riparian plant species richness along lateral and longitudinal gradients of water stress and flood disturbance, San Pedro River, Arizona, USA. *Journal of Arid Environments* 63, 785–813. <https://doi.org/10.1016/j.jaridenv.2005.03.026>
- Lower Putah Creek Coordinating Committee, 2005. Lower Putah Creek Watershed Management Plan.
- Lowney, C.L., Greco, S.E., 2003. Technical Memorandum: Flood Frequency Analysis of the Sacramento River at Bend Bridge.
- LSA, 2023. LOWER PUTAH CREEK RESTORATION PROJECT, NISHIKAWA REACH - Draft Initial Study/Mitigated Negative Declaration.
- Lydersen, J.M., Collins, B.M., 2018. Change in Vegetation Patterns Over a Large Forested Landscape Based on Historical and Contemporary Aerial Photography. *Ecosystems* 21, 1348–1363. <https://doi.org/10.1007/s10021-018-0225-5>
- Ma, R., Broadbent, M., Zhao, X., 2020. Historical Photograph Orthorectification Using SfM for Land Cover Change Analysis. *J Indian Soc Remote Sens* 48, 341–351. <https://doi.org/10.1007/s12524-019-01082-7>
- Maaß, A.-L., Schüttrumpf, H., 2019. Reactivation of Floodplains in River Restorations: Long-Term Implications on the Mobility of Floodplain Sediment Deposits. *Water Resources Research* 55, 8178–8196. <https://doi.org/10.1029/2019WR024983>
- Magilligan, F.J., Nislow, K.H., 2005. Changes in hydrologic regime by dams. *Geomorphology, Dams in Geomorphology* 71, 61–78. <https://doi.org/10.1016/j.geomorph.2004.08.017>
- Mahoney, J.M., Rood, S.B., 1998. Streamflow requirements for cottonwood seedling recruitment—An integrative model. *Wetlands* 18, 634–645. <https://doi.org/10.1007/BF03161678>
- Mallik, A.U., Richardson, J.S., 2009. Riparian vegetation change in upstream and downstream reaches of three temperate rivers dammed for hydroelectric generation in British Columbia, Canada. *Ecological Engineering* 35, 810–819. <https://doi.org/10.1016/j.ecoleng.2008.12.005>
- Marchetti, M.P., Moyle, P.B., 2001. Effects of Flow Regime on Fish Assemblages in a Regulated California Stream. *Ecological Applications* 11, 530–539. <https://doi.org/10.2307/3060907>
- Marren, P.M., Grove, J.R., Webb, J.A., Stewardson, M.J., 2014. The Potential for Dams to Impact Lowland Meandering River Floodplain Geomorphology. *The Scientific World Journal* 2014, e309673. <https://doi.org/10.1155/2014/309673>
- Maxwell, S.K., Meliker, J.R., Goovaerts, P., 2010. Use of land surface remotely sensed satellite and airborne data for environmental exposure assessment in cancer research. *J Expo Sci Environ Epidemiol* 20, 176–185. <https://doi.org/10.1038/jes.2009.7>
- McCarthy, T.S., 2006. Groundwater in the wetlands of the Okavango Delta, Botswana, and its contribution to the structure and function of the ecosystem. *Journal of Hydrology, Groundwater - surface water interactions in wetlands for integrated water resources management* 320, 264–282. <https://doi.org/10.1016/j.jhydrol.2005.07.045>

- McClain, C.D., Holl, K.D., Wood, D.M., 2011. Successional Models as Guides for Restoration of Riparian Forest Understory. *Restoration Ecology* 19, 280–289. <https://doi.org/10.1111/j.1526-100X.2009.00616.x>
- Medina, J.A.V., Atehortua, B.E.A., 2019. Comparison of maximum likelihood, support vector machines, and random forest techniques in satellite images classification. *Tecnura* 23, 13–26. <https://doi.org/10.14483/22487638.14826>
- Monmonier, M., 2002. Aerial Photography at the Agricultural Adjustment Administration: Acreage Controls, Conservation Benefits, and Overhead Surveillance in the 1930s. *Photogrammetric Engineering and Remote Sensing* 68.
- Moore, P.L., Holl, K.D., Wood, D.M., 2011. Strategies for Restoring Native Riparian Understory Plants Along the Sacramento River: Timing, Shade, Non-Native Control, and Planting Method. *San Francisco Estuary and Watershed Science* 9. <https://doi.org/10.15447/sfews.2014v9iss2art1>
- Morris, J.T., Drexler, J.Z., Vaughn, L.J.S., Robinson, A.H., 2022. An assessment of future tidal marsh resilience in the San Francisco Estuary through modeling and quantifiable metrics of sustainability. *Frontiers in Environmental Science* 10.
- Moyle, P.B., 2014. Novel Aquatic Ecosystems: The New Reality for Streams in California and Other Mediterranean Climate Regions. *River Research and Applications* 30, 1335–1344. <https://doi.org/10.1002/rra.2709>
- Moyle, P.B., Marchetti, M.P., Baldrige, J., Taylor, T.L., 1998. Fish Health and Diversity: Justifying Flows for a California Stream. *Fisheries* 23, 6–15. [https://doi.org/10.1577/1548-8446\(1998\)023<0006:FHADJF>2.0.CO;2](https://doi.org/10.1577/1548-8446(1998)023<0006:FHADJF>2.0.CO;2)
- National Inventory of Dams [WWW Document], 2023. URL <https://nid.sec.usace.army.mil/#/dams/search/sy=@stateKey:CA&viewType=map&resultType=dams&advanced=false&hideList=false&eventSystem=false> (accessed 8.9.23).
- Nienhuis, P.H., Leuven, R.S.E.W., 1998. Ecological concepts for the sustainable management of lowland river basins: A review, in: *New Concepts for Sustainable Management of River Basins*. Backhuys Publishers, pp. 7–33.
- Nobre, A.D., Cuartas, L.A., Hodnett, M., Rennó, C.D., Rodrigues, G., Silveira, A., Waterloo, M., Saleska, S., 2011. Height Above the Nearest Drainage – a hydrologically relevant new terrain model. *Journal of Hydrology* 404, 13–29. <https://doi.org/10.1016/j.jhydrol.2011.03.051>
- Northrup, W.L., 1965. Republican River channel deterioration, *Micellaneous Publications*. US Department of Agriculture.
- NRCS, 2015. Chapters 5 and 18, *National Engineering Handbook*, Part 630. USDA Natural Resource Conservation Service (NRCS).
- NRCS, 2007. Chapter 5, *National Engineering Handbook*, Part 654. USDA Natural Resource Conservation Service (NRCS).
- Nüchel, J., Bøcher, P.K., Svenning, J.-C., 2019. Topographic slope steepness and anthropogenic pressure interact to shape the distribution of tree cover in China. *Applied Geography* 103, 40–55. <https://doi.org/10.1016/j.apgeog.2018.12.008>
- O’Brien, M.J., 2001. Archaeology, Paleoecosystems, and Ecological Restoration, in: *The Historical Ecology Handbook*. Island Press.
- Olofsson, P., Foody, G.M., Herold, M., Stehman, S.V., Woodcock, C.E., Wulder, M.A., 2014. Good practices for estimating area and assessing accuracy of land change. *Remote Sensing of Environment* 148, 42–57. <https://doi.org/10.1016/j.rse.2014.02.015>



- Pagliuco, B., Scott, N., O-Keefe, C., Holycross, B., 2023. Klamath Reservoir Reach Restoration Prioritization Plan.
- Palmer, S.C.J., Kutser, T., Hunter, P.D., 2015. Remote sensing of inland waters: Challenges, progress and future directions. *Remote Sensing of Environment, Special Issue: Remote Sensing of Inland Waters* 157, 1–8. <https://doi.org/10.1016/j.rse.2014.09.021>
- Parker, C.B., 2006. The Arboretum Waterway [WWW Document]. UC Davis. URL <https://www.ucdavis.edu/news/arboretum-waterway> (accessed 7.20.23).
- Parker, C.B., 2003. Scholars eye non-native species invasions. UC Davis.
- Parker, K.C., Bendix, J., 1996. Landscape-Scale Geomorphic Influences on Vegetation Patterns in Four Environments. *Physical Geography* 17, 113–141. <https://doi.org/10.1080/02723646.1996.10642577>
- Pasternack, G.B., 2023. River Builder [WWW Document]. River Architect. URL [https://riverarchitect.github.io/RA\\_wiki/RiverBuilder](https://riverarchitect.github.io/RA_wiki/RiverBuilder) (accessed 12.3.23).
- Perry, L., Reynolds, L., Beechie, T., Collins, M., Shafroth, P., 2015. Incorporating climate change projections into riparian restoration planning and design: Riparian Restoration for a Changing Climate. *Ecohydrology* 8, n/a-n/a. <https://doi.org/10.1002/eco.1645>
- Petsch, D.K., Cionek, V.D.M., Thomaz, S.M., Dos Santos, N.C.L., 2023. Ecosystem services provided by river-floodplain ecosystems. *Hydrobiologia* 850, 2563–2584. <https://doi.org/10.1007/s10750-022-04916-7>
- Petts, G.E., Gurnell, A.M., 2005. Dams and geomorphology: Research progress and future directions. *Geomorphology, Dams in Geomorphology* 71, 27–47. <https://doi.org/10.1016/j.geomorph.2004.02.015>
- Piégay, H., Arnaud, F., Belletti, B., Bertrand, M., Bizzi, S., Carbonneau, P., Dufour, S., Liébault, F., Ruiz-Villanueva, V., Slater, L., 2020a. Remotely sensed rivers in the Anthropocene: state of the art and prospects. *Earth Surface Processes and Landforms* 45, 157–188. <https://doi.org/10.1002/esp.4787>
- Piégay, H., Arnaud, F., Belletti, B., Bertrand, M., Bizzi, S., Carbonneau, P., Dufour, S., Liébault, F., Ruiz-Villanueva, V., Slater, L., 2020b. Remotely sensed rivers in the Anthropocene: state of the art and prospects. *Earth Surface Processes and Landforms* 45, 157–188. <https://doi.org/10.1002/esp.4787>
- Pinder, J.E., Kroh, G.C., White\*, J.D., Basham May, A.M., 1997. The relationships between vegetation type and topography in Lassen Volcanic National Park. *Plant Ecology* 131, 17–29. <https://doi.org/10.1023/A:1009792123571>
- Poff, N.L., Hart, D.D., 2002. How Dams Vary and Why It Matters for the Emerging Science of Dam Removal: An ecological classification of dams is needed to characterize how the tremendous variation in the size, operational mode, age, and number of dams in a river basin influences the potential for restoring regulated rivers via dam removal. *BioScience* 52, 659–668. [https://doi.org/10.1641/0006-3568\(2002\)052\[0659:HDVAWI\]2.0.CO;2](https://doi.org/10.1641/0006-3568(2002)052[0659:HDVAWI]2.0.CO;2)
- Poff, N.L., Zimmerman, J.K.H., 2010. Ecological responses to altered flow regimes: a literature review to inform the science and management of environmental flows. *Freshwater Biology* 55, 194–205. <https://doi.org/10.1111/j.1365-2427.2009.02272.x>
- Politti, E., Bertoldi, W., Gurnell, A., Henshaw, A., 2018. Feedbacks between the riparian Salicaceae and hydrogeomorphic processes: A quantitative review. *Earth-Science Reviews* 176, 147–165. <https://doi.org/10.1016/j.earscirev.2017.07.018>

- Poole, G.C., Stanford, J.A., Frissell, C.A., Running, S.W., 2002. Three-dimensional mapping of geomorphic controls on flood-plain hydrology and connectivity from aerial photos. *Geomorphology* 48, 329–347. [https://doi.org/10.1016/S0169-555X\(02\)00078-8](https://doi.org/10.1016/S0169-555X(02)00078-8)
- Rango, A., Laliberte, A., Winters, C., 2008. Role of aerial photos in compiling a long-term remote sensing data set. *JARS* 2, 023541. <https://doi.org/10.1117/1.3009225>
- Richter, B.D., Baumgartner, J.V., Powell, J., Braun, D.P., 1996. A Method for Assessing Hydrologic Alteration within Ecosystems. *Conservation Biology* 10, 1163–1174. <https://doi.org/10.1046/j.1523-1739.1996.10041163.x>
- Richter, B.D., Richter, H.E., 2000. Prescribing Flood Regimes to Sustain Riparian Ecosystems along Meandering Rivers. *Conservation Biology* 14, 1467–1478.
- Roberts, W., Howe, J., Major, J., 1980. A SURVEY OF RIPARIAN FOREST FLORA AND FAUNA IN CALIFORNIA.
- Ronco, P., Fasolato, G., Nones, M., Di Silvio, G., 2010. Morphological effects of damming on lower Zambezi River. *Geomorphology* 115, 43–55. <https://doi.org/10.1016/j.geomorph.2009.09.029>
- Rosgen, D.L., 1997. A Geomorphological Approach to Restoration of Incised Rivers, in: *Proceedings of the Conference on Management of Landscapes Disturbed by Channel Incision*.
- Rosgen, D.L., 1996. *Applied River Morphology*. Wildland Hydrology, Pagosa Springs, CO.
- Rubin, H., 1988. *The Solano Water Story: A History of the Solano Irrigation District and the Solano Project*. Solano Irrigation District.
- Sagers, C.L., Lyon, J., Dale, E.E.Jr., 1996. Physical factors, functional groups and phytosociology: evaluating plant communities in the riparian zone of the Buffalo National River. *Proceedings of the Arkansa Water Resources Center 1996 Research Conference*.
- Salazar Loor, J., Fdez-Arroyabe, P., 2019. Aerial and Satellite Imagery and Big Data: Blending Old Technologies with New Trends, in: Dey, N., Bhatt, C., Ashour, A.S. (Eds.), *Big Data for Remote Sensing: Visualization, Analysis and Interpretation: Digital Earth and Smart Earth*. Springer International Publishing, Cham, pp. 39–59. [https://doi.org/10.1007/978-3-319-89923-7\\_2](https://doi.org/10.1007/978-3-319-89923-7_2)
- Samuels, P.G., 1990. Cross-section location in 1-D models. *Internation Conference on River Flood Hydraulics*.
- Sanderson, E., 2009. *Mannahatta: A Natural History of New York City*. Abrams, New York, New York.
- Schmidt, J.C., Webb, R.H., Valdez, R.A., Marzolf, G.R., Stevens, L.E., 1998. Science and Values in River Restoration in the Grand Canyon: There is no restoration or rehabilitation strategy that will improve the status of every riverine resource. *BioScience* 48, 735–747. <https://doi.org/10.2307/1313336>
- Schumm, S.A., 1969. River metamorphosis. Presented at the *Proceedings of the American Society of Civil Engineers*, pp. 255–273.
- Schwindt, S., Larrieu, K., Pasternack, G.B., Rabone, G., 2020. River Architect. *SoftwareX* 11, 100438. <https://doi.org/10.1016/j.softx.2020.100438>
- Shafroth, P.B., Auble, G.T., Stromberg, J.C., Patten, D.T., 1998. Establishment of woody riparian vegetation in relation to annual patterns of streamflow, Bill Williams River, Arizona. *Wetlands* 18, 577–590. <https://doi.org/10.1007/BF03161674>

- Sheykhoumousa, M., Mahdianpari, M., Ghanbari, H., Mohammadimanesh, F., Ghamisi, P., Homayouni, S., 2020. Support Vector Machine Versus Random Forest for Remote Sensing Image Classification: A Meta-Analysis and Systematic Review. *IEEE Journal of Selected Topics in Applied Earth Observations and Remote Sensing* 13, 6308–6325. <https://doi.org/10.1109/JSTARS.2020.3026724>
- Shields, F.D., Copeland, R.R., Klingeman, P.C., Doyle, M.W., Simon, A., 2003. Design for Stream Restoration. *Journal of Hydraulic Engineering* 129, 575–584. [https://doi.org/10.1061/\(ASCE\)0733-9429\(2003\)129:8\(575\)](https://doi.org/10.1061/(ASCE)0733-9429(2003)129:8(575))
- Soar, P.J., Thorne, C.R., 2011. Design discharge for river restoration, in: Simon, A., Bennett, S.J., Castro, J.M. (Eds.), *Stream Restoration in Dynamic Fluvial Systems*, Geophysical Monograph Series. American Geophysical Union, pp. 123–149. <https://doi.org/10.1029/2010GM001009>
- Solano County Water Agency, 2014. Lake Solano Sediment Study – 2013 Update.
- Solano County Water Agency, 2009. Lake Berryessa shapefile.
- Solano County Water Agency, 2005. Putah Creek LiDAR flight 2005.
- Solins, J.P., Thorne, J.H., Cadenasso, M.L., 2018. Riparian canopy expansion in an urban landscape: Multiple drivers of vegetation change along headwater streams near Sacramento, California. *Landscape and Urban Planning* 172, 37–46. <https://doi.org/10.1016/j.landurbplan.2017.12.005>
- Somach, S.L., 2000. Settlement - Putah Creek Cases.
- Sommer, T.R., Harrell, W.C., Swift, T.J., 2008. Extreme hydrologic banding in a large-river Floodplain, California, U.S.A. *Hydrobiologia* 598, 409–415. <https://doi.org/10.1007/s10750-007-9159-1>
- Stanford, J.A., Ward, J.V., Liss, W.J., Frissell, C.A., Williams, R.N., Lichatowich, J.A., Coutant, C.C., 1996. A General Protocol for Restoration of Regulated Rivers. *Regulated Rivers: Research & Management* 12, 391–413. [https://doi.org/10.1002/\(SICI\)1099-1646\(199607\)12:4/5<391::AID-RRR436>3.0.CO;2-4](https://doi.org/10.1002/(SICI)1099-1646(199607)12:4/5<391::AID-RRR436>3.0.CO;2-4)
- Stevens, M., Ryan, A., 1997. *Healing the Land, Healing the People: A Guidebook to the Ethnobotany of the Putah and Cache Creeks Ecoregion*.
- Stromberg, J.C., Tiller, R., Richter, B., 1996. Effects of Groundwater Decline on Riparian Vegetation of Semiarid Regions: The San Pedro, Arizona. *Ecological Applications* 6, 113–131. <https://doi.org/10.2307/2269558>
- Swanson, F.J., Kratz, T.K., Caine, N., Woodmansee, R.G., 1988. Landform Effects on Ecosystem Patterns and Processes. *BioScience* 38, 92–98. <https://doi.org/10.2307/1310614>
- Swetnam, T.W., Allen, C.D., Betancourt, J.L., 1999. Applied Historical Ecology: Using the Past to Manage for the Future. *Ecological Applications* 9, 1189–1206. [https://doi.org/10.1890/1051-0761\(1999\)009\[1189:AHEUTP\]2.0.CO;2](https://doi.org/10.1890/1051-0761(1999)009[1189:AHEUTP]2.0.CO;2)
- Teversham, J.M., 1973. *VEGETATION RESPONSE TO FLUVIAL ACTIVITY IN THE LILLOOET RIVER FLOODPLAIN*.
- Thanh Noi, P., Kappas, M., 2018. Comparison of Random Forest, k-Nearest Neighbor, and Support Vector Machine Classifiers for Land Cover Classification Using Sentinel-2 Imagery. *Sensors* 18, 18. <https://doi.org/10.3390/s18010018>
- Thayer, R.L., 2003. *LifePlace: Bioregional Thought and Practice*. University of California Press.

- Thompson, K., 1961. RIPARIAN FORESTS OF THE SACRAMENTO VALLEY, CALIFORNIA <sup>1</sup>. *Annals of the Association of American Geographers* 51, 294–315. <https://doi.org/10.1111/j.1467-8306.1961.tb00380.x>
- Thorne, J.H., Boynton, R.M., Flint, L.E., Flint, A.L., 2015. The magnitude and spatial patterns of historical and future hydrologic change in California’s watersheds. *Ecosphere* 6, art24. <https://doi.org/10.1890/ES14-00300.1>
- Tobias, M.M., Bostic, D.J., Sibbett, S.S., 2021. Route Logic of the Central Pacific Railroad, 1861–1869. *California History* 98, 74–99. <https://doi.org/10.1525/ch.2021.98.2.74>
- Tomic, S., 1998. Flood frequency analysis on regulated rivers (Ph.D.). ProQuest Dissertations and Theses. The University of Alabama, United States -- Alabama.
- Tomsett, C., Leyland, J., 2019. Remote sensing of river corridors: A review of current trends and future directions. *River Research and Applications* 35, 779–803. <https://doi.org/10.1002/rra.3479>
- Trabucchi, M., O’Farrell, P.J., Notivol, E., Comín, F.A., 2014. Mapping Ecological Processes and Ecosystem Services for Prioritizing Restoration Efforts in a Semi-arid Mediterranean River Basin. *Environmental Management* 53, 1132–1145. <https://doi.org/10.1007/s00267-014-0264-4>
- Tranmer, A.W., Caamaño, D., Clayton, S.R., Giglou, A.N., Goodwin, P., Buffington, J.M., Tonina, D., 2022. Testing the effective-discharge paradigm in gravel-bed river restoration. *Geomorphology* 403, 108139. <https://doi.org/10.1016/j.geomorph.2022.108139>
- Truan, M.L., Engilis, A.Jr., Trochet, J.R., 2010. Putah Creek Terrestrial Wildlife Monitoring Program: Comprehensive Report and Map Volume, 1997-2009. Department of Wildlife, Fish, and Conservation Biology, Museum of Wildlife and Fish Biology, University of California, Davis.
- Tsheboeng, G., 2018. Spatial variation of the influence of distance from surface water on riparian plant communities in the Okavango Delta, Botswana. *Ecological Processes* 7, 32. <https://doi.org/10.1186/s13717-018-0140-x>
- Tuil, J.L., 2019. A Historical Ecology of the Cache and Putah Creek Alluvial Plain in the Sacramento Valley of California (Dissertation). University of California, Davis.
- UC Berkeley GeoData Repository, 2023. Average Annual Precipitation (Inches): California, 1981-2010 (800m).
- Ullrich, P.A., Xu, Z., Rhoades, A. m., Dettinger, M. d., Mount, J. f., Jones, A. d., Vahmani, P., 2018. California’s Drought of the Future: A Midcentury Recreation of the Exceptional Conditions of 2012–2017. *Earth’s Future* 6, 1568–1587. <https://doi.org/10.1029/2018EF001007>
- University of California, Davis, 2005. Putah Creek Riparian Reserve Management Plan.
- Ureta, J.C., Zurqani, H.A., Post, C.J., Ureta, J., Motallebi, M., 2020. Application of Nonhydraulic Delineation Method of Flood Hazard Areas Using LiDAR-Based Data. *Geosciences* 10, 338. <https://doi.org/10.3390/geosciences10090338>
- U.S. Army Corps of Engineers, 2023a. HEC-ras.
- U.S. Army Corps of Engineers, 2023b. Cross Section Spacing and Hydraulic Properties [WWW Document]. URL <https://www.hec.usace.army.mil/confluence/rasdocs/ras1dtechref/latest/performing-a-dam-break-study-with-hec-ras/downstream-flood-routing-modeling-issues/cross-section-spacing-and-hydraulic-properties> (accessed 9.7.23).

- US Census Bureau, 2023. TIGER/Line Shapefiles.
- U.S. Fish and Wildlife Service, 1992. Lower Putah Creek Resource Management Plan (Report to Congress).
- U.S. Water Resources Council, Subcommittee on Hydrology, 1967. A uniform technique for determining flood flow frequencies—Bulletin No. 15.
- USDA, 2023. National Agriculture Imagery Program [WWW Document]. URL <https://naip-usdaonline.hub.arcgis.com/> (accessed 11.12.23).
- USGS, 2023. USGS Water Data for the Nation [WWW Document]. URL <https://waterdata.usgs.gov/nwis> (accessed 7.6.23).
- USGS, 2022. CalWater Hydrologic Unit boundaries [WWW Document]. The National Map Download v2. URL <https://apps.nationalmap.gov/downloader/> (accessed 8.14.23).
- Vaghti, M.G., Holyoak, M., Williams, A., Talley, T.S., Fremier, A.K., Greco, S.E., 2009. Understanding the Ecology of Blue Elderberry to Inform Landscape Restoration in Semiarid River Corridors. *Environmental Management* 43, 28–37. <https://doi.org/10.1007/s00267-008-9233-0>
- Van de Steeg, H.M., Blom, C.W.P.M., 1998. Impact of Hydrology on Floodplain Vegetation in the Lower Rhine System: Implications for Nature Conservation and Nature Development, in: *New Concepts for Sustainable Management of River Basins*. Backhuys Publishers, pp. 131–144.
- Vaught, D., 2007. *After the Gold Rush: Tarnished Dreams in the Sacramento Valley*. The Johns Hopkins University Press.
- Villada Arroyave, J.A., Crosato, A., 2010. Effects of river floodplain lowering and vegetation cover. *Proceedings of the Institution of Civil Engineers - Water Management* 163, 457–467. <https://doi.org/10.1680/wama.900023>
- Vondrasek, C.E., 2015. Delineating forested river habitats and riparian floodplain hydrology with LiDAR (Thesis).
- Weems, J., 2011. Interpreting a 1930s aerial survey photograph: the artfulness of technological images. *History and Technology* 27, 223–231. <https://doi.org/10.1080/07341512.2011.573275>
- West, T.S., Niezgodna, S.L., 2006. Estimating a Stream Restoration Design Discharge. Presented at the World Environmental and Water Resource Congress 2006, American Society of Civil Engineers, pp. 1–10. [https://doi.org/10.1061/40856\(200\)351](https://doi.org/10.1061/40856(200)351)
- Whipple, A.A., Grossinger, R.M., Davis, F.W., 2011. Shifting Baselines in a California Oak Savanna: Nineteenth Century Data to Inform Restoration Scenarios. *Restoration Ecology* 19, 88–101. <https://doi.org/10.1111/j.1526-100X.2009.00633.x>
- Wohl, E., Lane, S.N., Wilcox, A.C., 2015. The science and practice of river restoration. *Water Resources Research* 51, 5974–5997. <https://doi.org/10.1002/2014WR016874>
- Worley, L.C., Underwood, K.L., Diehl, R.M., Matt, J.E., Lawson, K.S., Seigel, R.M., Rizzo, D.M., 2023. Balancing multiple stakeholder objectives for floodplain reconnection and wetland restoration. *Journal of Environmental Management* 326, 116648. <https://doi.org/10.1016/j.jenvman.2022.116648>
- Wright, S., Schoellhamer, D., 2004. Trends in the Sediment Yield of the Sacramento River, California, 1957 - 2001. *SFEWS* 2. <https://doi.org/10.15447/sfews.2004v2iss2art2>
- Yates, G., 2003. Gravel and Temperature Surveys of Lower Putah Creek. Lower Putah Creek Coordinating Committee, Vacaville, CA.

Yochum, S.E., 2017. logPearson Frequency Analysis Spreadsheet for Analyses of Streamgage Records.

Yolo Bypass Working Group, Yolo Basin Foundation, Jones and Stokes, 2001. A Framework for the Future: Yolo Bypass Management Strategy.

## Appendix

**Table A.1.** Pre-dam Weibull-plotted flow frequency tables, sorted by flow rank.

Year	Event date	Gage height (ft)	Discharge (cfs)	Rank (m)	Probability exceedance (P)	P as %	Recurrence interval (yrs)
1940	2/27/1940	29.5	81000	1	0.02	2	52.00
1943	1/21/1943	29	70300	2	0.04	4	26.00
1942	2/6/1942	28.55	67200	3	0.06	6	17.33
1914	12/31/1913	39	60,000	4	0.08	8	13.00
1956	12/22/1955	26.73	55400	5	0.10	10	10.40
1925	2/11/1925	35.1	53,600	6	0.12	12	8.67
1916	1/3/1916	35	53,300	7	0.13	13	7.43
1937	2/4/1937	25.4	50800	8	0.15	15	6.50
1938	12/11/1937	24.8	48100	9	0.17	17	5.78
1953	12/7/1952	25.08	45700	10	0.19	19	5.20
1951	12/3/1950	24.32	41600	11	0.21	21	4.73
1941	4/4/1941	24.3	41400	12	0.23	23	4.33
1935	3/6/1935	23.2	41000	13	0.25	25	4.00
1915	2/2/1915	30	40,400	14	0.27	27	3.71
1936	2/21/1936	22.85	39200	15	0.29	29	3.47
1917	2/24/1917	29	37,300	16	0.31	31	3.25
1907	3/19/1907	29	37,300	17	0.33	33	3.06
1928	3/27/1928	31	34,700	18	0.35	35	2.89
1932	12/27/1931	21.8	34100	19	0.37	37	2.74
1921	1/30/1921	29.2	33,500	20	0.38	38	2.60
1909	1/8/1909	27.5	33,400	21	0.40	40	2.48
1954	1/17/1954	22.75	33000	22	0.42	42	2.36
1927	4/2/1927	29.2	31,300	23	0.44	44	2.26
1919	2/10/1919	26	30,000	24	0.46	46	2.17
1944	3/4/1944	21.4	29600	25	0.48	48	2.08
1911	3/7/1911	26.22	28,300	26	0.50	50	2.00
1906	1/19/1906	24	25,400	27	0.52	52	1.93
1952	1/14/1952	20.6	25100	28	0.54	54	1.86
1926	4/8/1926	25.5	24,500	29	0.56	56	1.79
1949	3/11/1949	19.67	22700	30	0.58	58	1.73
1930	12/15/1929	25.3	22,700	31	0.60	60	1.68
1923	12/10/1922	23.4	21,900	32	0.62	62	1.63
1945	2/1/1945	19.38	21700	33	0.63	63	1.58
1950	2/4/1950	19.27	21300	34	0.65	65	1.53
1922	2/19/1922	20.8	17,000	35	0.67	67	1.49
1946	12/27/1945	17.88	16500	36	0.69	69	1.44
1947	2/12/1947	17.3	14800	37	0.71	71	1.41
1913	1/19/1913	18.6	14,600	38	0.73	73	1.37
1924	2/8/1924	18.2	13,100	39	0.75	75	1.33
1910	12/9/1909	17.4	12,900	40	0.77	77	1.30
1934	12/30/1933	15.18	11700	41	0.79	79	1.27
1933	1/27/1933	14.67	10500	42	0.81	81	1.24
1908	2/2/1908	14.25	8,600	43	0.83	83	1.21
1929	2/4/1929	14.8	7,860	44	0.85	85	1.18
1948	3/24/1948	13.7	6540	45	0.87	87	1.16
1955	11/15/1954	12.78	4960	46	0.88	88	1.13
1931	1/23/1931	11.7	4820	47	0.90	90	1.11
1912	1/26/1912	10.9	4,530	48	0.92	92	1.08
1918	3/19/1918	9.8	3,790	49	0.94	94	1.06
1920	4/16/1920	9	2,830	50	0.96	96	1.04
1939	3/9/1939	7.95	1260	51	0.98	98	1.02

**Table A.2.** Post-dam Weibull-plotted flow frequency tables, sorted by flow rank.

Year	Event date	Gage height (ft)	Discharge (cfs)	Rank (m)	Probability exceedance (P)	P as %	Recurrence interval (yrs)
1983	3/2/1983	19.55	18,700	1	0.02	2	65.00
1970	1/24/1970	18.85	16,300	2	0.03	3	32.50
1997	1/26/1997	18.4	14,800	3	0.05	5	21.67
1998	2/8/1998	17.12	11,100	4	0.06	6	16.25
1982	4/12/1982	16.63	9,930	5	0.08	8	13.00
2004	2/18/2004	16.18	8,800	6	0.09	9	10.83
2019	2/27/2019	16.71	8,460	7	0.11	11	9.29
1965	1/7/1965	14.96	7,740	8	0.12	12	8.13
1974	3/30/1974	15.48	7,700	9	0.14	14	7.22
2006	3/7/2006	15.6	7,200	10	0.15	15	6.50
2017	2/21/2017	16.17	7,180	11	0.17	17	5.91
1986	3/16/1986	15	6,700	12	0.18	18	5.42
1984	12/26/1983	14.93	6,580	13	0.20	20	5.00
1969	2/15/1969	14.72	6,410	14	0.22	22	4.64
1967	1/31/1967	14.69	6,390	15	0.23	23	4.33
1975	3/25/1975	12.98	3,870	16	0.25	25	4.06
1996	3/13/1996	13.22	3,850	17	0.26	26	3.82
1995	1/9/1995	12.91	2,770	18	0.28	28	3.61
2005	3/23/2005	11.36	2,050	19	0.29	29	3.42
1999	3/26/1999	10.34	1,830	20	0.31	31	3.25
1980	2/19/1980	10.19	1,610	21	0.32	32	3.10
2003	12/16/2002	9.98	1,380	22	0.34	34	2.95
2000	6/14/2000	9.84	1,300	23	0.35	35	2.83
1958	2/18/1958	9.14	1,240	24	0.37	37	2.71
1968	3/17/1968	9.23	1,180	25	0.38	38	2.60
1973	3/21/1973	9.13	1,140	26	0.40	40	2.50
1978	1/14/1978	9.34	1,130	27	0.42	42	2.41
1971	3/28/1971	9.1	1,100	28	0.43	43	2.32
1963	1/31/1963	8.77	1,060	29	0.45	45	2.24
1981	6/25/1981	8.8	1,010	30	0.46	46	2.17
1976	5/13/1976	8.66	952	31	0.48	48	2.10
1959	2/16/1959	8.44	906	32	0.49	49	2.03
2011	3/20/2011	8.96	893	33	0.51	51	1.97
1985	7/12/1985	8.38	853	34	0.52	52	1.91
1993	1/20/1993	8.47	839	35	0.54	54	1.86
2014	7/1/2014	8.81	825	36	0.55	55	1.81
2001	6/22/2001	8.8	825	37	0.57	57	1.76
2013	6/10/2013	8.77	821	38	0.58	58	1.71
2012	6/18/2012	8.77	821	39	0.60	60	1.67
2007	7/31/2007	8.65	817	40	0.62	62	1.63
2010	1/20/2010	8.75	814	41	0.63	63	1.59
2021	7/8/2021	8.57	811	42	0.65	65	1.55
1977	4/25/1977	8.3	804	43	0.66	66	1.51
1987	6/25/1987	8.25	800	44	0.68	68	1.48
1979	7/16/1979	8.46	790	45	0.69	69	1.44
1966	9/11/1966	8.11	778	46	0.71	71	1.41
1988	6/3/1988	8.15	764	47	0.72	72	1.38
2002	7/26/2002	8.63	764	48	0.74	74	1.35
1972	7/16/1972	8.22	757	49	0.75	75	1.33
2009	6/2/2009	8.52	752	50	0.77	77	1.30
2020	7/8/2020	8.44	746	51	0.78	78	1.27
1989	6/23/1989	8.21	745	52	0.80	80	1.25
1992	8/23/1992	8.01	735	53	0.82	82	1.23
1994	6/24/1994	8.31	735	54	0.83	83	1.20

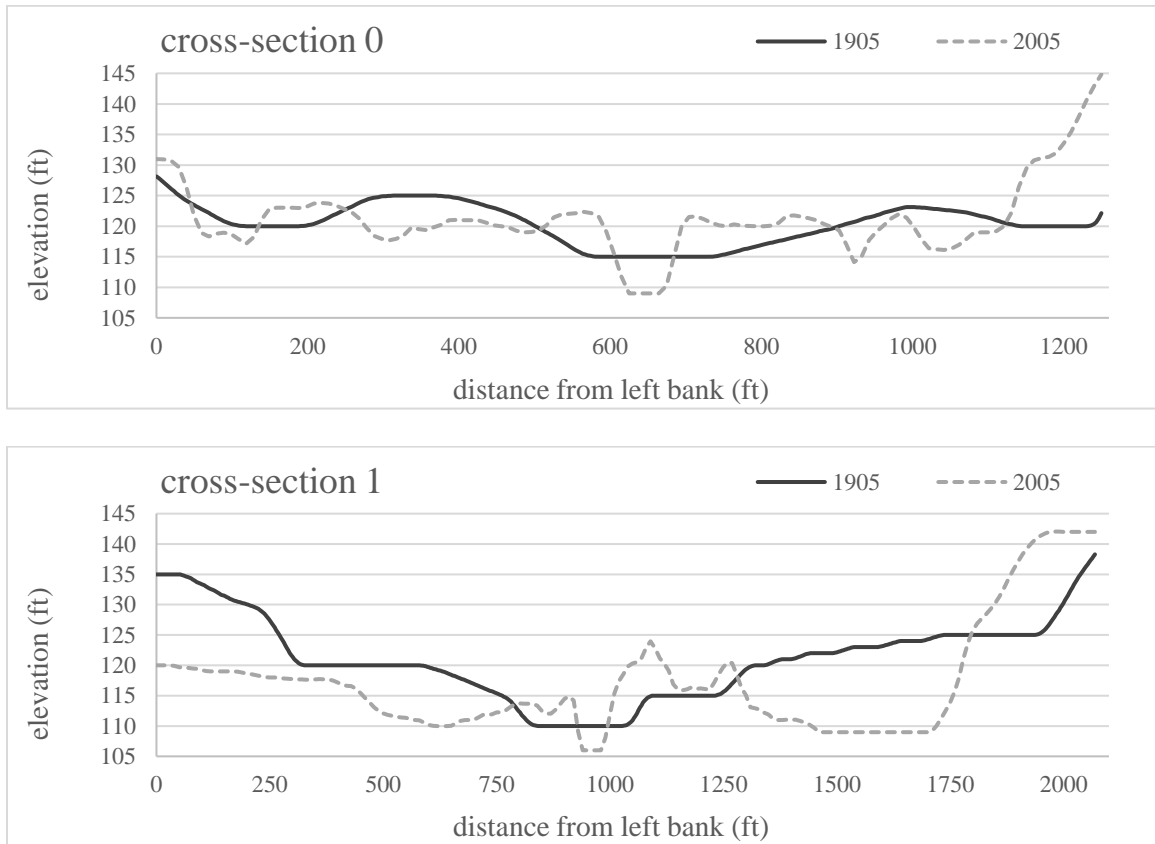
Table continued on next page.

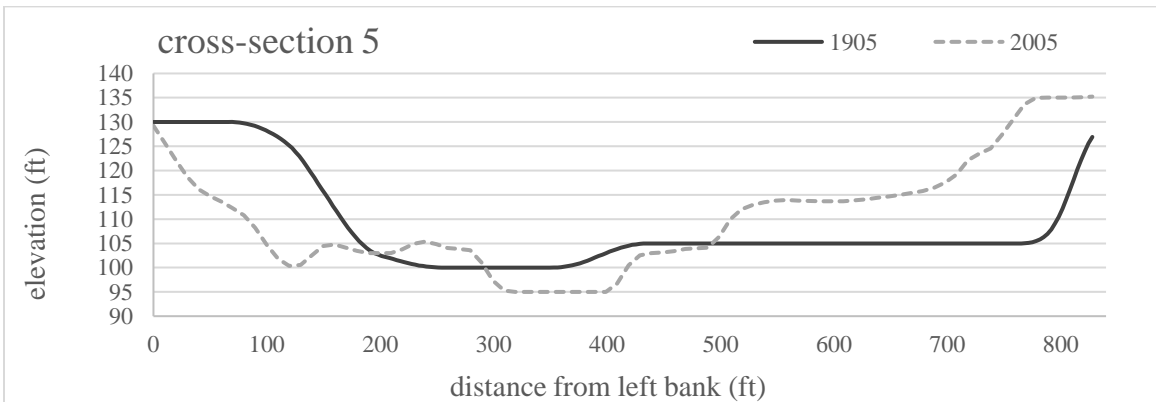
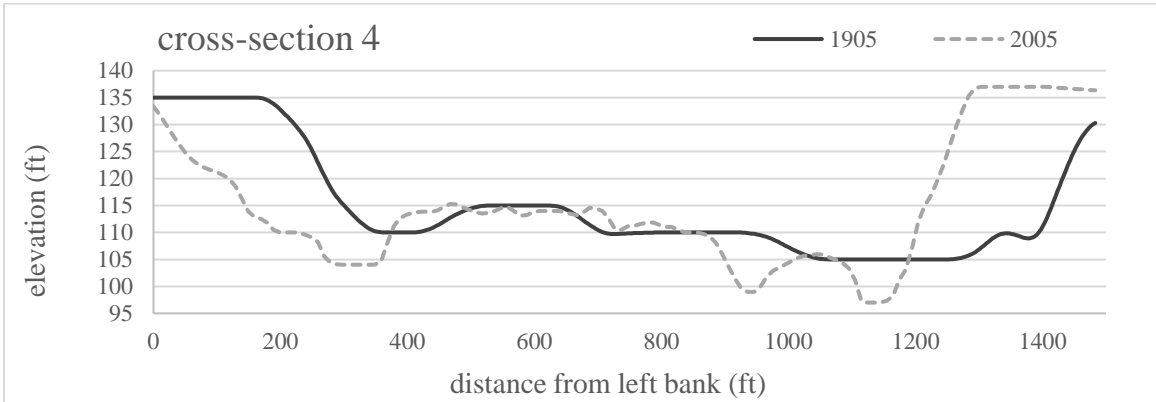
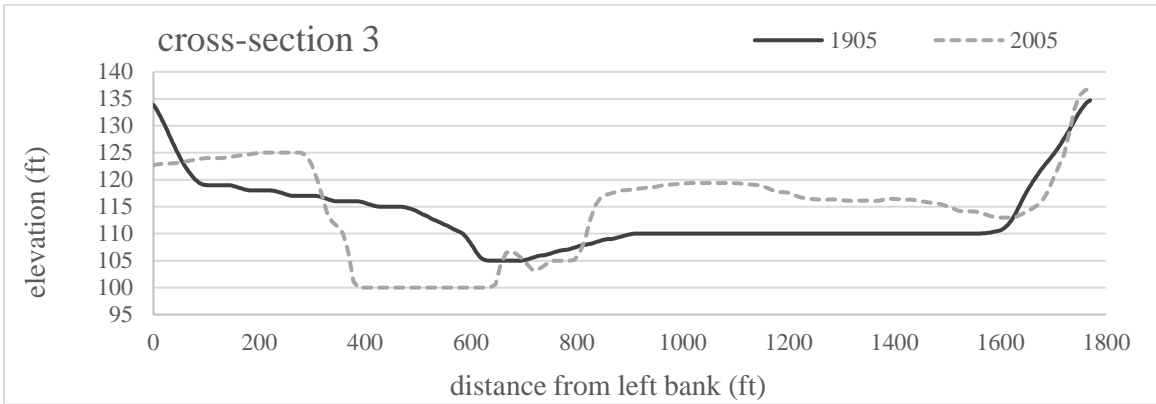
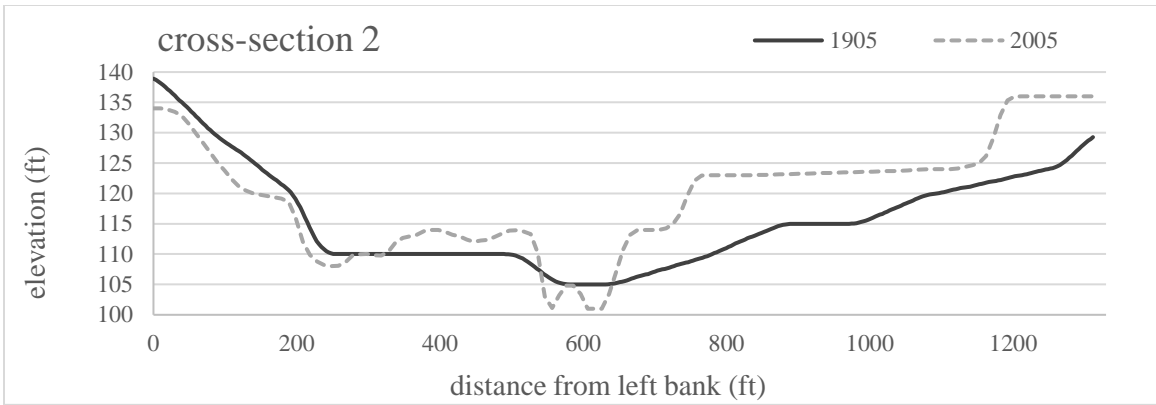


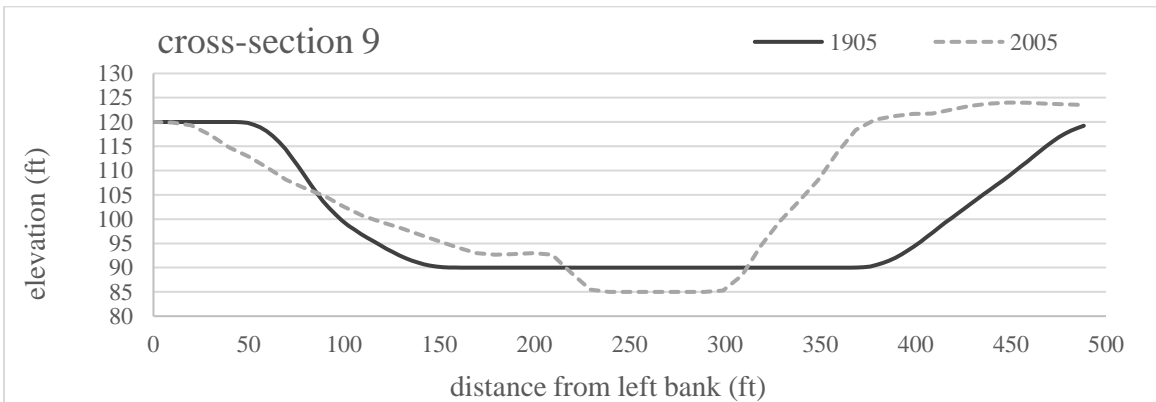
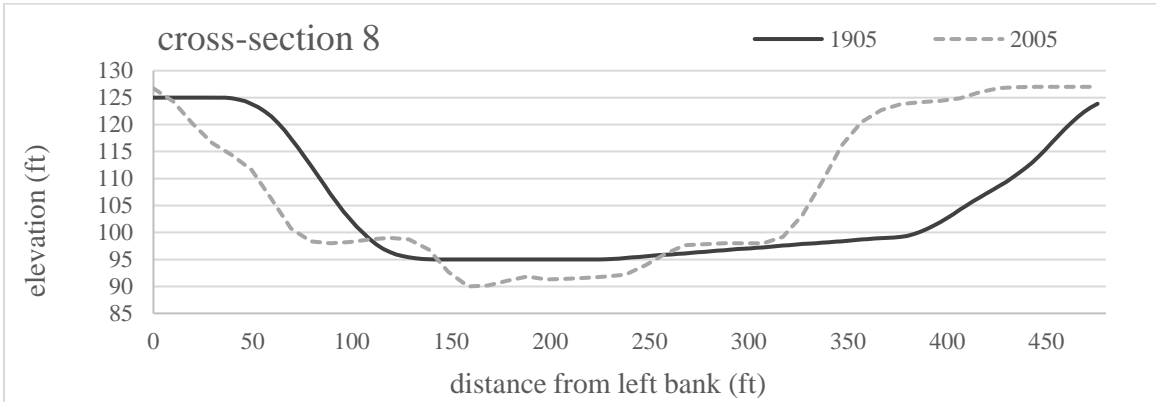
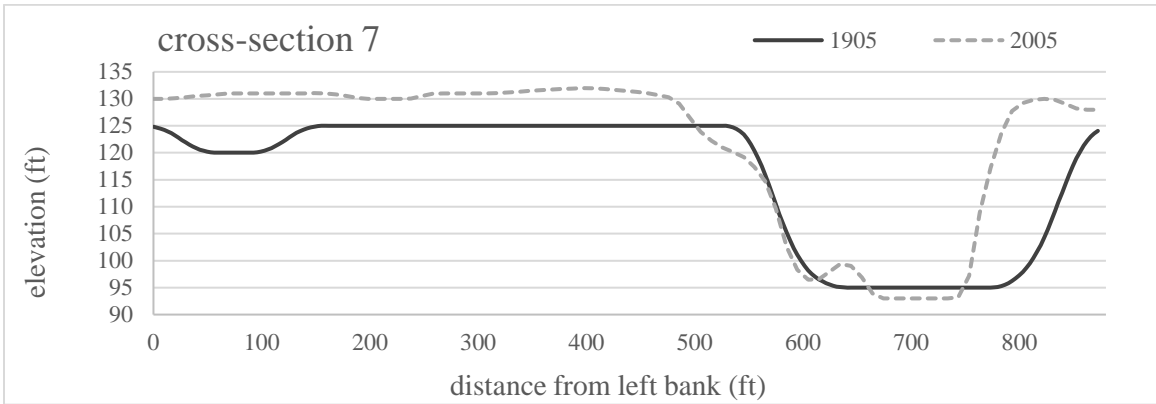
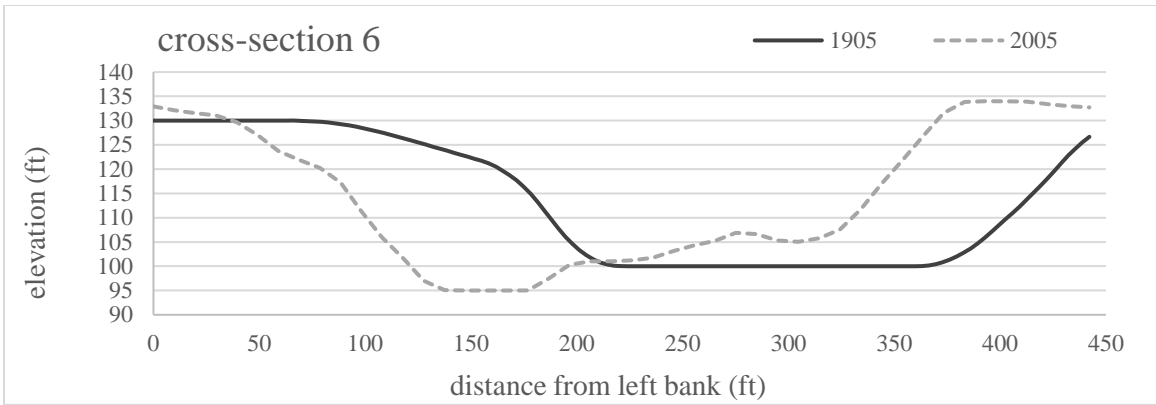
Continued from previous page: Post-dam Weibull-plotted flow frequency tables, sorted by flow rank.

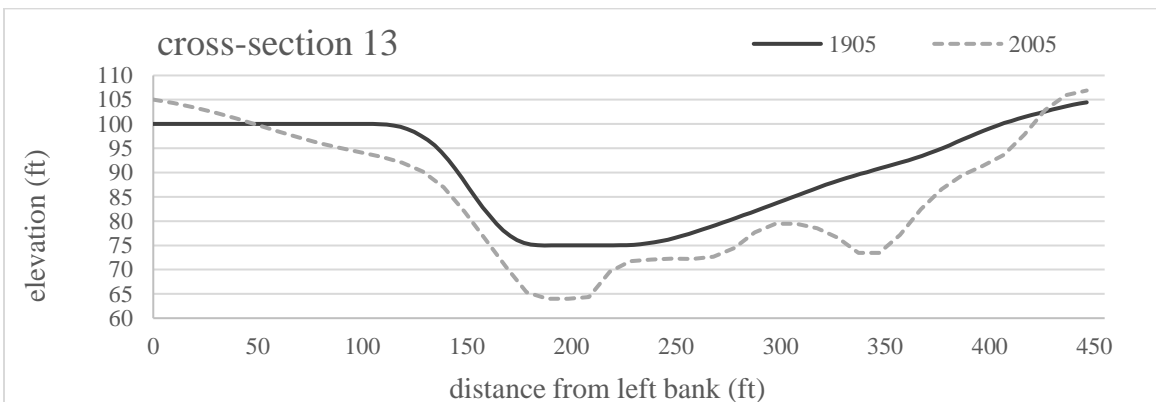
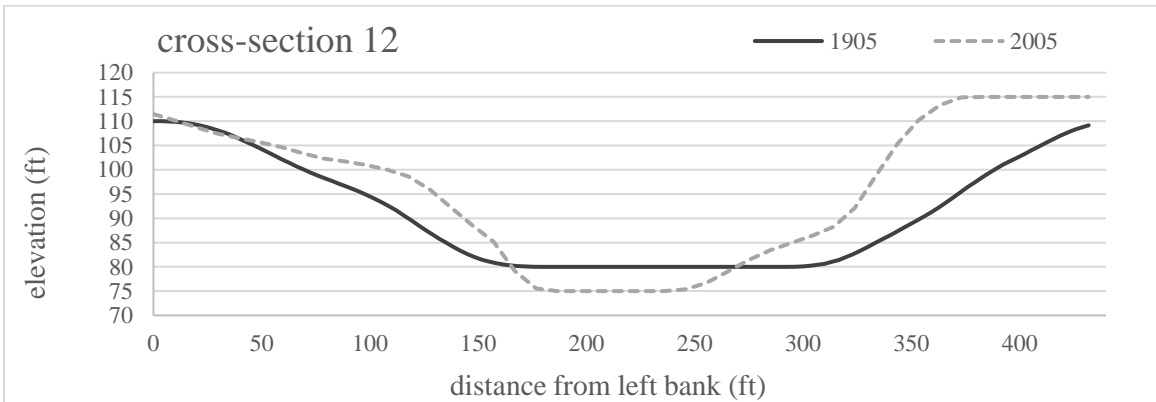
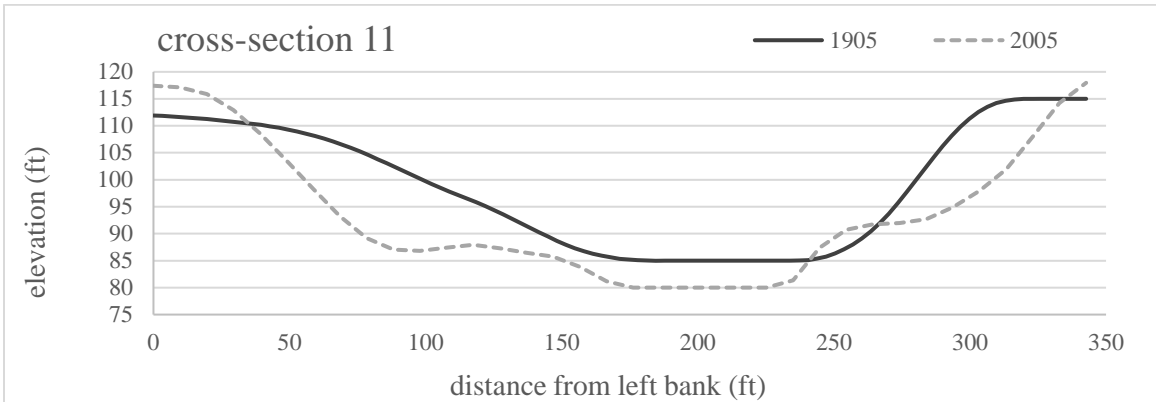
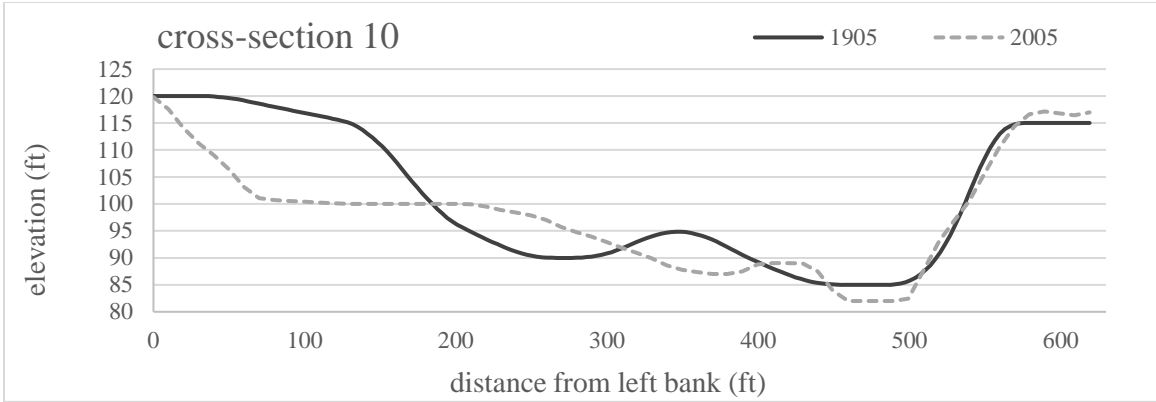
Year	Event date	Gage height (ft)	Discharge (cfs)	Rank (m)	Probability exceedance (P)	P as %	Recurrence interval (yrs)
2015	7/17/2015	8.68	735	55	0.85	85	1.18
2008	6/20/2008	8.52	731	56	0.86	86	1.16
1990	7/14/1990	8.14	721	57	0.88	88	1.14
2016	7/1/2016	8.49	686	58	0.89	89	1.12
2018	6/28/2018	8.33	665	59	0.91	91	1.10
1964	7/19/1964	7.75	658	60	0.92	92	1.08
1991	6/9/1991	7.82	645	61	0.94	94	1.07
1961	7/4/1961	7.55	585	62	0.95	95	1.05
1962	6/28/1962	7.38	524	63	0.97	97	1.03
1960	6/28/1960	6.84	397	64	0.98	98	1.02
1957	2/24/1957	6.7	368	65	1.00	100	1.00

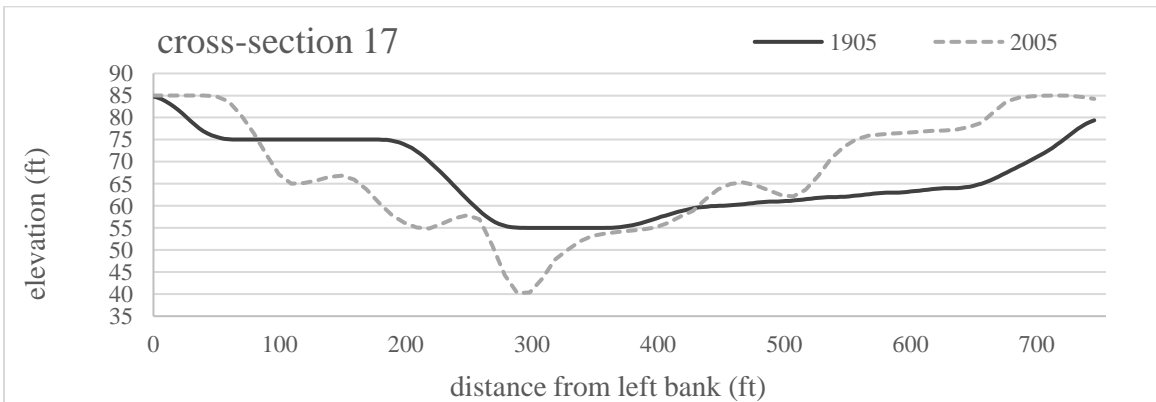
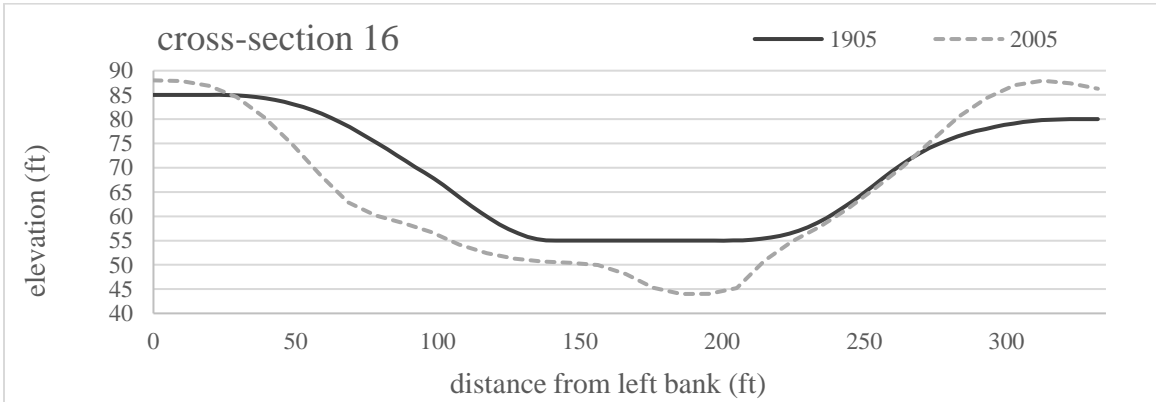
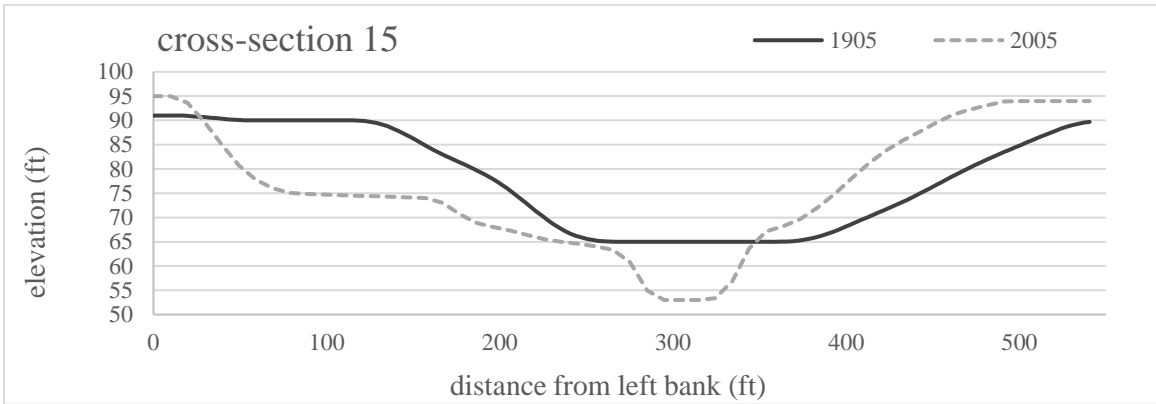
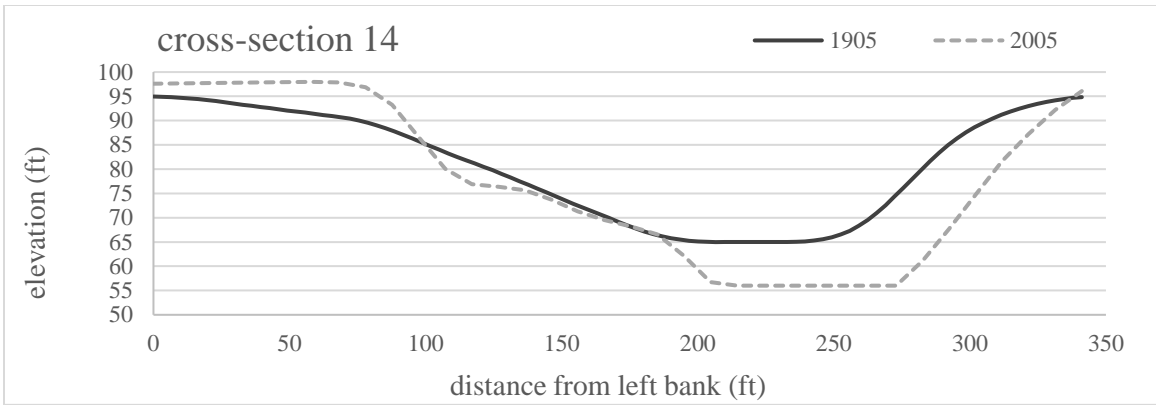
Figure A.1. Representative cross-sections from Chapter 1 geomorphic analyses.

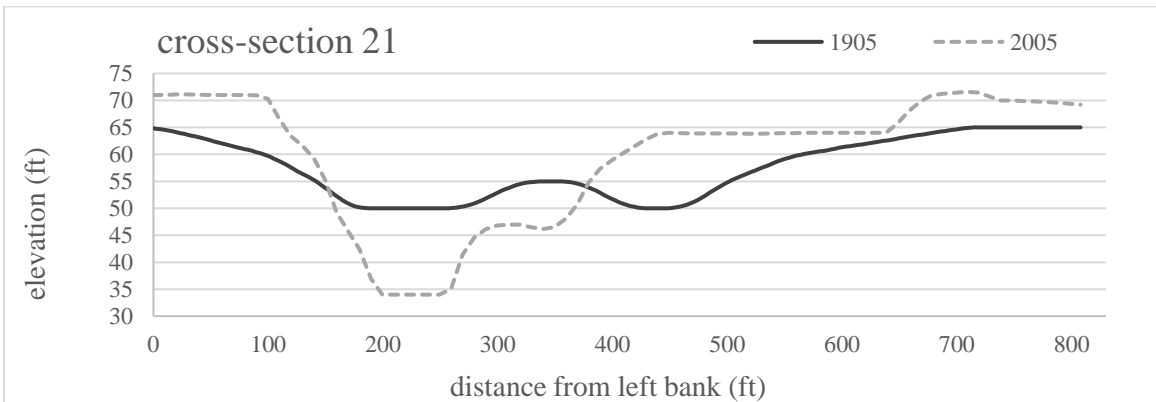
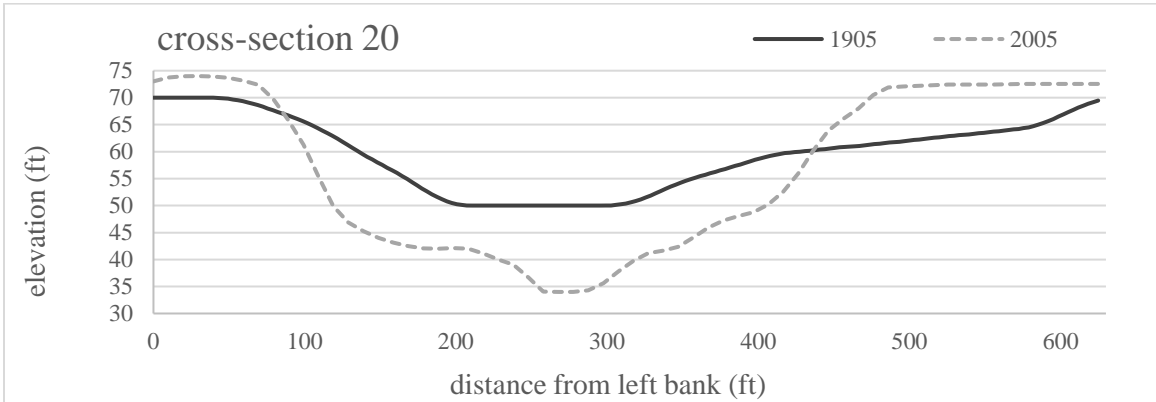
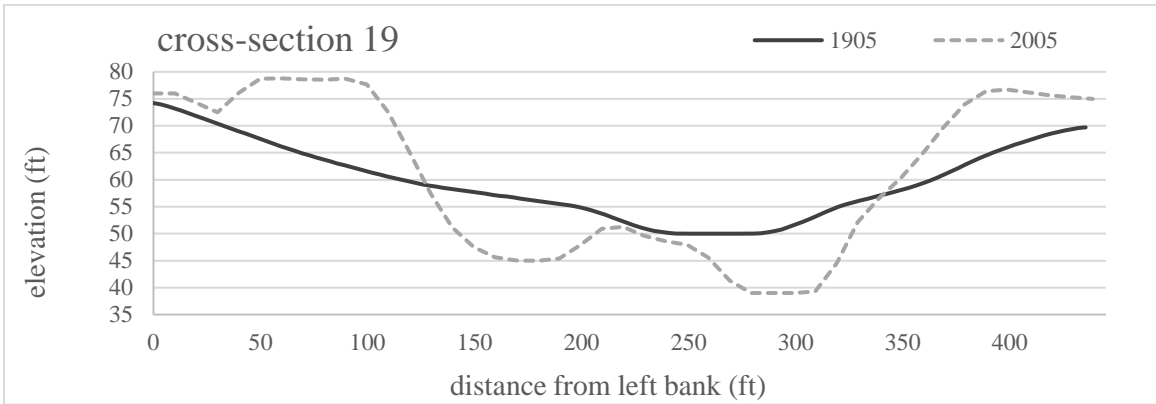
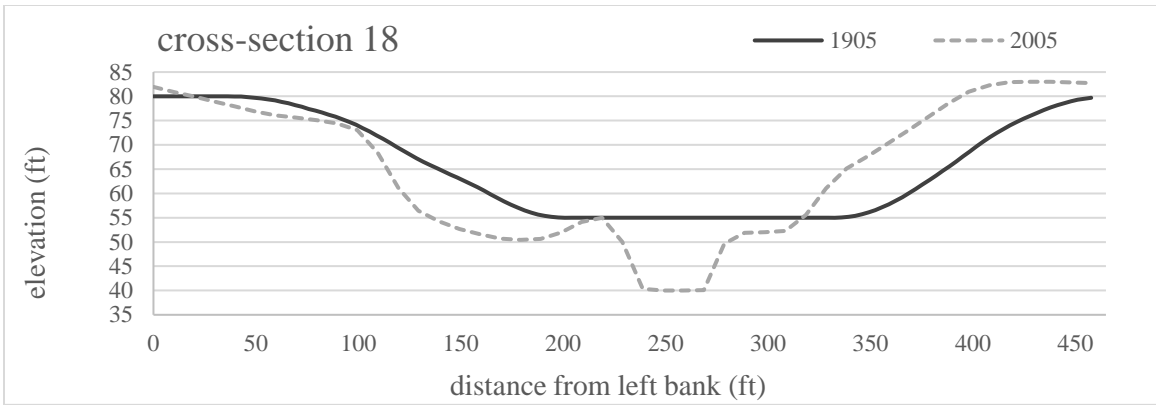


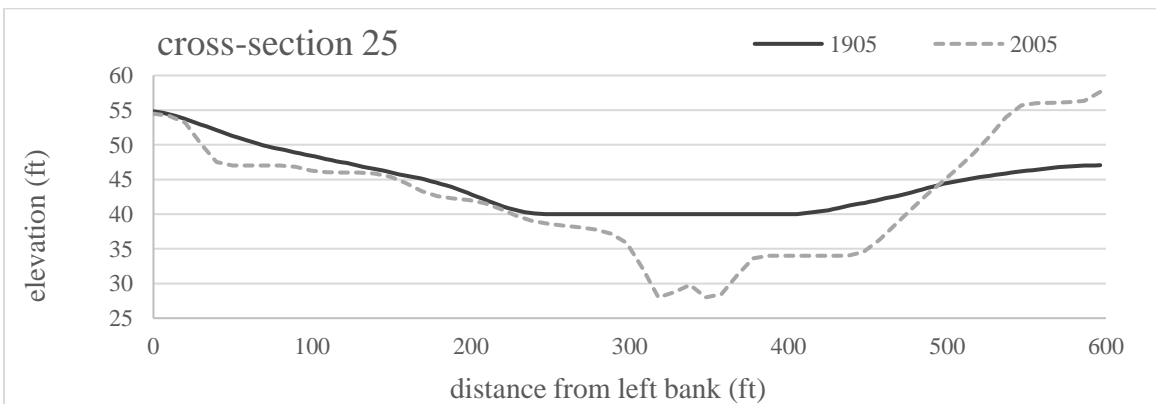
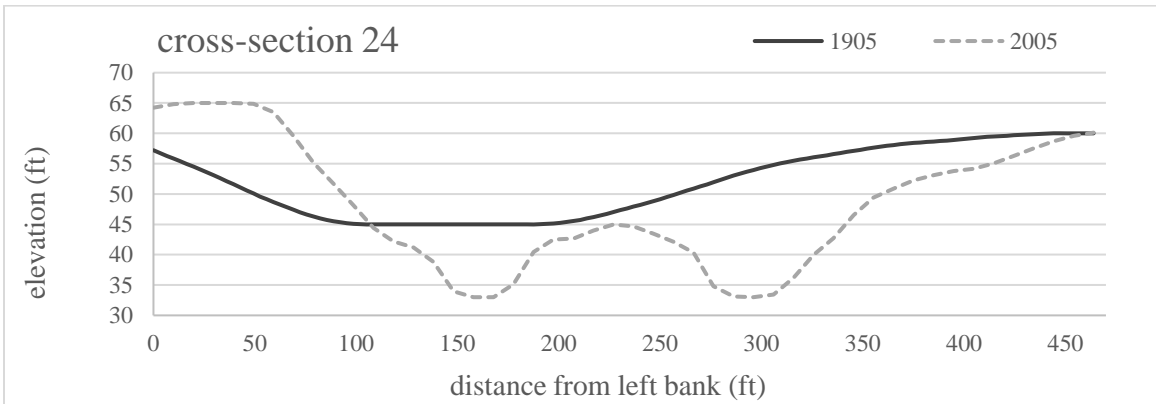
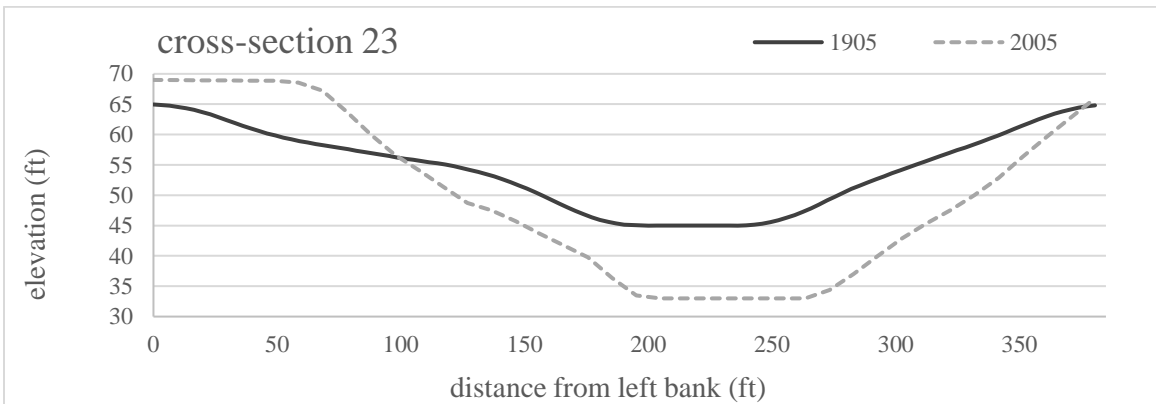
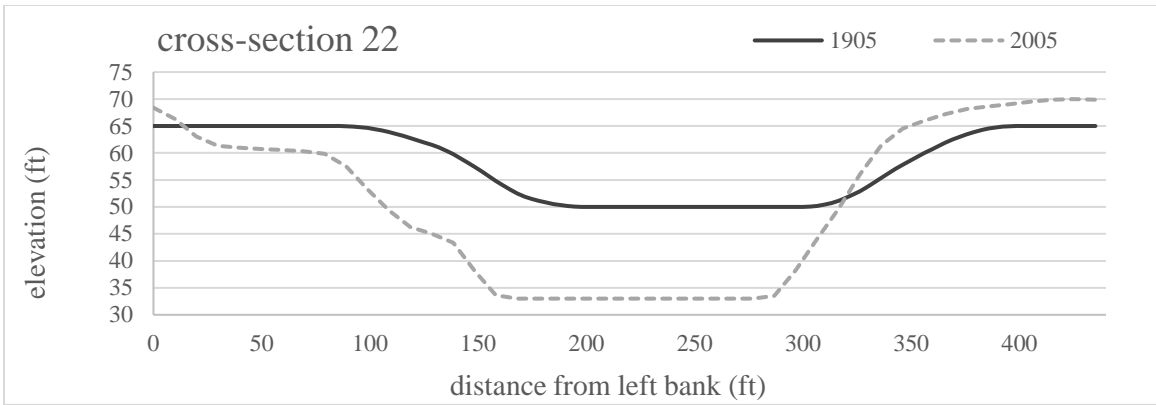


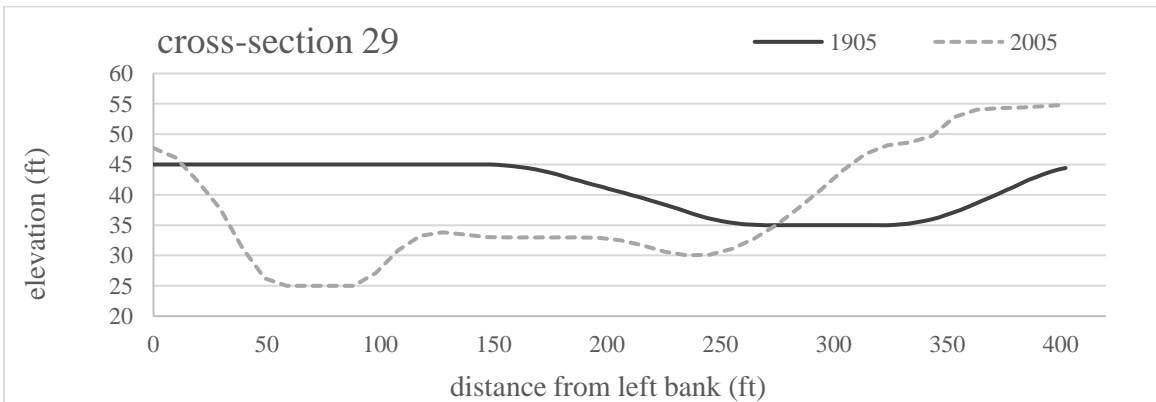
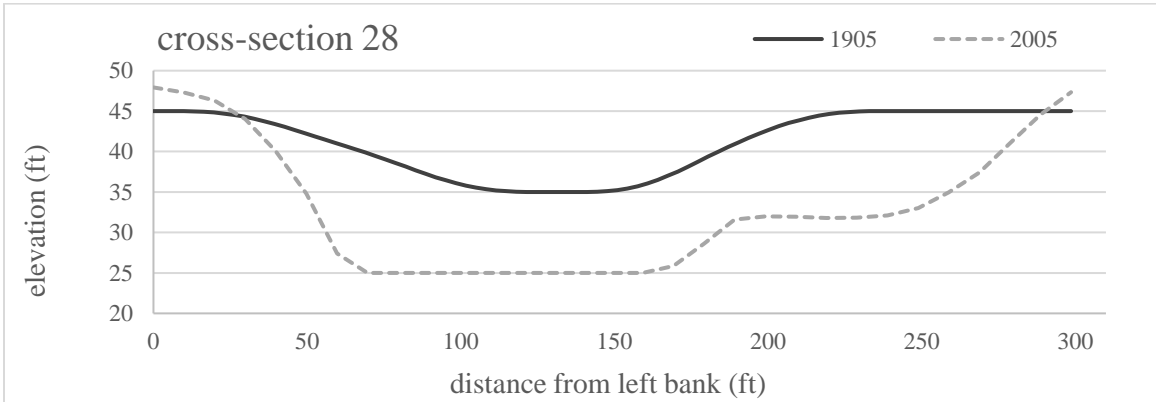
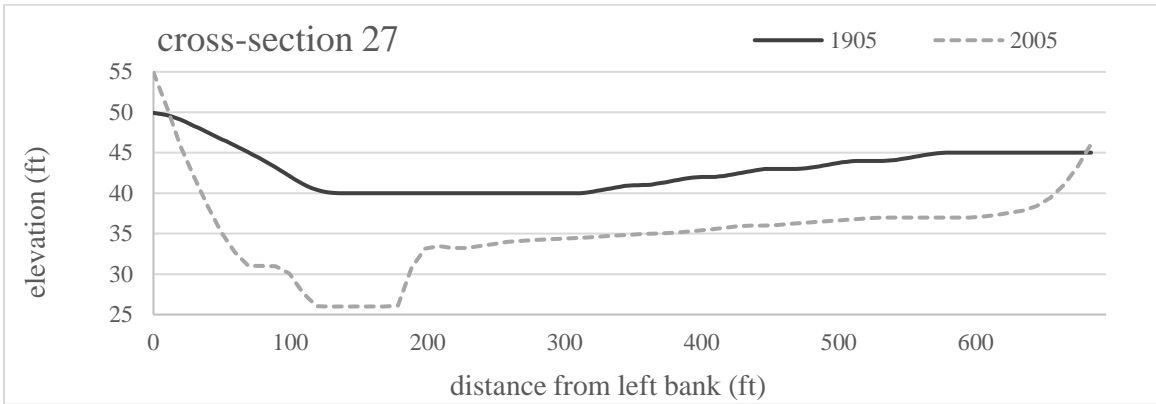
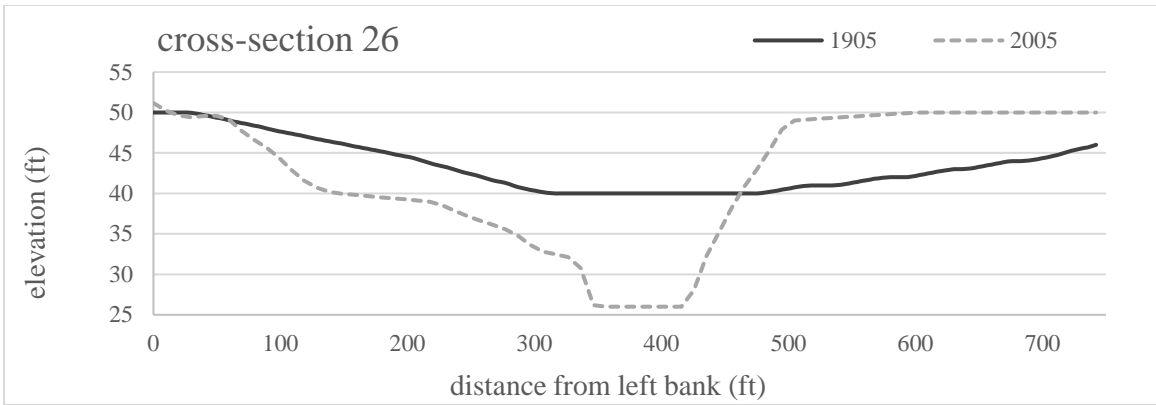




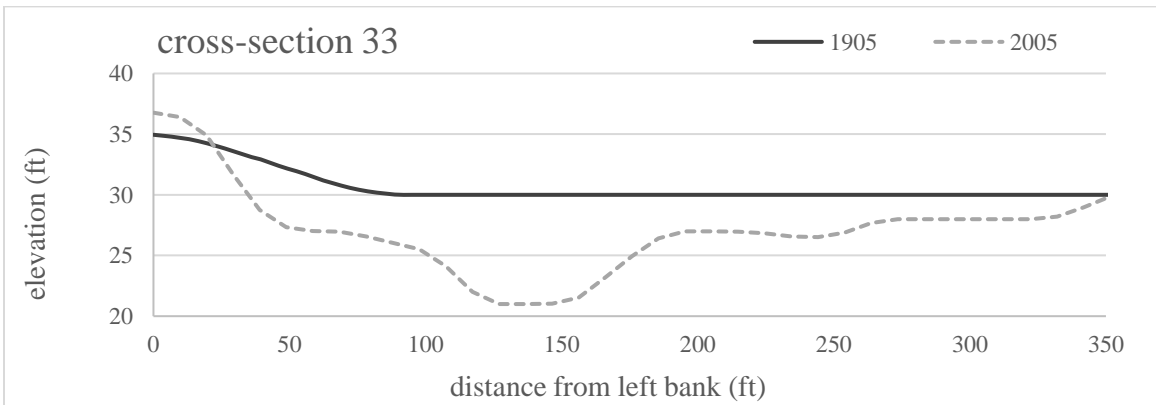
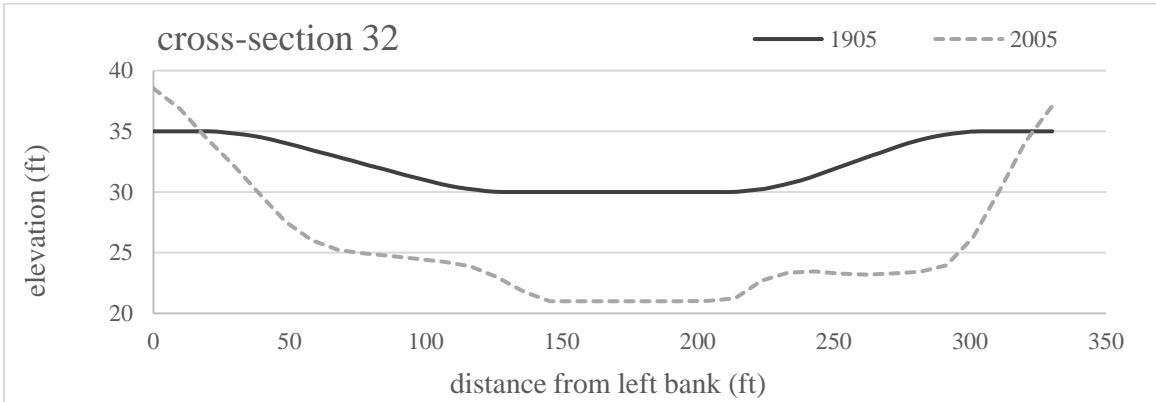
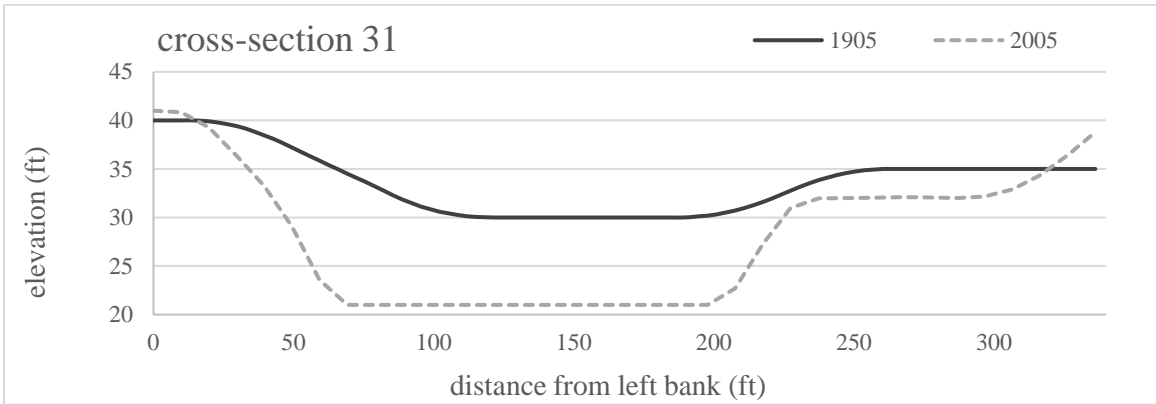
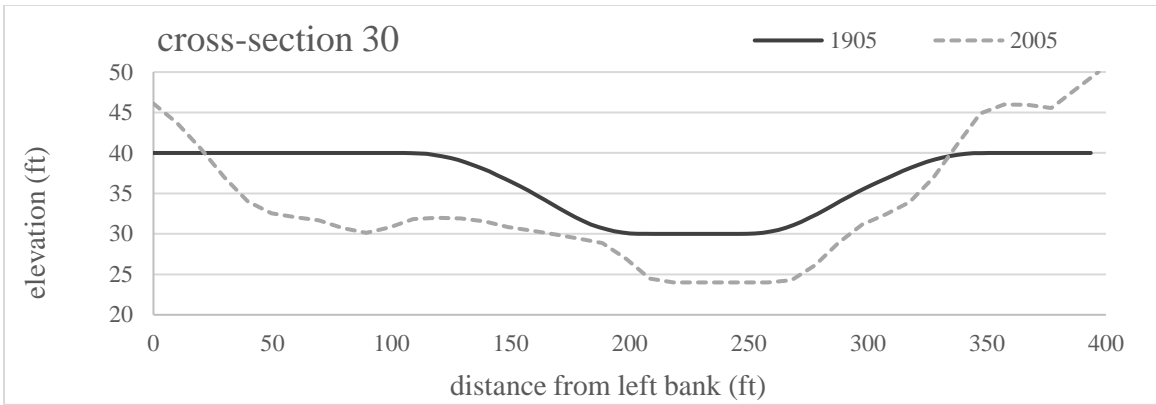


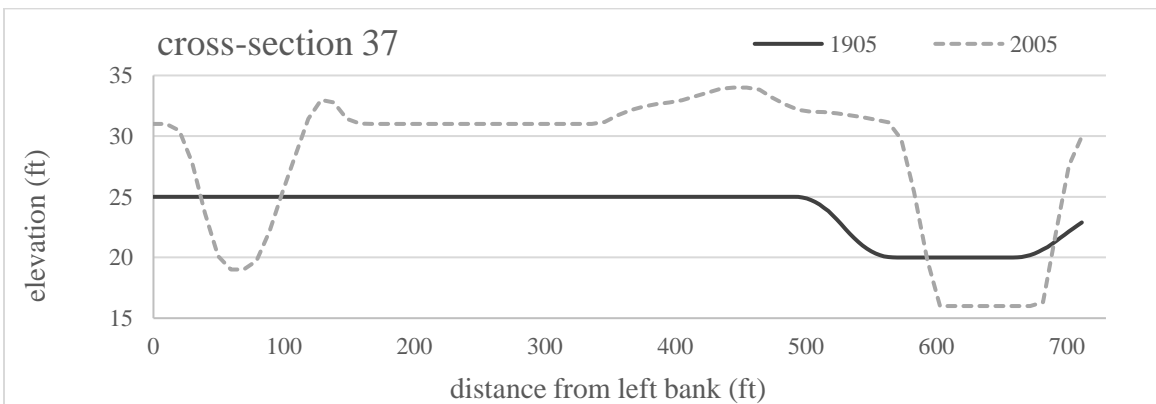
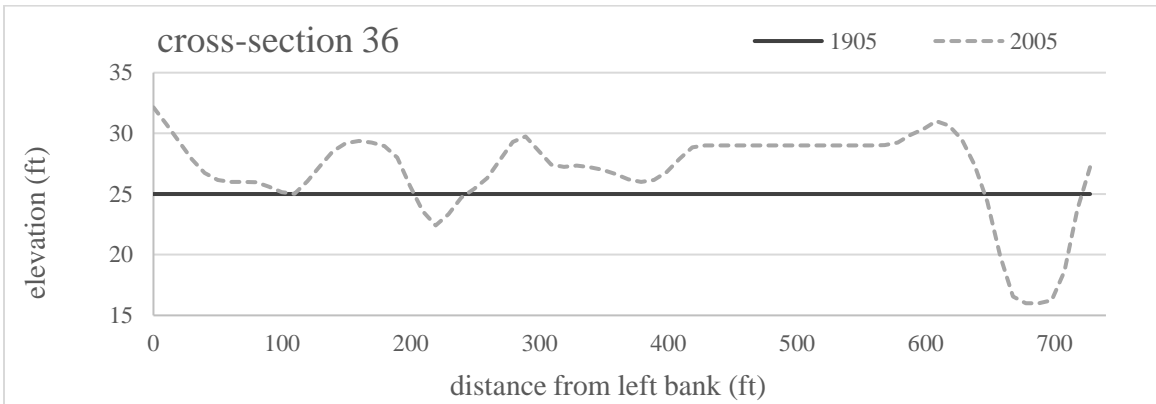
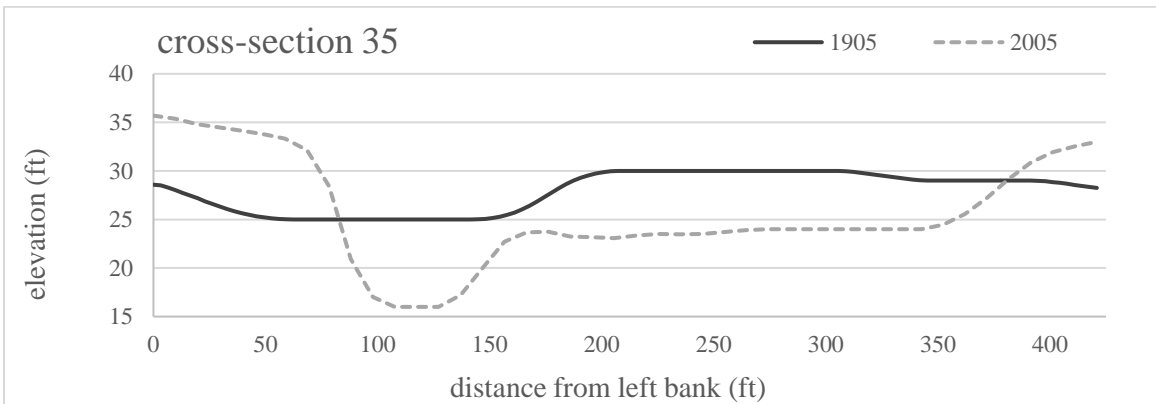
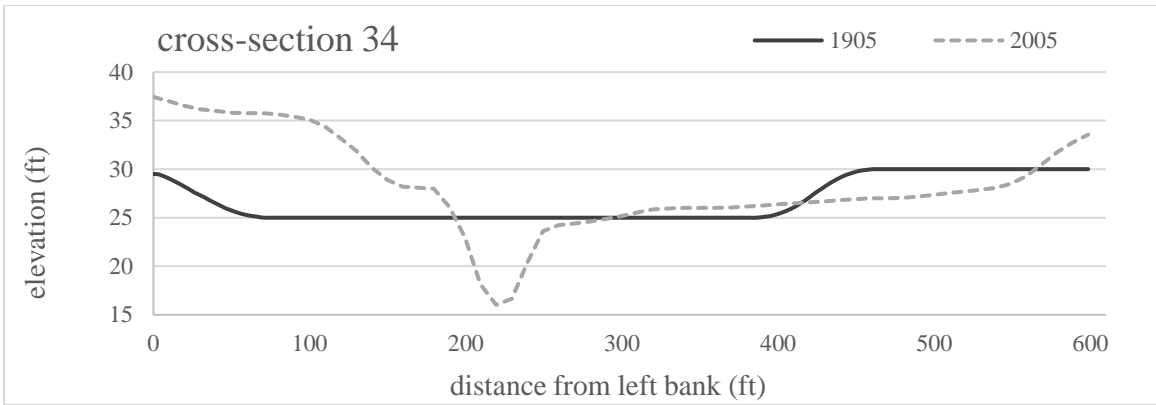












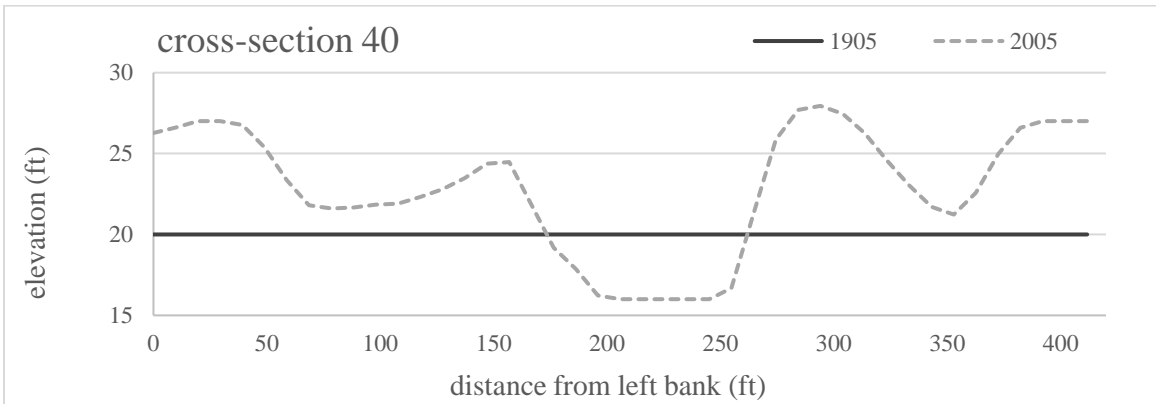
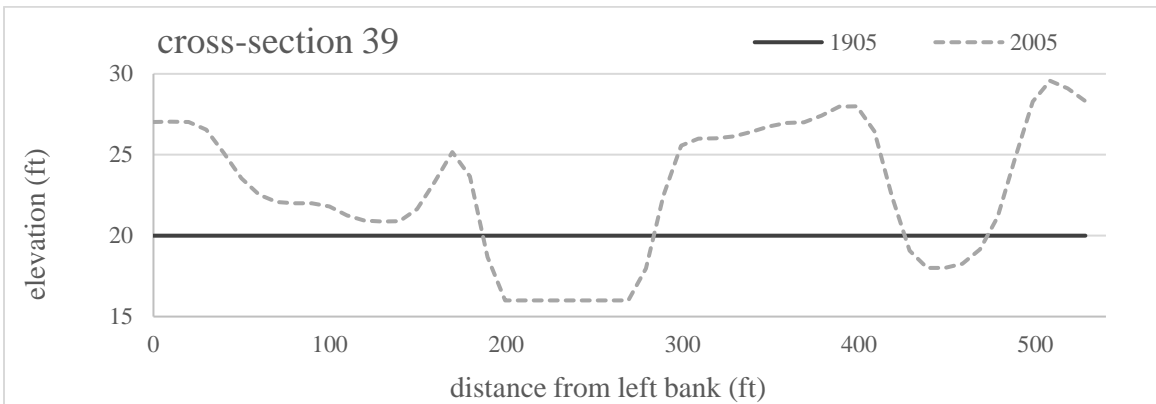
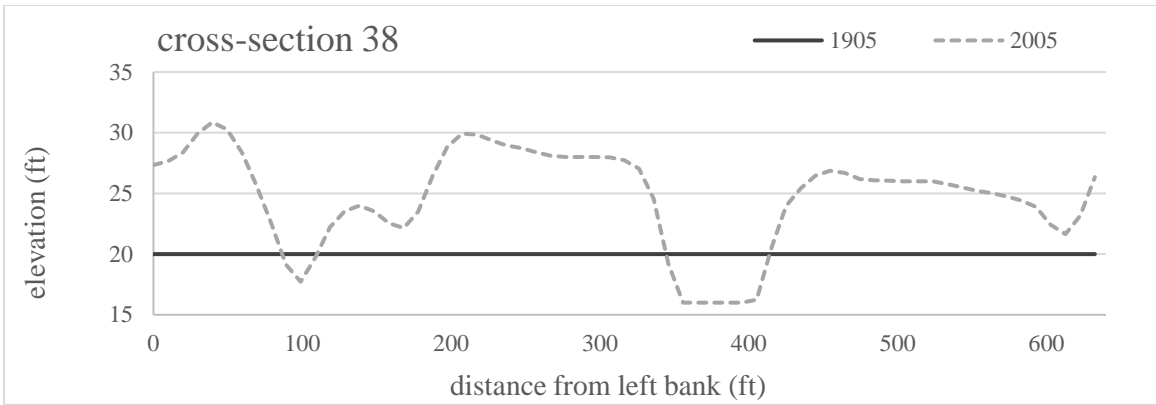


**Table A.3.** Reach-scale geomorphological statistics.

Reach #	downstream river-mile	upstream river-mile	upstream thalweg elevation (ft)	downstream thalweg elevation (ft)	thalweg elevation loss (ft)	stream centerline length (ft)	mean channel slope (%)	mean baseflow width (ft)	mean bank slope (deg.)	SD bank slope (deg)	mean bank slope (%)	SD bank slope (%)
1	1.54	2.05	16.00	16.00	0.00	2,717	0.00	88.36	5.4	6.4	9.5	11.2
2	2.05	3.28	16.13	16.00	0.13	6,476	0.00	57.62	4.9	7.5	8.6	13.2
3	3.28	4.07	17.00	16.13	0.87	4,181	0.02	69.74	5.4	7.9	9.5	13.9
4	4.07	5.20	21.00	17.00	4.00	5,960	0.07	42.13	5.7	6.7	10.0	11.8
5	5.20	5.56	22.00	21.00	1.00	1,890	0.05	130.66	6.6	7.5	11.6	13.2
6	5.56	6.46	25.00	22.00	3.00	4,758	0.06	60.71	8.0	8.1	14.1	14.2
7	6.46	7.40	26.00	25.00	1.00	4,964	0.02	81.07	5.6	8.3	9.8	14.6
8	7.40	8.15	28.00	26.00	2.00	3,952	0.05	50.88	4.9	6.8	8.6	11.9
9	8.15	8.93	33.00	28.00	5.00	4,120	0.12	44.78	9.1	7.6	16.0	13.3
10	8.93	9.73	34.00	33.00	1.00	4,219	0.02	84.18	7.6	9.3	13.3	16.4
11	9.73	10.78	39.00	34.00	5.00	5,534	0.09	34.37	10.4	10.3	18.4	18.2
12	10.78	11.32	40.00	39.00	1.00	2,850	0.04	63.07	11.8	11.8	20.9	20.9
13	11.32	12.31	43.33	40.00	3.33	5,236	0.06	33.50	10.9	10.3	19.3	18.2
14	12.31	13.10	48.00	43.33	4.67	4,194	0.11	35.34	12.6	11.2	22.4	19.8
15	13.10	15.55	62.23	48.00	14.23	12,905	0.11	35.43	11.0	10.3	19.4	18.2
16	15.55	16.25	74.00	62.23	11.77	3,690	0.32	29.20	10.6	9.2	18.7	16.2
17	16.25	16.65	75.00	74.00	1.00	2,136	0.05	81.79	9.3	10.5	16.4	18.5
18	16.65	17.06	79.00	75.00	4.00	2,144	0.19	54.08	10.1	9.0	17.8	15.8
19	17.06	17.47	80.00	79.00	1.00	2,208	0.05	81.69	11.2	11.0	19.8	19.4
20	17.47	18.41	85.00	80.00	5.00	4,928	0.10	57.31	9.0	9.7	15.8	17.1
21	18.41	19.13	90.00	85.00	5.00	3,830	0.13	47.64	10.9	11.1	19.3	19.6
22	19.13	20.27	96.00	90.00	6.00	5,988	0.10	69.89	8.0	10.0	17.6	17.6
23	20.27	20.71	98.00	96.00	2.00	2,353	0.08	52.75	5.1	7.3	12.8	12.8
24	20.71	21.65	104.00	98.00	6.00	4,940	0.12	93.59	4.6	6.7	8.1	11.8
25	21.65	22.75	109.00	104.00	5.00	5,834	0.09	40.27	4.6	6.0	8.1	10.5

**Table A.4.** Reach-scale area (acres) of each land cover type in the SVM classification of 2020 NAIP imagery.

Reach #	downstream river-mile	upstream river-mile	barren (ac)	herbaceous (ac)	shrub (ac)	riparian forest (ac)	valley oak (ac)	total area (ac)
1	1.54	2.05	1.2	8.1	2.1	8.7	4.0	24.1
2	2.05	3.28	31.1	17.2	4.3	18.8	17.2	88.5
3	3.28	4.07	0.8	9.1	2.4	9.3	7.9	29.5
4	4.07	5.20	0.6	1.8	3.1	21.9	16.5	43.9
5	5.20	5.56	0.4	1.5	0.3	4.6	6.1	12.9
6	5.56	6.46	0.4	4.6	1.4	12.0	15.7	34.2
7	6.46	7.40	1.3	28.3	1.2	7.1	8.8	46.6
8	7.40	8.15	1.2	29.7	1.0	7.1	5.1	44.1
9	8.15	8.93	0.6	9.5	2.7	10.0	7.7	30.4
10	8.93	9.73	0.9	7.0	0.8	9.2	12.7	30.6
11	9.73	10.78	1.4	14.8	3.4	16.4	16.9	52.9
12	10.78	11.32	5.1	2.2	0.3	6.8	7.7	22.2
13	11.32	12.31	0.9	9.9	0.5	13.4	24.9	49.6
14	12.31	13.10	0.1	4.8	1.9	7.6	18.2	32.6
15	13.10	15.55	1.0	22.7	8.6	22.9	50.6	105.9
16	15.55	16.25	2.7	5.7	2.4	7.6	13.4	31.8
17	16.25	16.65	0.5	1.4	0.6	2.9	5.6	10.9
18	16.65	17.06	0.8	2.7	2.6	4.3	5.7	16.1
19	17.06	17.47	1.5	2.1	1.0	3.0	5.3	12.9
20	17.47	18.41	1.0	8.9	1.8	10.8	14.5	36.9
21	18.41	19.13	0.4	4.9	0.8	7.3	10.4	23.7
22	19.13	20.27	5.5	13.4	2.7	10.7	12.8	45.0
23	20.27	20.71	2.0	9.5	2.5	6.4	9.6	30.1
24	20.71	21.65	2.3	16.5	14.1	12.0	23.7	68.6
25	21.65	22.75	10.3	73.2	26.1	16.4	18.6	144.7

**Table A.5.** Reach-scale relative area (%) of each land cover type in the SVM classification of 2020 NAIP imagery.

<b>Reach #</b>	<b>downstream river-mile</b>	<b>upstream river-mile</b>	<b>barren (%)</b>	<b>herbaceous (%)</b>	<b>shrub (%)</b>	<b>riparian forest (%)</b>	<b>valley oak (%)</b>	<b>combined shrub/riparian (%)</b>
1	1.54	2.05	4.8	33.6	8.7	36.2	16.7	44.9
2	2.05	3.28	35.1	19.4	4.9	21.2	19.4	26.1
3	3.28	4.07	2.7	30.8	8.1	31.7	26.7	39.8
4	4.07	5.20	1.3	4.1	7.1	50.0	37.5	57.1
5	5.20	5.56	2.8	11.9	2.4	35.8	47.0	38.3
6	5.56	6.46	1.3	13.5	4.0	35.1	46.1	39.1
7	6.46	7.40	2.7	60.7	2.5	15.1	19.0	17.7
8	7.40	8.15	2.8	67.4	2.2	16.1	11.5	18.3
9	8.15	8.93	2.0	31.1	8.7	32.8	25.4	41.6
10	8.93	9.73	3.1	23.0	2.6	30.0	41.3	32.6
11	9.73	10.78	2.6	28.0	6.4	31.1	31.9	37.5
12	10.78	11.32	23.1	9.9	1.4	30.8	34.8	32.2
13	11.32	12.31	1.8	19.9	1.1	27.0	50.2	28.1
14	12.31	13.10	0.3	14.8	5.8	23.3	55.8	29.1
15	13.10	15.55	1.0	21.5	8.1	21.6	47.8	29.7
16	15.55	16.25	8.4	18.0	7.5	24.0	42.1	31.5
17	16.25	16.65	4.3	12.5	5.8	26.3	51.2	32.1
18	16.65	17.06	4.7	16.7	16.2	26.9	35.4	43.2
19	17.06	17.47	11.6	16.2	8.0	23.3	41.0	31.3
20	17.47	18.41	2.7	24.0	4.8	29.2	39.3	34.0
21	18.41	19.13	1.6	20.5	3.5	30.8	43.7	34.3
22	19.13	20.27	12.2	29.7	6.0	23.7	28.4	29.7
23	20.27	20.71	6.6	31.7	8.3	21.4	31.9	29.7
24	20.71	21.65	3.4	24.0	20.6	17.4	34.6	38.0
25	21.65	22.75	7.1	50.6	18.1	11.3	12.9	29.4

**Table A.6.** Reach-scale area (acres) of each HAR zone from the random forest classification and zone analysis.

Reach #	downstream river-mile	upstream river-mile	aquatic (ac)	core riparian (ac)	marginal riparian (ac)	transition (ac)	valley oak (ac)	out-of-channel (ac)	in-channel area (ac)
1	1.54	2.05	5.2	11.3	7.6	7.2	0.0	0.0	31.3
2	2.05	3.28	9.9	15.0	14.1	60.1	0.1	0.0	99.3
3	3.28	4.07	6.8	7.6	7.2	15.4	1.4	0.0	38.5
4	4.07	5.20	5.5	25.2	7.8	15.8	0.1	0.0	54.3
5	5.20	5.56	4.5	3.6	3.0	3.6	1.0	0.0	15.7
6	5.56	6.46	6.3	18.2	3.0	5.4	10.0	0.0	42.9
7	6.46	7.40	10.6	6.7	17.1	15.0	8.5	0.1	57.9
8	7.40	8.15	4.7	6.0	4.5	20.8	25.8	0.7	61.8
9	8.15	8.93	4.1	11.6	5.0	6.8	9.0	2.4	36.5
10	8.93	9.73	9.0	3.1	2.4	6.6	12.5	20.7	33.6
11	9.73	10.78	5.1	9.9	6.9	9.4	7.8	23.5	39.0
12	10.78	11.32	4.4	2.0	1.9	3.9	2.8	11.4	15.0
13	11.32	12.31	4.6	4.1	4.1	12.8	10.4	23.2	36.0
14	12.31	13.10	3.6	3.7	3.3	6.2	4.0	16.0	20.8
15	13.10	15.55	11.7	9.3	9.7	28.0	24.3	46.6	83.1
16	15.55	16.25	2.7	6.4	4.5	9.3	9.3	8.7	32.2
17	16.25	16.65	4.3	1.9	2.1	2.7	4.5	6.4	15.5
18	16.65	17.06	2.9	5.5	2.5	3.2	4.5	4.3	18.4
19	17.06	17.47	4.2	2.0	1.9	3.5	2.9	5.0	14.4
20	17.47	18.41	6.7	11.4	5.3	15.7	8.6	9.7	47.7
21	18.41	19.13	5.3	6.2	4.0	4.8	4.8	14.0	25.1
22	19.13	20.27	10.0	12.9	8.0	8.3	8.5	31.8	47.7
23	20.27	20.71	3.7	7.1	6.5	21.0	15.5	12.3	53.9
24	20.71	21.65	10.5	24.0	13.6	33.7	49.2	18.2	131.0
25	21.65	22.75	6.2	47.2	40.9	69.1	51.6	29.7	214.9

**Table A.7.** Reach-scale relative area (%) of each HAR zone within the channel (< 30 ft HAR; excludes out-of-channel zone), based on the random forest classification and zone analysis.

<b>Reach #</b>	<b>downstream river-mile</b>	<b>upstream river-mile</b>	<b>aquatic (%)</b>	<b>core riparian (%)</b>	<b>marginal riparian (%)</b>	<b>transition (%)</b>	<b>valley oak (%)</b>	<b>combined riparian (%)</b>
1	1.54	2.05	16.7	36.1	24.3	22.9	0.0	60.4
2	2.05	3.28	10.0	15.1	14.2	60.6	0.1	29.3
3	3.28	4.07	17.7	19.9	18.8	40.0	3.6	38.7
4	4.07	5.20	10.1	46.3	14.3	29.0	0.2	60.7
5	5.20	5.56	29.0	23.2	18.9	22.7	6.3	42.1
6	5.56	6.46	14.6	42.4	7.1	12.5	23.4	49.4
7	6.46	7.40	18.3	11.5	29.6	26.0	14.6	41.1
8	7.40	8.15	7.6	9.7	7.2	33.7	41.8	16.9
9	8.15	8.93	11.3	31.9	13.7	18.5	24.7	45.5
10	8.93	9.73	26.8	9.2	7.0	19.7	37.2	16.2
11	9.73	10.78	13.0	25.4	17.7	24.0	19.9	43.1
12	10.78	11.32	29.0	13.1	12.9	26.1	18.9	26.0
13	11.32	12.31	12.8	11.4	11.3	35.5	29.0	22.7
14	12.31	13.10	17.1	18.0	15.9	29.7	19.2	33.9
15	13.10	15.55	14.1	11.2	11.6	33.7	29.3	22.9
16	15.55	16.25	8.4	19.7	13.9	29.0	29.0	33.6
17	16.25	16.65	28.0	12.2	13.7	17.2	28.9	25.9
18	16.65	17.06	15.6	29.6	13.3	17.1	24.3	43.0
19	17.06	17.47	29.0	13.7	13.1	24.1	20.1	26.9
20	17.47	18.41	14.1	23.8	11.2	32.9	18.1	35.0
21	18.41	19.13	21.0	24.6	16.0	19.2	19.2	40.6
22	19.13	20.27	21.0	27.0	16.9	17.3	17.9	43.8
23	20.27	20.71	6.9	13.2	12.1	39.1	28.8	25.3
24	20.71	21.65	8.0	18.3	10.4	25.7	37.6	28.7
25	21.65	22.75	2.9	22.0	19.0	32.1	24.0	41.0



**Table A.8.** Place names associated with each reach, in order from lowest-to-highest river-miles. Green = “reference,” yellow = “somewhat degraded,” orange = “moderately degraded,” red = “severely degraded.” See **Table 3.9** for ranking scheme.

Reach #	downstream river-mile	upstream river-mile	place names	sum ranking
1	1.54	2.05	end of the Putah Creek south levee	12
2	2.05	3.28	split channel	41
3	3.28	4.07	South Fork Preserve	36
4	4.07	5.2	no associated place names	10
5	5.2	5.56	no associated place names	29
6	5.56	6.46	easternmost end of UC Davis Riparian Reserve, south of and past the solar farm	4
7	6.46	7.4	Old Davis Road and Restoria project site	22
8	7.4	8.15	Railroad bridge	36
9	8.15	8.93	Interstate 80	6
10	8.93	9.73	UC Davis picnic grounds and Putah Creek north-south fork	41
11	9.73	10.78	Pedrick Road and westernmost end of UC Davis Riparian Reserve	12
12	10.78	11.32	Nishikawa project site	42
13	11.32	12.31	Glide Ranch	43
14	12.31	13.1	Stevenson Bridge	31
15	13.1	15.55	UC Davis Russell Ranch	41
16	15.55	16.25	Walnut Bayou Lane	22
17	16.25	16.65	no associated place names	34
18	16.65	17.06	no associated place names	10
19	17.06	17.47	Long-distance electricity transmission lines	40
20	17.47	18.41	El Rio Villa	31
21	18.41	19.13	Interstate 505	22
22	19.13	20.27	Winters Putah Creek Nature Park	13
23	20.27	20.71	Dry Creek confluence	36
24	20.71	21.65	Wintu Way and Putah Creek Road intersection	21
25	21.65	22.75	Winters Oxbow	15

**Figure A.2.** HAR zone maps by reach.

